Network Connectedness and Financial Technologies: from Systemic Risk to Investment Management

by

Paolo Pagnottoni
Matriculation no. 1050344

A thesis submitted for the degree of

Doctor of Philosophy

in

Applied Economics and Management

of the

University of Bergamo and University of Pavia

Supervisor:

Prof. Dr. Paolo Stefano Giudici

Faculty Tutor:

Prof. Dr. Paola Cerchiello

2020

In a real sense all life is interrelated. All men are caught in an inescapable network of mutuality, tied in a single garment of destiny. Whatever affects one directly, affects all indirectly.

MARTIN LUTHER KING
(1929 - 1968)

Invisible threads are the strongest ties.

FRIEDRICH NIETZSCHE
(1844 - 1900)

Acknowledgments

Going through the PhD has been like going through a new life. I met extraordinary people during this journey and from each of them I have learnt something that made up what I am right now. I have to thank many people for this.

I heartily thank my supervisor, for being the present guide who drove me throughout my PhD journey. I have learnt so many things from him, and not only academic ones. He is the person who built myself up as the researcher I am now, and the one who taught me lots of life things in what felt such a short time working with him. Thank you.

I thank my friends for being always around. They laughed with me when things were going right, cheered me up when things were going wrong, and built a part of me that is virtuously complementary to the professional one. The energy and examples you gave me have always been a motivation to do great in life.

I thank all my Lab colleagues for being always around, though I believe I should not thank them aside: I called them colleagues, but they are actually real friends as those above, besides being a true family to me. A family made of people that are always there, that always have a smile and that are both great academics and human beings. I already miss our Pavia Statistics group: you all made my time in the University.

I thank all the people whom I met in the various conferences, seminars and workshops. The inputs each of you gave me were crucial to improve my research skills and output. In particular, I thank Prof. Tomaso Aste for giving me the opportunity to spend a visiting period at the University College of London. I would have loved to stay there a bit more!

Last, but definitely not least, I thank my family for always supporting me in whatever I was convinced to do. A special thanks goes to my mother, who gave me all the opportunities in life, among which that of studying, bearing the difficulties coming from raising three kids mostly on her own. I bet my father would be proud of you, and of all of us.

Ringraziamenti

Il viaggio attraverso il dottorato è stato come percorrere una nuova vita. Ho incontrato persone straordinarie su questa strada e da ciascuna di esse ho imparato qualcosa che ha contribuito a costruire la persona che sono ora. Devo ringraziare diverse persone per questo.

Ringrazio il mio mentore, per essere stato la guida presente che mi ha accompagnato nel viaggio del dottorato. Ho imparato molte cose da lui, e non solo accademiche. Lui è la persona che ha costruito il ricercatore che sono oggi, e la persona che mi ha insegnato così tante cose importanti della vita in quello che mi è sembrato essere un così breve tempo trascorso lavorando con lui. Grazie di cuore.

Ringrazio i miei amici per la loro presenza. Hanno riso con me quando le cose andavano per il verso giusto, rincuoratomi quando le cose andavano per quello sbagliato, e costruito una parte di me che è virtuosamente complementare a quella professionale. L'energia e gli esempi che mi avete trasmesso sono sempre stati una ragione per dare il massimo nella vita.

Ringrazio tutti i miei colleghi del Laboratorio, anche loro per essere sempre presenti, nonostante io creda di non doverli ringraziare a parte: li ho chiamati colleghi, ma in realtà sono per me come i veri amici di cui sopra, oltre ad essere invero la mia famiglia. Una famiglia fatta di persone che ci sono sempre, che hanno sempre un sorriso per te e che sono grandi persone accademiche e, soprattutto, grandi esseri umani. Il nostro gruppo di Statistica di Pavia mi manca già: avete tutti reso speciale il mio vivere l'Università.

Ringrazio tutte le persone che ho incontrato durante le varie conferenze, seminari e workshop. Gli input che ciascuno di voi mi ha dato sono stati fondamentali per migliorare le mie competenze di ricerca e i miei output. In particolare, ringrazio il Prof. Tomaso Aste per avermi dato l'opportunità di trascorrere un periodo di visita presso l'University College di Londra. Mi sarebbe piaciuto molto stare un po' di più!

Infine, ringrazio la mia famiglia per avermi sempre supportato in qualunque cosa ero convinto di fare. Un ringraziamento speciale va a mia madre, che

mi ha dato tutte le opportunità possibili nella vita, tra cui quella di studiare, sopportando le difficoltà derivanti dal crescere tre bambini perlopiù sola. Scommetto che papà sarebbe fiero di te, e di tutti noi.

Abstract

The growing interest of research in econometric methods for systemic risk analysis fostered a rapid development of econometric spillover and network models to monitor the systemic risk in financial systems and improve investment management practices. The thesis contributes to the literature on econometric interconnectedness and investment management by developing new techniques for building models capable to reveal insights on the complex relationships in economic and financial systems. From a methodological viewpoint, the thesis mostly contributes to the econometric literature on interconnectedness measurement and to the financial one on portfolio management. From an empirical viewpoint, financial applications are offered for both traditional financial markets and the cryptocurrency one, whose relative importance in the global financial system is growing over time.

The contributions of this thesis to the literature are developed in seven self contained chapters. Chapter 2 proposes a Vector Error Correction model based spillover methodology to monitor return connectedness and lead-lag relationships of Bitcoin - and more generally financial - market exchanges. Chapter 3 extends the previous study by means of an in-depth analysis of intra-day data. Chapter 4 proposes a methodology to construct a basket based stablecoin whose value is stable over time and resilient to shocks in the currency market. Chapter 5 examines the lead-lag relationship between the European countries' sovereign CDS and bond market by means of the effective transfer entropy methodology. Chapter 6 introduces an artificial neural network framework for Bitcoin option pricing. Chapter 7 proposes an asset allocation methodology capable to take into account for the systemic risk impounded into network metrics when dealing with portfolio management, applied to the cryptocurrency space. Chapter 8 proposes a methodology based on chaos and dynamical systems theory for non-linear time series forecasting and investment strategy development.

Contents

1 General introduction **1**

2 Vector Error Correction Models and Bitcoin Exchange Connectedness **4**

2.1 Introduction 4
2.2 Proposal 7
2.3 Data 10
2.4 Empirical findings 17
2.4.1 Full sample results 18
2.4.2 Subsample results 21
2.4.3 Dynamic results 25
2.5 Conclusion 28

3 Intra-day Price Change Spillovers in Bitcoin Markets **31**

3.1 Introduction 31
3.2 Literature review 32
3.3 Methodology 35
3.4 Data 39
3.5 Empirical findings 48
3.6 Robustness 56
3.7 Conclusion 57

4 Basket-based Stablecoins to Mitigate Foreign Exchange Spillovers **60**

4.1 Introduction 60
4.2 Literature Review 63
4.2.1 Cryptocurrencies, stablecoins and e-money 63
4.2.2 Global currencies 65
4.2.3 Remittances and exchange rates 66
4.2.4 Our contribution 67
4.3 Methodology 67
4.3.1 Optimal control problem 68

4.3.2 VAR models and spillover analysis . . . 69
4.4 Data and empirical findings . . . 72
4.4.1 Data . . . 72
4.4.2 Optimal basket and stability analysis . . . 73
4.4.3 Spillover network analysis . . . 78
4.5 Conclusion . . . 85

5 Information Flow in the Credit Risk Market: Evidence from the European Sovereign CDS and Government Bonds 87
5.1 Introduction . . . 87
5.2 Literature review . . . 91
5.2.1 Price discovery process in CDS and Bond markets . . . 91
5.2.2 Transfer entropy in economic and financial contexts . . . 95
5.3 Methodology . . . 97
5.4 Data description and preliminary analysis . . . 101
5.5 Empirical results and discussion . . . 111
5.6 Conclusion . . . 116

6 Neural Network Models for Bitcoin Option Pricing 118
6.1 Introduction . . . 118
6.2 Methodology . . . 121
6.2.1 Tree models . . . 121
6.2.2 Finite difference method . . . 124
6.2.3 Monte Carlo simulation . . . 125
6.2.4 Neural networks to improve precision . . . 126
6.2.5 Performance assessment . . . 127
6.3 Data . . . 128
6.4 Empirical findings . . . 130
6.5 Robustness analysis . . . 132
6.5.1 Out-of-sample performance . . . 133
6.5.2 Cross-validation . . . 133
6.6 Conclusion . . . 135

7 Network Models to Enhance Automated Cryptocurrency Portfolio Management **138**
7.1 Introduction . . . 138
7.2 Methodology . . . 141
7.2.1 Random Matrix Theory . . . 141
7.2.2 The Minimal Spanning Tree . . . 142
7.2.3 Network centrality measures . . . 143
7.2.4 Portfolio construction . . . 144
7.3 Empirical findings . . . 146
7.3.1 Data description and network topology analysis . . . 146
7.3.2 Portfolio construction . . . 151
7.4 Conclusion . . . 160

8 Chaos Based Portfolio Selection: a Constant Chaoticity Approach **162**
8.1 Introduction . . . 162
8.2 The Constant Chaoticity Portfolio: methodology . . . 166
8.2.1 Phase space Reconstruction . . . 166
8.2.2 Lyapunov exponent . . . 168
8.2.3 The GenericPred Algorithm . . . 169
8.2.4 The Constant Chaoticity Portfolio formation . . . 170
8.3 Data and empirical results . . . 172
8.3.1 Data . . . 172
8.3.2 Forecasting stock prices . . . 175
8.3.3 Portfolio results . . . 177
8.4 Sensitivity analysis of the portfolio strategies . . . 182
8.4.1 Sensitivity to the underlying model parameters . . . 182
8.4.2 Sensitivity to the forecast horizon choice . . . 184
8.4.3 Overall sensitivity . . . 187
8.5 Conclusion . . . 189

9 Concluding remarks **192**

A Appendix **214**
A.1 Technical Details of Chapter 5 214
A.2 Technical Details of Chapter 7 214
A.3 Technical Details of Chapter 8 217
A.3.1 Hang Seng Index Results 217
A.3.2 Hang Seng Index Sensitivity 223

List of Tables

1 Bitcoin daily trading volume shares . . . 11
2 Summary Statistics of Returns . . . 14
3 Returns correlation matrix . . . 14
4 Returns partial correlation matrix . . . 15
5 Stationarity tests . . . 16
6 Cointegration (Max Eigenvalue test) . . . 17
7 Cointegration (Trace test) . . . 18
8 Directional Spillover Indexes (DSI) . . . 19
9 Net Pairwise Spillovers (NPS) . . . 21
10 Directional Spillover Indexes (DSI) - Subsample 1 . . . 22
11 Directional Spillover Indexes (DSI) - Subsample 2 . . . 23
12 Net Pairwise Spillovers (NPS) - Subsample 1 . . . 23
13 Net Pairwise Spillovers (NPS) - Subsample 2 . . . 24
14 Main events related to cryptocurrencies . . . 40
15 Bitcoin exchange features . . . 44
16 Summary Statistics of Returns . . . 47
17 Augmented Dickey-Fuller test . . . 48
18 Cointegration (Johansen Trace test) . . . 49
19 Optimal weights . . . 73
20 Volatility and Correlations between the RNVALs and basket based stable coin. . . . 76
21 Volatility of the RNVALs . . . 77
22 Currency spillovers . . . 79
23 Descriptive statistics for sovereign CDS premium and bond spread . . . 104
24 Augmented Dickey Fuller Test Statistics for sovereign CDS premium and bond spread . . . 106
25 Johansen Trace test and Johansen Maximum Eigenvalue test . 108
26 Effective transfer entropy estimates . . . 112
27 In-sample performance of neural network and classical models 131

28 Out-of-sample performance of neural network and classical models . . . 134
29 Summary statistics . . . 147
30 Cumulative Profits & Losses . . . 153
31 Value at Risk . . . 157
32 Sharpe Ratio . . . 157
33 Rachev Ratio . . . 158
34 Summary Statistics - STOXX Europe 50 . . . 174
35 Summary Statistics - Hang Seng . . . 175
36 Sharpe Ratio and Jensen's Alpha of different portfolio strategies 181
37 Sharpe Ratio and Jensen's Alphas at ten days forecasting window . . . 188
38 Robustness checks for the effective transfer entropy estimates significance . . . 215
39 Robustness checks for the effective transfer entropy estimates during the sovereign debt crisis . . . 216
40 Sharpe Ratio and Jensen's Alpha of different portfolio strategies 218
41 Sharpe Ratio and Jensen's Alpha of different portfolio strategies 227

List of Figures

1 Bitcoin exchange price evolution . . . 12
2 Exchange return deviation from daily average . . . 13
3 Total Spillover Index (TSI) . . . 26
4 Directional and Net Spillover Indexes . . . 27
5 Net Pairwise Spillovers (NPS) . . . 29
6 Bitstamp price (USD) . . . 45
7 Exchange continuous returns . . . 46
8 Total Spillover Index (TSI) . . . 50
9 Directional Spillover Indexes (DSI) . . . 52
10 Net Pairwise Spillover Indexes (NPSI) . . . 54

11 Robustness analysis 58
12 Time evolution of the Reduced Normalised Values and of the basket based stable coin (SAC) 74
13 Time evolution of the Reduced Normalised Values 75
14 Overall spillovers 80
15 From spillovers 80
16 To spillovers 81
17 Net spillovers 81
18 Spillover network (full sample) 83
19 Spillover networks (sub-samples) 84
20 CDS premium and bond spread for each sovereign entity . . . 103
21 Kernel density plot of CDS premium and bond spread first differences 109
22 Binomial tree 122
23 Trinomial tree 123
24 The multilayer perceptron neural network model 127
25 Real and predicted option prices 130
26 In-sample performance of neural network and "best" classical model 132
27 Out-of-sample performance of neural network and "best" classical model 135
28 Model performance distribution (call) 136
29 Model performance distribution (put) 136
30 Normalized cryptocurrency price series I 148
31 Normalized cryptocurrency price series II 149
32 MST September 2017- January 2018 150
33 MST June 2019- October 2019 150
34 MST thresholds and residuality coefficients 152
35 Performances of different portfolio strategies 154
36 Performances of selected portfolio strategies 155
37 Winning strategy portfolio weights 159

38 Highly risk adverse strategy portfolio weights 160
39 The price pattern prediction at five days forecasting horizon for the stock component 405780 (l'OREAL) of the STOXX Europe 50 176
40 Portfolio performances with five days forecasting horizon for the European case 179
41 Sensitivity analysis with five days forecasting horizon for the European case 183
42 The price pattern prediction at ten days forecasting horizon for the stock component 405780 (l'OREAL) of the STOXX Europe 50 185
43 Portfolio performance with ten days forecasting horizon 186
44 Sensitivity analysis with ten days forecasting horizon 190
45 Cumulative returns for selected portfolio strategies with shifting starting points. 219
46 Cumulative returns for selected portfolio strategies with different rolling estimation windows 220
47 The price pattern prediction at five days forecasting horizon for the stock component ID 0001.HK (CK Hutchison Holdings Limited) of the Hang Seng index 221
48 Portfolio performance with five days forecasting horizon, for the Asian case 222
49 Sensitivity analysis with five days forecasting horizon for the Asian case 224
50 Price pattern prediction at ten days forecasting horizon for the stock component ID 0001.HK (CK Hutchison Holdings Limited) of the Hang Seng index 225
51 Portfolio performance with ten days forecasting horizon, for the Asian case 226
52 Sensitivity analysis with ten days forecasting horizon for the Asian case 228

1 General introduction

Connectedness is a key topic arisen in the field of financial risk measurement and management. Connectedness features in important aspects of market risk, i.e. portfolio concentration and return connectedness, credit risk - default connectedness -, systemic risk, that is system-wide connectedness, counter-party risk - bilateral and multilateral contractual connectedness, as well as business cycle risk, with intra- and inter-country real activity - see Diebold and Yilmaz (2009). Connectedness and systemic risk are therefore fundamental related concepts in economic and financial fields.

World crises such as the global financial crisis of 2007 - 2009 and the Covid-19 outbreak have stressed the importance to examine the global systems as a network of interconnected entities, where linkages play a fundamental role in the contagion dynamics. Against this, researchers have proposed several spillover and network models which can help monitoring the systemic risk in financial systems.

Connectedness is key to understand price discovery processes and lead-lag relationships among financial actors. It becomes of fundamental importance also in the investment management field, where knowing the relationships existing among financial assets becomes crucial in the allocation problem, as well as prior knowledge of leadership dynamics may enhance arbitrage opportunities.

This thesis aims to contribute to the existing literature both from a methodological and empirical viewpoint, i.e. providing new methodological tools and extending the use of existing ones, and uncovering insights on modern economic and financial systems. The thesis mainly contributes to the literature on the interconnectedness and information flow, methods to construct a stable basket-based stablecoin, novel methodologies for option pricing and asset allocation; providing empirical applications not only to traditional financial markets, but also to the fintech space. Indeed, several applications are developed on the cryptocurrency market, a nascent market with unprecedented characteristics which deserve to be explored.

The contributions are presented in seven self contained chapters.

In chapter 2 we present a Vector Error Correction model (VECM) based spillover methodology that builds upon the law of one price to determine return connectedness of securities across financial market exchanges. We apply the methodology to a set of Bitcoin market exchanges and determine which are the leader and the follower in the shock transmission mechanisms.

In chapter 3 we make use of the interconnectedness tools to extend the analysis reported in chapter 2. In particular, we analyze the intra-day price change spillovers across Bitcoin exchanges and get indication of the lead-lag relationships among the platforms at intra-day level.

In chapter 4 we propose a methodology to construct basket based stablecoins whose value is relatively stable over time. We discuss the main policy implications of adopting a basket based stablecoin whose weights are derived by minimizing variability rather than a single digital currency, potentially more sensitive to market factors.

In chapter 5 we examine the lead-lag relationship between the sovereign CDS and bond market of a set of representative European Union countries by means of effective transfer entropy. The effective transfer entropy allows, differently from previous studies, to examine the post sovereign crisis period, overcoming the need for the two markets to be cointegrated in order to conduct the analysis.

In chapter 6 we analyze a nascent market, i.e. the Bitcoin option market, and provide a tool to Bitcoin option pricing. The methodology proposed builds upon classical option pricing methods such as Monte Carlo simulation, trinomial tree, finite difference method, and combines them through an artificial neural network to improve the pricing precision.

In chapter 7 we illustrate a method to construct a portfolio taking into account for the network centrality of the assets to be included. The algorithm is able to determine the weights as a function of the systemic risk aversion of the investor, which determines whether to take to a greater extent core or peripheral assets; we apply this algorithm to the cryptocurrency space.

In chapter 8 we propose a methodology based on chaos and dynamical systems theory for non-linear time series forecasting and investment strategy development. We construct Constant Chaoticity Portfolios (CCP) and evaluate their performances relative to several competing alternatives on the survival components of the STOXX Europe 50 index and the Hang Seng index.

Chapter 2 has been published as: Giudici, Paolo, & Pagnottoni, Paolo. 2020. Vector error correction models to measure connectedness of Bitcoin exchange markets. *Applied Stochastic Models in Business and Industry*, **36**(1), 95–109.

Chapter 3 has been published as: Giudici, Paolo, & Pagnottoni, Paolo. 2019a. High Frequency Price Change Spillovers in Bitcoin Markets. *Risks*, **7**(4), 111.

Chapter 4 is currently under review process as: Giudici, Paolo, Pagnottoni, Paolo, & Leach, Thomas. 2020a. Libra or Librae? Basket based stablecoins to mitigate foreign exchange volatility spillovers. *available at SSRN*.

Chapter 5 is currently under review process as: Caserini, Nicoló, & Pagnottoni, Paolo. 2020. Information Flow in the Credit Risk Market: Evidence from the European Sovereign CDS and Government Bonds. *Working Paper*.

Chapter 6 has been published as: Pagnottoni, Paolo. 2019. Neural Network Models for Bitcoin Option Pricing. *Frontiers in Artificial Intelligence*, **2**, 5.

Chapter 7 has been published as: Giudici, Paolo, Pagnottoni, Paolo, & Polinesi, Gloria. 2020. Network models to enhance automated cryptocurrency portfolio management. *Frontiers in Artificial Intelligence*, **3**, 22.

Chapter 8 is currently under review process as: Spelta, Alessandro, Pecora, Nicoló, & Pagnottoni, Paolo. 2020. Chaos Based Portfolio Selection: a Constant Chaoticity Approach. *Working Paper*.

2 Vector Error Correction Models and Bitcoin Exchange Connectedness

Based on the paper:
Giudici, Paolo, & Pagnottoni, Paolo. 2020. Vector error correction models to measure connectedness of Bitcoin exchange markets. *Applied Stochastic Models in Business and Industry*, **36**(1), 95–109.

2.1 Introduction

Connectedness is gaining much importance in financial econometrics and risk management. The study of return connectedness is key to assess market risk and, in particular, to understand which are the market exchanges whose shocks in price are transmitted to the others; or which are those that receive shocks from the others and adjust their prices consequently. In other words, the study of connectedness across market exchanges is fundamental for price discovery purposes, that is, to determine the leader-follower relationships between markets. This becomes particularly interesting when analyzing nascent markets with peculiar features, such as the cryptocurrency one.

Several researches dealt with econometric connectedness measures development and interdependency measurement. Diebold and Yilmaz (2012) propose measures for the total and directional volatility spillovers, based on forecast error variance decompositions from vector autoregressive models (VARs). Diebold and Yılmaz (2014) relate the above said forecast error variance decompositions to a network topology representation, and apply it to measure the connectedness of financial firms. Also Billio et al. (2012) develop different econometric measures of connectedness and systemic risk, focusing in the finance and insurance sectors specifically. In Ahelegbey et al. (2016), the authors propose a Bayesian graph-based approach to solve the identification issue in Vector Autoregressive (VAR) models, as well as it contributes to the econometric literature on financial interconnectedness.

The available literature on price discovery on cryptocurrency (Bitcoin)

exchanges is quite limited. The first researchers addressing this issue are Brandvold et al. (2015), who found that Mt.Gox - a leading exchange which went bankrupt right after their analysis - and BTC-e were the leaders of price discovery. A more recent study by Pagnottoni and Dimpfl (2019) makes use of the Hasbrouck (1995a) and Gonzalo and Granger (1995a) methodologies taking into account also the impact of exchange rates. They find Chinese exchanges to be the ones leading price discovery during their analyzed period. More recently, Giudici and Abu-Hashish (2019) employ a VAR model, that embeds into its correlation structure the connectedness among eight Bitcoin exchanges. All previous papers have the merit of being the first ones in the field but, on the other hand, they are limited as they lack either a less restrictive modelling strategy (as is the case of the first two papers) or do not take into account important econometric aspects such as cointegration and stationarity of the considered series (as is the case with the third paper).

Recently, some studies which examine interconnectedness and spillovers in the cryptocurrency market arose.Koutmos (2018) studied interconnectedness among 18 major cryptocurrencies and found - among others - a growing interdependence among them. Another noticeable example is given by Yi et al. (2018), who investigate static and dynamic volatility connectedness among eight typical cryptocurrencies and build a volatility connectedness network that links 52 cryptocurrencies by using the LASSO-VAR for estimating high-dimensional VARs. Finally, Corbet et al. (2018b) investigate the dynamic relationships, particularly volatility spillovers, between major cryptocurrencies (Bitcoin, Litecoin and Ripple) and other financial assets through the Diebold and Yilmaz (2012) generalized variance decomposition technique.

As previously stated, a limitation the existing literature on interconnectedness among cryptocurrencies is that all contributions employ a generalized VAR model, which does not take a potential cointegration structure of the series into account, a phenomena that is particularly evident when studying connectedness among market exchanges prices concerning the same asset,

such as the Bitcoin. We aim to improve the latter contributions, and suggest a model that, while fully grounded on an econometric approach, builds a comprehensive statistical model. To this aim, we rely on the order-invariant forecast error variance decomposition proposed by Diebold and Yilmaz (2012).

Indeed, Diebold and Yilmaz (2012) develop measures of directional spillovers in a generalized VAR framework, which are suitable for several applications. However, when the time series under consideration are integrated of order one ($I(1)$), the VAR model is not suitable to model them in levels. Moreover, if the same time series additionally show a significant co-movement around a common stochastic trend, i.e. they are cointegrated, Engle and Granger (1987) show it is reasonable to model them as a VEC model (VECM), whose error correction term accounts for the common stochastic trend driving prices.

In line with the previous comment, here we make use of an extension of the Diebold and Yilmaz (2012) methodology with a generalized VECM [1]. To the best of our knowledge, this is the first application of such a technique to measure connectedness of exchange platforms, particularly of Bitcoin. The methodology allows us to study market exchange connectedness at different levels: pairwise and system-wide, as well as both from a static and time-varying point of view, accounting for the common stochastic trend driving the fundamental Bitcoin price.

We therefore contribute, from a methodological viewpoint, to the econometric literature - particularly for what concerns price discovery and connectedness of market exchanges - by employing an extension of the Diebold and Yilmaz (2012) connectedness measure, which relies on VECM rather than VAR models. The model allows to shed further light on price discovery in Bitcoin markets, extending the conclusions in Pagnottoni and Dimpfl (2019) and Giudici and Abu-Hashish (2019) and, in particular, characterizing which are the leaders and followers in price formation among the considered

[1] This is in line with Pesaran and Shin (1998a), who extend the generalized impulse analysis to VECMs.

exchanges, along time.

The chapter proceeds as follows. Section 2 contains our methodological proposal. Section 3 presents the analyzed data and provide their preliminary analysis. In Section 4 we discuss the empirical results obtained. Section 5 concludes.

2.2 Proposal

We denote the Bitcoin price of an exchange i at time t as X_t^i, while its logarithm as x_t^i. We are in the situation in which the same asset is traded across different platforms. In such a framework the law of one price prescribes that prices related to the same good should not deviate in the long run. Strictly speaking, the no-arbitrage condition implies, when Bitcoin prices are expressed in the same currency, that there exist linear combination of their (log-) prices yielding a stationary process.

The considerations from above make us expect there is a cointegration structure among our variables. Thus, the theoretical econometric framework delineated by Engle and Granger (1987) suggests us to exploit the VECM. Namely, let us denote the continuous returns for a generic exchange i at time t as:

$$\Delta x_t^i = x_t^i - x_{t-1}^i \tag{2.1}$$

where $i = 1, 2, \cdots, n$ and n is the number of exchanges considered.

Note that continuous returns are the first difference of the exchange prices in log levels. Defining $\Delta x_t = (\Delta x_t^1, \cdots, \Delta x_t^i, \cdots, \Delta x_t^n)'$ with $i = 1, 2, ..., n$, the model assumes the following form:

$$\Delta x_t = \alpha\beta' x_{t-1} + \sum_{i=1}^{k-1} \zeta_i \Delta x_{t-i} + \varepsilon_t \tag{2.2}$$

with α being the $(n \times h)$ adjustment coefficient matrix, β the $(n \times h)$ cointegrating matrix, ζ_i the $(n \times n)$ parameter matrices with $i = 1, ..., n$, k

the autoregressive order and ε_t is a zero-mean white noise process having variance-covariance matrix Σ. We denote as h the cointegrating rank. In our case, the time series in levels should show one common stochastic trend, i.e. economic theory suggests that the cointegrating rank of the system is $h = n - 1$.

From the VECM$(k-1)$ in (2.2) one can derive the equivalent $n-$variable VAR(k) representation, that is:

$$x_t = \sum_{i=1}^{k} \Phi_i x_{t-i} + \varepsilon_t \tag{2.3}$$

where $\Phi_1, \Phi_2, ..., \Phi_k$ with $i = 1, ..., n$ are the $(n \times n)$ autoregressive parameter matrices. This is done recalling that $\alpha\beta' = \sum_{i=1}^{k} \Phi_i - I_n$ and $\Psi_i = -\sum_{j=i+1}^{k} \Phi_j$.

Equation 2.3 is the starting point of the approach developed by Diebold and Yilmaz (2012). Indeed, to retrieve the impact of shocks on the system variables to others, we rewrite the VAR model in (2.3) into its vector moving average (VMA) representation:

$$x_t = \varepsilon_t + \Psi_1 \varepsilon_{t-1} + \Psi_2 \varepsilon_{t-2} + \cdots \tag{2.4}$$

where we denote as $\Psi_1, \Psi_2, ...$ the $(n \times n)$ matrices containing the VMA coefficients. The vector moving average coefficients are such that the recursion $\Psi_i = \Phi_1 \Psi_{i-1} + \Phi_2 \Psi_{i-2} + ... + \Phi_i \Psi_1$ holds true, with $\Psi_i = 0 \ \forall i < 0$ and $\Psi_1 = I_n$.

The VMA representation of the system is fundamental to evaluate the effect of a shock in one system variable on the others thanks to the impulse response functions and variance decomposition tools. In particular, the variance decomposition allows to decompose the H-step-ahead error variance in predicting x_i due to shocks to x_j, $\forall j \neq i$ and $\forall i = 1, ..., n$.

In our contribution we rely, as in Diebold and Yilmaz (2012), on the Koop et al. (1996) and Pesaran and Shin (1998b) (KPPS) H-step-ahead forecast

errors. They have the advantage to be invariant to the variable ordering, unlike the popular although restrictive Cholesky factorization, which would require an ordering of the Bitcoin exchange prices *a priori* with regards to the influence of shocks across the system variables.

Taking two generic variables x_i and x_j, Diebold and Yilmaz (2012) define the own variance shares as the proportion of the H-step ahead error variance in forecasting x_i due to shocks in x_i itself, $\forall i = 1, ..., n$, whereas the cross variance shares (spillovers) are defined as the H-step ahead error variance in predicting x_i due to shocks in x_j, $\forall i = 1, \cdots, n$ with $j \neq i$.

That said, using $\theta_{ij}^g(H)$ to denote the KPSS H-step forecast error variance decompositions, with $h = 1, \cdots, H$, we have:

$$\theta_{ij}^g(H) = \frac{\sigma_{jj}^{-1} \sum_{h=0}^{H-1} (e_i' \Psi_h \Sigma e_j)^2}{\sum_{h=0}^{H-1} (e_i' \Psi_h \Sigma \Psi_h' e_j)} \tag{2.5}$$

where σ_{jj} is the standard deviation of the innovation for equation j and e_i represents the selection vector with one as element i and zeros elsewhere.

However, we have that $\sum_{h=0}^{H-1} \theta_{ij}^g(H) \neq 1$, i.e. the sum of the row elements of the generalized variance decomposition is not equal to 1. That is the reason why in the calculation of the spillover indexes, Diebold and Yilmaz (2012) proposed to normalize the entries of the variance decomposition matrix by the row sum, that is:

$$\tilde{\theta}_{ij}^g(H) = \frac{\theta_{ij}^g(H)}{\sum_{j=1}^n \theta_{ij}^g(H)}. \tag{2.6}$$

By construction we have that $\sum_{j=1}^n \tilde{\theta}_{ij}^g(H) = 1$ as well as $\sum_{j,i=1}^n \tilde{\theta}_{ij}^g(H) = n$.

From the use of the total contributions to the forecast error variance decomposition we estimate the Total Spillover Index (TSI) as:

$$TSI(H) = \frac{\sum_{\substack{j=1 \\ j \neq i}}^n \tilde{\theta}_{ij}^g(H)}{\sum_{j,i=1}^n \tilde{\theta}_{ij}^g(H)} \cdot 100 = \frac{\sum_{\substack{j=1 \\ j \neq i}}^n \tilde{\theta}_{ij}^g(H)}{n} \cdot 100 \tag{2.7}$$

Moreover, we also get the Directional Spillovers Indexes (DSI) to measure respectively through Equations (2.8) and (2.9) the spillover from exchange i to all exchanges J, as well as the spillover from all exchanges J to exchange i as:

$$DSI_{J\leftarrow i}(H) = \frac{\sum_{\substack{j=1 \\ j\neq i}}^{n} \tilde{\theta}^{g}_{ji}(H)}{\sum_{j,i=1}^{n} \tilde{\theta}^{g}_{ij}(H)} \cdot 100 \tag{2.8}$$

$$DSI_{i\leftarrow J}(H) = \frac{\sum_{\substack{j=1 \\ j\neq i}}^{n} \tilde{\theta}^{g}_{ij}(H)}{\sum_{j,i=1}^{n} \tilde{\theta}^{g}_{ij}(H)} \cdot 100. \tag{2.9}$$

We also derive the Net Spillover Index (NSI) from market i to all other markets J as:

$$NSI_{J\leftarrow i}(H) = DSI_{i\leftarrow J}(H) - DSI_{J\leftarrow i}(H). \tag{2.10}$$

Finally, we derive the Net Pairwise Spillovers (NPS) to measure the difference between the gross shocks transmitted from market i to j and gross shocks transmitted from j to i as:

$$PNS_{ij}(H) = \left(\frac{\tilde{\theta}^{g}_{ij}(H)}{\sum_{q=1}^{n} \tilde{\theta}^{g}_{iq}(H)} - \frac{\tilde{\theta}^{g}_{ji}(H)}{\sum_{q=1}^{n} \tilde{\theta}^{g}_{jq}(H)} \right) \cdot 100. \tag{2.11}$$

By means of the variance decompositions, these measures allow to analyze exchange spillovers both from a system-wide and a net pairwise viewpoint. Outcomes are presented in the results Section.

2.3 Data

We consider for our empirical analysis what is arguably the most relevant cryptocurrency nowadays existing: Bitcoin. We indeed examine Bitcoin exchange prices denominated in USD on a daily basis during a time-frame from

18 May 2016 and 30 April 2018, as in Giudici and Abu-Hashish (2019). Data were collected from https://www.investing.com/crypto/bitcoin and through the CryptoCompare API. With the aim to study system-wise connectedness as well as the pairwise one among Bitcoin trading venues, we consider eight Bitcoin exchanges, i.e. Bitfinex, Coinbase, Bitstamp, Hitbtc, Gemini, ItBit, Kraken, Bittrex. We remark that the investigated exchanges are geographically widespread, with their daily trading volumes summing up to more than 75% at the ending date of the sample, as illustrated in Table 1.

Table 1: Bitcoin daily trading volume shares

Exchange	Daily Volume Share
Bitfinex	27.37%
Coinbase	12.45%
Bitstamp	11.05%
Kraken	9.97%
Hitbtc	8.56%
Gemini	3.08%
Bittrex	1.84%
ItBit	1.61%
Total	75.93%

Note: The table from above shows daily trading volume shares for the considered exchanges at the end of the sample period considered (30 April 2018). We synthesized data retrieved from https://data.bitcoinity.org/markets.

The Bitcoin price dynamics of the considered exchanges are illustrated in Figure 1.

From Figure 1 note that prices related to the eight Bitcoin exchanges follow a common pattern, a result in line with economic expectations, as we are investigating the same asset traded on different venues. Furthermore,

Figure 1: Bitcoin exchange price evolution

Note: The figure from above illustrates the eight Bitcoin exchange price series related to the full sample period.

given the dynamics of Bitcoin prices over time, it is reasonable to expect that in our case we deal with non-stationary time series - arguably $I(1)$.

However, we also provide a plot of the difference between the return of each series and the average return across exchanges in Figure 2.

What emerges from a visual inspection of Figure 2 is that prices (and returns) may vary quite consistently across platforms. Specifically, there are some dates in which the misalignment across exchanges prices is particularly marked. The summary statistics in Table 2 give an overview of the features of the dataset and confirm the previous claims.

As a preliminary analysis, we compute the pairwise correlation existing among the exchange returns and test for their significance. Results are contained in Table 3.

Table 3 confirms that, as we are investigating the same asset traded on different platforms, returns exhibit high pairwise correlations. However, some exchanges present lower pairwise correlations with the others, meaning that

Figure 2: Exchange return deviation from daily average

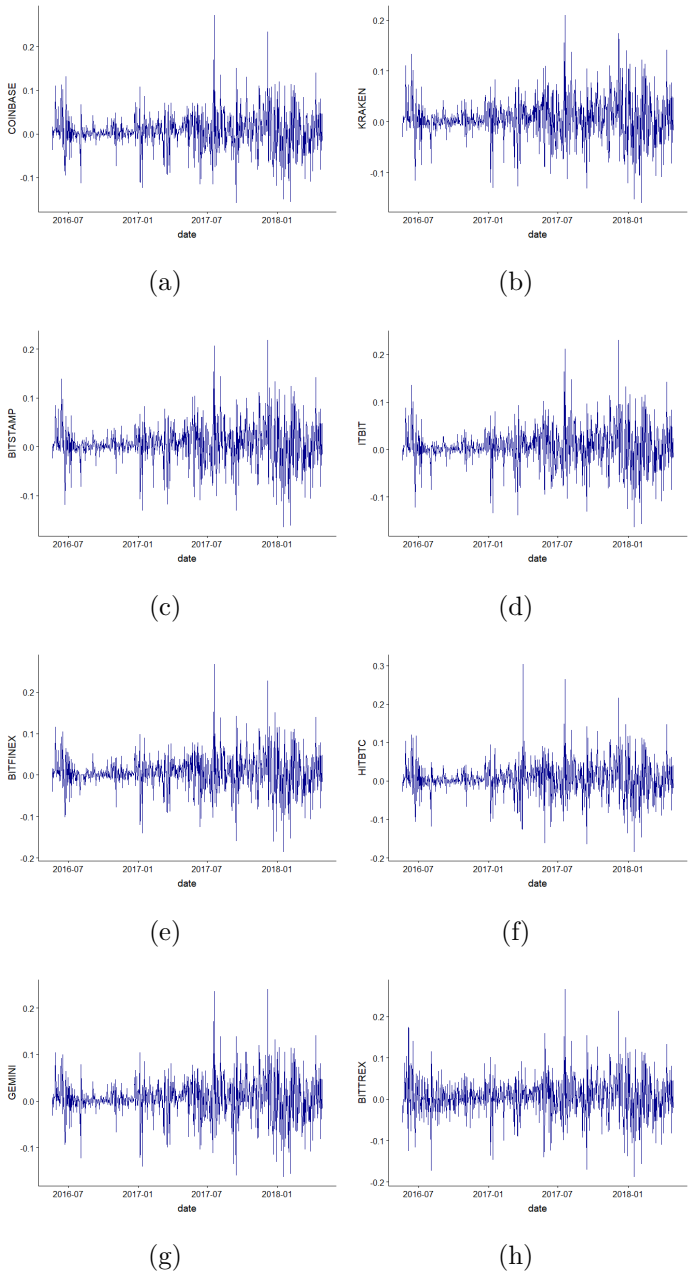

(a) (b)

(c) (d)

(e) (f)

(g) (h)

*Note:*The figure shows the return deviation of each exchange from the daily return average of the exchanges. The plot refers to the full sample period.

Table 2: Summary Statistics of Returns

	Coinbase	Kraken	Bitstamp	Itbit	Bitfinex	Hitbtc	Gemini	Bittrex
Mean	0.0042	0.0042	0.0042	0.0042	0.0042	0.0042	0.0042	0.0042
Median	0.0042	0.0049	0.0041	0.0040	0.0042	0.0036	0.0033	0.0028
Maximum	0.2406	0.1906	0.1976	0.2073	0.2372	0.2653	0.2154	0.2364
Minimum	-0.1707	-0.1728	-0.1782	-0.1770	-0.2038	-0.2023	-0.1764	-0.2069
Std. Dev.	0.0449	0.0442	0.0440	0.0440	0.0458	0.0473	0.0453	0.0500
Skewness	0.0471	-0.2035	-0.1763	-0.1685	-0.1743	0.0527	-0.1779	-0.1906
Kurtosis	6.2512	5.0798	5.5469	5.7150	6.2570	6.7983	5.9265	5.5252

Note: The table include relevant summary statistics for returns related to the analyzed exchanges considering the entire sample period.

Table 3: Returns correlation matrix

	Coinbase	Kraken	Bitstamp	Itbit	Bitfinex	Hitbtc	Gemini	Bittrex
Coinbase	1.0000	0.7737	0.9459	0.9155	0.9674	0.9263	0.9784	0.8858
Kraken	0.7737	1.0000	0.8224	0.7896	0.7670	0.7298	0.7703	0.7211
Bitstamp	0.9459	0.8224	1.0000	0.9609	0.9504	0.9030	0.9499	0.8807
Itbit	0.9155	0.7896	0.9609	1.0000	0.9161	0.8722	0.9200	0.8525
Bitfinex	0.9674	0.7670	0.9504	0.9161	1.0000	0.9277	0.9682	0.8948
Hitbtc	0.9263	0.7298	0.9030	0.8722	0.9277	1.0000	0.9215	0.8542
Gemini	0.9784	0.7703	0.9499	0.9200	0.9682	0.9215	1.0000	0.8922
Bittrex	0.8858	0.7211	0.8807	0.8525	0.8948	0.8542	0.8922	1.0000

Note: The table illustrates the return correlation matrix related to the full sample. Significance tests show that correlations are all significant at 1% significance level.

Table 4: Returns partial correlation matrix

	Coinbase	Kraken	Bitstamp	Itbit	Bitfinex	Hitbtc	Gemini	Bittrex
Coinbase	1.0000	0.0656	0.0373	0.0209	0.2652	0.1830	0.5843	0.0014
Kraken	0.0656	1.0000	0.3316	-0.0022	-0.0694	-0.0236	-0.0455	0.0251
Bitstamp	0.0373	0.3316	1.0000	0.6380	0.2366	0.0529	0.1232	0.0701
Itbit	0.0209	-0.0022	0.6380	1.0000	-0.0407	0.0016	0.0500	0.0240
Bitfinex	0.2652	-0.0694	0.2366	-0.0407	1.0000	0.2249	0.2571	0.1668
Hitbtc	0.1830	-0.0236	0.0529	0.0016	0.2249	1.0000	0.0378	0.0774
Gemini	0.5843	-0.0455	0.1232	0.0500	0.2571	0.0378	1.0000	0.1164
Bittrex	0.0014	0.0251	0.0701	0.0240	0.1668	0.0774	0.1164	1.0000

Note: The table illustrates the return partial correlation matrix related to the full sample. All partial correlations are significant at a 1% significance level.

their dynamics has a weaker link with that of the other analyzed exchanges. In particular, we find that Kraken has a weak link with the other exchanges during the analyzed timespan. As a matter of fact, considering that we are analysing prices related to the same asset, correlation involving Kraken are low on a relative basis, as it is also proved by the values of correlations between other platforms. Note that all correlations are tested and found to be significant at all conventional significance levels, with p-values well below 1%.

Moreover, to control for the effect of the other exchanges in the pairwise relationship, we compute the partial correlations of the Bitcoin exchange returns. Results are shown in Table 4.

First of all, partial correlations further support our previous considerations. Indeed, Kraken shows a negative partial correlation with as much as 4 of the other exchanges out of 7, further confirming its dissimilar behaviour. Secondly, partial correlations already suggest that the interconnectedness among returns of different exchanges is of heterogeneous nature. Indeed,

Table 5: Stationarity tests

ADF Tests								
	Coinbase	Kraken	Bitstamp	Itbit	Bitfinex	Hitbtc	Gemini	Bittrex
$log(p_t)$	0.8622	0.8653	0.8660	0.8646	0.8589	0.8598	0.8613	0.8547
$\Delta log(p_t)$	<0.0010	<0.0010	<0.0010	<0.0010	<0.0010	<0.0010	<0.0010	<0.0010
KPSS Tests								
	Coinbase	Kraken	Bitstamp	Itbit	Bitfinex	Hitbtc	Gemini	Bittrex
$log(p_t)$	<0.0100	<0.0100	<0.0100	<0.0100	<0.0100	<0.0100	<0.0100	<0.0100
$\Delta log(p_t)$	>0.1000	>0.1000	>0.1000	>0.1000	>0.1000	>0.1000	>0.1000	>0.1000

Note: The table above illustrates the resulting p-values for the Augmented Dickey-Fuller (ADF) and the Kwiatkowsky, Phillips, Schmidt and Shin (KPSS) tests for the entire sample period. The tests in levels are executed including a constant but no time trend, as well as the KPSS ones do not include trends. Both tests are conducted using an optimal lag length determined according to the Bayes-Schwarz information criterion, as well as on a 5% significance level. The minimum p-value reported is 0.001 for the ADF and 0.01 KPSS tests, while the maximum p-value reported for the KPSS test is 0.1.

while most of the exchanges show positive partial correlations, some of which of a relatively high magnitude (being the highest +0.5843 for Coinbase and Gemini), a few of them show negative partial correlation (being the lowest −0.0694 for Bitfinex and Kraken).

As a further preliminary analysis, we perform stationarity and cointegration tests, to ensure that the series we analyze meet the features we expect.

To test for (non-)stationarity, we conduct the Augmented Dickey-Fuller (ADF) - see Dickey and Fuller (1979)- and Kwiatkowsky, Phillips, Schmidt and Shin (KPSS) - see Kwiatkowski et al. (1992) - tests on prices, expressed in log-levels. The results from the tests are reported in Table 5.

From Table 17 note that both tests point towards non-stationarity of

Table 6: Cointegration (Max Eigenvalue test)

h	Statistics	Critical Value	p-value	eigVal
0	215.0009	48.8789	<0.0010	0.2613
1	171.1194	42.7706	<0.0010	0.2142
2	167.6692	36.6291	<0.0010	0.2103
3	136.1324	30.4392	<0.0010	0.1745
4	122.6643	24.1605	<0.0010	0.1587
5	57.1105	17.7966	<0.0010	0.0773
6	32.6407	11.2252	<0.0010	0.0449
7	4.9952	4.1302	0.0302	0.0070

Note: The table above illustrates the statistics, critical values, p-values end eigenvalues for the Johansen Maximum Eigenvalue test for cointegration for the full sample period. The test does not include any costant or time trend, neither in the model specification nor in the cointegrating relationship. The minimum p-value reported is 0.001.

the Bitcoin log-prices, while when first differencing the time series, the tests provide support towards stationarity, for all conventional significance level (10%, 5%, 1%). We may then argue that the series are found to be $I(1)$.

As far as cointegration is concerned, we conduct the Johansen Maximum Eigenvalue and the Trace tests - see Johansen (1991). As mentioned in the Methodology Section, we expect the cointegrating rank of the system to be $h = n - g = 8 - 1 = 7$, given that we have the same asset (Bitcoin) traded on different platforms and we therefore reasonably expect the series to be driven by $g = 1$ common stochastic trend. The results of the Maximum Eigenvalue and Trace test are presented in Table 6 and Table 7, respectively.

Tables 6 and 7 show that, although the evidence is not particularly strong, the p-values associated to the tests are low enough to reject their null hypotheses at a 1% significance level, when compared to the alternative $h = 7$,

Table 7: Cointegration (Trace test)

h	Statistics	Critical Value	p-value	eigVal
0	907.3326	154.8020	<0.0010	0.2613
1	692.3317	121.7464	<0.0010	0.2142
2	521.2123	92.7173	<0.0010	0.2103
3	353.5431	67.6430	<0.0010	0.1745
4	217.4107	46.5743	<0.0010	0.1587
5	94.7464	29.5103	<0.0010	0.0773
6	37.6359	16.3589	<0.0010	0.0449
7	4.9952	6.9399	0.0302	0.0070

Note: The table above illustrates the statistics, critical values, p-values end eigenvalues for the Johansen Trace test for cointegration related to the full sample period. The minimum p-value reported is 0.001.

meaning that tests point to a cointegrating rank of 7, which is consistent with the fundamental economic law of "one underlying asset - one price".

2.4 Empirical findings

As already anticipated, we study connectedness and lead-lag relationships across Bitcoin exchanges both from a static point of view and from a dynamic one. In Subsection 2.4.1 we will present the full sample results. In Subsection 2.4.2 we split the sample in order to investigate connectedness and leaderships before and after a period of arguable structural break. In Subsection 2.4.3 we perform a dynamic analysis to study the evolution of connectedness and price discovery on Bitcoin exchanges.

Table 8: Directional Spillover Indexes (DSI)

	Coinbase	Kraken	Bitstamp	Itbit	Bitfinex	Hitbtc	Gemini	Bittrex
FROM	10.7430	11.6435	11.0222	11.0059	10.6811	10.8392	10.7684	10.6276
TO	12.1979	5.9122	10.2804	10.3914	12.5541	11.1419	12.0487	12.8043
NET	**1.4549**	**-5.7313**	**-0.7418**	**-0.6145**	**1.8730**	**0.3027**	**1.2803**	**2.1767**

Note: The table shows the directional return spillover indexes "from" others (FROM), "to" others (TO), as well as the net ones (NET) for the full sample period. Values are expressed in percentage terms.

2.4.1 Full sample results

Here we present our results on the spillover analysis related to the full sample period, that is from 18 May 2016 to 30 April 2018. All results are based on a vector error correction model of order 2, where the order is determined using the Bayes-Schwarz Information Criterion (BIC), and a generalized variance decomposition of the $H = 10$ step ahead forecast errors [2].

The Total Spillover Index (TSI) based on the full sample is 87.33%. The high value of the index shows that Bitcoin exchange prices, as we expect, are highly interconnected among each other. In other words, a consistent portion of the forecast error variance of the system is due to contributions among exchanges, rather than on the own contribution of single exchanges.

We then provide outcomes for the "from", "to" and "net" Directional Spillover Indexes (DSI) in Table 8.

Looking at the results in Table 8, we may argue that the directional spillovers have quite similar magnitude across all exchanges, with Kraken being the most influenced when shocks in other venues occur, and with Bittrex being the least influenced exchange. When looking at the directional

[2]The choice of $H = 10$ step ahead forecast errors for the generalized variance decomposition is made for the sake of consistency and comparability with Diebold and Yilmaz (2012).

spillovers to others, however, the picture slightly changes. Exchanges still show quite similar magnitudes regarding spillovers to others, with Bittrex surprisingly resulting as the one giving more spillover to others, followed by Bitfinex and Coinbase. This is likely due to a high peak that is registered in one single data point which influences our results. This explanation is further clarified in the dynamic analysis, and it is related to the anomalous return misalignment discussed in the previous Section. On the other hand, the exchange having the smallest impact towards the others in the system is Kraken, which counts only about 5.91% of directional spillover to others, a relatively low value when compared to the rest of the exchanges analyzed.

The interpretation of the net directional spillovers in Table 8 is immediate, given that they represent the difference between the gross shocks transmitted to and received from other platforms. We can see that the exchange showing the strongest positive net contribution is Bittrex (+2.18%) - consistently with what commented before -, followed by Bitfinex (+1.87%) and Coinbase (+1.45%). Gemini (+1.28%) and Hitbtc (+0.30%) also show a positive net contribution to others, despite a lower magnitude. Itbit (−0.61%), Bitstamp (−0.74%) and Kraken (−5.73%), instead, show a negative net return spillover, meaning that the return shocks they receive is greater than those transmitted to all other exchanges. This is particularly true for Kraken, that is the exchange resulting more sensitive to return shocks occurring in other platforms.

To provide a wider picture of connectedness, we also investigate Net Pairwise (return) Spillovers (NPS) between exchanges, whose results are presented in a tabular fashion in Table 9. In this way we are able to assess the pairwise net contribution to return shocks of each exchange with the remaining ones, investigating pairwise connectedness.

From Table 9, the net pairwise spillover outcomes are in line with what observed before. On one hand, Bittrex transmits return spillovers to all other exchanges, with the biggest contribution being the one towards Kraken. On the other hand, Kraken is the most influenced exchange from a price

Table 9: Net Pairwise Spillovers (NPS)

	Coinbase	Kraken	Bitstamp	Itbit	Bitfinex	Hitbtc	Gemini	Bittrex
Coinbase	-	-7.21	-2.23	-2.12	0.48	-1.1	-0.19	0.73
Kraken	7.21	-	4.97	5.12	7.61	5.99	7.03	7.92
Bitstamp	2.23	-4.97	-	0.12	2.57	1.06	2.04	2.88
Itbit	2.12	-5.12	-0.12	-	2.44	0.94	1.91	2.75
Bitfinex	-0.48	-7.61	-2.57	-2.44	-	-1.58	-0.61	0.31
Hitbtc	1.1	-5.99	-1.06	-0.94	1.58	-	0.93	1.95
Gemini	0.19	-7.03	-2.04	-1.91	0.61	-0.93	-	0.86
Bittrex	-0.73	-7.92	-2.88	-2.75	-0.31	-1.95	-0.86	-

Note: The table contains the net pairwise return spillovers for the full sample period. Values are expressed in percentage terms.

settlement point of view, receiving return spillovers from all other platforms. We may additionally notice that the magnitude of spillovers towards Kraken are relatively high.

The analysis of net pairwise spillovers helps in discriminating between the leader and follower Bitcoin exchanges, in terms of transmitting information about price changes to others. Besides the already mentioned Bittrex, we can identify Bitfinex as a leading exchange, given its influence exerted to all other markets except for Bittrex. We also identify Coinbase as a leading exchange, whereas Bitstamp and Itbit are followers. The remaining exchanges show both positive and negative pairwise spillovers, meaning their behaviour is dissimilar with respect to the exchanges analyzed.

We remark that, overall, the size of return spillovers appears quite linked to the trading volume sizes of the exchanges themselves. In other words, exchanges whose trading volume is large generally show positive net contributions to return spillovers, whereas for smaller ones the same quantity is mostly negative.

2.4.2 Subsample results

It could be inferred from Figure 1 that the Bitcoin price series exhibits a possible structural break. Indeed the series has a positive trend, building up to mid December 2017, immediately followed by a downward trend. This phenomenon has attracted a lot of attention in the community and it should be strictly linked to the leadership evolution of the exchanges and their interconnectedness, which deserve to be investigated.

The previous setup motivates our approach, that consists of splitting the analysis into two subsamples, denoted as subsample 1 (18 May 2016 - 15 December 2017) and subsample 2 (16 December 2017 - 30 April 2018). We then conduct the same analysis as described before and analyze connectedness and price discovery in the two periods of interest. All results refer to vector error correction models of order determined through the BIC, and $H = 10$ step ahead forecast errors for the generalized variance decomposition.

From Tables 10 and 11 our expectations are confirmed. Overall, connectedness seems to be quite stable in magnitude. Despite that, the size of net return spillovers among Bitcoin exchanges shrinks in the period after the price surge which occurred until the end of 2017. Besides different magnitudes, the exchanges additionally show different directions of the net contribution in terms of return spillover. To illustrate, Bitstamp and Itbit turn from showing a negative net spillover in the first phase, whereas they exhibit a positive net contribution for the second phase - i.e. the Bitcoin price decline. Furthermore, the exchange that in the previous Section showed the strongest positive net return spillover to others reveal to be highly weaker in its magnitude of contribution when considering the Bitcoin price decline timespan.

To complete the overview, we investigate the net pairwise spillovers related to the two subsamples, which are presented in a tabular fashion in Tables 12 and 13.

Pairwise results further confirm our expectations regarding the potential change in exchange connectedness between the two analyzed sub-periods. In

Table 10: Directional Spillover Indexes (DSI) - Subsample 1

	Coinbase	Kraken	Bitstamp	Itbit	Bitfinex	Hitbtc	Gemini	Bittrex
FROM	12.44	5.85	9.74	9.63	12.38	11.62	12.29	13.35
TO	10.71	11.65	11.10	11.11	10.70	10.77	10.73	10.53
NET	**1.73**	**-5.80**	**-1.36**	**-1.48**	**1.68**	**0.85**	**1.56**	**2.82**

Note: The table shows the directional return spillover indexes "from" others (FROM), "to" others (TO), as well as the net ones (NET) for the subsample 1 (18 May 2016 -15 December 2017). Values are expressed in percentage terms.

Table 11: Directional Spillover Indexes (DSI) - Subsample 2

	Coinbase	Kraken	Bitstamp	Itbit	Bitfinex	Hitbtc	Gemini	Bittrex
FROM	11.23	7.59	11.53	11.62	11.28	11.56	11.36	11.28
TO	10.89	11.40	10.85	10.84	10.89	10.81	10.88	10.89
NET	**0.33**	**-3.82**	**0.68**	**0.78**	**0.40**	**0.75**	**0.49**	**0.39**

Note: The table shows the directional return spillover indexes "from" others (FROM), "to" others (TO), as well as the net ones (NET) for the subsample 2 (16 December 2017 - 30 April 2018). Values are expressed in percentage terms.

Table 12: Net Pairwise Spillovers (NPS) - Subsample 1

	Coinbase	Kraken	Bitstamp	Itbit	Bitfinex	Hitbtc	Gemini	Bittrex
Coinbase	-	-7.60	-3.14	-3.29	0.04	-0.80	-0.20	1.12
Kraken	7.60	-	4.46	4.36	7.44	6.54	7.42	8.56
Bitstamp	3.14	-4.46	-	-0.13	3.00	2.23	2.94	4.15
Itbit	3.29	-4.36	0.13	-	3.12	2.36	3.06	4.26
Bitfinex	-0.04	-7.44	-3.00	-3.12	-	-0.84	-0.15	1.18
Hitbtc	0.80	-6.54	-2.23	-2.36	0.84	-	0.64	2.06
Gemini	0.20	-7.42	-2.94	-3.06	0.15	-0.64	-	1.22
Bittrex	-1.12	-8.56	-4.15	-4.26	-1.18	-2.06	-1.22	-

Note: The table contains the net pairwise return spillovers for the subsample 1 (18 May 2016 -15 December 2017). Values are expressed in percentage terms.

Table 13: Net Pairwise Spillovers (NPS) - Subsample 2

	Coinbase	Kraken	Bitstamp	Itbit	Bitfinex	Hitbtc	Gemini	Bittrex
Coinbase	-	-4.04	0.33	0.42	0.04	0.40	0.15	0.03
Kraken	4.04	–	4.44	4.57	4.31	4.60	4.23	4.34
Bitstamp	-0.33	-4.44	-	0.10	-0.30	0.05	-0.18	-0.31
Itbit	-0.42	-4.57	-0.10	-	-0.42	-0.05	-0.27	-0.43
Bitfinex	-0.04	-4.31	0.30	0.42	-	0.36	0.10	-0.01
Hitbtc	-0.40	-4.60	-0.05	0.05	-0.36	-	-0.25	-0.36
Gemini	-0.15	-4.23	0.18	0.27	-0.10	0.25	-	-0.12
Bittrex	-0.03	-4.34	0.31	0.43	0.01	0.36	0.12	-

Note: The table contains the net pairwise return spillovers for the subsample 2 (16 December 2017 - 30 April 2018). Values are expressed in percentage terms.

line with the considerations from above, pairwise net return spillovers lose their original size when considering the second subsample.

In particular, we can notice that Kraken behaves as a follower throughout the whole analyzed period. Indeed, even though magnitudes of spillovers are indisputably bigger when considering the first subsample, it keeps receiving price change spillovers from other exchanges during the second time frame in a considerable manner. In contrast, as already suggested by the net spillovers, some of the exchanges change their behaviour from one phase to the other. This is particularly true for Bittrex, showing most of its pairwise net contributions changing not only magnitude but also sign from one period to the other. We may therefore conclude that the leadership composition of the exchanges also varies accordingly over time. This is in line with what found in the price discovery studies by Brandvold et al. (2015) and Pagnottoni and Dimpfl (2019), which rely on the Hasbrouck (1995a) information shares and on the Gonzalo and Granger (1995a) common factor weights approaches. Both researches find that information shares are dynamic and significantly evolve over time.

The latter findings highlight the importance of tuning the right estimation time-spans in order to get meaningful insights. This further motivates our dynamic analysis, which is performed in Subsection 2.4.3.

2.4.3 Dynamic results

As noticed by Diebold and Yilmaz (2012), the full sample outcomes provide information about the "average" or "unconditional" features of connectedness. However, in most applications, it is of interest to examine the exchange connectedness dynamics over time. This is the reason why in this subsection we perform a dynamic analysis by means of rolling window estimations. In detail, we fix a rolling estimation window of 125 day and a 10-step ahead

forecast horizon for the variance decomposition [3]. As already anticipated, the dynamic analysis should be also able to better explain the outcomes of the "unconditional" connectedness measures derived before.

At first, we examine the Total Spillover Index (TSI), whose plot is illustrated in Figure 3.

Figure 3: Total Spillover Index (TSI)

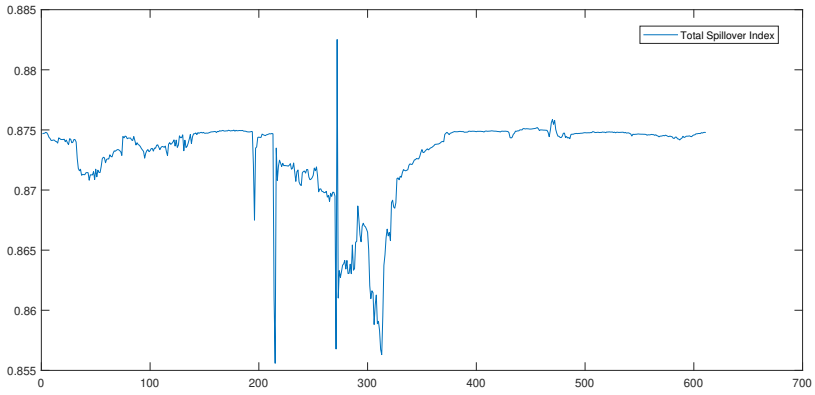

Note: The plot contains the dynamic total spillover index for the period 22 September 2016 - 30 April 2018. The rolling window set for the estimations is $w = 125$ days

We may notice two different cycles in the Bitcoin return spillover evolution across the exchanges. After a first period of relative stability for the index, from observation 171 (4 November 2016) to roughly 371 (25 May 2017) we can notice some turbulences. Indeed, the index becomes more volatile during this second phase, with exchanges weakening their overall connectedness, behaving more dissimilarly than before. This is particularly true for some of the exchanges. However, from the end of May 2017 onwards the TSI goes back towards its initial values and remains quite stable. The most relevant

[3]Repeating the analysis with different choices of the rolling estimation window and forecast horizon steps - i.e. increasing and decreasing them up to 50% of the fixed choices - shows that results do not change appreciably.

Figure 4: Directional and Net Spillover Indexes

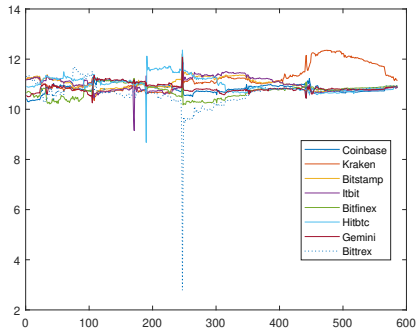

(a) From

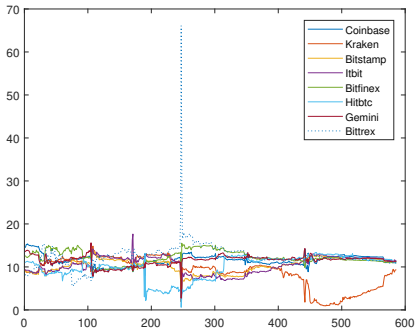

(b) To

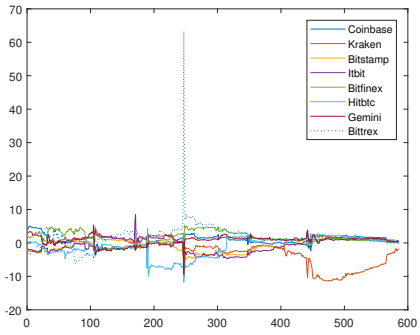

(c) Net

Note: The figure from above illustrates the dynamic "from", "to" and "net" return spillover indexes for the period 22 September 2016 - 30 April 2018. The rolling window set for the estimations is $w = 125$ days. Values are expressed in percentage terms.

peaks correspond to the dates we have discussed in the data Section, i.e. the points in time in which we have a strong misalignment in Bitcoin prices of the analyzed exchanges. Those misalignment are likely due to exits and entrances of big players in the market.

We then analyze the DSI "from" and "to" others, as well as the NSI, which are illustrated in Figure 4.

From Figure 4 note that peaks in the TSI are mainly caused by single exchange returns, whose misalignment create turbulences in the spillover indexes. The clearest example is the spillover from Bittrex to others, whose

influence on 24 May 2017 becomes suddenly high and almost immediately levels out. This occurrence has likely influenced our full sample results about Bittrex being a return spillover transmitter.

However, what we are interested in is the dynamic leader-follower relationship among exchanges, which can be visually inspected by jointly examining the three Figures. In this regard, results are again in line with those obtained in the full sample analysis: besides Bittrex, Bitfinex appears to be the exchange receiving the least and contributing the most to others in terms of return spillovers over time, immediately followed by Coinbase. In both cases, the magnitude of their influence varies over time. Notice also that Kraken is the exchange being the most influenced from others. From the beginning of May 2017, its return spillover contribution to others starts declining, whereas the one transmitted by others begins to rise. It is interesting to notice that Kraken's follower behaviour begins with the surge in Bitcoin prices, a day in which exchanges connectedness are arguably expected to experience some changes. This marks the beginning of a "follower phase" for Kraken, which lasts until the end of the sample, where we see its net contribution converging to its previous values.

As a final step, we investigate the evolution of the net pairwise spillovers between exchanges over time. We focus on the net pairwise spillovers between the four platforms showing the weakest net spillovers in the full sample analysis, namely Kraken, Bitstamp, Itbit and Hitbtc, whose dynamics are shown in Figure 5. Although Kraken mostly dominates small exchanges during the first period of analysis (roughly until May 2015), it starts losing its positive influence by then, and receives return spillovers. It is clear that spillovers show some kind of ciclicity. However, taking the Bitstamp-Hitbtc plot as an example, we may argue that major exchanges (in terms of trading volumes) generally show larger magnitudes of transmitted shocks, with respect to received shocks, as expected.

In general, the dynamic analysis gives insights about the dynamic nature of return spillovers. Indeed, the composition of leader-follower exchanges is

Figure 5: Net Pairwise Spillovers (NPS)

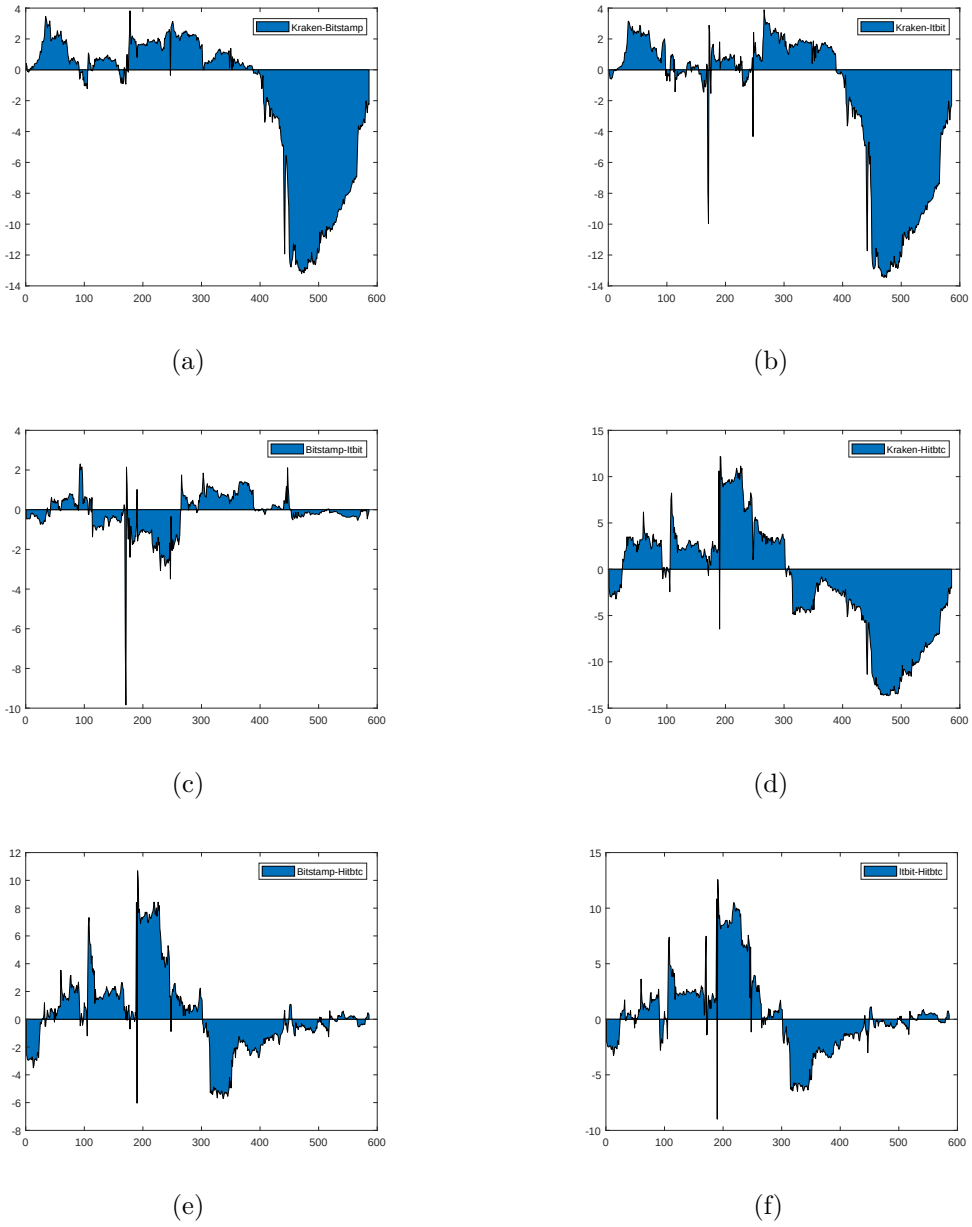

(a) (b)

(c) (d)

(e) (f)

Note: The figures from above illustrate the net pairwise return spillovers between the four selected exchanges - that is Kraken, Bitstamp, Itbit and Hitbtc - for the period 22 September 2016 - 30 April 2018. The rolling window set for the estimations is $w = 125$ days. Values are expressed in percentage terms.

time-varying and may consistently change over time. Again, this is in line with the stream of literature about price discovery on Bitcoin exchanges - see Brandvold et al. (2015) and Pagnottoni and Dimpfl (2019).

2.5 Conclusion

In this chapter we employ an extension of the Diebold and Yilmaz (2012) forecast error variance decomposition, which relies on a cointegrated vector error correction framework, in order to estimate return spillovers across Bitcoin exchanges. We believe that our proposal can be extended, without loss of generality, to other cryptocurrencies, as well as to traditional markets.

From a methodological point of view, we adapt the generalized variance decomposition technique introduced by Diebold and Yilmaz (2012). While Diebold and Yilmaz (2012) derive measures for the directional spillovers across markets within a generalized VAR framework, we apply their methodology to the case in which the same asset (Bitcoin) is traded on multiple exchanges. Since we deal with $I(1)$ price series related to a unique asset - i.e. arguably cointegrated -, we rely on a generalized VECM framework to derive directional spillovers.

From an empirical viewpoint, our results show that Bitfinex and Coinbase are the leader exchanges in the price formation process, transmitting a significant portion of return spillover to other exchanges. Moreover, we find Kraken among the follower exchanges. This is in line with the fact that the exchanges in which most of the trading volumes lie are generally also the ones giving substantial contribution to other markets from a price discovery point of view.

In addition, our results show that return spillovers across Bitcoin exchanges are dynamic and sensibly evolve over time. In other words, the leader-follower compositions are not constant in time and may consistently evolve. This is in line with what observed by Brandvold et al. (2015) and Pagnottoni and Dimpfl (2019), who concluded that information shares are dynamic and may consistently evolve over time.

3 Intra-day Price Change Spillovers in Bitcoin Markets

Based on the paper:
Giudici, Paolo, & Pagnottoni, Paolo. 2019a. High Frequency Price Change Spillovers in Bitcoin Markets. *Risks*, **7**(4), 111.

3.1 Introduction

The study of connectedness is a key topic arising in the field of financial econometrics. As Diebold and Yilmaz (2009) state, connectedness features in important aspects of market risk, i.e. portfolio concentration and return connectedness, credit risk - default connectedness -, systemic risk, that is system-wide connectedness, counter-party risk - bilateral and multilateral contractual connectedness, as well as business cycle risk, with intra- and inter-country real activity connectedness.

In particular, throughout the study of return and volatility connectedness of financial assets is able to retrieve system-wide and pairwise connectedness measures that are useful to assess the systemic risk of financial groups and/or single entities. Furthermore, the study of directional connectedness is able to shed light on which are leading assets in terms of shock transmission and, rather, which are those that follow others in the process. This contributes to the stream of econometric literature studying price discovery.

However, in the financial literature there is lack of studies exploring interconnectedness related to the same asset traded on different exchange platforms. Indeed, it is widely known that prices of the same good traded on different venues may consistently vary across exchange markets and that this is possibly due to lead-lag relationships existing across exchanges. This contribution aims to fill this gap, as the study of system-wide connectedness can give insights on how much different trading platforms are synchronized in terms of returns (and, therefore, market prices), as well as the study of directional connectedness is able to shed light on the lead-lag relationship

among exchange markets. Indeed, unlike previous studies, we explore dynamic return connectedness among different exchange markets trading the same good: Bitcoin.

The methodology we employ can be applied, without loss of generality, to the rest of the cryptocurrency market as well as to other financial products. To illustrate, studying interconnectedness and price discovery on the same asset or commodity returns when traded on different exchange platforms might give some insights on where the price formation process takes primarily place. Moreover, this technique may be applied to highly integrated markets to effectively measure spillovers taking into account for the common stochastic trends driving the co-movement of the underlying variables, as it can be the case for spot and future markets.

3.2 Literature review

Much research in the field of financial econometrics has dealt with how econometric connectedness measures development. To illustrate, Billio et al. (2012) build systemic risk and econometric measures of interdependency which are suitable to be used in the finance and insurance sectors. Diebold and Yilmaz (2012) develop overall and directional measures for return and volatility spillovers which are built upon forecast error variance decompositions deriving from vector autoregressive models (VARs). In a related work, Diebold and Yılmaz (2014) extend their previously developed measures to a network topology representation of the forecast error variance decomposition, linking the econometric connectedness literature to that of financial networks. More recently and following the same approach, Baruník and Křehlík (2018) propose a framework based on the spectral representation of variance decompositions to measure connectedness among financial variables which arise due to heterogeneous frequency responses.

Nowadays the existing literature focuses largely on measures applied to interconnectedness between financial entities belonging to different groups in terms of geography, financial sectors, etc. To illustrate, Diebold and Yilmaz

(2013) study the dynamics of global business cycle connectedness for a set of real output of six developed countries between 1962 and 2011. Demirer et al. (2018) study the global bank equity connectedness linking the publicly-traded subset of the world's top 150 banks during the period 2003-2014. Baruník et al. (2016) explore asymmetries in volatility spillovers that emerge due to bad and good volatility with the use of data regarding most liquid U.S. stocks across seven different sectors.

Since the birth of cryptocurrencies, a stream of literature started focusing on interconnectedness, spillover analyses and shock transmissions involving the cryptocurrency market. Fry and Cheah (2016) borrow some modelling strategies from econophysics to study shocks and crashes in cryptocurrency markets and show that in the period of negative bubble there is a spillover from Ripple to Bitcoin. Yi et al. (2018) use a LASSO-VAR to estimate a volatility connectedness network linking as much as 52 different cryptocurrencies. In Koutmos (2018) the authors explore connectedness across 18 cryptocurrencies finding growing interdependencies among them. Corbet et al. (2018b) analyze dynamic volatility spillovers between traditional financial assets such as gold, bond, equities and the global volatility index (VIX) and three major cryptocurrencies, i.e. Bitcoin, Litecoin, and Ripple, through the Diebold and Yilmaz (2012) methodology, finding evidence of a relative isolation of the latter category with respect to the traditional ones. Using the same technique, Ji et al. (2019) study connectedness across six large cryptocurrencies and show that Litecoin and Bitcoin belong to the centre of the connected network of returns, besides proving that connectedness is stronger via negative returns rather than via positive ones. Zięba et al. (2019) use instead minimum spanning trees (MSTs) to form cryptocurrency clusters and VAR models to examine the transmissions of demand shocks within clusters. They conclude that Bitcoin's role, which was dominant until 2017, has then diminished as well as that they show the presence of causal relationships between cryptocurrencies, excluding Bitcoin. Antonakakis et al. (2019) employ a TVP-FAVAR connectedness approach in order to investigate the transmis-

sion mechanism among 9 major cryptocurrencies. They conclude that total cryptocurrency connectedness shows large dynamic variability and that, despite Bitcoin still preserves its influencing role in the market, Ethereum has recently become the number one transmitting cryptocurrency.

Some research on price discovery of cryptocurrencies has recently emerged. Specifically, on Bitcoin exchanges. Brauneis and Mestel (2018) investigate efficiency and predictability of a set of cryptocurrency returns time series, concluding that they become less efficient and predictable when liquidity raises. Brandvold et al. (2015) discovered through information share measures that Mt.Gox and BTC-e were leaders of the price formation process during their analyzed period. On the other hand Pagnottoni and Dimpfl (2019), who analyzed a subsequent timespan, concluded the decreased role of BTC-e and the increased one of Chinese exchange platforms in the price discovery mechanism by means of the Hasbrouck (1995a) and Gonzalo and Granger (1995a) techniques. Recently, Giudici and Abu-Hashish (2019) and Giudici and Pagnottoni (2020) have also focused on price discovery, analyzing bitcoin daily prices, respectively with a VAR and a VECM model.

Against this background, our contribution is the extension of the Diebold and Yilmaz (2012) methodology for high frequency data, which takes into account the non-stationary and cointegrated behaviour of the analyzed time series. In other words, we rely on vector error correction models (VECMs) rather than VARs to derive the forecast error variance decompositions and build dynamic connectedness measures, contributing both from a methodological and economic viewpoint. This is done by analyzing 5 major Bitcoin intraday exchange prices, i.e. Bitstamp, Gemini, Coinbase, Kraken and Bittrex. We conclude that total and directional connectedness consistently evolve over time, and that, overall, Bitfinex and Gemini are leading exchanges during the analyzed period, while Bittrex is a follower.

We also remark that our contribution bears some similarities with Koutmos (2018), in particular as far as the methodology to measure spillovers is concerned. Indeed, Koutmos (2018) decompose volatility and return shocks

among 18 major cryptocurrencies by means of the technique outlined by Diebold and Yilmaz (2009), which is based on a VAR framework. However, in the present contribution we look at return spillovers in Bitcoin exchanges, meaning the same cryptocurrency trading on different venues, rather than at spillovers among cryptocurrencies themselves. Thus, we also rely on an extension of the methodology used in Diebold and Yilmaz (2009), with the aim of taking into account for the peculiar non-stationary and cointegrated behaviour of the time series analyzed through VECMs rather than VARs. The focus on Bitcoin allows us to determine interconnectedness and lead-lag relationships of market exchanges trading Bitcoin.

The chapter proceeds as follows. Section 2 illustrates the employed methodology. Section 3 presents the data analyzed and provide their preliminary analysis. In Section 4 we discuss the empirical results obtained. Section 5 provides a robustness analysis. Section 6 concludes.

3.3 Methodology

The methodology builds on the law of one price, stating that the prices of the same good traded on different venues should not deviate in the long run. In other words, the absence of arbitrage implies that (log-)price series related to the same asset and denominated in the same currency should yield to a stationary process when linearly combined. Furthermore, when time series exhibit non-stationary, and, particularly, $I(1)$ behaviour as Bitcoin prices do, we must take cointegration of the series into account. We thus make use of the econometric vector error correction framework designed by Engle and Granger (1987) to deal with the cointegration problem.

We denote continuous returns for a generic exchange i at time t as:

$$\Delta x_t^i = x_t^i - x_{t-1}^i \tag{3.1}$$

where $i = 1, 2, \cdots, n$ and n is the number of exchanges considered, x_t^i is the Bitcoin (log-)price of an exchange i at time t.

We define $\Delta x_t = (\Delta x_t^1, \cdots, \Delta x_t^i, \cdots, \Delta x_t^n)'$ with $i = 1, 2, ..., n$. In line with the notations above, the vector error correction model assumes the following form:

$$\Delta x_t = \alpha\beta' x_{t-1} + \sum_{i=1}^{k-1} \zeta_i \Delta x_{t-i} + \varepsilon_t \tag{3.2}$$

with α being the $(n \times h)$ adjustment coefficient matrix, β the $(n \times h)$ cointegrating matrix, ζ_i the $(n \times n)$ parameter matrices with $i = 1, ..., n$, k the autoregressive order and ε_t is the zero-mean white noise process having variance-covariance matrix Σ and h the cointegrating rank. Financial theory suggests that, in this case, the time series in levels shall follow one common stochastic trend, which means having a cointegrating rank of the system which is $h = n - 1$.

Recall that by means of the recursive computations $\alpha\beta' = \sum_{i=1}^{k} \Phi_i - I_n$ and $\Psi_i = -\sum_{j=i+1}^{k} \Phi_j$ one is able to retrieve the equivalent non-stationary $n-$variable VAR(k) representation from the VECM($k-1$) in (3.2), which is:

$$x_t = \sum_{i=1}^{k} \Phi_i x_{t-i} + \varepsilon_t \tag{3.3}$$

where $\Phi_1, \Phi_2, ..., \Phi_k$ with $i = 1, ..., n$ are the $(n \times n)$ autoregressive parameter matrices.

Note that Diebold and Yilmaz (2012) start from a stationary VAR as the one in (3.3) to build their methodology.

We may also rewrite the systems from above in the vector moving average (VMA) representation, namely:

$$x_t = \varepsilon_t + \Psi_1 \varepsilon_{t-1} + \Psi_2 \varepsilon_{t-2} + \cdots \tag{3.4}$$

where $\Psi_1, \Psi_2, ...$ the $(n \times n)$ denote the matrices of VMA coefficients. The VMA coefficients are recursively computed as $\Psi_i = \Phi_1 \Psi_{i-1} + \Phi_2 \Psi_{i-2} + ... + \Phi_i \Psi_1$, having $\Psi_i = 0 \ \forall i < 0$ and $\Psi_1 = I_n$.

As it is widely accepted in the financial econometric literature, the variance decomposition tools are used to evaluate the impact of shocks in one system variable on the others. Strictly speaking, variance decompositions decompose the H-step-ahead error variance in forecasting x_i which is due to shocks to x_j, $\forall j \neq i$ and $\forall i = 1, ..., n$.

In this chapter we make use of the KPPS H-step-ahead forecast error variance decompositions, as Diebold and Yilmaz (2012) do. This is because we avoid imposing an a priori ordering of Bitcoin exchange prices regarding the influence of shocks across the system variables, as popular techniques like the Cholesky identification scheme do - see for reference on the Cholesky factorization, for instance, Keating (1996). Indeed, the KPPS H-step-ahead forecast errors are convenient as they are invariant with respect to the variable ordering.

As already stated, Diebold and Yilmaz (2012) found their methodology on the H-step ahead forecast error variance decomposition. Considering two generic variables x_i and x_j, they define the own variance shares as the proportion of the H-step ahead error variance in predicting x_i due to shocks in x_i itself, $\forall i = 1, ..., n$. On the other hand, the cross variance shares (spillovers) are defined as the H-step ahead error variance in forecasting x_i due to shocks in x_j, $\forall i = 1, \cdots, n$ with $j \neq i$.

In other words, denoting as $\theta_{ij}^g(H)$ the KPPS H-step forecast error variance decompositions, with $h = 1, \cdots, H$, we have:

$$\theta_{ij}^g(H) = \frac{\sigma_{jj}^{-1} \sum_{h=0}^{H-1} (e_i' \Psi_h \Sigma e_j)^2}{\sum_{h=0}^{H-1} (e_i' \Psi_h \Sigma \Psi_h' e_i)} \tag{3.5}$$

with σ_{jj} being the standard deviation of the innovation for equation j and e_i the selection vector, i.e. a vector having one as i^{th} element and zeros elsewhere. Intuitively, the own variance shares and cross variance shares (spillovers) measure the contribution of each variable to the forecast error variance of itself and the other variables in the system, respectively, thus giving a measure of the importance of each variable in predicting the others.

Note that the row sum of the generalized variance decomposition is not equal to 1, meaning $\sum_{h=0}^{H-1} \theta_{ij}^{g}(H) \neq 1$. Diebold and Yilmaz (2012) circumvent this problem by normalizing each entry of the variance decomposition matrix by its own row sum, i.e.

$$\tilde{\theta}_{ij}^{g}(H) = \frac{\theta_{ij}^{g}(H)}{\sum_{j=1}^{n} \theta_{ij}^{g}(H)}. \tag{3.6}$$

This tackles the above mentioned issue and yields to $\sum_{j=1}^{n} \tilde{\theta}_{ij}^{g}(H) = 1$, and $\sum_{j,i=1}^{n} \tilde{\theta}_{ij}^{g}(H) = n$.

As a measure of the fraction of forecast error variance coming from spillovers, Diebold and Yilmaz (2012) define the total spillover index (TSI):

$$TSI(H) = \frac{\sum_{\substack{j=1 \\ j \neq i}}^{n} \tilde{\theta}_{ij}^{g}(H)}{\sum_{j,i=1}^{n} \tilde{\theta}_{ij}^{g}(H)} \cdot 100 = \frac{\sum_{\substack{j=1 \\ j \neq i}}^{n} \tilde{\theta}_{ij}^{g}(H)}{n} \cdot 100. \tag{3.7}$$

Moreover, we also make use of directional spillovers indexes (DSI) to measure, respectively through Equations (3.8) and (3.9), the spillover from exchange i to all other exchanges J (cfr. Equation (3.8)) and the spillover from all exchanges J to exchange i (cfr. Equation (3.9)) as:

$$DSI_{J \leftarrow i}(H) = \frac{\sum_{\substack{j=1 \\ j \neq i}}^{n} \tilde{\theta}_{ji}^{g}(H)}{\sum_{j,i=1}^{n} \tilde{\theta}_{ij}^{g}(H)} \cdot 100 \tag{3.8}$$

$$DSI_{i \leftarrow J}(H) = \frac{\sum_{\substack{j=1 \\ j \neq i}}^{n} \tilde{\theta}_{ij}^{g}(H)}{\sum_{j,i=1}^{n} \tilde{\theta}_{ij}^{g}(H)} \cdot 100. \tag{3.9}$$

Directional spillovers may be conceived as providing a decomposition of total spillovers into those coming from - or to - a particular variable. In other words, they measure the fraction of forecast error variance which comes from (or to) one of the variables included in the system - and, hence, the importance of the variable itself in forecasting the others. From the definitions of

directional spillover indexes, it is natural to build a net contribution measure, impounded in the net spillover index (NSI) from market i to all other markets J, namely:

$$NSI_i(H) = DSI_{J \leftarrow i}(H) - DSI_{i \leftarrow J}(H). \tag{3.10}$$

Another very important metric to measure the difference between the gross shocks transmitted from market i to j and gross shocks transmitted from j to i is the net pairwise spillover (NPS), defined as:

$$PNS_{ij}(H) = \left(\frac{\tilde{\theta}^g_{ij}(H)}{\sum_{q=1}^{n} \tilde{\theta}^g_{iq}(H)} - \frac{\tilde{\theta}^g_{ji}(H)}{\sum_{q=1}^{n} \tilde{\theta}^g_{jq}(H)} \right) \cdot 100. \tag{3.11}$$

All the metrics discussed above are able to yield insights regarding the mechanisms of market exchange spillovers both from a system-wide and a net pairwise point of view. Furthermore, performing the analyses on rolling windows we are able to study the dynamics of spillover indexes over time.

3.4 Data

Our empirical analysis examines the most widely known and capitalized cryptocurrency in current times: Bitcoin. We consider Bitcoin exchange prices expressed in USD sampled on hourly basis. We analyze a 1 year time-frame which ranges from 1 July 2017 to 30 June 2018, counting 8750 observations[4]. The analyzed timespan includes two sub-periods of great interest for crypto investors: the spectacular price growth in 2017 and its correction in 2018. The period is chosen to be quasi-symmetric around bull and bear times.

During the two sub-periods many events involving cryptocurrencies occurred and some of them have meaningfully affected their price dynamics, mostly Bitcoin. The main events are summarized in Table 14. Some notable

[4]Exchange prices were collected from http://www.cryptodatadownload.com/data.

events include: in the beginning of September 2017, People's Bank of China ban of fund raising by Initial Coin Offerings (ICOs) was linked this with a 5 % drop in the Bitcoin price. This was followed by the dramatic announcement by the Chinese authority to shut down trading of cryptocurrencies at national level; in early December, the approval of Bitcoin futures by the Commodities Futures Trading Commission (CFTC) had a high impact on Bitcoin investors. Bitcoin price spectacularly grew from around 10,000 USD a coin when the news broke to a high just below 20,000 USD on 18 December; at the beginning of 2018 the South Korean regulators banned anonymous bank accounts being used to buy and sell cryptocurrencies. After that move, Bitcoin price declined from just below 11,000 USD to a daily low of 10,179 USD. The Bitcoin price fall then continued and was accompanied by many negative news regarding cryptocurrencies. Indeed, during the first half of 2018, the exchange platform Bitconnect shut down, Coincheck was hacked and Coinsecure was robbed, leading to unavoidable price declines. Moreover, the Bitcoin price suffered from the moves of the Chinese government towards blocking all websites that enable cryptocurrency trading and ICOs and foreign platforms that enable bitcoin trading in February, as well as from the social network bans on advertisements for ICOs and token sales.

Table 14: Main events related to cryptocurrencies

Date	Event	Description
1) 01/08/2017	Bitcoin Cash hard fork	Bitcoin forked into two derivative digital currencies, the Bitcoin (BTC) chain with 1 MB blocksize limit and the Bitcoin Cash (BCH) chain with 8 MB blocksize limit.
2) 04/09/2017	China banning ICOs	People's Bank of China banned fund raising by Initial Coin Offerings (ICOs) referring to the threat to economic and financial stability. Largely due to the high amount of suspicious ICOs accused of illegally raising money and aiding intentional fraud.

3) 16/09/2017	China exiting local trading	Chinese authorities announced a ban on trading cryptocurrencies at national exchange services. Firstly, leaked documents were online just four days after the ban of ICOs, on 8 September. On 15 September the Chinese platforms Huobi and OKCoin announced that they will halt trading for local customers by 31 October.
4) 24/10/2017	Japan establish a self-regulatory industry body	The Financial Services Agency (FSA), the responsible overseer of banking, securities, insurance, and exchange sector of Japan, set up the Japan Virtual Currency Exchange Association (JVCEA) - a consortium of 16 FSA-approved domestic cryptocurrency exchanges - to establish as a certified fund settlement business association.
5) 24/10/2017	Coinbase received New York state banking license	Coinbase Custody received a license to operate as an independent qualified custodian, i.e. a Limited Purpose Trust Company chartered by the New York Department of Financial Services (NYDFS).
6) 28/11/2017	Bitcoin price $ 10,000	Bitcoin price reaches the level of $ 10,000.
7) 01/12/2017	CFTC Bitcoin futures approval	The Commodities Futures Trading Commission (CFTC) approved the request by CME Group and Cboe Global Markets to launch bitcoin futures. The two markets, which were launched on December 10 and 18 respectively, allow investors to bet on the future price of Bitcoin.
8) 17/12/2017	Bitcoin price $ 20,000	Bitcoin price reaches the level of $ 20,000.
9) 19/12/2017	Yapian filed for bankruptcy	Yapian, a company owning the Youbit cryptocurrency exchange in South Korea, filed for bankruptcy following a hack, saying it lost 17% of its assets.

10) 08/01/2018	China scrutinizing mining	The Public Bank of China started to investigate Bitcoin mining and outlined the plan to deter Bitcoin miners by limiting power consumption.
11) 08/01/2018	Korean crypto bank accounts investigation	Korean financial authorities launched an investigation into cryptocurrency-related services provided by local banks. In particular, the Financial Intelligence Unit (FIU) - a body under the Financial Services Commission (FSC) which monitors illegal financial activities - and the Financial Supervisory Commission - the country's financial supervisor - were looking into cryptocurrency-related virtual accounts at six local banks to check their compliance with anti-money laundering regulations.
12) 16/01/2018	Bitconnect exchange shut-down announcement	Bitconnect announced it would shut down its cryptocurrency exchange and lending operation after North Carolina and Texas regulators issued a cease-and-desist order against it, stating it was suspected of being fraudulent.
13) 22/01/2018	South Korean regulation about anonymity	South Korea brought in a regulation requiring all Bitcoin traders to reveal their identity, hence banning anonymous trading of Bitcoins.
14) 26/01/2018	Coincheck hacked	Japan's largest cryptocurrency OTC market, Coincheck, was hacked and as much as 530 million US dollars of NEMs were stolen, causing Coincheck to suspend trading.
15) 05/02/2018	China's announcement of blocking foreign trading	With the aim of preventing Chinese investors from financial risks, as in September 2017, China's authorities announced their willingness to ban trading of cryptocurrencies by blocking internet access to foreign trading platforms.
16) 07/03/2018	Irregular trades	Compromised Binance API keys were used to place irregular trades.
17) Late 03/2018	Social network bans	Facebook, Google, and Twitter banned advertisements for ICOs and token sales.

18) 13/04/2018	Coinsecure robbery	Coinsecure, one of India's biggest exchange platforms, lost 438 Bitcoins as a result of a theft. Based on the prices at the time of the occurrence of the event this translates to approximately 3 million $ (i.e. roughly 190 million rupees in local currency).

Note: The table reports major events related to cryptocurrencies during the sample period analyzed in the chapter, i.e. 1 July 2019-30 June 2019.

We study return connectedness of five major Bitcoin market exchanges, meaning Bitstamp, Gemini, Coinbase, Kraken and Bittrex[5]. The main features of the Bitcoin exchange platforms analyzed in this study are summarized in Table 15. Bitstamp and Kraken are two of the oldest cryptocurrency exchanges existing, whereas Gemini, Coinbase and Bittrex are relatively newer ones. Except for Bitstamp, whose headquarter is located in UK, all the exchanges included in the sample are US-based. The number of traded pairs varies quite much across exchanges, with Bitstamp and Gemini being the ones trading the smallest number coin pairs and Bittrex the one showing more variety of trading pairs. Trading fees are generally quite comparable across the analyzed exchanges, whereas trading volumes during the analyzed time-frame are all above 5 million USD and the time to withdraw or deposit fiat currencies is generally between 1 to 5 business days, except for Gemini, which shows lower trading volumes and higher withdrawal and deposit time of fiat currencies. As far as the supported currencies, Kraken is the one supporting the biggest number of fiat currencies, whereas Gemini and Bittrex support only USD and USDT respectively.

[5]The five exchanges were selected accounting for their total market capitalization and data availability over the time period studied.

Table 15: Bitcoin exchange features

	Bitstamp	Gemini	Coinbase	Kraken	Bittrex
Launched	Jul 2011	Oct 2014	May 2014	Jul 2011	Feb 2014
Headquarter location	UK	USA	USA	USA	USA
Trading pairs	14	15	53	95	355
BTC trading volume during analyzed period	6.37 M	2.63 M	7.46 M	5.46 M	NA
Trading fees	0.10%-0.25%	0.00%-0.25%	0.10%-0.30%	0.00%-0.25%	0.25%
Fiat currencies withrawal / deposit time	1-5 business days	4-5 business days	1-5 business days	1-5 business days	-
Supported currencies	USD, EUR	USD	USD, EUR, GBP	CAD, EUR, GBP, JPY, USD	USDT

Note: The table summarizes the characteristics of the Bitcoin exchanges investigated in the study at the date of 05/10/2019. Maker fees may be smaller than taker fees and fees may be lower for high trading sizes.

Given that in our analysis we consider the price of the same crypto (Bitcoin) traded on different venues, prices exhibit almost identical dynamics - i.e. they co-move. Therefore, without loss of generality, we plot the Bitstamp price series during the considered period in Figure 6, highlighting the main events related to cryptocurrencies described in Table 14.

Figure 6: Bitstamp price (USD)

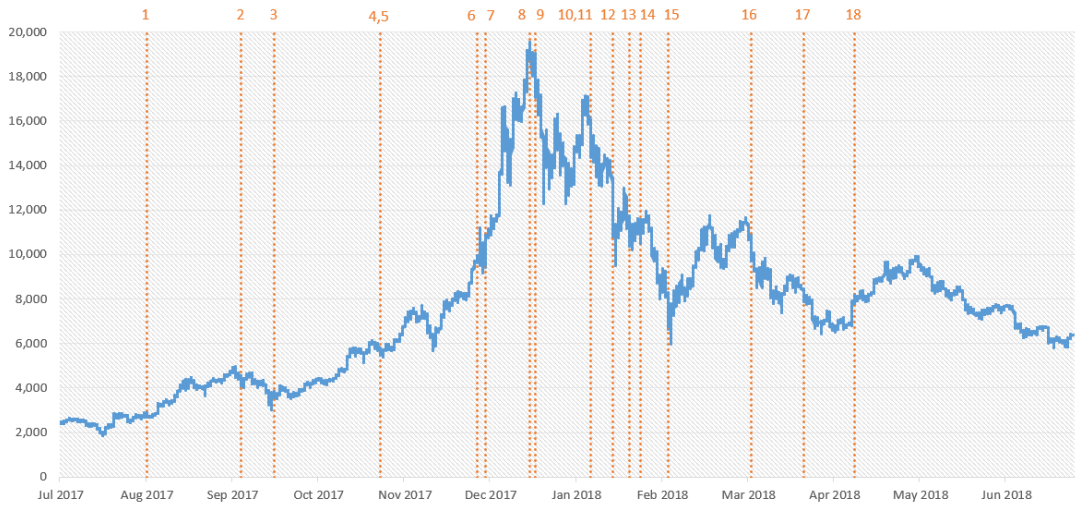

Note: The figure shows the Bitstamp price series (USD) related to the sample period 1 July 2017 - 30 June 2018. Dotted lines indicate the dates at which the main events related to cryptocurrencies described in Table 14 occurred.

A simple visual inspection yields to the conclusion that the upward and downward trend periods split the sample into two almost equal time-frames. More importantly, from an econometric point of view it can be noticed that the Bitcoin price series seem to be highly non-stationary in levels, arguably $I(1)$. This consideration, together with the non-deviation of Bitcoin exchange prices in the long run prescribed by the law of one price, makes us expect a cointegrating relationship among the Bitcoin price series we analyze.

For the sake of completeness, we also plot the continuous returns of the exchange price series in Figure 7.

Figure 7: Exchange continuous returns

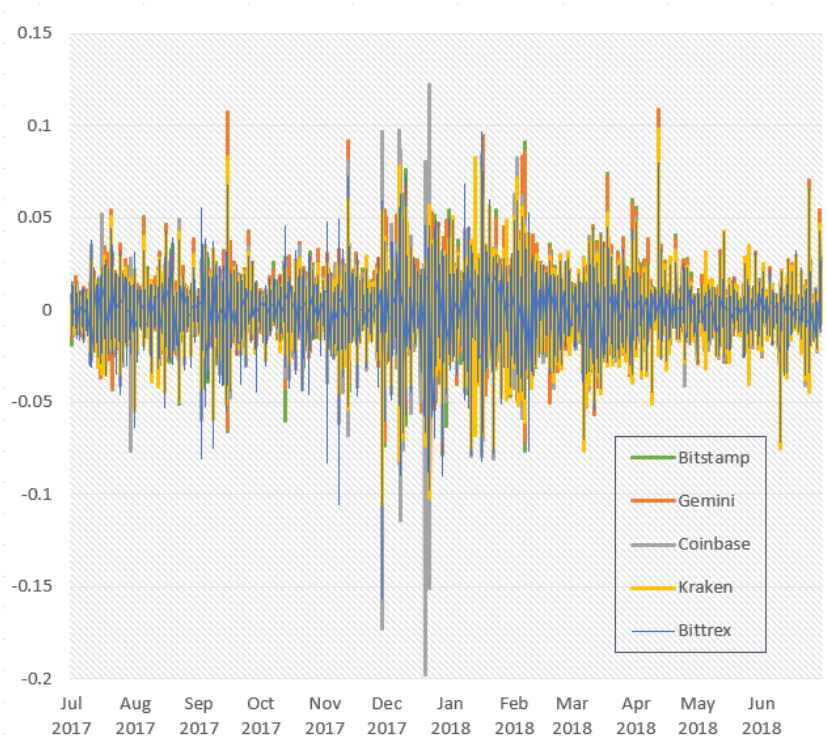

Note: The figure illustrates the analyzed Bitcoin exchange continuous returns during the sample period 1 July 2017 - 30 June 2018.

Table 16: Summary Statistics of Returns

	Bitstamp	Gemini	Coinbase	Kraken	Bittrex
Mean	0.0001	0.0001	0.0001	0.0001	0.0001
Median	0.0002	0.0001	0.0009	0.0006	0.0006
Maximum	0.1079	0.1083	0.1220	0.0980	0.0969
Minimum	-0.1076	-0.1222	-0.1979	-0.1052	-0.1565
Std. Dev.	0.0122	0.0121	0.0122	0.0115	0.0124
Skewness	0.0497	0.1303	-1.3244	-0.5429	-0.9601
Kurtosis	8.0090	9.3869	25.3352	9.4711	11.2719

Note: The table includes relevant summary statistics for returns related to the analyzed exchanges considering the entire sample period.

In this case we notice a few data points in which there is a consistent disequilibrium in returns, meaning that they diverge quite drastically. This suggests that some exchanges behave dissimilarly to others during certain periods. The latter proposition is also supported by the summary statistics contained in Table 16. Again from an econometric point of view, the graph showing continuous returns provides evidence to the hypothesis that Bitcoin price series are $I(1)$ time series, which will be empirically tested in the following.

As a preliminary analysis, we need to ensure that the analyzed time series are characterized by a non-stationary and cointegrated behaviour. To this aim, we conduct two widely employed stationarity and cointegration tests.

To test for (non-)stationarity, we perform the Augmented Dickey-Fuller (ADF) tests - see Dickey and Fuller (1979) - on prices, expressed in log-levels. The test results are shown in Table 17.

The ADF test provides strong support towards the non-stationarity of the price series in log-levels, whereas it provides evidence for stationarity of their first differences - i.e. of continuous returns. This is true for all

Table 17: Augmented Dickey-Fuller test

	Bitstamp	Gemini	Coinbase	Kraken	Bittrex
p-value$_{log-levels}$	0.7669	0.7718	0.7232	0.7945	0.7440
p-value$_{log-returns}$	<0.0100	<0.0100	<0.0100	<0.0100	<0.0100

Note: The table shows the resulting p-values for the Augmented Dickey-Fuller (ADF) test considering the entire sample period. The test in levels includes a constant but no time trend in the model specification. The minimum p-value reported is 0.01.

conventional significance level. Therefore, we can claim that the Bitcoin price series analyzed are $I(1)$ time series.

To test for cointegration, we employ the Johansen trace test, as proposed by Johansen (1991). In line with our methodological approach, we expect to find a cointegrating rank of the system which amounts to $h = n - g = 5 - 1 = 4$. This is because the law of one price entails that prices related to the same asset should be driven by $g = 1$ unique common stochastic trend. The test outcomes are illustrated in Table 18.

The test statistics allows us to reject the null hypothesis of a cointegrating rank h of at most 3 against the alternative of a cointegrating rank of 4. In other words, the test suggests a cointegrating rank of the system $h = 4$, i.e. the presence of $g = 1$ common stochastic trend driving the fundamental Bitcoin price, in line with our previous considerations. This guarantees assumptions are met and the methodology can be soundly applied to our real data.

3.5 Empirical findings

In this chapter we investigate Bitcoin exchange return connectedness from a dynamic viewpoint. In other words, rather than estimating spillover measures on the full sample period, which would provide the "average" or "un-

Table 18: Cointegration (Johansen Trace test)

	Test stat	Critical 10%	Critical 5%	Critical 1%
h <= 4	3.10	6.50	8.18	11.65
h <= 3	188.84	15.66	17.95	3.52
h <= 2	752.42	28.71	31.52	37.22
h <= 1	1627.95	45.23	48.28	55.43
h = 0	3230.01	66.49	70.60	78.87

Note: The table illustrates the test statistics statistics and critical values for the Johansen Trace test for cointegration for the full sample period. The test does not include any costant or time trend, neither in the model specification nor in the cointegrating relationship.

conditional" connectedness, we estimate spillover indexes on rolling windows, with the aim to explore the dynamic features of exchange interconnectedness. In particular, we set a predictive horizon for the variance decomposition of $H = 12$. As far as the approximating model is concerned, we use a VECM lag length of 2, corresponding to a lag length of 3 in its vector autoregressive representation. We then consider a one-sided estimation rolling window of $w = 336$ hours - corresponding to two weeks [6].

Firstly, we derive the total return spillover index and provide its plot - together with the Bitstamp Bitcoin price related to the same period - in Figure 4.7.

The total return spillover index ranges from a minimum of 72.24% to a maximum of 79.79%, with an average value of 78.13% over the examined period. This suggests that system-wide return connectedness is relatively high when considering Bitcoin exchanges.

[6]The first two choices are in line with (Diebold and Yılmaz, 2014), who fix their forecast horizon to $H = 12$ for the variance decomposition and the lag length of the approximating VAR model to 3. The second choice is pursued for empirical reasons, meaning that we consider the previous two full Bitcoin trading weeks to carry on the estimations.

Figure 8: Total Spillover Index (TSI)

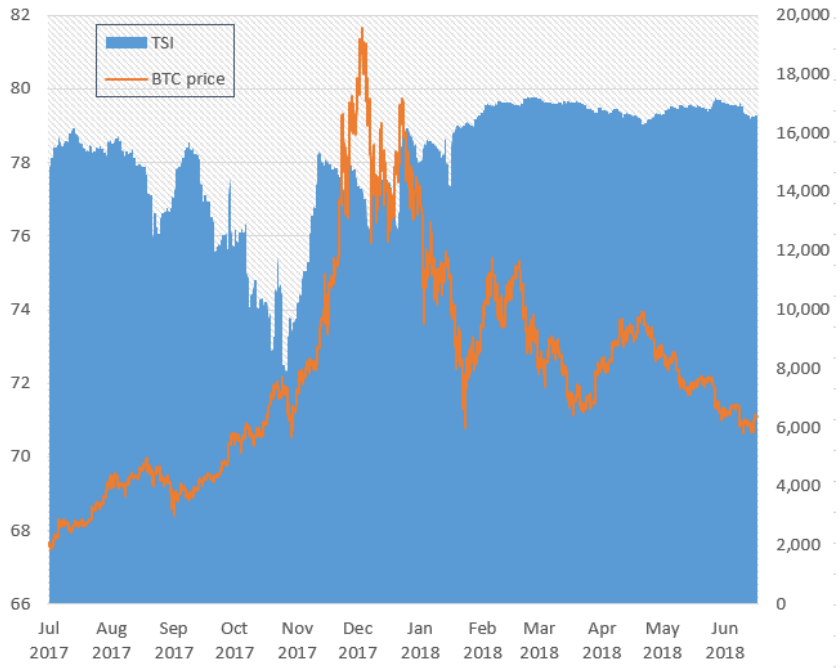

Note: The plot illustrates the total return spillover index versus the Bitstamp Bitcoin price series. The rolling window set for the estimations is 2 weeks. Values for the total spillover index are expressed in percentage terms, while the Bitcoin price is denominated in USD.

Similarly to the Bitcoin price, the total spillover index seems to show two main cycles: one in which the index witness a downward trend, as well as a following one where it steadily grows and finally smooths out. However, its dynamics are not synchronized with that of the Bitcoin price. This suggests that both in hype and correction periods interconnectedness may either lower or increase depending on specific market features.

In our case, system-wide connectedness generally falls during the first cycle, specifically until the beginning of November 2017, period in which the Bitcoin price starts an unprecedented year-end rally. Right after the minimum peak of the index, Bitcoin prices began to surge like never before,

and the index goes back rapidly to its previous values. This means that, while during the first price growth phase we encounter interconnectedness among Bitcoin exchanges lowers, contagion effects begin to be more consistent during the year-end Bitcoin price hype. During the second cycle the total spillover index wiggles and grows at first, whereas it levels out and stabilizes in the range 79%-80% starting from February 2018. This also coincides with the end of the hard correction of Bitcoin price, after which exchange interconnectedness becomes relatively steady.

After that, we study the directional return spillover indexes, i.e. the "from", "to" and "net" spillover indexes. A plot illustrating their dynamics over the considered time-frame is contained in Figure 9.

At first glance, one may notice that the range of variation related to the directional spillovers to others is wider than that of the directional spillovers from others. Indeed, while the return spillover indexes from others range from a minimum of 7.80% to a maximum of 19.23%, the spillovers indexes to others show a minimum of 0.47% and a maximum of 39.32% during the studied period. This reflects into an as wide range for the net return spillover indexes, with values between -18.57% and 30.13%.

In general, we find that to some extent there is a kind of equilibrium with regards to the directional spillovers from and to others, as well as in the net ones. During most part of the analyzed period, Bitcoin exchanges can be split into two groups: those who transmit return spillovers to others, namely Bitstamp and Gemini, and those who instead receive return spillovers, i.e. Bittrex, Coinbase and Kraken. This can be immediately stated by a visual inspection of the net spillover indexes in Figure 9, which give us a hint on the leading and following Bitcoin exchanges during the analyzed time-frame. Moreover, we may add that the dynamics and magnitude of the directional return spillovers is quite similar within the same group.

However, there is a specific period in which the equilibrium witnesses a substantial instability. This is related to the same period in which the total return spillover index starts to rise after a steady decline. The directional

Figure 9: Directional Spillover Indexes (DSI)

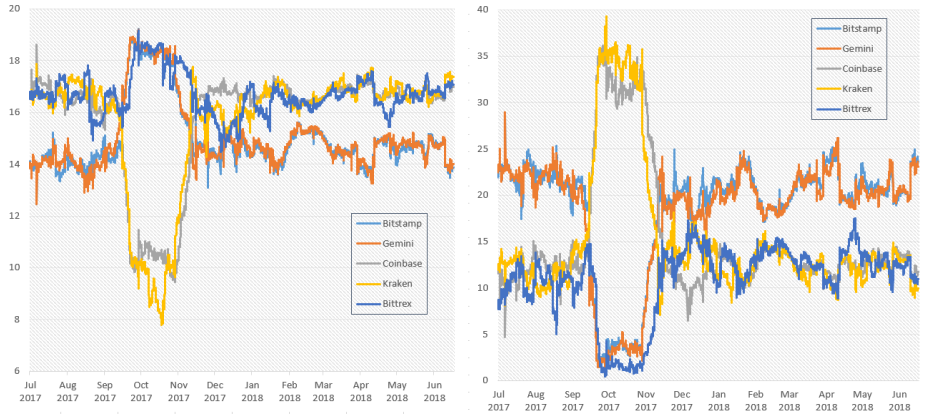

(a) From (b) To

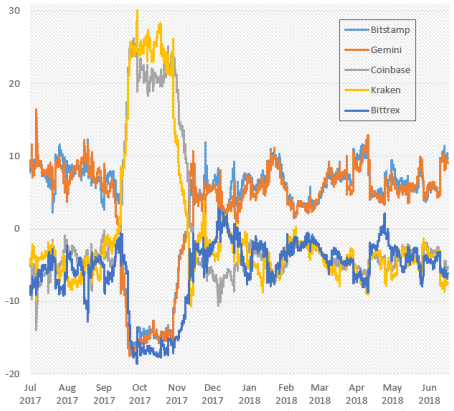

(c) Net

Note: The figure shows the directional return spillover indexes "from" others (From), "to" others (To), as well as the net ones (Net). The rolling window set for the estimations is 336 hours - corresponding to 2 weeks. Values are expressed in percentage terms.

spillover indexes suggest that in this phase Kraken and Coinbase rapidly start transmitting return spillovers to others and they keep doing that until the dramatic year-end price surge, whereas Bitstamp and Gemini receive spillovers during the same phase, together with Bittrex. The strong change in leadership pushes from 20% to 5% the transmitted spillover contributions of the two exchanges leading before in less than one month, besides making that of Bittrex drop to almost null values.

Bittrex is the unique exchange which constantly emerges as a return spillover receiver - even more in the latter mentioned timespan - is Bittrex, being its net spillover index values as much as 96.98% of the times below 0. This is in line with the fact that leading exchanges are generally those in which most of the trading volumes lie, as Bittrex is the smallest exchange we selected in terms of trading volumes.

After the year-end Bitcoin price surge, directional spillover indexes go back to their previous equilibrium. Indeed, the down market not only brings system-wide connectedness to its previous levels, but also re-establishes the exchange ranking in terms of return shock transmitted. In particular, despite some fluctuations from the end of 2017 onwards Bitstamp and Gemini re-confirm their previous leading position, while Bittrex, Kraken and Coinbase that of follower.

Finally, we explore the net pairwise spillover indexes, which give us information on how return shocks are transmitted across Bitcoin market exchanges, from a pairwise viewpoint. We plot the net pairwise spillover indexes in Figure 10.

Figure 10: Net Pairwise Spillover Indexes (NPSI)

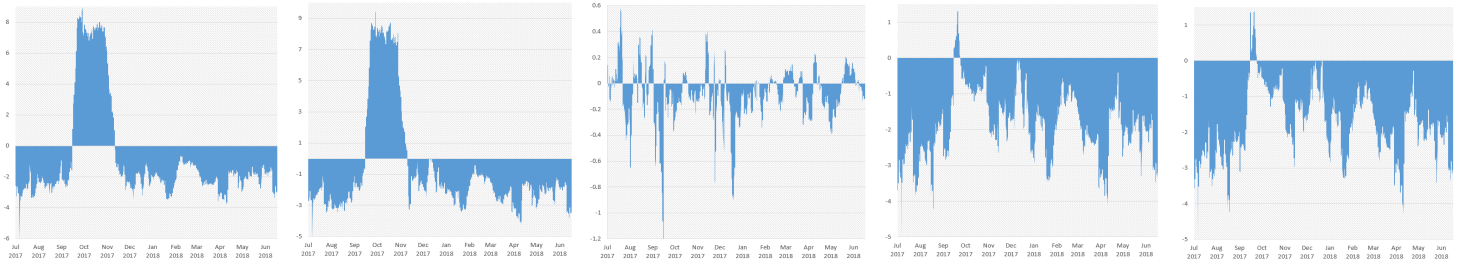

(a) Coinbase-Bitstamp (b) Kraken-Bitstamp (c) Gemini-Bitstamp (d) Bittrex-Bitstamp (e) Bittrex-Gemini

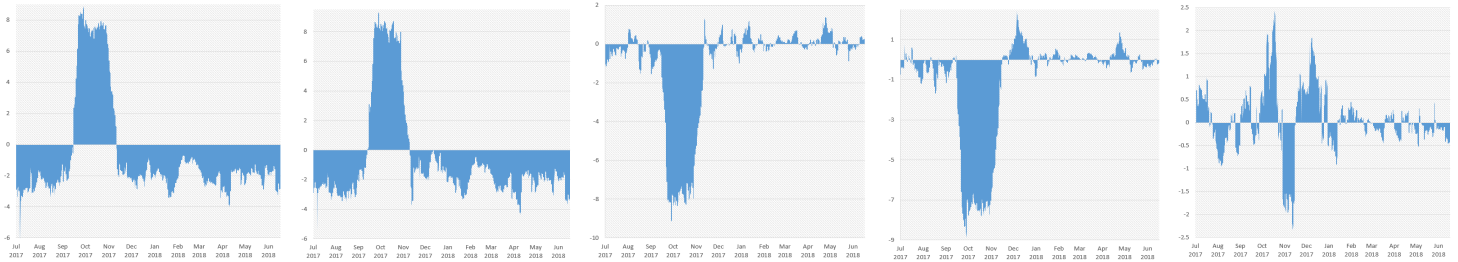

(f) Coinbase-Gemini (g) Kraken-Gemini (h) Kraken-Bittrex (i) Bittrex-Coinbase (j) Coinbase-Kraken

Note: The figure illustrates the net pairwise return spillover indexes. The rolling window set for the estimations is 336 hours - corresponding to 2 weeks. Values are expressed in percentage terms.

First of all, pairwise spillover indexes vary in wide ranges, meaning that pairwise connectedness relationships show considerably different magnitudes across exchange pairs. To illustrate, the narrowest range of variation can be found in the pairwise spillover index between Gemini and Bitstamp, which shows a minimum of -3.56 and a maximum of 1.07, whereas the widest range in the index is that of Bitstamp and Coinbase, that is from -6.19% to 8.88% - more than three times the latter one.

The study of net pairwise spillover indexes provides more depth to the conclusions on the exchange interconnectedness that emerged from the total and directional spillover indexes analysis. Overall, Bitstamp and Gemini transmit a significant portion of return spillovers to all other exchanges, with Bittrex being the most affected. However, in line with the earlier findings, during the period before the year-end price hype, Coinbase and Kraken transmit shocks to all other exchanges, with relatively high and comparable magnitudes.

It is interesting to study the interaction between the exchanges on the top of the ranking. The net pairwise spillover index between Gemini and Bitstamp oscillates around the zero line and assumes relatively low values. From a visual inspection Bitstamp seems to dominate Gemini in terms of return spillover transmission, both in terms of timespan and magnitude. As a matter of fact, the net pairwise spillover index Gemini-Bitstamp assumes negative values as much as almost two thirds (66.58%) of the times. Moreover, the contribution of Gemini towards Bitstamp does rarely overcome a value of 0.4 as opposed to the return spillovers transmitted from Bitstamp to Gemini, which not only double but even triple in size.

For the sake of ranking completeness, we also investigate the relationship between Coinbase and Kraken. It is not clear from a graphical point of view which exchange contributes more in terms of return spillover. Contribution magnitudes show quite comparable ranges, and the number of times Coinbase transmits shocks to Kraken is almost the same as the opposite situation (49.01%). It is clear that the two exchanges interact in a different way with

respect to the two leading ones, as their net pairwise spillover index oscillates much less around 0. This means their role of transmitter and receiver are more stable over time than in the previous case.

To summarise our empirical contribution in a nutshell, we are able to shed further light on price discovery among bitcoin exchange markets. Previous papers, such as Brandvold et al. (2015) and Pagnottoni and Dimpfl (2019) and Giudici and Pagnottoni (2020) found that the exchange markets with higher traded volumes are typically the ones that drive prices and spillovers. Differently from the previous papers, based on daily price data, we have considered high frequency data. The analysis of this data leads to confirm the conclusions from the previous papers. In addition, it allows an important discovery on the dynamic nature of return spillovers: although stable to some extent, the lead-lag relationship among Bitcoin exchanges is dynamic and witnesses notable changes over time. These changes may be fundamental for both policy makers and investors, which should monitor them for the purpose of an efficient decision making process and investment decision, respectively.

3.6 Robustness

In this section we propose a robustness analysis of our results with respect to the choices of the parameters used in the modelling strategy. To illustrate, we examine the total return spillover index for alternative rolling windows w set for the model estimations and alternative predictive horizons H. We increased and decreased the window width and predictive horizon by +50% and -50%, resulting in window width choices of $w = 168, 336, 504$ and predictive horizon choices of $H = 6, 12, 18$. [7] In this way we investigate the robustness of the total spillover index when considering rolling estimation

[7] A similar robustness analysis is performed by Diebold and Yılmaz (2014). By means of increasing and decreasing the estimation parameters by +50% and -50%, we are coherent with their choices with regards to the forecast horizon ($H = 6, 12, 18$), while we take into account an even wider range of rolling window widths ($w = 168, 336, 504$ as opposed to $w = 75, 100, 125$), ensuring a punctual robustness check of our outcomes.

windows of 1, 2 and 3 weeks as well as predictive horizons of $\frac{1}{4}$, $\frac{1}{2}$ and $\frac{3}{4}$ of a day. Plots related to the alternative total spillover indexes are illustrated in Figure 11.

The total spillover index seems to be just slightly influenced by changes in the window width w. As one may expect, the larger the rolling window the smoother is the index, whereas tighter windows yield to a more fluctuating one. However, in our case, we can state that results are qualitatively unaffected by the choice of the rolling window.

The index appears to be more sensitive to the choice of the forecast horizon H to compute the forecast error variance decompositions rather than to the rolling window. However, there is much more similarity in the behaviour of the spillover index between choices of the forecast horizons H of 12 and 18 rather than those of 6 and 12. This suggests that a judicious predictive horizon choice should grant stability of the index without losing information about its surge or decline and related magnitude. More importantly, the dynamics of the indexes show quite similar patterns, which just differ in their scale of values. This means that - once more - the qualitative interpretation of our results is not influenced by the choice of the predictive horizon H.

To conclude, our empirical outcomes appear robust with respect to the rolling window set for the estimation and the predictive horizons used in the forecast error variance decompositions.

3.7 Conclusion

This chapter explores system-wide and directional connectedness, along with price discovery mechanisms among five major Bitcoin exchange markets. This is done by extending the Diebold and Yilmaz (2012) forecast error variance decomposition from a VAR to a VECM framework, which enables us to take into account the non-stationary and cointegrated behaviour of the time series analyzed.

We remark that the methodological improve illustrated above is neither exclusively tied to Bitcoin exchange platforms, nor to cryptocurrency ones.

Figure 11: Robustness analysis

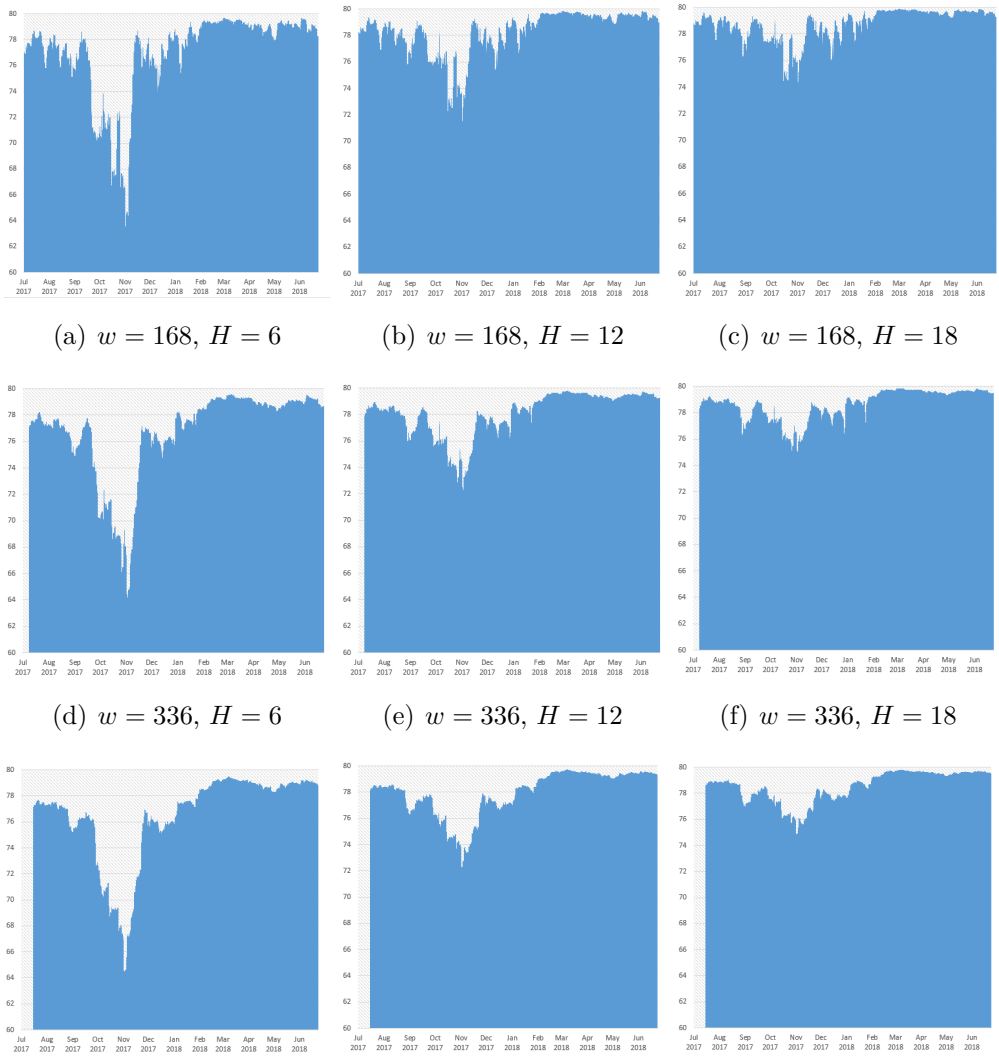

(a) $w = 168$, $H = 6$ (b) $w = 168$, $H = 12$ (c) $w = 168$, $H = 18$

(d) $w = 336$, $H = 6$ (e) $w = 336$, $H = 12$ (f) $w = 336$, $H = 18$

(g) $w = 504$, $H = 6$ (h) $w = 504$, $H = 12$ (i) $w = 504$, $H = 18$

Note: The figure shows the total spillover index with estimation window widths w of 168, 336 and 504 hours - corresponding to 1, 2 and 3 weeks respectively - and predictive horizons H of 6, 12 and 18 hours. Values are expressed in percentage terms.

Indeed, this technique can be extended to the study of interconnectedness among all exchange platforms trading the same financial products.

Our results show that overall connectedness strongly evolves over time and, in particular, it generally decreases during bull market times and decreases during down market periods. We also find that Bitfinex and Gemini can be all over considered as leading exchanges in the price formation process, being mostly transmitter of a significant portion of return spillover during the considered timespan. On the other hand, we identify Bittrex as follower, given it acts as a receiver of return shocks during the whole time period considered.

We also highlight the dynamic nature of return spillover across Bitcoin exchanges, as they considerably evolve over time. This means that the lead-lag relationships existing among Bitcoin exchanges is not constant and it is subject to changes over time.

From a practical viewpoint, our results suggest that, to predict the direction of price movements and contagion effects, potential investors should pay attention to spillovers and particularly to the exchanges that have the highest trading volumes - in general. However, also that the time dynamics should be taken into account, with a particular eye on events that may affect price volatilities and spillovers. This is true also for policy makers, who can come up with more efficient decision making by monitoring spillover effects due to events belonging to the regulatory framework.

Future research may include different model paradigms, based on Bayesian analysis - as in Giudici et al. (2003), Figini and Giudici (2011) -, on network models - as in Giudici and Bilotta (2004) - or on extreme value models - as in Calabrese and Giudici (2015).

4 Basket-based Stablecoins to Mitigate Foreign Exchange Spillovers

Based on the paper:
Giudici, Paolo, Pagnottoni, Paolo, & Leach, Thomas. 2020a. Libra or Librae? Basket based stablecoins to mitigate foreign exchange volatility spillovers. *available at SSRN*.

4.1 Introduction

Carney (2019) posed the question of whether a Synthetic Hegemonic Currency (SHC) would be best provided by the public sector. The rationale being that a global currency, underpinned by a basket of reserve assets, could better support global outcomes. For example, an SHC could dampen the dominating influence of the US dollar on global trade, alleviate spillovers to exchange rates from shocks to the US economy, and trade across countries would become less dependent on the dollar.

Discussions around global currencies, have been reignited in the overarching debate around central bank digital currency (CBDC) and stablecoins. Most notably, Facebook announced plans for its own privately issued stablecoin that would emulate the characteristics of an SHC. In the most recent iteration of Facebooks proposition, the idea is to supply digital tokens that are pegged to major currencies, i.e. LibraUSD would be pegged to the US dollar. Moreover, there will be another token whose value is derived from a weighted basket of the currencies provided on the platform. Currently, the exact composition of the underlying basket and its targeted exchange rate is unspecified. In this chapter, we assume that the objective is to devise a digital currency whose exchange rate fluctuations are minimised against several currencies, hence a global stablecoin. Facebooks plans have been met with some resistance from regulators and face intense scrutiny before receiving any kind of regulatory approval.

Why have regulators reacted with such caution to Facebook's plans to

issue a stablecoin? Firstly, as a tech-giant Facebook can push Libra to its vast user-base, approximately 2.41 billion monthly active users.[8] To put this into perspective, currently it is estimated there around 40 million bitcoin wallets and 1 million daily users.[9] Facebook would have to successfully penetrate 2% of its user base to match what is an upper bound on a proxy for the size of bitcoins user base, the most frequently used cryptoasset. There is consequently significant potential for Facebook to rapidly acquire a vast user base for its digital currency.

Against this background, we investigate the empirical aspects of the design of a currency basket i.e. "Librae" in the sense that the value is composed of several currencies. First, we consider the optimal weights of the basket of underlying reference currencies, such as those included in the International Monetary fund Special Drawings Rights (SDRs). After computing the optimal weights we construct the historical values of the currency and compare the volatility against a set of major currencies, wel also use the value of SDRs as a reference for currency baskets.

For the optimal allocation of weights in the currency basket we follow Hovanov et al. (2004) to compute a basket whose value's variance is minimised against the currencies contained in the basket. We construct a reference basket that contains the Dollar (USD), the Euro (EUR), the Yen (JPY), the Renminbi (CNY) and the Pound Sterling (GBP), the same currencies that are employed for the determination of the IMF's Special Drawing Rights (SDR) basket. Currently, Facebook has not made explicit which currencies it intends to use in the basket. The weights are determined by minimising the variance of a portfolio of currencies, expressed in Reduced Normalised Values (RNVALs). The benefit of using the RNVALs is that the value of each currency is expressed in how much it varies against others included in the portfolio, therefore removing fluctuations in an underlying base currency. We use daily data from January 2002 up until November 2019. Comparing

[8]https://newsroom.fb.com/company-info/

[9]The number of bitcoin wallets: https://www.statista.com/statistics/647374/worldwide-blockchain-wallet-users/ and the number of active wallets: https://coinmetrics.io/.

our weights with those of the SDR, less weight is given to the dollar, and more weight on the Euro and Renminbi.

By construction, our basket based currency should be the least varying in comparison to those contained in the basket, and our results confirm this. However, it is of interest to see how our basket fares against currencies outside of the basket, for example against the currencies of the most important remittance markets. The comparison can answer a very important question, that is: is the exchange rate of the SHC less volatile then the exchange rate of the dollar and, consequently, could a basket currency increase the utility of individuals that make remittances? To answer this question, we recompute the currency invariant indices with the inclusion of additional currencies, namely the Indian Rupee, the Mexican Peso, the Philippine Peso and the Nigerian Naira. Our empirical findings show that, overall, the basket has the lowest volatility. Therefore acting as a safe store of value for overseas workers savings. The basket can be used as a hedge against fluctuations between the the domestic and foreign currencies of individuals that rely on remittances. that could be held in the basket currency. The IMF's SDRs, performs almost as well. Stablecoins based on single-currencies in this respect perform worse, although during the crisis the dollar had a lower volatility.

We then study the currencies which mostly determine volatility spillovers among exchange rates, using the framework of Diebold and Yılmaz (2014). Specifically, we build a spillover network decomposition analysis of the currencies up to April 2020, thus including the period of the Covid-19 outbreak. Our spillover network decomposition shows that the USD is the currency whose dynamics has the largest impact on the others, especially in terms of exporting contagion, although in the latest period CNY has begun overtaking. As a consequence, a shock to USD, expressed by a one standard deviation decrease in its normalised value with respect to the other currencies, causes a shock on all currencies and, through high order contagion, on the USD itself, leading to a new lower equilibrium. Differently, a shock in the value of the SHC, caused by a shock of a currency in the basket, is offset

by the diversification effect and, therefore, the starting equilibrium is maintained. This implies that remittances converted in basket based stablecoin better maintain their value, with respect to those converted in dollars (or dollar based stable coins).

The rest of the chapter is organised as follows, Section 4.2 contains a review of the relevant literature, Section 4.3 outlines our proposed methodologies, Section 4.4 presents our data and the empirical findings, and finally in Section 4.5 we conclude.

4.2 Literature Review

4.2.1 Cryptocurrencies, stablecoins and e-money

Cryptocurrencies were first conceived with the advent of Bitcoin, large attributed by the work of Nakamoto et al. (2008). This was the first decentralized payment system based on maintaining a public transaction ledger. Since then, as many as 5,500 cryptocurrencies exist as of 24 May 2020. With respect to the analysis of cryptocurrencies, the research covers a vast array of topics. Several dealt with the description and functioning of cryptocurrencies (Segendorf, 2014; Dwyer, 2015b). Issues surrounding cryptocurrrencies from a legal perspective are discussed, for example, in Murphy et al. (2015). Cheng and Dai (2020) demonstrate the inflow capital control evasion phenomenon in cryptocurrencies and show that the relative CNY to USD bitcoin price, indicating capital inflow volume reacts more negatively to carry trade returns.

Many studies analyse cryptocurrencies and their features from a quantitative viewpoint. As an example, Corbet et al. (2018c) investigate the dynamic spillovers of cryptocurrencies with other financial assets, and find that the two categories of financial instruments are isolated. With a similar methodology, Giudici and Pagnottoni (2020) explore the dynamic relationship of Bitcoin exchanges and show their relative importance in transmitting information of fundamental Bitcoin price changes. Katsiampa et al. (2019)

examine the volatility interaction of eight cryptocurrencies through the Diagonal BEKK and Asymmetric Diagonal BEKK methodologies and find that despite shocks in Bitcoin are the longest lasting, the cryptocurrency is not dominant. Bouri et al. (2019) evaluate the effectiveness of several technical trading rules in cryptocurrency markets and provide support to the best performances of moving average based strategies.

Research on stablecoins is instead quite limited. The Financial Stability Board (2019) defines a 'stablecoin' as a crypto-asset designed to maintain a stable value relative to another asset (typically a unit of currency or commodity) or a basket of assets. Bullmann et al. (2019) make the following distinctions between types of stablecoins.

- **Tokenised funds** - denote stablecoins that are a claim on a pool of collateral that consists of funds, including cash, electronic money, commercial bank money or central bank reserve deposits e.g. Tether, Utility Settlement Coin
- **Off-Ledger Collateralised** - stablecoins that are a claim on a pool of collateral that is comprised of various assets e.g. multiple currencies, T-Bills etc
- **On-Ledger Collateralised** - stablecoins that are a claim on a pool of underlying collateral that is held on a blockchain e.g. Dai
- **Algorithmic** - take users expectations into account to stabilise the value of the coin (mostly conceptual) e.g. BasisCoin

At present, tokenised funds and off-ledger collateralised are the most common occurring instances of stablecoins. The Libra concept, would fall into the later as the foundation has plans to invest the funds that are received in return for stablecoins. Stablecoins replicate close substitutes for cash, similarly to electronic money. This is not the first time that electronic money has been on the agenda for central banks and policy makers, after a flurry of innovations in this space, in 1996 and 1998 respectively the BIS and ECB

published reports addressing the regulation of e-money and the implications for monetary policy.[10] For various reasons, these forms of e-money never really troubled the concerns of policy makers of the time.[11]. However, discussions around digitised forms of money have reared their head once again.

4.2.2 Global currencies

A global currency as put forward recently by Carney (2019) could address certain issues in the international monetary system. Keynes originally suggested the *bancor* as a unit of account of his proposed International Clearing Union, intended to fix to the dual dollar gold system. The solution was eventually conceived by the IMF who approved the Special Drawing Rights (SDRs) in 1967. The IMF's issuance of SDRs could be seen as a supranational currency issued by central banks, although the SDR does not fulfil all functions of money. Whilst serving as a store of value and unit of account, SDRs are only used by some central banks and international institutions as a means of exchange to pay each other (Ocampo, 2019). For this, they may not be strictly considered as a"true" global currency.

A boost to the importance of SDRs was given in 2009, when China called for reforms to the international monetary system by adopting the SDR as a reserve asset. Against these developments, Humpage (2009) suggests that while the adoption of the SDR as a reserve asset is technically feasible, it would not reduce the dollar's role any time soon. Many foreign-exchange transactions, even excluding US residents, are denominated and settled in dollars. Producers typically invoice their products in dollars, which keeps their prices in line with their competitors and simplifies cross-border price comparisons among producers (Gopinath et al., 2016). Given the persistent importance of the US dollar, the question is whether this will remain so under the fintech transformation that is changing the financial world. And, in particular, whether a dollar based stable coin is more likely to be adopted

[10] See European Central Bank (1998); Bank for International Settlements (1996)

[11] For example, see Levene (2006)

than a basket based one.

4.2.3 Remittances and exchange rates

A stablecoin backed by a basket of currencies could be an attractive asset for foreign workers that make remittances to families in their home countries. In particular, where its value is not directly tied to the domestic currency. Under the status quo, an appreciation in the value of the domestic currency can reduce the remittances ratio because workers want to to keep the additional earning from the appreciation of the currency. On the other hand, workers based in foreign countries, where the value of the domestic currency is declining, may remit money on an urgent basis. Flore (2018) recently notes the impact that blockchain could have on reducing costs in remittance markets.

One specific challenge for countries that face large inflows of worker remittances could lead to the emergence of "Dutch disease," that is, remittance inflows could result in an appreciation of the equilibrium real exchange rate that would tend to undermine the international competitiveness of domestic production, particularly that of nontraditional exports. Barajas et al. (2011) note that reasonable modifications in the modelling of the factors driving remittances, or in the various macroeconomic roles that remittances may play, could moderate or even reverse the expected impact of remittance flows on the equilibrium value of the real exchange rate. Acosta et al. (2009) discuss two mechanisms by which this occurs, the first mechanism is demonstrated in the Salter-Swan-Conder-Dornbusch model, which points to a “spending effect,” by which the increase in wealth following higher capital inflows from remittances, combined with exogenous tradable prices, causes the prices of nontradable goods and services to rise. These higher prices lead to an expansion in the non-tradable sector. By definition, an increase in the price of nontradables relative to the price of tradables translates into real exchange rate appreciation. The second mechanism is that remittances tend to increase household aggregate wealth. An increase in household wealth may lead to a decrease in labor supply as households substitute more leisure for

work. A shrinking labor supply, in turn, puts upward pressure on wages. Rising wages raise production costs, and higher production costs can lead to a further contraction of the tradable sector. Both the resource reallocation effects and the labor effects can cause an appreciation of the exchange rate, thereby reducing the international competitiveness of the tradable sector, and may lead to tradable sector contraction, higher wages, and higher production costs.

A basket based currency could dampen some of these effects as it is less susceptible to appreciation and depreciation of the domestic and foreign currencies. However, the effects are likely to be ambiguous and depend on how the stablecoin is used. If it gains acceptability in the home currency this could leads to new episodes of dollarisation, whereas if the currency is only used as a medium of exchange the effect could be negligible.

4.2.4 Our contribution

Our proposal combines the background of the previous streams of literature, namely: the need of a global currency, which is "optimal" in terms of minimum volatility (maximum stability), and resilient to exchange rate shocks; with the emergence of fintech technologies, and of blockchain based stable coins in particular. Against this background, we contribute to the previous literature, from an economic viewpoint, by answering the following research question: is a basket based stable coin better than a single currency one, in terms of stability? To answer this question, we contribute to the literature, from a methodological viewpoint, with two main innovations: i) we provide a methodology to build a minimum variance basket of currency, to derive the optimal weights for a 'global stablecoin'; ii) we provide a methodology aimed at assessing contagion spillovers among foreign exchange markets, based on Diebold and Yilmaz variance decomposition model.

4.3 Methodology

In this section we outline the methodologies employed in our empirical application. Firstly, we describe the optimal control problem which yields to the optimal stablecoin weights. Secondly, we introduce our VAR model and, based on it, we study the spillover effects across the currencies in the basket to determine their interconnectedness and, therefore, to understand which are the most relevant ones in terms of shock transmission.

4.3.1 Optimal control problem

We aim to build a basket of predetermined (reference) currencies with optimal weights, namely, weights which minimize the variability of a basket based stablecoin. This translates into an optimal control problem which minimize the variance of the basket constructed with the above mentioned currencies.

Hovanov et al. (2004) show that the values of any given currency depends on the base currency chosen. The latter fact creates ambiguity in evaluating the currency itself and its dynamics. To overcome this issue, Hovanov et al. (2004) proposed a reduced (to the moment t_0) normalized value in exchange (RNVAL) of the i-th currency:

$$\mathrm{RNVAL}_i\left(t/t_0\right) = \frac{c_{ij}(t)}{\sqrt[n]{\prod_{k=1}^{n} c_{kj}(t)}} \Big/ \frac{c_{ij}\left(t_0\right)}{\sqrt[n]{\prod_{k=1}^{n} c_{kj}\left(t_0\right)}} = \sqrt[n]{\prod_{k=1}^{n} \frac{c_{ik}(t)}{c_{ik}\left(t_0\right)}}. \tag{4.1}$$

By reducing to the moment t_0 and normalizing each currency observation by the geometric average of the other currencies at that specific point in time, the RNVAL allows the computation of a unique optimal, minimum variance currency basket, despite the base currency choice. The minimum variance currency basket is derived by searching the optimal weight vector w^* which solves the following optimal control problem:

$$\mathrm{Min}\left(S^2(w) = \sum_{i,j=1}^{n} w_i w_j \,\mathrm{cov}(i,j) = \sum_{i=1}^{n} w_i^2 s_i^2 + 2\sum_{i,j=1}^{n} w_i w_j \,\mathrm{cov}(i,j)\right) \tag{4.2}$$

subject to

$$\begin{cases} \sum_{i=1}^{n} w_i = 1 \\ w_i \geq 0 \end{cases}$$

The optimal control problem in Equation (4.2) yields to the minimum variance weights which enable us to construct the stablecoin value.

4.3.2 VAR models and spillover analysis

We evaluate spillovers through the methodology by Diebold and Yilmaz (2012). As in their seminal paper, we start from estimating a Vector AutoRegressive (VAR) model, that is :

$$x_t = \sum_{i=1}^{k} \Phi_i x_{t-i} + \varepsilon_t \tag{4.3}$$

where x_t being the $(n \times 1)$ vector of first differences in RNVALs at time t, Φ_i the $(n \times n)$ VAR parameter matrices, k the autoregressive order, ε_t a zero-mean white noise process having variance-covariance matrix Σ_ε, with n being the number of currencies considered in order to build the basket. Note that the VAR model is built on the variables' first differences, as this ensure the stationarity of the analyzed time series.

The VAR in Equation (4.3) may also be rewritten in its corresponding vector moving average (VMA) representation, that is

$$x_t = \varepsilon_t + \Psi_1 \varepsilon_{t-1} + \Psi_2 \varepsilon_{t-2} + \cdots \tag{4.4}$$

where $\Psi_1, \Psi_2, ...$ the $(n \times n)$ are the matrices of VMA coefficients. The VMA coefficients are recursively computed as $\Psi_i = \Phi_1 \Psi_{i-1} + \Phi_2 \Psi_{i-2} + ... + \Phi_i \Psi_1$, having $\Psi_i = 0 \ \forall i < 0$ and $\Psi_1 = I_n$.

As it is widely accepted in the financial econometric literature, the variance decomposition tools are used to evaluate the impact of shocks in one

system variable on the others. Strictly speaking, variance decompositions decompose the H-step-ahead error variance in forecasting x_i which is due to shocks to x_j, $\forall j \neq i$ and $\forall i = 1, ..., n$.

In this contribution we make use of the KPPS H-step-ahead forecast error variance decompositions, as Diebold and Yilmaz (2012) do. This is because we avoid imposing an a priori ordering exchange rates regarding the influence of shocks across the system variables, as popular techniques like the Cholesky identification scheme do. Indeed, the KPPS H-step-ahead forecast errors have are convenient as they are invariant with respect to the variable ordering.

As already stated, Diebold and Yilmaz (2012) found their methodology on the H-step ahead forecast error variance decomposition. Considering two generic variables x_i and x_j, they define the own variance shares as the proportion of the H-step ahead error variance in predicting x_i due to shocks in x_i itself, $\forall i = 1, ..., n$. On the other hand, the cross variance shares (spillovers) are defined as the H-step ahead error variance in forecasting x_i due to shocks in x_j, $\forall i = 1, \cdots, n$ with $j \neq i$.

In other words, denoting as $\theta_{ij}^g(H)$ the KPPS H-step forecast error variance decompositions, with $h = 1, \cdots, H$, we have:

$$\theta_{ij}^g(H) = \frac{\sigma_{jj}^{-1} \sum_{h=0}^{H-1} (e_i' \Psi_h \Sigma e_j)^2}{\sum_{h=0}^{H-1} (e_i' \Psi_h \Sigma \Psi_h' e_i)}, \tag{4.5}$$

with σ_{jj} being the standard deviation of the innovation for equation j and e_i the selection vector, i.e. a vector having one as i^{th} element and zeros elsewhere. Intuitively, the own variance shares and cross variance shares (spillovers) measure the contribution of each variable to the forecast error variance of itself and the other variables in the system, respectively, thus giving a measure of the importance of each variable in predicting the others.

Note that the row sum of the generalized variance decomposition is not equal to 1, meaning $\sum_{h=0}^{H-1} \theta_{ij}^g(H) \neq 1$. Diebold and Yilmaz (2012) circumvent this problem by normalizing each entry of the variance decomposition matrix

by its own row sum, i.e. :

$$\tilde{\theta}_{ij}^{g}(H) = \frac{\theta_{ij}^{g}(H)}{\sum_{j=1}^{n} \theta_{ij}^{g}(H)}. \tag{4.6}$$

This tackles the above mentioned issue and yields to $\sum_{j=1}^{n} \tilde{\theta}_{ij}^{g}(H) = 1$, and $\sum_{j,i=1}^{n} \tilde{\theta}_{ij}^{g}(H) = n$.

As a measure of the fraction of forecast error variance coming from spillovers, Diebold and Yilmaz (2012) define the total spillover index (TSI):

$$TSI(H) = \frac{\sum_{\substack{j=1 \\ j \neq i}}^{n} \tilde{\theta}_{ij}^{g}(H)}{\sum_{j,i=1}^{n} \tilde{\theta}_{ij}^{g}(H)} \cdot 100 = \frac{\sum_{\substack{j=1 \\ j \neq i}}^{n} \tilde{\theta}_{ij}^{g}(H)}{n} \cdot 100. \tag{4.7}$$

Moreover, we also make use of directional spillovers indexes (DSI) to measure, respectively through Equations (4.8) and (4.9), the spillover from exchange i to all other exchanges J (cfr. Equation (4.8)) and the spillover from all exchanges J to exchange i (cfr. Equation (4.9)) as:

$$DSI_{J \leftarrow i}(H) = \frac{\sum_{\substack{j=1 \\ j \neq i}}^{n} \tilde{\theta}_{ji}^{g}(H)}{\sum_{j,i=1}^{n} \tilde{\theta}_{ij}^{g}(H)} \cdot 100 \tag{4.8}$$

$$DSI_{i \leftarrow J}(H) = \frac{\sum_{\substack{j=1 \\ j \neq i}}^{n} \tilde{\theta}_{ij}^{g}(H)}{\sum_{j,i=1}^{n} \tilde{\theta}_{ij}^{g}(H)} \cdot 100. \tag{4.9}$$

Directional spillovers may be conceived as providing a decomposition of total spillovers into those coming from - or to - a particular variable. In other words, they measure the fraction of forecast error variance which comes from (or to) one of the variables included in the system - and, hence, the importance of the variable itself in forecasting the others. From the definitions of directional spillover indexes, it is natural to build a net contribution measure, impounded in the net spillover index (NSI) from market i to all other markets J, namely:

$$NSI_i(H) = DSI_{J \leftarrow i}(H) - DSI_{i \leftarrow J}(H). \tag{4.10}$$

Another very important metric to measure the difference between the gross shocks transmitted from market i to j and gross shocks transmitted from j to i is the net pairwise spillover (NPS), defined as:

$$PNS_{ij}(H) = \left(\frac{\tilde{\theta}^g_{ij}(H)}{\sum_{q=1}^{n} \tilde{\theta}^g_{iq}(H)} - \frac{\tilde{\theta}^g_{ji}(H)}{\sum_{q=1}^{n} \tilde{\theta}^g_{jq}(H)} \right) \cdot 100. \tag{4.11}$$

All the metrics discussed above are able to yield insights regarding the mechanisms of market exchange spillovers both from a system-wide and a net pairwise point of view. Furthermore, performing the analyses on rolling windows we are able to study the dynamics of spillover indexes over time.

4.4 Data and empirical findings

4.4.1 Data

To test our proposal, we make use of historical data, according to a retrospective analysis. In particular, we use daily foreign exchange rate data over the period January 2002 - November 2019, obtained from *investing.com*. To build our optimal basket of currencies, we collect data relative to the foreign exchange pairs between the currencies that are included in the IMF's Special Drawings Rights: the US dollar, the Chinese Renmimbi, the Euro, the British pound and the Japanese Yen. According to our research assumption, we will assume that the obtained basket of currencies correspond to a stable coin which can be exchanged and compared with a single currency based stablecoin, for example based on the US dollar. This, in particular, for foreign individuals sending remittances to their home country. To understand the relationship between major currencies and remittances we also collect data on the largest remittance markets - namely, the Indian Rupee, Mexican Peso,

Table 19: Optimal weights

Currency	USD	CNY	EUR	GBP	JPY
Optimal Weights	0.17	0.2	0.23	0.19	0.21
IMF SDR Weights	0.42	0.11	0.31	0.08	0.08

Note: Weights of the currency in the chose basket, according to our methodology (Optimal) and the IMF Special Drawing Rights (IMF SDR)

Philippines Peso, Nigerian Naira. Moreover, for what concerns the volatility analysis, we divide the sample into subsets which define the pre-crisis period (2002-2008), crisis period (2009-2011) and post-crisis period (2012-2019).

Finally, for the sake of comparison with a widely known basket-based currency such as the IMF SDR, we also collect data relative to the foreign exchange pair of the dollar with the IMF Special Drawing Rights.

4.4.2 Optimal basket and stability analysis

First of all, we compute the RNVALs as described in Section 4.3. The resulting weights are contained, together with those of the IMF SDR, in Table 19.

From Table 19 note that our method yields weights which are relatively equal among each other, in fact each are approximately a fifth, with a slightly heavier weighting on the EUR. The weights are quite different from the weights of the IMF SDR, which are highly concentrated on the USD dollar. Fluctuations of SDRs will strongly be correlated with fluctuations in USD and EUR. The SAC distributes the weights more evenly across the basket to minimise the variations in fluctuations. Since, the basket is comprised of hard currencies the diversification tends to work since the currencies move systematically over time relative to one another. Such that, if the value a particular currency depreciates relative to the SAC, but simultaneously there is an appreciation of another currency, their movements would tend to cancel

each other, all else the same. Note, that China has managed a floating peg against the USD and hence these two currencies are likely to be strongly linked. In the SDR these two currencies make up 53% of the basket compared to 37% in the SAC. Indicating, perhaps more diversification is needed to offset movements in the dollar. To better interpret the results, Figure 12 represents the time series of the Reduced Normalised Values of all considered currencies in the basket, along with our basket based stable coin, in the considered period.

Figure 12 shows the evolution of the RNVALs of the currencies composing the basket during the whole sample period. From Figure 12 note that, after a first period of small turbulences, the time series start to diverge roughly from the beginning of 2006 onwards. From that point in time onwards, two clusters seem to emerge from the graph: the first one includes USD and CNY, while the second one pertains EUR, GBP and JPY. This is arguably due to the fact that, for many years, the CNY value was pegged to the dollar and, therefore, its dynamics over time shows quite similar patterns to that of the USD. Note that, as expected by construction, the Reduced Normalised Value of the basket based stable coin lies in the middle, "mediating" between the different currencies, and compensating single deviations with diversification benefits.

For the sake of analyzing the world's emerging market currencies with the highest portions of remittances, we recompute the RNVALs including them. The corresponding graphical representation is contained in Figure 13. In the figure we have included, besides our basket based stable coin, another one that employs the same weights as the Special Drawing Rights.

Figure 13 shows that emerging market currencies such as the Mexican Peso (MXN) and the Philippine Peso (PHP) appreciate consistently with respect to the other fiat currencies in the basket over time. All the other currencies, instead, seem to belong to another cluster, in the sense that they do not follow an upward trend as the previous ones, but rather fluctuate below the value of 1, with different patterns. The only exception is the

Figure 12: Time evolution of the Reduced Normalised Values and of the basket based stable coin (SAC)

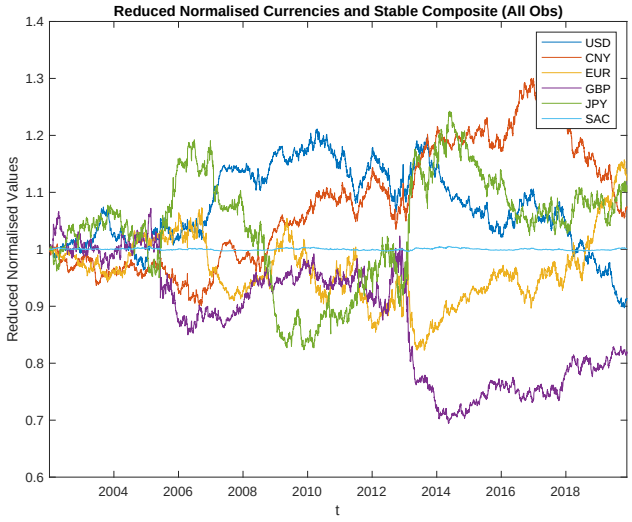

Note: Time evolution of the Reduced Normalised Values and of the basket based stable coin (SAC)

Figure 13: Time evolution of the Reduced Normalised Values

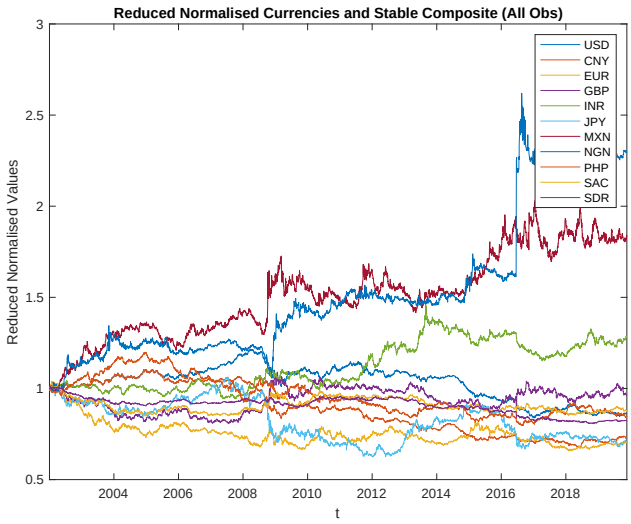

Note: Time evolution of the Reduced Normalised Value of the basket currencies (USD, CNY, EUR,GBP, JPY), of the considered emerging market currencies (INR, MXN, NGN, PHP) and of the basket based stable coins (SAC, SDR)

Indian rupee (INR), whose value grows over time, although not with the same magnitude as MXN and PHP do. Note that both basket based stable coins lie in the middle, similarly as in Figure 12, although their Reduced Normalised values fluctuate. This because the baskets are built using only five currencies, but are normalised with respect to all nine included in Figure 13.

To understand more precisely which stable coin is more stable (Libra: single currency based, or Librae: basket based), Table 20 presents their volatilities, measured by their standard deviations in the considered time period. The table presents also the correlations between the currencies, which help in the interpretation of the results.

Table 20 shows, as far as correlations are concerned, that USD and CNY exhibit relatively strong negative or little correlation with others currencies in the basket, but are weakly positive between themselves, consistently with

Table 20: Volatility and Correlations between the RNVALs and basket based stable coin.

	USD	CNY	EUR	GBP	JPY	SAC
USD	1	0.14	-0.68	0.01	-0.41	0.02
CNY	0.14	1	-0.4	-0.8	0.17	0.02
EUR	-0.68	-0.4	1	0.26	-0.09	0.03
GBP	0.01	-0.8	0.26	1	-0.64	0.02
JPY	-0.41	0.17	-0.09	-0.64	1	0.02
SAC	0.02	0.02	0.03.	0.02	0.02	1
σ	0.07	0.1	0.06	0.1	0.09	0.002

what observed in Figure 12. Moreover, one can clearly notice that the EUR acts as a good diversifier, as its pairwise correlations are quite low if compared to those between other currencies. More importantly, from the correlation matrix we can deduce that the stablecoin shows correlations with the other currencies whose values are very close to zero. Low correlations with the other currencies is a clear sign of the goodness of our stablecoin in being isolated with respect to the fiat currencies' dynamics and, therefore, arguably stable. In terms of volatility, the standard deviations show that the most volatile currency is CNY, followed by JPY and USD. Our stablecoin exhibits a standard deviation magnitude which is much lower than those of the other currencies and about ten times lower than that of the least volatile one, namely EUR. This is a clear sign of stability of the proposed stablecoin, as opposed to an hypothetical stablecoin pegged to one single currency.

To determine whether a basket-based stablecoin would be a more valuable and more stable alternative than a stablecoin pegged to a single currency, especially for remittances, we can, in analogy with 13, compare the volatility of our stablecoin with that of a SDR based basket, and with the currencies of the most important emerging markets in terms of remittances. Table 21

Table 21: Volatility of the RNVALs

	USD	CNY	EUR	GBP	INR	JPY	MXN	NGN	PHP	SAC	SDR
σ_{all}	0.09	0.14	0.07	0.06	0.13	0.11	0.23	0.41	0.10	0.04	0.05
σ_{pre}	0.04	0.03	0.08	0.05	0.02	0.05	0.10	0.07	0.06	0.04	0.02
σ_{cri}	0.05	0.05	0.03	0.06	0.03	0.10	0.09	0.10	0.03	0.03	0.02
σ_{post}	0.1	0.06	0.03	0.04	0.08	0.07	0.16	0.39	0.04	0.03	0.05

Note: Volatility of the RNVALs of the basket currencies, of the emerging market currencies, and of the two basket based stable coins, over the whole period (all), the pre-crisis period (pre), the crisis period (cri) and the post-crisis period (post).

contains the comparison, over the whole period and also in three distinct periods, corresponding to the pre-crisis period, the crisis period and the post-crisis period.

From Table 21 first row, it is clear that overall the stablecoin exhibits lower values of volatility, when compared to the other traditional fiat currencies. The other rows in the Table show that is often the case, although especially during pre-crisis and crisis period few currencies exhibit slightly lower volatilities, depending on how and when they were affected by the global financial crisis. However, we can notice that the stablecoin's volatility is much more stable than that of the other currencies which, although for some period slightly lower, show quite relevant jumps in magnitude. Moreover, the proposed stablecoin exhibit lower volatilities over the whole time period if compared to the single currencies in the basket and to the single emerging market currencies. This can be read as a strength of our stablecoin, as it could function as a better medium of exchange than a country's single currency, in particular as far as remittances are concerned. Note also that the SDR is a valid alternative to our stable coin, possibly easier to implement, from a political consensus viewpoint.

Table 22: Currency spillovers

	USD	CNY	EUR	GBP	JPY	FROM
USD	44.94	35.33	13.02	6.67	0.04	11.01
CNY	34.49	49.40	10.76	5.34	0.00	10.12
EUR	15.81	15.22	62.29	6.48	0.19	7.54
GBP	11.4	10.21	6.28	69.58	2.53	6.08
JPY	0.41	0.14	0.01	3.94	95.51	0.90
TO	12.42	12.18	6.01	4.49	0.55	35.66

4.4.3 Spillover network analysis

We now consider spillovers between exchanges, to evaluate the price change connectedness of the currencies that compose the basket, and to understand which is the relative importance of each of the currencies in transmitting shocks. In this way, we are also able to determine which currencies potentially cause strong (or weak) price changes in our proposed stablecoin value.

As far as specifications are concerned, VAR models are built on price changes in reduced normalised values (RNVALs). We use a VAR lag determined by a Bayes-Schwarz information criterion (BIC) that penalises over-parameterisation compared to other widely employed information criteria. The optimal number of lag determined by the BIC is 1. We use a $H = 100$ step-ahead forecast horizons for forward iteration of the system. Additionally, dynamic spillovers use a rolling estimation window of length 100 observations.

Firstly, we provide an analysis of unconditional price change spillovers, that are spillovers evaluated on the whole sample period. The results are shown in Table 22.

From Table 22 note that there are two currencies which are highly interconnected with the others, meaning USD and CNY, whereas EUR, GBP and in particular JPY are more isolated in terms of return connectedness. Furthermore, the scene appears to be dominated by USD and CNY, whose

Figure 14: Overall spillovers

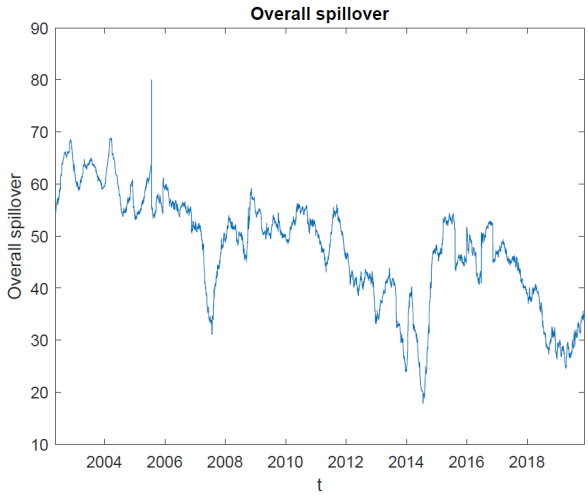

contributions in terms of price change spillovers towards other currencies are much higher than those of the remaining currencies in the basket.

The analysis of dynamic spillovers is able to clarify the results obtained in the unconditional spillover analysis by means of observing the evolution of spillovers over time. Figure 14 shows the results.

Figure 14 depicts the overall dynamic spillover plotted over the sample period. The overall spillover within the basket ranges from a minimum of 17.87% to a maximum of 80.00%. It seems that the overall spillover follows a generally decreasing trend, as it starts from 54.51% at the beginning of the sample period, while it diminishes to 34.43% at the end of the studied time frame.

Dynamic directional spillovers can shed light on which of the currencies transmit price change spillovers to others and which of them receive price change spillovers from others. We plot from, to, net and pairwise spillovers in Figures 15, 16 and 17, respectively.

From the joint analysis of Figures 15, 16 and 17 we can highlight that that USD is the most influential currencies in terms of return spillovers. Indeed, the magnitude of spillovers received from others is weak compared to that

Figure 15: From spillovers

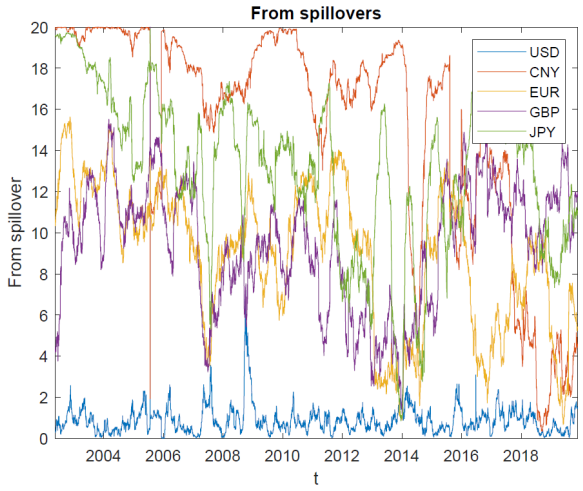

Figure 16: To spillovers

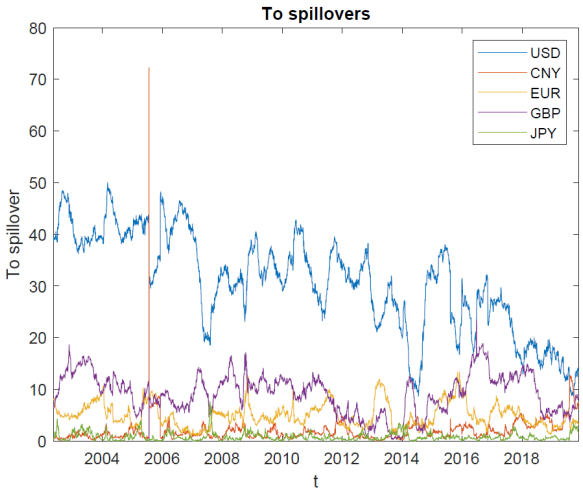

Figure 17: Net spillovers

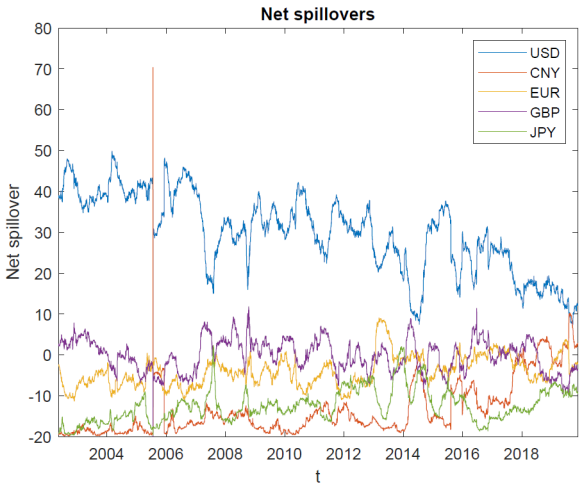

transmitted to others. Moreover, the net spillover dynamics summarizes the dominant position of the USD, being it always positive and taking relatively high values over the sample period. However, the magnitude of spillovers transmitted by USD follows a negative trend over time, meaning the currency is gradually losing its potentiality to contribute to the evolution of the others, perhaps due to the affirmation of emerging economies in the latter period, especially after the 2009 crisis. CNY is indeed emerging as a dominant currency during the recent times. Despite that, the latter considerations are in line with the full sample results obtained above, which point to the dominance of USD as a spillover transmitting currency.

Differently from what emerged in the full sample analysis, instead, the dynamic analysis shows that CNY has not been such a leading currency in transmitting price change shocks from an historical viewpoint. Indeed, the full sample result is arguably driven by a noticeable spike which occurred on 21 July 2005. Indeed, during that day the Chinese Central Bank officially announced the abandonment of the eleven-year-old peg to the dollar and pegged the CNY to a basket of currencies whose composition was not disclosed. This caused a prompt revaluation to CNY 8.11 per USD, as well

as to 10.07 CNY per euro. However, the peg to the dollar was reinstituted as the financial crisis strengthened in July 2008. These results indicate that CNY does not particularly contribute to the price change evolution of the other currencies in the basket, although it can exert shocks through sudden policy decisions.

The dominance of the USD and, to a lesser extent, of CNY emerges also when analyzing the directed network structure of the currencies in terms of net pairwise spillovers represented in Figure 18. In this context, the network edges are represented by the currencies in the basket, whereas edges represent the magnitude of net pairwise spillovers for each currency pair.

To verify the loss of importance of the dollar, we can extend the spillover network analysis to cover the Covid-19 outbreak period of March-April 2020. Specifically, we analyze two subsamples with the year 2020 as cutting point, to detect major changes in country forex spillover dynamics.

The spillover network gives a ranking in terms of spillover transmission capacity and, therefore, price discovery. The most influential currency in terms of price change shock transmission is USD, followed by CNY and, to a lesser extent, GBP. The two receivers are instead JPY and, at most, EUR. The highest influence is given by USD towards EUR, followed by CNY to JPY. This suggests that the contagion occurs to a greater extent within Asian currencies and across American and European ones.

However, the picture is different when analyzing spillovers during two distinct sub-samples: one ranging from September 2017 to December 2019, and another one from January 2020 to April 2020, both depicted in Figure 19. Indeed, overall interconnectedness has increased in the second sub-sample, likely due to the Covid-19 outbreak, thus markets move more similarly as a consequence of the epidemic. This is equivalent to say there are more contagion dynamics occurring since the Covid-19 outbreak and that magnitude of information transmitted from the currencies sharply increased after the Covid-19 crisis. Moreover, they highlight that the contagion dynamics is very different from that of the pre-crisis period. USD is no longer dominant,

Figure 18: Spillover network (full sample)

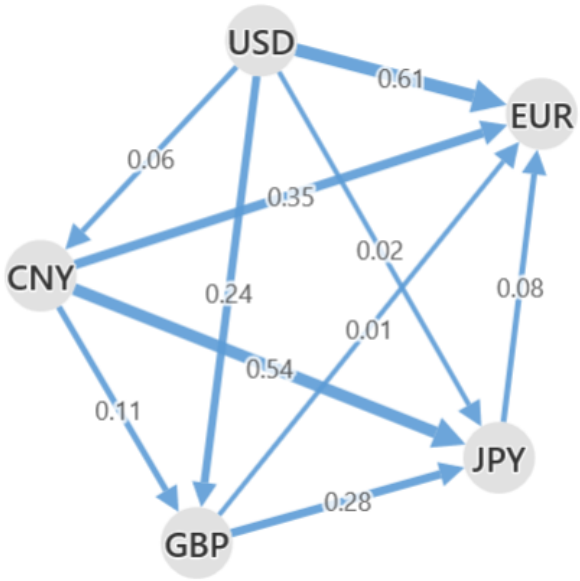

Note: The figure represents the spillover network of the currencies included in the basket over the full sample period. The nodes are represented by the currencies included in the basket. The magnitude of the links is represented by the net pairwise spillovers between each currency pair.

whereas Asian countries with CNY and JPY, which encountered the Covid-19 outbreak before others, turn out to be the strongest currency shock propagators, along with an augmented relative importance of GBP. This suggests that the spillover dynamics has been somehow linked to the virus spread, meaning financial shocks occurred first in the countries first hit by the virus, specifically the Asian ones, and then awareness gradually spread through the Euro zone and the United States. It also highlights the importance of monitoring the spillover dynamics in the basket both to have a systemic risk indicator and to determine lead-lag relationships among currencies in the basket when designing basket-based stablecoins.

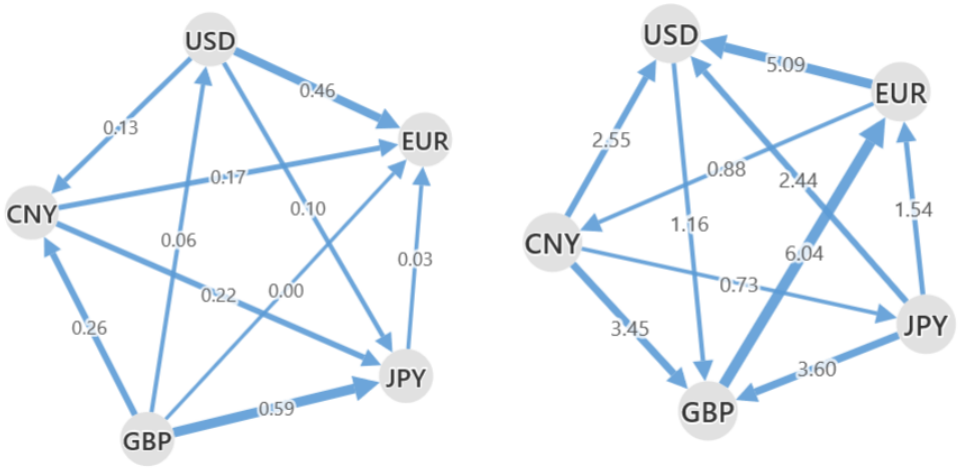

Figure 19: Spillover networks (sub-samples)

Note: The figure represents the spillover network of the currencies included in the basket. The first representation corresponds to the period September 2017 to December 2019 (panel a), while the second one from January 2020 to April 2020 (panel b). The nodes are represented by the currencies included in the basket. The magnitude of the links is represented by the net pairwise spillovers between each currency pair.

4.5 Conclusion

In this chapter we present a methodology to build a basket based stable coin whose weights can maximise stability over a long time period. The weights have been calculated, retrospectively, for the period that follows 2002, and show a distribution more even than the IMF Special Drawing Rights weights.

The proposed stable coin (Librae) appears to be less volatile than single currencies and, therefore, with respect to single currency stable coins (Libra). It can thus constitute a valuable proposal especially for workers who live abroad and make remittances to their own country, a market segment with a high potential of being attracted by payments in stablecoins.

We have also proposed a variance decomposition technique based on a

VAR model aimed at showing which currencies mostly impact the Foreign Exchange market and whether a single currency or a basket based stablecoin is more resilient to currency shocks. Our results show that the dollar is the currency which mostly impact the market, and that a basket based coin is better than a dollar based one, from a stability and value maintenance viewpoint. However, CNY is taking over as spillover transmitter and USD is gradually losing its influence over time, especially with regards to the latest period, characterised by the Covid-19 otubreak.

With a basket based stablecoin it is possible to offset the risk of currencies shocks. This is of relevance for different policy purposes and, in particular, for emerging markets and countries having high remittances. Indeed, by holding stablecoins rather than single currencies the risks associated to currency shocks are mitigated and stablecoins holder can count on a currency whose value is less volatile than traditional fiat currencies and, thereby, more reliable. The latter fact has also positive consequences on cross-border payments side, provided that the stability of the stablecoin mitigates the foreign exchange risk, thus contributing to the fact that buyers and sellers give or receive an amount of money whose value is less sensitive to variations over time.

Future research may consider basket that dynamically evolve over time ("AI baskets"), although these are bound to be more difficult to achieve consensus. Furthermore, currency volumes in circulation may be taken to account, along with the technical characteristics of the coins (for example: cybersecurity, redeemability, reliability), from a different, more theoretical, viewpoint.

5 Information Flow in the Credit Risk Market: Evidence from the European Sovereign CDS and Government Bonds

Based on the paper:
Caserini, Nicoló, & Pagnottoni, Paolo. 2020. Information Flow in the Credit Risk Market: Evidence from the European Sovereign CDS and Government Bonds. *Working Paper*.

5.1 Introduction

The rapid development of credit derivative products, in particular by the first decade of 2000, led to a remarkable financial innovation which could considerably improve the protection of market participants against the exposure to the credit risk of a specific entity. Among credit derivatives, credit default swap (CDS) has become one of the most widely traded instruments, especially in the aftermath of the collapse of the investment bank Lehman Brothers in September 2008. When the market pricing of government and company debt was significantly affected during the crisis outbreak, investors all over the world widely used the CDS market to hedge their credit exposures as well as to extend their investment opportunities. The CDS premium, which depends on the default probability of the underlying entity, played a growing role as an instrument through which information on credit risk is disclosed, potentially in competition with the bond market (Coudert and Gex, 2013). Indeed, the CDS premium should be approximately equal to the spread of a bond over a risk-free rate on the same reference entity and of the same maturity, since both instruments price the credit risk associated with a specific underlying entity. As a consequence, an approximate arbitrage relation between the bond spread and the CDS premium exists, as clearly discussed by Duffie (1999).

In light of this, the literature on credit risk started to investigate the

dynamic relationship between the CDS and the bond market, in order to assess which of these two assets is faster at incorporating information about the credit risk of the underlying entity in their prices. In other words, the relation between the CDS and bond market has been explored to investigate which market leads the price discovery process. Many researches devoted particular attention to the information leadership of credit risk in CDS and bond markets using data on corporate entities. In this context, econometric approaches based on cointegration revealed that the CDS market moves quicker than the bond one in terms of price discovery. Such results, mostly referring to the global financial crisis, are closely related to the relative size and liquidity of the CDS and the corporate bond market. As discussed in detail by Coudert and Gex (2013), market participants are more prone to benefit of particular information regarding a given company by trading a CDS rather than a bond, due to the greater liquidity of the CDS market. Consequently, liquidity seems to play an important role in fostering a market's leadership in the price discovery process.

This finding in the corporate framework led a branch of the literature to investigate the relationship between the CDS and the bond market across governments, in order to examine which market is the most efficient in pricing the information of the sovereign credit risk, and especially to examine if the CDS market could be entitled as a leader in the price discovery process for sovereign entities as well. However, as opposed to the corporate framework, results are found to be very mixed and ambiguous for sovereigns, as discussed by Augustin (2014). Different authors suggest that these discrepancies in the price discovery analysis may be related for example to the relative liquidity of both markets (see Ammer and Cai (2011)) or to market frictions, such as counterparty risk and funding costs (see Arce et al. (2013)) or to differences in how bond spread are calculated (see Gyntelberg et al. (2013)). As a consequence, no unique results have been found on the leadership between the two markets so far.

As a common point discussed by the extant literature, the arbitrage rela-

tion between the CDS premium and the bond spread is not perfect. Market imperfections, such as the cheapest-to-deliver (CTD) option, unavailability of instruments with exactly matching maturity dates, or liquidity premia can impair the relationship between the two markets in the long-run. Indeed, the existence of a long-run equilibrium relationship is not always proved and, when the lack of this assumption occurs, information measures based on Vector Error Correction Models (VECM) cannot be applied. This is usually circumvented by means of the Granger causality test based on a Vector Autoregressive Model (VAR), able to detect lead-lag relationship between the two markets when no evidence of cointegration is found. However, as for the VECM, Granger causality requires restrictive assumptions for the linear dynamics of the model. Thus, the failure to provide the existence of a long-run equilibrium relationship between the two time series and the restrictive assumptions for the linear dynamics of the models require additional techniques to detect a possible interaction between the CDS and the bond market.

In this chapter we cope with the missing cointegration relation between the CDS premium and the bond spread, and we measure the interactions between the CDS and the bond markets by means of the practical background proposed by Dimpfl and Peter (2013). It consists of an alternative methodology which uses the concept of transfer entropy to examine the information flow between the CDS and the corporate bond market. Based on the concept of Shannon Entropy developed in information theory by Shannon (1948), transfer entropy has been subsequently introduced by Schreiber (2000) to measure the dependency between two variables in time. Such a measure is a model-free approach able to detect statistical dependencies without being restricted to linear dynamics. Indeed, the use of the transfer entropy does not require the assumptions of the standard models, like cointegration in the present context, and can be applied more easily in a variety of areas in research.

Against this background, our aim is to analyze the interactions between

the CDS and the government bond market for countries of the European Union, and to address the question of which market is the first to reflect new information in pricing sovereign credit risk. Given the puzzling conclusions for sovereign entities provided by the literature so far, we aim to shed some light on the price discovery leadership between the CDS and bond markets. This is done through the transfer entropy methodology outlined by Dimpfl and Peter (2013). Therefore, our contribution to the literature is mainly twofold.

Firstly, we contribute by applying transfer entropy to the CDS and bond market in the sovereign context. As a matter of fact, due to the increasing evidence of the highly nonlinear market interactions in the framework of econophysics, transfer entropy has become an appealing tool and has been widely used from the quantification of information flow between stock indices (Marschinski and Kantz, 2002) to the interaction between exchange rates and stock markets (Sensoy et al., 2014). However, to the best of our knowledge, there is no study yet examining price discovery in the sovereign CDS and bond market using such a technique, which allows us to overcome restrictive assumptions on the data.

Secondly, the choice of the selected period from 1 January 2010 to 31 December 2018 gives a relevant contribution to the reference literature. Indeed, most of the analyses conducted on European countries did not deeply investigate the relationship between the two markets after 2012, when still the situation in the Eurozone was changing drastically, especially for the countries with slower economic growth and higher spread. On the contrary, analyzing a wider timespan allows us to yield results for both the European sovereign crisis and the post-crisis period, characterized by very low bond yields.

Results show evidence of a significant bi-directional information flow between the CDS and the bond market and a clear dominance of the bond market from a price discovery point of view. In particular, during the period which covers the sovereign debt crisis, the information flow from the bond to

the CDS market is more remarkable with respect to that from the CDS to the bond market, especially for core countries of the European Union with lower yield. During the post-crisis period, less information flow between both markets is observed and a few sovereigns behave dissimilarly, although generally speaking the bond market still dominates the CDS market in terms of price discovery.

Our results on the dominance of the bond market might give relevant insights for policy makers and market participants. From a risk management prospective, our findings highlight the importance of the bond spread as a reliable market indicator of sovereign credit risk during a crisis period, provided that it is able to respond faster to economic fundamentals and global financial market factors. This suggests to policy makers that an extensive use of the CDS market as a hedging instrument does not directly lead to a consequent increase of funding costs of the sovereigns, and hence to high level of bond spread. In addition, institutional investors can benefit to know which market has a leadership role on the other, so to take advantage of market imperfections and to set up profitable arbitrage strategies.

The remainder of this chapter is structured as follows. Section 2 provides a literature review on the relation between the CDS and the bond market and on the transfer entropy. Section 3 introduces the concept of transfer entropy. In section 4 the data will be presented and analyzed. Section 5 illustrates and discusses the empirical outcomes. Section 6 concludes.

5.2 Literature review

This contribution relates to a branch of the literature based on the relation between the CDS and the bond markets and especially on the identification of the leading market in pricing the credit risk. To give a better understanding of the fundamental empirical and methodological framework, we firstly introduce the literature regarding price discovery and efficiency between the two markets. After that, we discuss the methodological background linked to our analysis.

5.2.1 Price discovery process in CDS and Bond markets

As explained in theory by Duffie (1999), the spread on a par floating-rate bond over a risk-free benchmark should be equal to the CDS premium for the same entity and maturity, since both markets offer a similar exposure to the credit risk of the underlying entity. Therefore, the two markets are linked by an approximate arbitrage relationship. Against this background, the CDS premium and the bond spread should be cointegrated and driven by a common stochastic trend, interpreted in this case as the efficient price of credit risk. This relationship led many researchers to analyze the dynamic behavior of the two assets, in order to ascertain the informationally dominant market.

The pillar methodologies of the price discovery analysis in this field were applied in first place by Blanco et al. (2005). They used a VECM to find an equilibrium long-run relation between the pricing in the two markets for a sample of 33 investment-grade North American and European firms in a restricted period of 18 months between 2001 and 2002. As far as the firms for which the equilibrium holds are concerned, the empirical measures of Hasbrouck (1995b) and Gonzalo and Granger (1995b) highlight that the CDS market leads the bond market in determining the price of credit risk. Consecutive studies found the predominance of the CDS market with respect to the bond market in corporate entities (e.g., Zhu (2006); Baba and Inada (2009); Molleyres (2018)), and a common point of the aforementioned literature regards the discussion of various market imperfections that can hinder the equal price of the two markets in the long term, making the arbitrage relationship not perfect. Such market imperfections move the so-called "basis", defined as the difference between the premium on the CDS and the corresponding bond spread on the same entity and with the same maturity, away from the theoretical value of zero. The arbitrage opportunity due to such deviations from the parity led various researches to analyze the topic from two main viewpoints.

On the one hand, a branch of literature discusses empirical causes of a

non-zero basis, especially in the area of sovereign entities in times of market stress (e.g., Ammer and Cai (2011); Palladini and Portes (2011); Arce et al. (2013); Fontana and Scheicher (2016); Gyntelberg et al. (2017)). Among the main factors that can deviate the basis away from the theoretical value of zero, particular attention has been dedicated to the CTD option. By means of the CTD option, the buyer of the CDS has the incentive to deliver the lowest valued bond of the underlying entity in case of default, causing disadvantage for the seller and a higher CDS premium. Liquidity premia is another factor that can, for example, increase the bond spread if the risk-free bond market is more liquid than the risky bond. The counterparty risk of the seller of a CDS can also affect the basis, due to the over-the-counter nature of the respective derivative market. The perception of a lower quality of the contract sold may affect the price of the CDS, hence yielding to a negative value of the basis.

On the other hand, a wide stream of literature employ a variety of investigation strategies to examine the relationship between the two markets with the aim of identifying the leading one in terms of price discovery in sovereign contexts. Ambiguous results in sovereign entities can be found in the literature, with consequent considerations regarding the key determinants of price discovery. The relationship has initially been investigated among emerging countries. Chan-Lau and Kim (2004) examined the equilibrium price relationship and the price discovery process for eight emerging sovereigns in the period between 2001 and 2003, but the mixed results accomplished by the Granger causality test combined with the price discovery measures did not deliver to the authors any strong conclusion about the price discovery leadership. Using data for nine emerging sovereigns for the period from 2001 to 2005, Ammer and Cai (2011) found that bond spread leads the CDS premium more often than what had been found for investment-grade corporate entities. This finding has been reported for emerging economies that have issued more bonds, confirming the key determinant role of liquidity in capturing the relative contribution to price discovery, as discussed by Chakravarty et al.

(2004). In contrast, Li and Huang (2011) found that in emerging sovereigns the CDS market plays a greater role than the bond market in the price discovery process for the period between 2004 and 2008, by means of an empirical analysis based on VECM and Granger causality tests.

Consecutive studies have been conducted on European economies, and still divergent results persisted. Fontana and Scheicher (2010) studied weekly CDS premia and bond spreads of ten countries of the European Union for the period between 2006 and 2010 and found heterogeneous otucomes on the lead-lag relationship between the two markets. Delis and Mylonidis (2011) focused on Southern European countries with fiscal vulnerabilities, such as Greece, Italy, Portugal, and Spain, performing a series of rolling Granger causality test and showed that the CDS market Granger causes the government bond market after since the start of the global financial crisis in 2007. A notable contribution in the methodology has been proposed by Delatte et al. (2012), who used a Panel Smooth Transition Error Correction Model to overcome the restricting hypothesis of the linear specifications. The model, applied to eleven European Union countries in the phase of the global financial crisis, revealed the bond market of core European economies as leader of the price discovery process during calm periods. A leadership in the CDS market was instead found during distress periods. A considerable contribution to the extant literature is that of Coudert and Gex (2013), who focused on the interaction between the two markets during the global financial crisis, from the beginning of 2007 to 2010. By means of the Gonzalo and Granger (1995b) measure, they showed the leadership of the CDS market in the price discovery process for a sample of 17 financial companies. However, the same analysis conducted on 18 sovereigns, including both advanced and emerging economies, delivered different results and highlighted a leader role of the bond market for low-yield government issuers. Recently, Agiakloglou and Deligiannakis (2020) investigated the relationship for eight European Union countries between the two markets using Granger causality. They did not find evidence of cointegration between the two markets during calm period,

and conclude that the bond market led the price discovery process during the post-crisis period. Another recent analysis has been conducted by Patanè et al. (2019), who analyzed the link between the CDS premium and the bond spread for core and peripheral countries in the Eurozone during a wider timespan, ranging from 2011 to 2018. When cointegration was found, they concluded that the bond market played a leader role in the price discovery process during the period of financial distress, and only during the subsequent period between 2014 and 2018 the CDS market gained more importance.

The ambiguity of results in the literature may be caused by the differences in the analyzed timespans and by the different maturities of the relative assets used in the analysis, as discussed in Gyntelberg et al. (2013). Additionally, different econometric procedures are usually implemented, due for example to the nonlinearity mechanism between the bond market and the CDS market, as discussed in Delatte et al. (2012), and to the lack of cointegration that motivates the use of the Granger causality test. In order to overcome these problems, this chapter gives a considerable contribution to the sovereign analysis proposed by the literature so far, making use of a model-free approach, which enables us to circumvent restrictive assumptions and model configurations.

5.2.2 Transfer entropy in economic and financial contexts

Various time series analysis approaches have been recently introduced in order to widen the class of statistical measures applied in social sciences. The growing evidence of nonlinear market interactions animated the literature to investigate the stock markets making a considerable use of methods borrowed from the statistical physics. Among these, the development of the transfer entropy turned out to be a very useful instrument to quantify information flows between financial time series. The concept of transfer entropy has been originally introduced by Schreiber (2000), based on the theory of Shannon entropy, to quantify the statistical coherence between systems evolving in time. As explained by the author, the mutual information developed by

Shannon (1948) was widely used to quantify the overlap of information content of two systems. However, since the mutual information does not express dynamical or directional information, the transfer entropy concept has been developed upon it, taking the dynamics of information transport into account (Schreiber, 2000, p. 461).

The introduction of the transfer entropy delivered to the financial literature an appealing tool to estimate information flows between time series in different contexts. One of the first research analyzing the information flows between financial time series has been accomplished by Marschinski and Kantz (2002). They proposed a modified version of the transfer entropy, called the effective transfer entropy, which overcomes the likely biased estimates due to small sample effects yielded by the methodology of Schreiber (2000). The authors investigated the information flow between the Dow Jones Industrial Average and the DAX stock index. The improvement of their results performed by the straightforward implementation of the estimator paved the way to a new measure able to quantify the information flows between various financial time series.

A stream of literature started to apply the transfer entropy and the modified version proposed by Marschinski and Kantz (2002) across international financial markets. Baek et al. (2005) focused on the daily closure price of 135 stocks listed on NYSE of different business sectors in order to investigate which industry influences at most the whole market. Kwon and Yang (2008a) examined the information flow between the S&P 500 index, the Dow Jones index and the stock price of 125 individual companies. Similarly, Kwon and Yang (2008b) analyzed the strength and direction of information flows among 25 stock indices. Reddy and Sebastin (2008) studied the interactions between the Indian stock and commodity market, while Sensoy et al. (2014) investigated the information flow between exchange rates and stock prices in different emerging countries.

Dimpfl and Peter (2013) offer a contribution to the literature which is very close to ours, as they studied the relationship between the corporate

CDS and the bond market through the transfer entropy methodology. Because of a possible lack of cointegration between CDS premium and bond spread, price discovery measures that rely on the existence of a cointegration relationship cannot be applied. To cope with this, they quantified the information flow between the two markets using the effective transfer entropy on 27 iTraxx Europe companies from January 2004 to December 2011. The provided results showed the dominance of the CDS market in pricing the credit risk, especially during the financial crisis period, in line with the existing literature (see Blanco et al. (2005)). In addition, Dimpfl and Peter (2013) proposed to assess the statistical significance of the estimated information flows through a bootstrap procedure of the underlying Markov process, which allows to derive the distribution of the estimated transfer entropy under the null hypothesis of no information flow and to subsequently evaluate the significance of results.

In this chapter we employ the transfer entropy methodology and the statistical significance metrics proposed by Dimpfl and Peter (2013) to the sovereign framework, rather than to the corporate one. In this way we are able to investigate the relation between the CDS premium and the bond spread for every sovereign analyzed, even as regards to the countries for which a cointegrating relationship is not supported by the data.

5.3 Methodology

The concept of transfer entropy in the context of time series has been firstly introduced by Schreiber (2000), and the foundations of such methodology are based on the information theory originally proposed by Shannon (1948). Shannon (1948) constructed a measure for uncertainty by averaging the amount of information gained from a certain state of a random variable over all possible states that can be assumed by the random variable itself

[12]. In order to address a theoretical explanation, consider a discrete random variable J with probability distribution $p(j)$, where j denotes the different outcomes that the variable J can take. According to Shannon (1948), the average number of bits needed to optimally encode independent draws from the distribution of J is given by

$$H_j = -\sum_j p(j)\, log\,(p(j)), \tag{5.1}$$

where the *log* is taken to be to the base 2 in order to indicate bits as units in which the information is measured, and the sum extends over all states j that can be assumed by the variable J. Strictly speaking, the higher the entropy measured by H_j, the higher is the uncertainty about the random variable J. Therefore, the Shannon entropy in Equation (5.1) shows the largest amount of uncertainty when all possible states of J are equally likely to be observed.

The Shannon entropy combined with the concept of Kullback-Leibler distance (see Kullback and Leibler (1951)) allows to measure the information flow between two processes. The Kullback-Leibler distance is used to measure the difference between two probability distributions, assuming that one of them represents an approximation of the other. As mentioned by Schreiber (2000), the Kullback entropy gives the excess number of bits needed in the encoding when a different probability distribution is used. In the bivariate case, the Kullback entropy is known as the formula for mutual information. In addition to J, consider another discrete random variable I with probability distribution $p(i)$. The corresponding Kullback entropy of the two random variables I and J, whose joint probability distribution is defined by $p_{IJ}(i,j)$, is given by

$$M_{IJ} = \sum_{i,j} p_{IJ}(i,j)\, log\, \left(\frac{p_{IJ}(i,j)}{p(i)p(j)}\right), \tag{5.2}$$

[12]As shown in the related literature, the quantity $log(1/p_j)$, with p_j indicating the probability of the event j, gives the amount of information that can be gained from the particular outcome j. The average amount of information per outcome over the total n outcomes, presented as $\sum_{j=1}^{n} p_j\, log\,(1/p_j)$, brings to the formula of Shannon (1948).

where $p(i)$ and $p(j)$ represent the marginal probability distributions of I and J, and the sum extends over all states i and j which can be assumed by the variables I and J, respectively. The mutual information in Equation (5.2) measures the deviation from the independence of the two random variables, and can be thought of as the reduction of uncertainty about one variable given by the knowledge of the other. However, it must be mentioned that the direction of information cannot be distinguished due to the symmetry of the measure.

For the application of these measures in time series context, Schreiber (2000) introduced a dynamical structure by considering transition probabilities. The relative measure to quantify the information flows is derived under the assumption that the dynamical structure of a discrete random variable I corresponds to a stationary Markov process of order k, implying that the probability to observe I at time $t+1$ in state i conditional on the k previous observations is $p(i_{t+1}|i_t, ..., i_{t-k+1}) = p(i_{t+1}|i_t, ..., i_{t-k})$. The average number of bits needed to encode one more state - or one more time series observation in the present case - if the previous states are known is then represented by

$$h_I(k) = -\sum_i p(i_{t+1}, i_t^{(k)})\, log\, (p(i_{t+1}|i_t^{(k)})), \tag{5.3}$$

where $i_t^{(k)} = (i_t, ..., i_{t-k+1})$. In the case of two processes I and J, still assuming that both are stationary Markov processes with k and l representing their respective order, Schreiber (2000) proposed to quantify the information flow from J to I by measuring the deviation from the generalized Markov property $p(i_{t+1}|i_t^{(k)}) = p(i_{t+1}|i_t^{(k)}, j_t^{(l)})$. The deviation from this assumption, embodied in the Kullback-Leibler distance, defines the transfer entropy (TE), which is computed as

$$TE_{J\to I}(k,l) = \sum_{i,j} p(i_{t+1}, i_t^{(k)}, j_t^{(l)})\, log\, \left(\frac{p(i_{t+1}|i_t^{(k)}, j_t^{(l)})}{p(i_{t+1}|i_t^{(k)})}\right), \tag{5.4}$$

where $TE_{J\to I}$ measures the amount of information flow from process J to process I. If the previous observations of J do not affect the transition

probability of I, then the transfer entropy $TE_{J\to I}$ is zero and no information flow in this direction is found. Since the transfer entropy is an asymmetric measure, $TE_{I\to J}$ can be similarly computed and it measures the information flow from I to J. Hence the difference between $TE_{J\to I}$ and $TE_{I\to J}$ allows to discover the dominant direction of the information flow.

As mentioned in Schreiber (2000), common choices of the order of the Markov process for l are $l = k$ or $l = 1$, and the last is usually preferred. Thus, the analysis in the current study is conducted by setting $k = l = 1$.

Since the transfer entropy measure in Equation (5.4) is constructed for discrete data, a partition of the time series into discretized values is necessary to conduct it for continuous ones, as it is frequently done in empirical applications. Following Dimpfl and Peter (2013), the symbolically encoded series $S(t)$ is obtained by partitioning the time series $y(t)$ into three bins as follows:

$$S(t) = \begin{cases} 1 & \text{for } \; y(t) \leq q_1 \\ 2 & \text{for } \; q_1 < y(t) < q_2 \\ 3 & \text{for } \; y(t) \geq q_2 \end{cases}. \tag{5.5}$$

In this way it is possible to replace each value of the time series y_t by a corresponding integer (1,2,3). As we will discuss further, the distribution of changes in the CDS premium and bond spread series motivates the choice of the quantiles in this setting.

Most of the related studies on financial time series data are conducted using a modification of the above transfer entropy, proposed by Marschinski and Kantz (2002). The adjustment suggested by the authors derives by the fact that small sample effects may lead the estimates of the transfer entropy to be biased. Therefore, a modified version called effective transfer entropy (ETE) is obtained by subtracting from the transfer entropy shown in Equation (5.4) the transfer entropy computed by using a shuffled version of the time series of the variable J. The effective transfer entropy can be formulated as follows:

$$ETE_{J\to I}(k,l) = TE_{J\to I}(k,l) - TE_{J_{\text{shuffled}}\to I}(k,l), \tag{5.6}$$

where the transfer entropy calculated with a shuffled version of the series J is represented by $TE_{J_{\text{shuffled}} \to I}(k, l)$. This methodology nullifies both the statistical dependencies between the two time series J and I and the time series dependencies of J, since a new time series is generated by a realignment of randomly drawing values from the time series J. As a consequence, $TE_{J_{\text{shuffled}} \to I}(k, l)$ converges to zero when the sample size increases and values of $TE_{J_{\text{shuffled}} \to I}(k, l)$ different from zero are due to small sample effects. As mentioned by Dimpfl and Peter (2013), it is common to shuffle the series many times and to use the transfer entropy estimate averaged over the replications in order to calculate the effective transfer entropy.

To conduct inference on the estimated information flows, we rely on the methods discussed in Dimpfl and Peter (2013). In other words, we assess statistical significance of the transfer entropy estimates by bootstrapping the underlying Markov process n times. By means of this procedure, the statistical dependencies between the series J and I are eliminated, but the dependencies within them are retained. Consequently, the distribution of the estimates under the null hypothesis of no information flow can be obtained by repeating the estimation of the transfer entropy using the simulated time series. Given the bootstrapped distribution of the transfer entropy estimates, the dominant direction of the information flow can be confirmed by deriving standard errors and p-values for the effective transfer entropy.

5.4 Data description and preliminary analysis

We analyze daily data on five-year sovereign CDS premia and sovereign bond yields for eight countries of the European Union, i.e. Italy, Belgium, Austria, France, the Netherlands, Ireland, Portugal and Spain. The sample includes what are arguably the core countries of the European Union (Belgium, Austria, France and the Netherlands) and peripheral countries with higher spreads (Italy, Ireland, Portugal and Spain). The time period examined ranges from 1 January 2010 to 31 December 2018. The time series of CDS premia and bond yields are collected from Thomson Reuters Datas-

tream. The time series of CDS premia and sovereign bond yields have the same maturity as well as they are all denominated in Euro.

The use of five-year maturity contracts with respect to the ten-year is justified by the higher liquidity of the CDS market, especially when the sovereign debt crisis intensified, as documented in Gyntelberg et al. (2013). The analysis of five-year maturity contracts is also in line with most of the extant literature.

In order to determine the government bond spread, the difference between the five-year bond yield of each sovereign and a five-year risk-free rate has to be computed. The risk-free rate is usually chosen between the swap rate or the bond yield of the country considered as less risky of a certain area. The use of the swap rate would be justified by the introduction in the analysis of Germany, which is the benchmark of the Euro area and hence usually used as the risk-free rate. Nevertheless, using the Euro interest swap rate yields negative values of the bond spread related to countries with high creditworthiness in the sample. To avoid this, the five-year German bond yield is used as risk-free rate in the present contribution, as it benefited from a lower interest rate on debt with respect to the other countries in the sample.

The sample period is selected to analyze the relationship between the two markets in crucial times for the European Union, i.e. from the beginning of the sovereign debt turmoil to the post-crisis period. Such a wide period allows us to adequately separate the sample into two phases and to independently conduct two selected sub-period analyses, one for the sovereign crisis period and the other for the post-crisis period. The phase from 2010 to the end of 2014 aims to detect the leading market for credit risk considering a larger interval of time than that usually adopted by previous literature. By doing so, the results are carried out both for the great intensity phase of the crisis in 2011 and 2012, when longer-term refinancing operations and bail-out programs were conducted by the International Monetary Fund and European Union institutions, and for the end of the year 2014, marked by the decline of government bond spreads due to the start of the programme of Outright

Monetary Transactions implemented by the European Central Bank. These results are then compared with the ones of the period from 2015 to the end of 2018, characterized by a relatively tranquil period and flattening of the analyzed curves, as a result of the European Central Bank monetary policies, the quantitative easing started at the beginning of 2015 and a lower trading activities in the CDS market as well.

The dynamics of the CDS premium and bond spread time series across countries are shown in Figure 20. During the sample period considered, both markets increased and reached their maximum level between 2011 and 2013, the peak of the European debt crisis. This effect levelled out and low levels of both CDS premium and bond spread can be observed in the subsequent years.

From the descriptive statistics reported in Table 23 we may notice a clear distinction between the core and peripheral countries. A significant similarity among the core countries consists of their low mean and volatility of both CDS premium and bond spread. This group maintains an average of the CDS premium below 61 basis points for the entire sample period. In contrast, there is a marked heterogeneity across the peripheral countries. The Portuguese's credit risk is the one with the highest and most volatile figures across the sample. The Portuguese CDS premium reached the maximum level of 1521.50 basis point in January 2012, when the country was going through what was arguably one of the most severe moment of its economic crisis. A similar level is reached by Ireland, followed by Italy and Spain.

Before we employ our approach, we need to ensure that the time series we model are stationary. We test for stationarity to detect the order of integration of each time series by means of the Augmented Dickey Fuller (ADF). The results of the ADF tests for the entire sample period in levels and on first difference are reported in Table 24. The t-statistics of the ADF test indicate that the null hypothesis of a unit root cannot be rejected at a 5% significance level for all countries for both CDS premium and bond spread. The results for the other two sub-periods are also reported in Table 24. The

Figure 20: CDS premium and bond spread for each sovereign entity

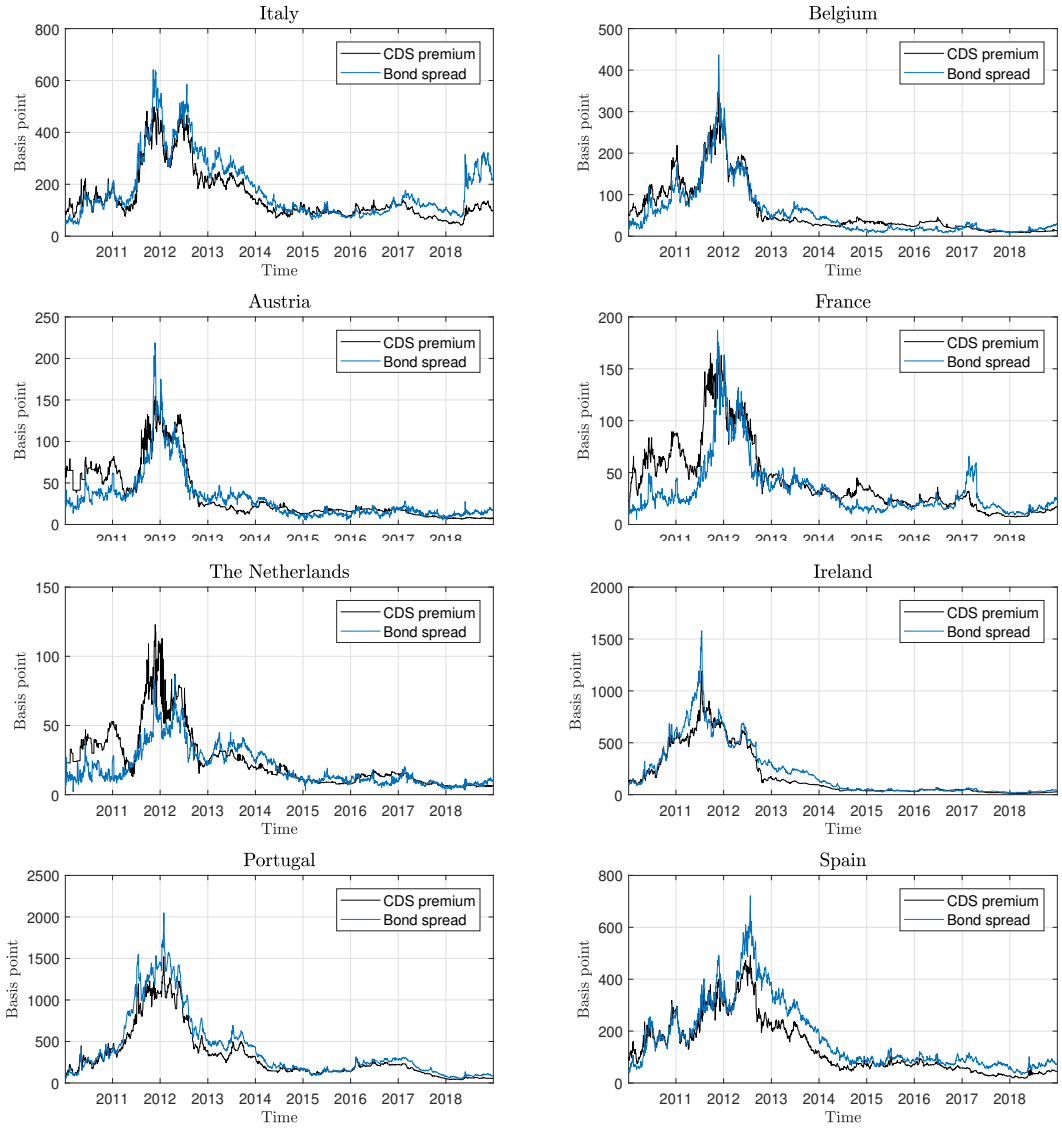

Note: The figure shows the time series of five-year CDS premium and bond spread (calculated over the five-year German bond yield) quoted in basis point, for the countries of the European Union, relative to the period 4 January 2010 - 31 December 2018.

Table 23: Descriptive statistics for sovereign CDS premium and bond spread

		CDS premium				Bond spread			
Country	Period	Mean	St.Dev.	Min	Max	Mean	St.Dev.	Min	Max
Italy	Full sample	153.02	97.372	42.04	498.66	184.37	118.89	45.35	641.91
	2010 - 2014	200.65	107.52	69.25	498.66	232.48	131.74	45.35	641.91
	2015 - 2018	93.51	22.60	42.04	140.50	124.27	60.11	64.12	324.62
Belgium	Full sample	60.44	62.78	8.37	341.98	55.82	62.85	7.63	436.68
	2010 - 2014	92.00	69.14	21.53	341.98	87.59	69.43	11.06	436.68
	2015 - 2018	21.01	9.65	8.37	45.96	16.13	5.22	7.63	34.44
Austria	Full sample	34.41	32.74	6.47	159.23	31.20	29.06	5.18	218.94
	2010 - 2014	51.23	35.74	12.18	159.23	44.99	32.88	6.39	218.94
	2015 - 2018	13.40	4.58	6.47	23.04	13.94	3.56	5.18	28.10
France	Full sample	42.30	33.64	7.15	171.56	33.10	27.41	5.03	186.97
	2010 - 2014	61.62	33.98	21.03	171.56	44.07	31.85	5.03	186.97
	2015 - 2018	18.16	7.34	7.15	37.73	19.39	9.24	9.08	65.59
Netherlands	Full sample	24.59	21.03	5.34	122.91	19.86	14.02	2.17	85.85
	2010 - 2014	36.44	21.70	10.62	122.91	28.02	14.06	2.17	85.85
	2015 - 2018	9.77	3.29	5.34	17.95	9.65	2.80	3.16	20.31
Ireland	Full sample	183.11	230.29	11.43	1191.2	220.43	263.13	15.23	1579.40
	2010 - 2014	304.04	249.93	35.72	1191.2	66.70	276.49	32.93	1579.40
	2015 - 2018	32.03	12.77	11.43	70.23	37.68	10.74	15.23	71.75
Portugal	Full sample	323.87	303.82	38.29	1521.50	403.42	386.39	53.82	2049.60
	2010 - 2014	474.16	334.58	73.11	1521.50	593.89	427.5	55.38	2049.60
	2015 - 2018	136.11	65.77	38.29	286.38	165.47	74.80	53.82	315.78
Spain	Full sample	134.87	106.11	17.71	492.07	173.03	129.90	31.87	721.59
	2010 - 2014	200.37	101.50	45.42	492.07	248.51	131.57	39.93	721.59
	2015 - 2018	53.04	20.01	17.71	105.03	78.75	18.00	31.87	135.44

Note: The table reports descriptive statistics for daily five-year CDS premium and bond spread, calculated over the five-year German bond yield denominated in Euro. Min and Max are the minimum and the maximum value of the time series. The measures are reported for the full sample (4 January 2010 - 31 December 2018), together with two sub-periods (4 January 2010 - 31 December 2014 and 1 January 2015 - 31 December 2018).

null hypothesis of a unit root cannot be rejected at any conventional significance level for all the time series during the period between 2010 and 2014, given the increasing default probability of the sovereign states. We obtain a different result for bond spreads during the recovery phase for countries such as Belgium, Austria, France, the Netherlands, Ireland, and Spain, when the persistence of low bond yield led to a stationary behaviour of the time series. The ADF test statistics applied on the first difference series indicates that the unit root hypothesis is always rejected for every period and every country, hence stationarity is confirmed. Thus we model returns for our analysis.

We analyze then the cointegrating relationship between CDS premium and bond spread. We argue that this is not always proven for such time series, making it necessary to find alternative methodologies such as the transfer entropy measures to investigate their price discovery process. We examine cointegration through the Johansen Trace and Maximum Eigenvalue tests, whose results are reported in Table 25. It is clear that the hypothesized cointegrating relationship between the two time series is not always supported by the data. With respect to the entire sample period, cointegration is not confirmed by both tests for three out of eight countries. Furthermore, the absence of a long-run relation between the two markets in the two sub-periods is observed for almost all the entities. According to the Maximum Eigenvalue test, cointegration is found to be statistically significant at 5% only for France, Ireland and Portugal during the period between 2010 and 2014. The same test on the period between 2015 and 2018 shows significant cointegrating relationships at 5% for Austria and Ireland, and no evidence is found for the remaining countries. This finding revealed the difficulty to assess a cointegration relationship between the CDS premium and the bond spread during period of low financial stress, as also discussed by previous studies (see Fontana and Scheicher (2010) and Agiakloglou and Deligiannakis (2020)).

To derive the information flow between the CDS premium and the bond spread with the transfer entropy methodology we need to partition the observations of the time series into discretized values following Equation (5.5). By

Table 24: Augmented Dickey Fuller Test Statistics for sovereign CDS premium and bond spread

Country	Period	CDS premium		Bond spread	
		Levels	First diff.	Levels	First diff.
Italy	Full sample	-1.9493	-24.4419***	-2.1405	-13.3398***
	2010 - 2014	-1.7448	-18.44188***	-1.7541	-23.1969***
	2015 - 2018	-2.4759	-11.0051***	-1.5857	-11.6793***
Belgium	Full sample	-1.4441	-25.8122***	-1.7834	-19.5834***
	2010 - 2014	-1.3301	-19.2251***	-1.7038	-16.1998***
	2015 - 2018	-1.3364	-24.4883***	-2.5819**	-19.6293***
Austria	Full sample	-1.4497	-12.8408 ***	-2.0691	-15.5855***
	2010 - 2014	-1.4975	-23.3357***	-1.6974	-11.6827***
	2015 - 2018	-0.7302	-21.4159***	-4.3960***	-18.6868***
France	Full sample	-1.4860	-19.9528***	-1.9453	-14.8564***
	2010 - 2014	-1.6458	-15.6494***	-1.5316	-12.9203***
	2015 - 2018	-2.3474	-15.5197***	-2.5611*	-31.3841***
Netherlands	Full sample	-1.6904	-15.8882***	-2.3439	-19.7682***
	2010 - 2014	-1.5946	-11.8021***	-2.4914	-14.5612***
	2015 - 2018	-1.1279	-31.4867***	-2.8448*	-10.8596***
Ireland	Full sample	-1.0174	-15.9963***	-1.5047	-12.2163***
	2010 - 2014	-0.8586	-11.8729***	-1.3901	-13.0456***
	2015 - 2018	-1.5047	-7.7359***	-3.1551**	-17.9393***
Portugal	Full sample	-1.3646	-14.5825 ***	-1.2912	-16.2117***
	2010 - 2014	-1.4751	-21.9709***	-1.2268	-12.0775***
	2015 - 2018	-1.0341	-21.2223***	-1.1538	-13.7751***
Spain	Full sample	-1.5630	-27.9765***	-1.6611	-22.1389***
	2010 - 2014	-1.6186	-20.8201***	-1.6841	-21.3086***
	2015 - 2018	-1.6881	-13.5407***	-3.2488**	-14.3744***

Note: The table reports the t-statistic of the ADF test statistics in levels and on the first difference for the entire sample period, together with two sub-periods. The null hypothesis for the test is non-stationarity. The ADF test is based on regressions including constant term but no time trend. The 95% critical value of the ADF t-statistic for regression including a constant term is -2.86. ***, **, * indicate rejection of the null hypothesis at 1%, 5%, and 10% significance level, respectively.

Table 25: Johansen Trace test and Johansen Maximum Eigenvalue test

Country	Period	Trace test		Max eigenvalue test	
		$r = 0$	$r = 1$	$r = 0$	$r = 1$
Italy	Full sample	12.6636	3.5528	9.1108	3.5528
	2010 - 2014	16.6830	3.2921	13.3909	3.2921
	2015 - 2018	8.8900	2.1608	6.7291	2.1608
Belgium	Full sample	16.7774	2.0553	14.7221*	2.0553
	2010 - 2014	10.4195	1.9459	8.4737	1.9459
	2015 - 2018	16.0767	2.7258	13.3508	2.7258
Austria	Full sample	26.2266***	2.3656	23.8611***	2.3656
	2010 - 2014	15.3661	1.4629	13.9032	1.4629
	2015 - 2018	19.3988*	0.8567	18.5421**	0.8567
France	Full sample	27.1848***	3.4234	23.7613***	3.4234
	2010 - 2014	19.7876*	3.0508	16.7367**	3.0508
	2015 - 2018	21.8275**	7.3840	14.4435*	7.3840
Netherlands	Full sample	17.6276	2.5617	15.0660*	2.5617
	2010 - 2014	12.6264	3.2052	9.4213	3.2052
	2015 - 2018	11.7675	1.7461	10.0214	1.7461
Ireland	Full sample	30.9152***	1.5878	29.3273***	1.5878
	2010 - 2014	20.9281**	1.4414	19.4867**	1.4414
	2015 - 2018	18.5605*	1.3054	17.2551**	1.3054
Portugal	Full sample	31.1199***	1.6343	29.4857***	1.6343
	2010 - 2014	19.2433*	1.5246	17.7187**	1.5246
	2015 - 2018	14.2060	2.4542	11.7519	2.4542
Spain	Full sample	20.2142***	4.3596	15.8545**	4.3596
	2010 - 2014	13.4069	4.4084	8.9985	4.4084
	2015 - 2018	18.1568*	2.3025	15.8543*	2.3025

Note: The table reports the results of the Trace test and the Maximum Eigenvalue test. The tests include a constant but no time trend. The number of lags up to 15 included in the VECM is determined by the AIC based on a VAR in first differences. r indicates the number of cointegrating relations. The null hypothesis of the tests is $r = 0$, indicating the absence of cointegration, and $r = 1$, indicating one cointegrating relation. ***, **, * indicate rejection of the null hypothesis at 1%, 5%, and 10% significance level, respectively.

doing so, the series are partitioned into three bins. The analysis is conducted setting the 0.05 quantile for q_1 and the 0.95 quantile for q_2, maintaining a large intermediate bin. This partition of the time series permits to obtain a symbolically encoded series where extreme negative values are contained in the first bin, while the third bin contains extreme positive values. The motivation of this choice depends on the excessive kurtosis found in the distribution of the series of the CDS premium and bond spread series in first difference, which are illustrated together with their associated normal distributions in Figure 21. The series deviate from the normal distribution, showing fatter tails and a peaked center. If a market is found to be informationally dominant, the extreme changes in this market should be incorporated consequently into the other market's price. Thus, the data in the tails of the distribution of the first difference series turn out be of extreme relevance. By keeping the intermediate bin large, extreme changes can be identified more clearly, especially when a significant amount of noise in the series occurs, as in the present case.

The modelling strategies for the estimation of the effective transfer entropy are based on the paper of Behrendt et al. (2019). The estimates are calculated by setting the number of shuffles equal to 100 and the number of bootstrap replications to obtain the distribution of the entropy estimates under the null hypothesis of no information flow to 300. The robustness analysis reported in the Appendix confirms the stability of our results with respect to the different modelling strategies.

5.5 Empirical results and discussion

The effective transfer entropy estimates for the entire sample and the two subperiods 2010-2014 and 2015-2018 are reported in Table 26. We also illustrate the net information flow from the CDS to the bond market, meaning that when this quantity is positive, the CDS informationally dominates the bond market, whereas when it is negative, the bond market leads.

As far as the entire sample period is concerned, the null hypothesis of no

Figure 21: Kernel density plot of CDS premium and bond spread first differences

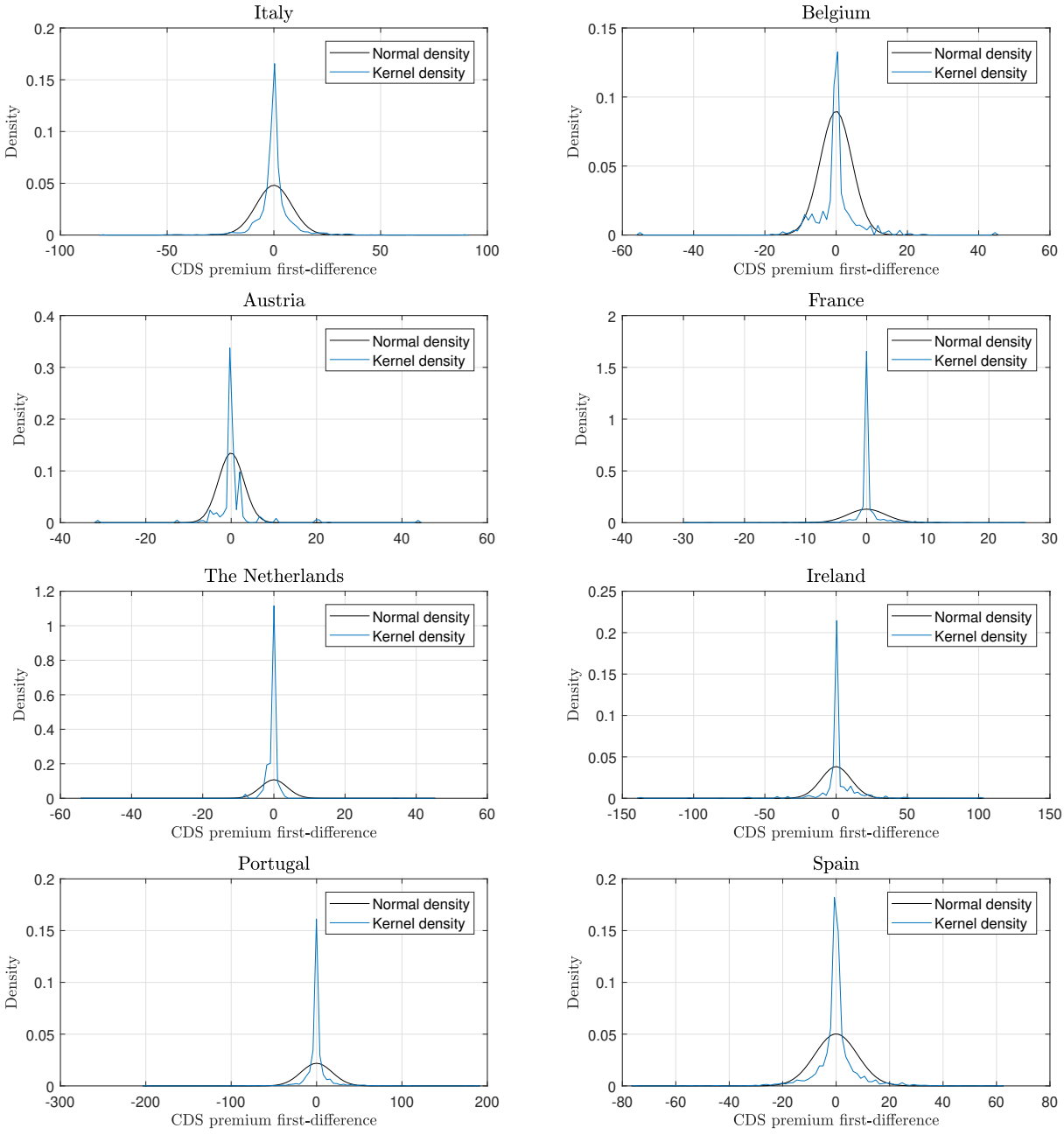

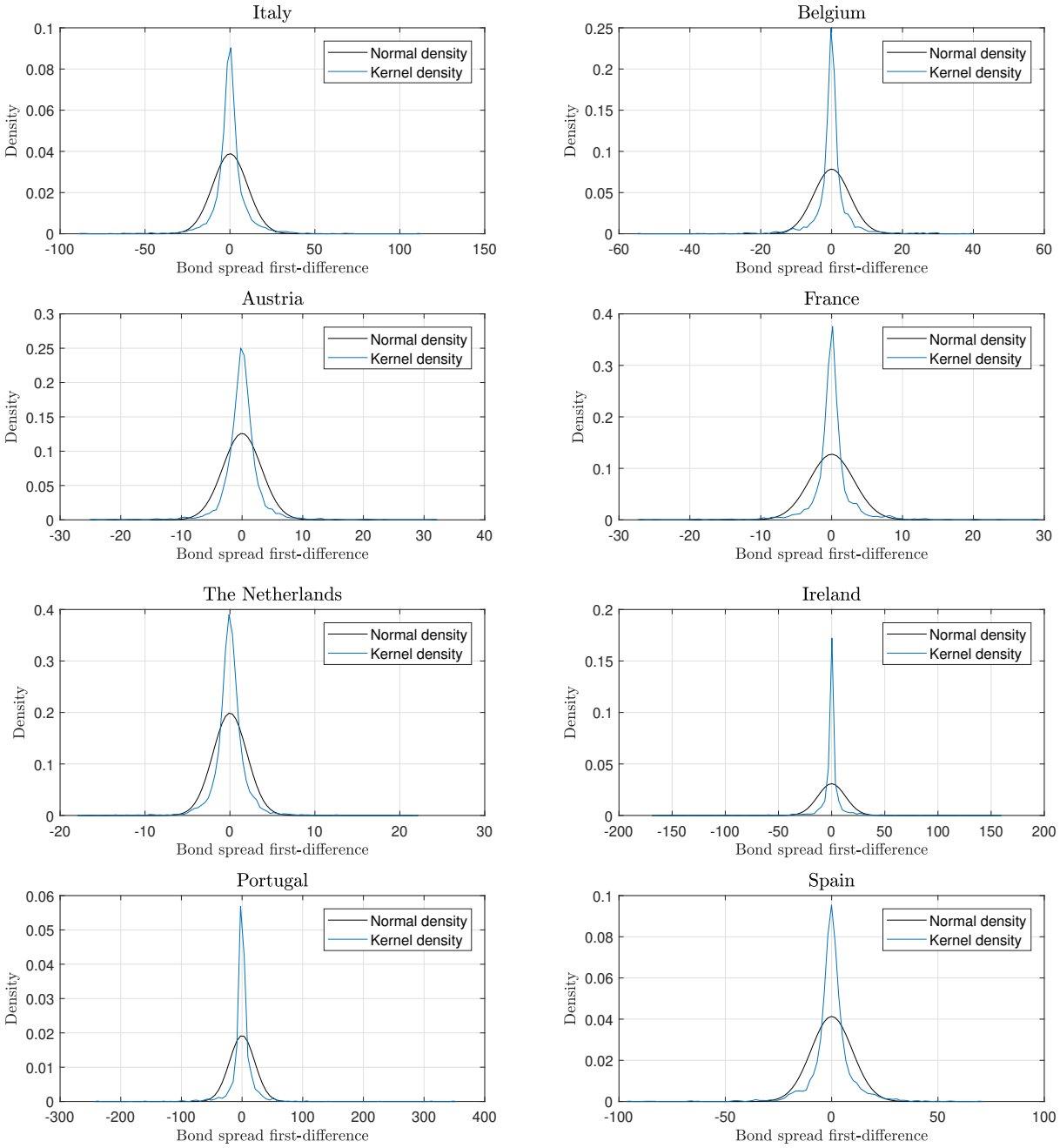

Note: The figure shows the kernel density of CDS premium and bond spread first differences for the countries of the European Union, relative to the period 4 January 2010 - 31 December 2018.

Table 26: Effective transfer entropy estimates

Country	Period	$ETE_{CDS\to BS}$	Std. Err.	$ETE_{BS\to CDS}$	Std. Err.	NIF
Italy	2010 - 2018	0.00969***	0.00135	0.00971***	0.00143	-0.00002
	2010 - 2014	0.00499**	0.00246	0.01534***	0.00263	-0.01036
	2015 - 2018	0.00154	0.00295	0.01027***	0.00292	-0.00873
Belgium	2010 - 2018	0.02205***	0.00151	0.02825***	0.00142	-0.00620
	2010 - 2014	0.00142	0.00251	0.01094***	0.00229	-0.00952
	2015 - 2018	0.00000	0.00306	0.00000	0.00311	0.00000
Austria	2010 - 2018	0.01295***	0.00153	0.02006***	0.00150	-0.00712
	2010 - 2014	0.00656**	0.00246	0.01206***	0.00251	-0.00549
	2015 - 2018	0.00000	0.00299	0.00000	0.00294	0.00000
France	2010 - 2018	0.02350***	0.00137	0.03105***	0.00148	-0.00754
	2010 - 2014	0.00789**	0.00252	0.02203***	0.00240	-0.01414
	2015 - 2018	0.00510**	0.00302	0.02941***	0.00296	-0.02431
Netherlands	2010 - 2018	0.00780***	0.00142	0.00979***	0.00144	-0.00198
	2010 - 2014	0.00461*	0.00236	0.01313***	0.00265	-0.00852
	2015 - 2018	0.00424*	0.00307	0.00217	0.00301	0.00208
Ireland	2010 - 2018	0.02187***	0.00144	0.03363***	0.00145	-0.01176
	2010 - 2014	0.00918***	0.00234	0.01561***	0.00245	-0.00643
	2015 - 2018	0.00175	0.00294	0.01199***	0.00296	-0.01024
Portugal	2010 - 2018	0.02452***	0.00149	0.02592***	0.00149	-0.00140
	2010 - 2014	0.01226***	0.00249	0.02844***	0.00239	-0.01618
	2015 - 2018	0.00555**	0.00315	0.00771**	0.00319	-0.00216
Spain	2010 - 2018	0.00624***	0.00152	0.00916***	0.00145	-0.00293
	2010 - 2014	0.00624***	0.00241	0.00805***	0.00264	-0.00181
	2015 - 2018	0.00904**	0.00307	0.00264	0.00292	0.00640

Note: The table reports the results of the effective transfer entropy estimates. The third and the fourth columns show the estimates of the effective transfer entropy from the CDS to the bond market ($ETE_{CDS\to BS}$) and the standard error (Std. Err). The fifth and the sixth columns show the estimates of the effective transfer entropy from the bond to the CDS market ($ETE_{BS\to CDS}$) and the standard error (Std. Err.). The last column reports the net information flow (NIF), the difference between $ETE_{CDS\to BS}$ and $ETE_{BS\to CDS}$. ***, **, * indicate rejection of the null hypothesis of no information flows at 1%, 5%, and 10% significance level, respectively.

information flow between the CDS and the bond market can be rejected at any conventional significance level for all the European countries. In other words, there is a significant bi-directional information flow between the two markets. The net information flow shows a larger information transmission from the bond to the derivative market. Hence, the results suggest that the bond spread dominates the market for credit risk for all the countries of the analysis. The largest net information flow is found for Ireland, followed by countries of the core group such as France, Austria, and Belgium. The high estimate of the effective transfer entropy from the bond to the CDS market is noteworthy also for Spain, the Netherlands, and Portugal, while for Italy a relatively smaller net information flow is observed.

When considering the period 2010-2014, we find again a clear dominance of the bond market across all the countries. Specifically, bi-directional information flow is not found to be statistically significant at any conventional significance level for every sovereign, and such finding reveals an interesting distinction between core and peripheral countries.

For core countries, the effective transfer entropy from the bond to the CDS market is larger and with higher significance than the one in the opposite direction. This is the case for Austria, France, and even more remarkable for the Netherlands. With respect to the analysis conducted on the full sample, the information flow for France and the Netherlands shows a huge increase from the bond to the CDS market.

For peripheral countries, there is still significant bi-directional information flow. The interactions between the CDS and the bond market are relatively strong and significant in both directions for Ireland, Portugal, and Spain. The net information flow still reveals the dominance of the bond market also in the periphery.

These outcomes are in line with the previous literature. The results for the core countries lead to the same conclusion of Coudert and Gex (2013) and Fontana and Scheicher (2010), who found a leadership of the bond market in low yield sovereigns during the high stress caused by the financial crisis.

Similar outcomes are also derived by Patanè et al. (2019), who found a dominant role of the bond market for Germany and France during the period between April 2011 and May 2014. According to the results of Coudert and Gex (2013) and Fontana and Scheicher (2010), the bond market leads the price discovery process in countries exhibiting low bond yields. During the period of the crisis, investors could have moved their own positions towards these sovereign bond markets, considered as arguably safe. Indeed, the CDS market has been less used by the investors to hedge their credit exposure on countries with a low probability of default. Additionally, the liquidity of the government bond market of core economies is greater than the one of the CDS market, given the higher size of the respective market. To illustrate, the International Monetary Fund reports that at the end of 2011 the total government debt outstanding was 50 trillion USD, whereas the size of the sovereign CDS reached only 3 trillion USD[13]. This could have played a role in determining the bond asset as the leader market, since the market that is able to incorporate faster the information of the underlying entity is usually the most liquid one.

During the crisis period, the bond market dominated the CDS one also when considering countries with higher spread. The effective transfer entropy from the bond market exceeds that from the CDS market for all the four sovereigns, confirming the bond market as the dominant one in the sovereign credit risk sphere. Previous results in the literature regarding the leader market in the price discovery process could not lead to a specific conclusion. Even though the effective transfer entropy estimates of the core countries are in line with the findings of Coudert and Gex (2013) and Fontana and Scheicher (2010), results for countries with weak fiscal vulnerabilities are in contrast to them, but in line with others: Arce et al. (2013) showed that the bond market led the price discovery process during the crisis period in the

[13]For further details, see the Global Financial Stabilty Report of April 2013: https://www.imf.org/en/Publications/GFSR/Issues/2016/12/31/Old-Risks-New-Challenges.

Eurozone for peripheral countries; Gyntelberg et al. (2017) found evidence of bond leadership in the Irish market.

In addition to liquidity, counterparty risk may have also played a role in contrasting the leadership of the derivative market in the price discovery process. Due to the over-the-counter nature of the derivative market in question, a negative effect on the CDS price may be the consequence of a high counterparty risk of the seller of the CDS contract, and hence a lower quality of the protection sold. Therefore, the lower quality of the protection sold may have affected the capability of the derivative market in reflecting better than the bond market the credit risk of the sovereign entities. This explanation has been proved by Arce et al. (2013), who showed how the contribution of the bond market becomes greater after an increase in the counterparty risk.

In light of what has emerged, the bond market holds a dominant role during the entire period of the debt sovereign crisis, from the drastic increase of risk among the countries to a more stable financial situation after the implementations of programs by the European Central Bank. The interest rate could have also played an important role in determining the dominance of the bond market. Especially for the safest governments, investors might have moved their own positions towards the bond markets when the yield was constantly decreasing, expecting a greater price of the sovereign bond in the future and making a considerable profitable investment.

In addition to the literature so far, we examine how the relationship between the two markets evolved in the aftermath of the European debt crisis over the period 2015-2018. This period is characterized by very low bond yields, and for many countries the time series of bond spread and CDS premia do not even satisfy a cointegrating relationship.

In general, the information transmission between the two markets heavily decreased in this period. In addition, although the bond market is still broadly dominant with respect to the CDS one, there are some differences in the behaviour of the European countries in the sample.

The lower information flow on the period 2015-2018 is not surprising. A difficulty to verify a cointegrating relationship, hence a co-movement between the CDS and the bond market during no-crisis periods is a common result of the literature. During periods of low financial turbulence, the higher safety of the sovereign debts could lead the market participants to make less use of the credit derivative market to protect their own exposure. As a matter of fact, CDS premia are relatively constant in the aftermath of the crisis, due to the lower trading activities in the CDS market. As explained by Fontana and Scheicher (2010), for the period before the financial crisis of 2008 CDS premia and bond spreads across sovereigns exhibited weaker relationships due to the lower arbitrage forces between the two markets. The low information flow in the period after the sovereign crisis confirm the weaker relationship of the two markets during such times.

The information flows highlight the existence of three main groups of countries in terms of behaviour. The first one is composed by Italy, France, Ireland and Portugal, whose leading market remains the bond one, as it was during the sovereign debt crisis period. The second group consists of the Netherlands and Spain, which show that the CDS market became informationally dominant to the detriment of the bond one during the post-crisis period. The last group is the one including countries for which there is no information flow between the two markets, i.e. Belgium and Austria.

In detail, effective transfer entropy estimates are found to be statistically significant in both directions only for France and Portugal, and the two estimates still confirm the role of the bond market in incorporating faster the information of the sovereign credit risk. Information flow is significant only in one direction for Italy, Ireland, Spain and the Netherlands, and as far as the latter two countries evidence provides that the CDS market dominates the bond one, though with lower levels of significance. Hence the results related to the recovery period do not reveal a unique market leader across all analyzed countries, but they suggest that - even if to a smaller extent - the bond market is still dominating the CDS one.

Overall, our results show significant information transmission between the CDS and the bond market across all the countries for the whole period 1 January 2010 - 31 December 2018 and a clear dominance of the bond market. When focusing on the crisis period, the effective transfer entropy confirms that information on the sovereign credit risk are expected to be reflected initially in the bond market. This strong conclusion cannot be drawn for every country during the post-crisis period, when the information flow between the two markets decreased.

5.6 Conclusion

This chapter explores the dynamic relationship between the CDS premium and the bond spread of European Union countries using the concept of effective transfer entropy. The lack of a cointegrating framework between the CDS premium and the bond spread requires alternative methodologies to detect the informationally dominant market between the CDS and the bond one. Hence, we make use of a model-free approach, without being restricted to linear dynamics, to discover which market incorporates faster the information on sovereign credit risk.

Our results show a significant bi-directional information flow between the CDS and the bond market for the European Union countries, and a dominant position for the bond market. During the European debt crisis, we find a strong predominance of the bond market, especially as regards to core countries. During the post-crisis period, the information flow between the CDS and the bond market significantly weakens in almost all countries, mainly due to the lower turmoil and trading activities in the CDS market. However, although some countries behave dissimilarly, we still find an overall predominance of the bond market also during the recovery period.

Our findings have a direct implication for policy makers, who can rely on the bond spread as a market indicator of sovereign credit risk during periods of financial distress. This result addresses the issue to know whether an extensive use of the CDS market could fuel a sovereign crisis. The leadership of

the bond market overcomes this possibility, suggesting that the CDS market can be used as hedging instrument without a direct impact on the financial position and stability of the sovereigns. Our results can also enhance profitability on arbitrage activities for institutional investors, who can take advantage of the knowledge of which asset has an influence over the other and profit from the theoretical deviation between the two markets.

6 Neural Network Models for Bitcoin Option Pricing

Based on the paper:
Pagnottoni, Paolo. 2019. Neural Network Models for Bitcoin Option Pricing. *Frontiers in Artificial Intelligence*, **2**, 5.

6.1 Introduction

Stock options are a category of financial derivatives which became widely employed by investors and speculators during the last few decades. Nevertheless, investors may ineffectively manage their portfolios if they are not able to value options in a proper way. For this reason, a reliable methodology capable to yield an option's current price or forecast is fundamental for investors in order to produce a rigorous decision making. This is particularly true when considering non-mature and volatile markets like the cryptocurrency one.

The theory of option pricing is broad and involves various types of pricing techniques, largely parametric ones. The most widely known option pricing method is arguably the one defined by Black and Scholes (1973). Although this technique has been widely employed by practitioners, its strict set of assumptions, as well as subjectivity with respect to the parameter choices, often yields to unreliable results to some extent. To illustrate, the leptokurtic behavior of return distributions and the volatility smiles and skews are features that cannot be captured by such a simplistic technique.

Besides the Black-Scholes model and its modifications, other parametric models have been developed and became widely used, among which the (binomial and trinomial) tree models, the finite difference method and the Monte Carlo simulation. While tree models converge to the Black-Scholes one in case the time occurring between steps is small enough, other methodologies take into consideration pricing aspects that these two models do not. Indeed, the Monte Carlo simulation allows for random shocks other than

those provided by the volatility and the movement probabilities of the tree models, whereas the finite difference method relies on a different simulation scheme. This is the reason why in this chapter examines and includes tree models, the Monte Carlo simulation and the finite difference method as pricing methodologies.

Alongside the category of classical derivative and option pricing models, non-parametric models such as neural networks gradually emerged, mainly thanks to their improved predictive performance with respect to the former techniques. Yao et al. (2000) predicts prices related to the Nikkei 225 index futures using back-propagation neural networks. Their results show that, despite the Black-Scholes model is still good for pricing at-the-money options, the neural network outperforms it, in particular when considering volatile markets. Another research conducted by Liang et al. (2009) motivates our contribution, as the authors use classical models (binomial tree, finite difference method and Monte Carlo simulation) in a first stage to forecast the option price and refine those forecasts through neural networks and support vector machines in a second stage. This technique allows to notably reduce forecast error, i.e. it substantially improves price forecasts in their Hong Kong option market framework. Nonetheless, there are many other examples on neural network models for derivative securities pricing which found that neural networks outperform classical models - see, for instance, Hutchinson et al. (1994), Malliaris and Salchenberger (1996), Amilon (2003), Binner et al. (2005), Lin and Yeh (2005).

Research related to the cryptocurrency market, as the phenomenon itself, is relatively new. Despite that, there is a massive interest of the academic community in investigating this new market and its peculiar features from all points of view, with a particular focus on Bitcoin. Indeed, since Nakamoto (2008) introduced the concept of Bitcoin as a purely peer-to-peer version of electronic cash, researches developed following different and multidisciplinary fields. Some researchers provide a general descriptional analysis of the cryptocurrency framework. To illustrate, in Dwyer (2015a) we may find

a detailed overview on technical issues of Bitcoin and the cryptocurrency market in general. Also White (2015) goes through the key concepts of cryptocurrencies, while focusing on the so called "Altcoins".[14] Kaplanov (2012) describes the usage, the mining process, exchange, acceptance and storage of Bitcoin in details, and it analyses the regulatory issues linked to this market. A further study by Kroll et al. (2013) examines the Bitcoin mining process thoroughly. An informative and useful collection of all modelling methodologies applied to the Bitcoin sphere can be found in Fantazzini et al. (2017). Another stream of the literature, with studies conducted by Brandvold et al. (2015) and Pagnottoni and Dimpfl (2019), finds the leader and follower Bitcoin exchanges of the price discovery process through an econometric analysis of its price across different exchange. A related analysis, provided by Giudici and Pagnottoni (2020), studies system-wide and pairwise connectedness among Bitcoin exchanges and provides further insights on price discovery on Bitcoin exchange platforms.

Despite the quite wide set of studies in the cryptocurrency area, to the best of our knowledge there is not yet any research trying to address option pricing related to Bitcoin (or cryptocurrency) derivatives. The aim of this study is to propose a pricing methodology that is feasible to price cryptocurrency options. Without loss of generality, the chapter focuses on european style Bitcoin put and call options which became recently available on the market. To this end, the study makes use of a two stage approach. The first stage consists of option pricing through parametric approaches such as tree models, finite difference method and Monte Carlo simulation. In the second stage, artificial neural networks are employed in order to combine the parametric option pricing approaches and capture the residual errors by learning schemes in the current status of the option market. Their performance is then compared to the conventional option pricing techniques obtained in the first stage. Results point to the predominance of the neural network mod-

[14] "Altcoin" stands for "alternative coin". The term is used to indicate all cryptocurrencies except for Bitcoin.

els with respect to the conventional methods in pricing Bitcoin options and, therefore, in capturing their real price dynamics. As a robustness check, an out-of-sample analysis confirm the previous result, as well as a cross validation analysis through random sub-sampling reveals that - despite there is still some room for improvement - results are arguably stable and the neural network is a suitable model in order to price options written on Bitcoin.

The remainder of the chapter proceeds as follows. Section 2 outlines the methodology employed. Section 3 describes and analyzes the data. Section 4 presents the results. Section 5 illustrates the robustness analysis conducted. Section 6 concludes.

6.2 Methodology

This section briefly introduces the classical parametric option pricing techniques used in this chapter: specifically, tree models, finite difference method and Monte Carlo simulation. After that, I discuss the neural network model and the comprehensive approach for option pricing.

The following notation will be used. S represents the underlying asset price, C is the option price, K is the options' exercise price, σ denotes the asset price volatility, r represents the risk-free interest rate, Δt is the time interval (i.e. the time period length) and T is the time to maturity.

6.2.1 Tree models

Tree models are widely used not only to price European style options, but also closed-form American options, as they can account for the early exercise feature. Milestone references for binomial trees are the ones of Cox et al. (1979) and Rendleman and Bartter (1979). Further extensions are proposed by Boyle (1977), Nelson and Ramaswamy (1990), Hull and White (1990a).

In the binomial tree setup, the underlying asset price $S_{t,i}$ with $t = 0, 1, 2, ..., n-1$ may either experience an up movement to $S_{t+1,i}$ or a down movement to $S_{t+1,i+1}$, with $t = 1, 2, ..., n$. This happens according to an

upward rate u and a downward rate d, which Cox et al. (1979) define as:

$$u = e^{\sigma\sqrt{\triangle t}}, \qquad d = e^{-\sigma\sqrt{\triangle t}} \tag{6.1}$$

where $\triangle t = \frac{T}{n}$ denotes the time step from t to $t+1$ and n the total number of time steps in the binomial tree.

A graphical representation of a n-step binomial tree is illustrated in Figure 22. Arrows constitute possible paths for the price dynamics, whereas nodes represent the underlying price $S_{t,i}$ from which the option price $C_{t,i}$ is computed. Option prices are then recursively computed from the last ones to the first one, going backwards, according to the following:

$$C_{t-\triangle t,i} = e^{-r\triangle t}(pC_{t,i+1} + (1-p)C_{t,i}) \tag{6.2}$$

where r is the risk-free rate, and the probabilities of up (p) and down (p_d) movements are defined as

$$p = \frac{e^{r\triangle t} - d}{u - d}, \qquad p_d = 1 - p. \tag{6.3}$$

The trinomial tree (Figure 23) works in a similar way. However, in this setup, the underlying asset price $S_{t,i}$ with $t = 0, 1, 2, ..., n-1$ may either experience an up movement to $S_{t+1,i}$, a middle movement to $S_{t+1,i+1}$ or a down movement to $S_{t+1,i+2}$, with $t = 1, 2, ..., n$. This happens according to an upward rate u, downward rate d and middle rate m defined as:

$$u = e^{\sigma\sqrt{2\triangle t}}, \qquad d = e^{-\sigma\sqrt{2\triangle t}}, \qquad m = 1. \tag{6.4}$$

In this case, the probabilities of up (p), down (p_d) and middle (p_m) movements are defined as:

Figure 22: Binomial tree

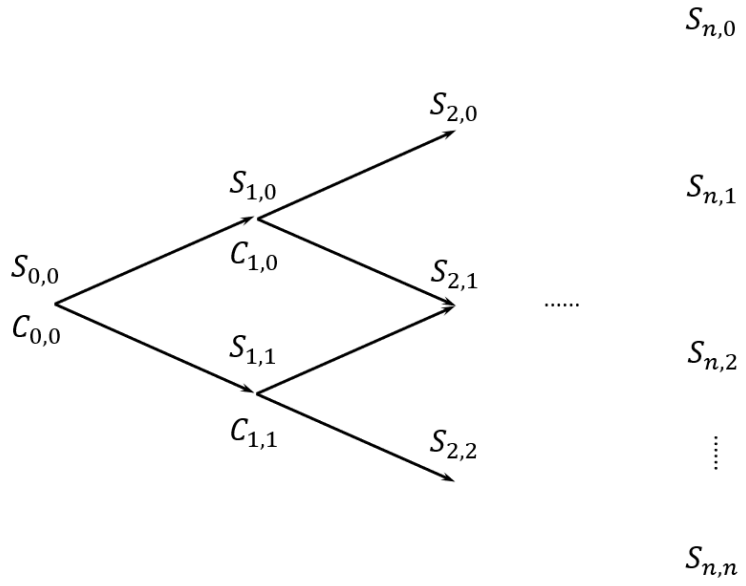

Figure 23: Trinomial tree

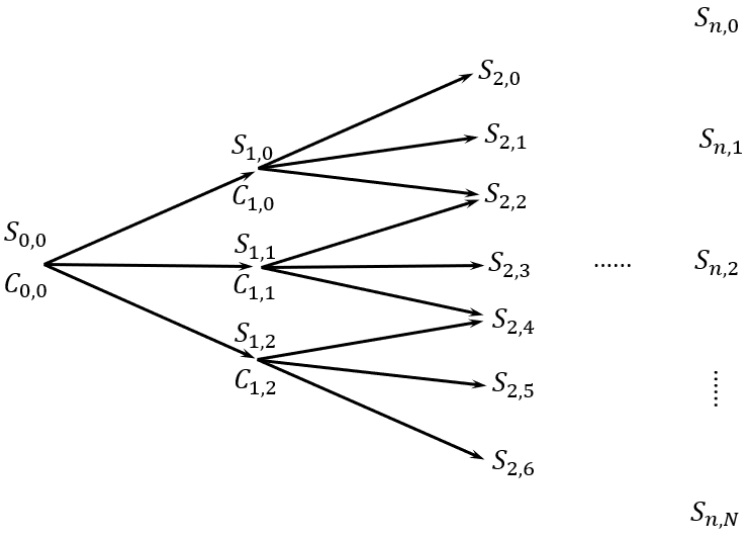

$$p = (\frac{e^{(r)\frac{\Delta t}{2}} - e^{-\sigma\sqrt{\frac{\Delta t}{2}}}}{e^{\sigma\sqrt{\frac{\Delta t}{2}}} - e^{-\sqrt{\frac{\Delta t}{2}}}})^2, \qquad p_d = (\frac{e^{\sigma\frac{\Delta t}{2}} - e^{(r)\frac{\Delta t}{2}}}{e^{\sigma\sqrt{\frac{\Delta t}{2}}} - e^{-\sqrt{\frac{\Delta t}{2}}}})^2, \qquad p_m = 1 - (p + p_d). \tag{6.5}$$

Among the advantages of using the trinomial trees, computational efficiency as well as precision are of our interest. Indeed, the trinomial tree should yield to more precise prices with less time steps if compared to the binomial counterpart.

6.2.2 Finite difference method

As extensively described in Brennan and Schwartz (1977), the finite difference method allows to price options through the solution of some differential equations with respect to the option prices. These equations are transformed into difference equations, whose solutions are iteratively solved by CPUs.

According to the finite difference method, the time to maturity T is segmented into p equally sized time periods Δt, whereas the asset price is segmented into q steps of length ΔS, ranging from a minimum of 0 to a maximum of S_{max}. This can be represented as a grid in which the horizontal line is the number of periods and the vertical one the asset prices.

In the present case, the application uses the so called explicit finite difference method, which solves the differential equations in a forward way, as elucidated by Hull and White (1990b). The reason behind our choice is that the explicit finite difference method is arguably more efficient than the implicit one, which in contrast solves the differential equations backwards. In particular, the equation to be solved is the well known partial differential equation of Black-Scholes, i.e. :

$$\frac{\partial C}{\partial t} + \frac{1}{2}\sigma^2 S^2 \frac{\partial^2 C}{\partial S^2} + rS\frac{\partial C}{\partial S} = rC \tag{6.6}$$

Where $i = 1, 2, ..., p$ and $j = 1, 2, ..., q$. The discrete version of Equation (6.6) is:

$$-\frac{C_{i,j} - C_{i-1,j}}{\Delta t} = \frac{1}{2}\sigma^2 \frac{C_{i,j+1} - 2\,C_{i,j} + C_{i,j-1}}{\Delta S^2} + \\ + rS\frac{C_{i,j} - 2\,C_{i,j-1}}{2\Delta S} - rC_{i+1,j}. \tag{6.7}$$

The option price can then be derived as:

$$C_{i,j} = \frac{1}{1 + r\Delta t}(pC_{i+1,j+1} + p_m C_{i+1,j} + p_d C_{i+1,j-1}) \tag{6.8}$$

where the probabilities associated with an up, middle or down movement are, respectively:

$$p = S_j r \frac{\Delta t}{2\Delta S} + \frac{1}{2} S_j^2 \sigma^2 \frac{\Delta t}{\Delta S^2} \tag{6.9}$$

$$p_m = 1 - S_j^2 \sigma^2 \frac{\Delta t}{\Delta S^2} \tag{6.10}$$

$$p_d = -\frac{S_j r \Delta t}{2\Delta S} + \frac{1}{2} S_j^2 \sigma^2 \frac{\Delta t}{\Delta S^2} \tag{6.11}$$

For a detailed explanation of the finite difference method, refer to Brennan and Schwartz (1977) and Hull and White (1990b).

6.2.3 Monte Carlo simulation

The Monte Carlo simulation is used to obtain the underlying asset price at the option maturity by means of averaging a sufficiently high number of stochastic asset price paths, obtained by assuming that the underlying price follows a log-normal distribution, that is simulating L scenarios for the underlying price evolution as:

$$S_T = S_t e^{(r-\frac{1}{2}\sigma)(T-t)+\sigma\sqrt{T-t}\Delta W_t} \tag{6.12}$$

where W_t denotes a standard Wiener process at time t.

After that, option prices are found by discounting that average result backwards. In other words, given the payoffs at maturity T of call and put options respectively as:

$$C_T = max(0, S_T - K), \qquad P_T = max(0, K - S_T) \tag{6.13}$$

the resulting call and put prices are obtained as an average of the L simulated scenarios, i.e. :

$$C_t = \frac{1}{L}\sum_{l=1}^{L} C_l, \qquad P_t = \frac{1}{L}\sum_{l=1}^{L} P_l \tag{6.14}$$

where $l = 1, 2, ..., L$.

6.2.4 Neural networks to improve precision

Option prices dynamics depend on several variables as well as on an economic environment and rules that continuously change. Despite parametric methods mimic the behavior of real option prices, it may be argued that they do not fully reflect the actual market evolution of option prices.

To cope with that, similarly to Liang et al. (2009), this chapter defines a two-step procedure in order to consistently evaluate option prices. The first step consists of pricing options according to the three parametric methods described above, i.e. tree models, finite difference method and Monte Carlo simulation. The prices obtained in the first step are then used as input training vector of a neural network model in the second step. As a consequence, once the main information regarding an option's price are captured through the parametric methods in the first step, the machine learning neural network

can concentrate its modelling power to approximate the nonlinear features of the option pricing errors. A graphical representation of the model can be found in Figure 24.

Figure 24: The multilayer perceptron neural network model

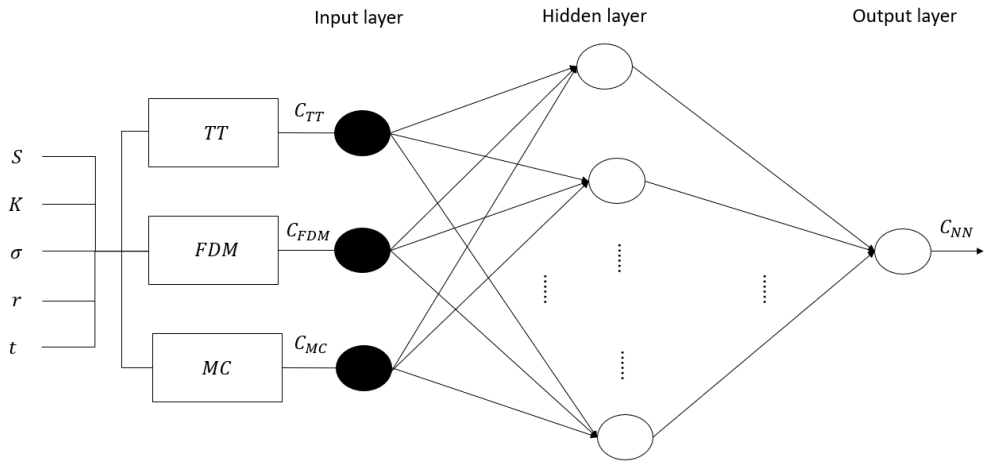

Note: The following notation is used: NN stands for the neural network model, TT corresponds to the trinomial tree, FDM represents the finite difference method and MC for the Monte Carlo simulation.

It is well known that the option market is a complex system with nonlinear characteristics. This further motivates our approach, since the use of a particular kind of neural network model, the multilayer perceptron one, allows to account for these features. Indeed, through the multilayer perceptron neural network one is able to include include hidden layers and nonlinear activation functions that may capture the non linearity of the option market. An organic description of multilayer perceptron neural networks can be found, for example, in Haykin et al. (2009).

6.2.5 Performance assessment

In this Subsection the the assessment criteria used to evaluate our models are presented. Performances of our pricing methods are judged according to three widely employed measures, i.e. the mean absolute error (MAE), mean squared error (MSE) and the mean absolute percentage error (MAPE). These criteria are defined by

$$MAE = \frac{1}{N}\sum_{n=1}^{N}|A_{t,n} - F_{t,n}| \tag{6.15}$$

$$MAPE = \frac{1}{N}\sum_{n=1}^{N}|\frac{A_{t,n} - F_{t,n}}{A_{t,n}}| \tag{6.16}$$

$$MSE = \frac{1}{N}\sum_{n=1}^{N}(A_{t,n} - F_{t,n})^2 \tag{6.17}$$

where A is the actual option value and F is the fitted value obtained by the corresponding pricing model, being t the specific time at which the option is evaluated and N the number of observations. Additionally, we remark that newly conceived model validation metrics could be used in order to further evaluate model predictive accuracy - see the RG or RGA measure in Agosto et al. (2019) and Agosto and Raffinetti (2019).

6.3 Data

An option market for cryptocurrencies - and Bitcoin - is gradually emerging. I analyze data from deribit.com, a platform offering trading of futures and European style options written on Bitcoin. In particular, the corresponding underlying on which the options are written consists of the deribit BTC index[15].

[15]Detailed information regarding the deribit BTC index can be found on www.deribit.com

Data are collected from 16 May 2018 to 15 July 2018, on a daily basis, every day at the same time (11:00 UTC). To be precise, the retrieved data are the deribit BTC index and all available option prices related to that day (European calls and puts).

Following Liang et al. (2009) the analysis is restricted to options having a time to maturity comprised between 5 and 20 days, as well as to in-the-money options having a spread which is lower than 50%. In this way it is possible to overcome price fluctuations related to the expiration effect and liquidity problems linked to the long term time to maturity options, as well as to eliminate outliers reflecting expectations which are somehow not rational and may heavily affect results. Furthermore, the choice of such a maturity range is in line with the peculiar short term feature of cryptocurrency options, whose maturities are generally smaller than the ones related to traditional option markets. To illustrate, the majority of options in our full dataset were issued only 8 days before maturity.

Given the set of restrictions adopted above, the dataset ends up with a total number of 281 call and 695 put prices. In the current analysis, the first 10 weeks will be used for the estimation purposes, while the last two weeks will be used for out-of-sample performance assessment.

As far as the parameter specifications, a 15-day historical volatility for the deribit BTC index and the 2-month Libor interest rate as risk-free rate are used. Moreover, the finite difference method has a grid of size $3T$ and the Monte Carlo simulation involves 10,000 repetitions.

The neural network involves several specifications, too. Firstly, the study relies on the widely spread backpropagation algorithm for the parameter estimation. Secondly, the most widely employed activation functions are tested in order to choose the one ensuring the best performance in terms of fitting[16]. Results indicate that the sigmoid function is the one ensuring the smallest sizes of prediction error. Thirdly, an analysis of the optimal

[16]In particular, the following activation functions are tested: sigmoid, taylor, identity, tanh, softplus, gauss.

number of hidden layers and neurons in the network is conducted, following the iterative procedure described in Stathakis (2009). Results suggest a model having 2 neurons and 1 hidden layer.

6.4 Empirical findings

In this section results are presented distinguishing between call and put options.

Without loss of generality, a plot of a representative option price evolution against one of the parametric methods (the trinomial tree) prediction is shown in Figure 25. Overall, classical parametric option pricing methods (i.e. trinomial tree, finite difference method and Monte Carlo simulation) lead to price predictions which are consistently lower than the actual option prices, both in the put and the call cases. Consequently, it may be argued that options written on Bitcoin are systematically overpriced by the platform when considering the parametric methods in question. Notwithstanding this, theoretical prices yielded by parametric methods converge to the real option prices as the time to maturity becomes smaller. This is in line with the behavior of the traditional markets for option exchanges, where a small time to maturity leads to a convergence of theoretical and real option prices.

Figure 25: Real and predicted option prices

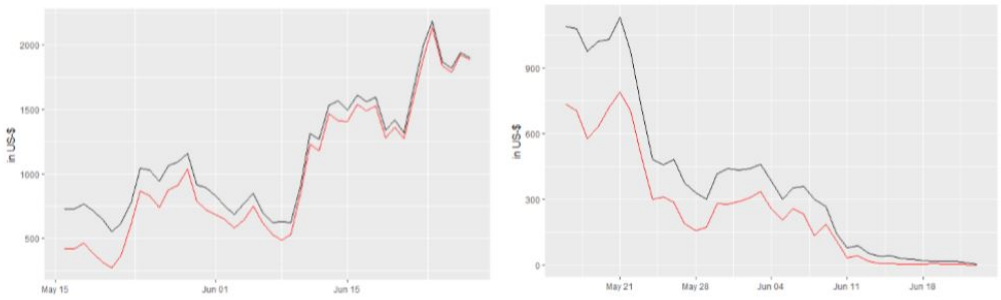

Note: Real option prices (black) against trinomial tree price predictions (red) for the option expiring on 29 June 2018, $K = 8000$, call (left) and put (right).

Prediction errors associated with each category of options are illustrated in Table 26. Absolute and relative model performance measures are quite comparable across the considered classical parametric methods. Besides that, it is clear that the neural network outperforms them in terms of prediction accuracy. This is also graphically represented in Figure 26, which shows the model performance metrics of the neural network against those of the "best" classical model, meaning the parametric model among the ones used in this study showing the lowest prediction error. To illustrate, when comparing the neural network and the "best" classical model performances the MAPE lowers by 6% in the call case and 7.33% in the put one, the MAE by 21.58% (call) and 0.4% (put) as well as the MSE by 64.07% (call) and 51.75% (put). This is mainly due to the fact that the multilayer perceptron neural network can deal with the complexity and non-linearity of the option market and the cryptocurrency market. Indeed, price predictions yielded in the first step by the conventional approach are then refined into the second step by the neural network, which focuses on lowering the errors existing between the real option prices and the predicted ones.

The obtained results are in accord with the existing literature on option pricing through non-parametric methods and, particularly, neural networks - see Hutchinson et al. (1994), Malliaris and Salchenberger (1996), Amilon (2003), Binner et al. (2005), Lin and Yeh (2005). Indeed, all these studies point to an overall predominance of neural network based models in pricing options with respect to conventional methodologies. It may be argued that this holds true also for particular markets like the cryptocurrency one, whose particular features are well captured by non-parametric models such as the neural network.

6.5 Robustness analysis

With the aim of testing the robustness of our model, this Section provides an out-of-sample performance analysis as well as a cross-validation analysis through repeated random sub-sampling.

Table 27: In-sample performance of neural network and classical models

-	**TT**	**FDM**	**MC**	**NN**
-	**Call**			
MAPE	0.0713	0.0713	0.0716	0.0670
MAE	42.78	42.79	43.2	33.55
MSE	5362.41	5362.65	5401.13	1926.66
-	**Put**			
MAPE	0.0546	0.0547	0.0546	0.0506
MAE	56.00	56.05	56.08	33.63
MSE	4764.71	4764.81	4765.29	2299.11

Note: The following notation is used: NN represents the neural network model, TT corresponds to the trinomial tree, FDM stands for finite difference method and MC for the Monte Carlo simulation.

Figure 26: In-sample performance of neural network and "best" classical model

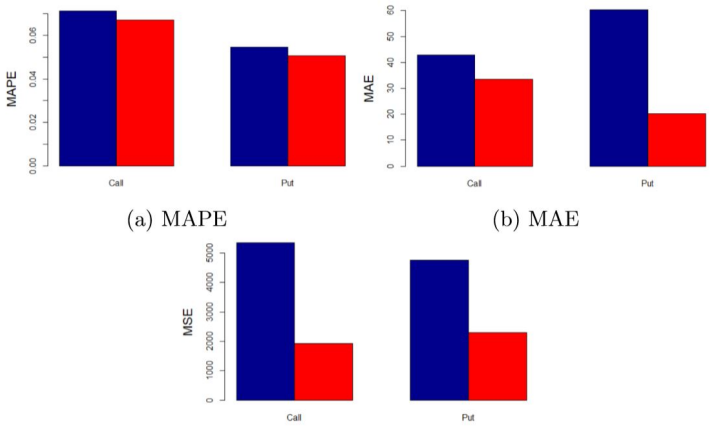

(a) MAPE

(b) MAE

(c) MSE

Note: The figure compares the in-sample performance of the neural network model (red) and "best" classical model (blue).

6.5.1 Out-of-sample performance

The out-of-sample performance is tested on the options available on the deribit platform between 1 August 2018 and 15 August 2018. Options are selected according to the same criteria described in Section 3. The final out-of-sample dataset consists of 29 call and 47 put option prices.

Results of the out-of-sample performance of the investigated models are illustrated in Table 28. At a first glance, one may notice that results linked to both absolute and relative performances change quite consistently. This is mainly due to the different structure of the out-of-sample dataset, in particular to the different maturities and market expectations.

As also depicted in Figure 27, it is clear that the neural network model proposed still outperforms the considered parametric methods. In addition, the difference in performance is even higher than the in-sample one. When comparing the performance of the neural network and the "best" classical

Table 28: Out-of-sample performance of neural network and classical models

	TT	**FDM**	**MC**	**NN**
Call				
MAPE	0.0429	0.0429	0.0425	0.0283
MAE	26.64	26.65	26.77	17.93
MSE	1016.11	1016.28	1026.79	441.94
Put				
MAPE	0.0642	0.0643	0.0642	0.035
MAE	73.4	73.4	73.23	41.45
MSE	6668.17	6667.56	6646.12	2978.26

Note: The following notation is used: NN represents the neural network model, TT corresponds to the trinomial tree, FDM stands for finite difference method and MC for the Monte Carlo simulation.

model, the MAPE lowers by 33.41% in the call case and 45.48% in the put one, the MAE by 32.7% (call) and 43.4% (put) as well as the MSE by 55.23% (call) and 55.06% (put). This provides further support to the fact that the neural network is a feasible model to price Bitcoin options.

6.5.2 Cross-validation

To further assess the robustness of our proposed model, the approach of repeated random sub-sampling for cross-validation purposes is adopted. In other words, the dataset is randomly split into training and validation set for 50 times and then the methodology and procedures described in this study are repeated. In this way, one is able to determine whether the neural network performance achieved in the results section are stable, as well as to evaluate the model's relative performance after random sub-sampling with respect to the conventional option pricing methods.

Results linked to the random sub-sampling procedure are illustrated through the boxplots contained in Figure 28 (call case) and Figure 29 (put case).

Figure 27: Out-of-sample performance of neural network and "best" classical model

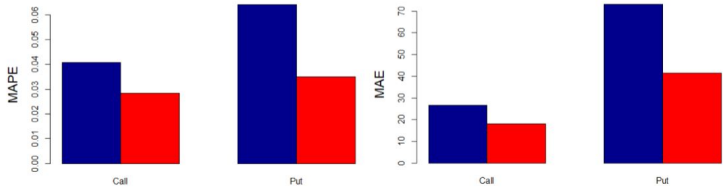

(a) MAPE

(b) MAE

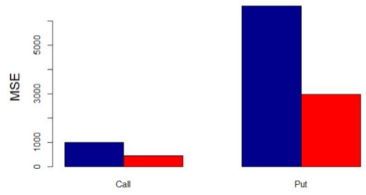

(c) MSE

Note: The figure compares the out-of-sample performance of the neural network model (red) and "best" classical model (blue).

Overall, outcomes are satisfactory provided that performance variability lies in ranges which are arguably not too wide. To illustrate, the interquartile ranges for MAPE and MAE are respectively less than 3% and below 10 USD in the call case, whereas in the put case they amount to roughly 1% and 5 USD.

Furthermore, comparing the distributions of the assessment criteria with the results in Table 28, it may be noticed that even in the context of resampling the neural network achieves again satisfactory results in terms of precision. Indeed, despite the MAPE results coming from the repeated random sub-sampling are partly worse than those of classical option pricing methods, the absolute assessment criteria still point to a substantial improvement when considering the neural network model rather than the conventional option pricing methods.

To conclude, there may be room for improvement in the modelling strat-

Figure 28: Model performance distribution (call)

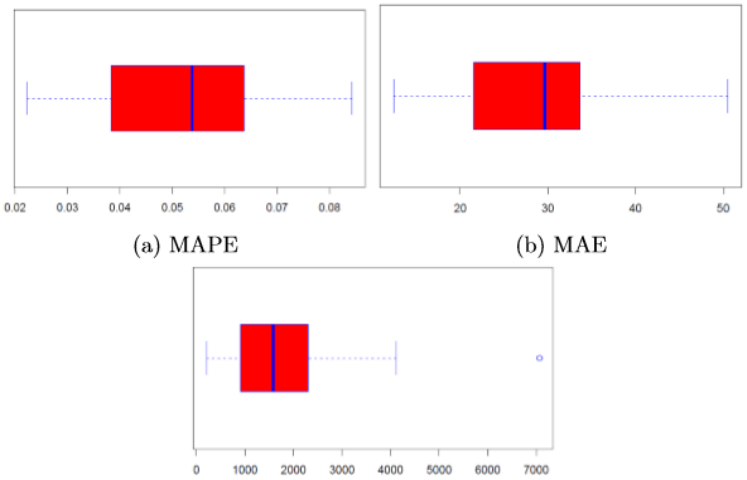

(a) MAPE (b) MAE

(c) MSE

Figure 29: Model performance distribution (put)

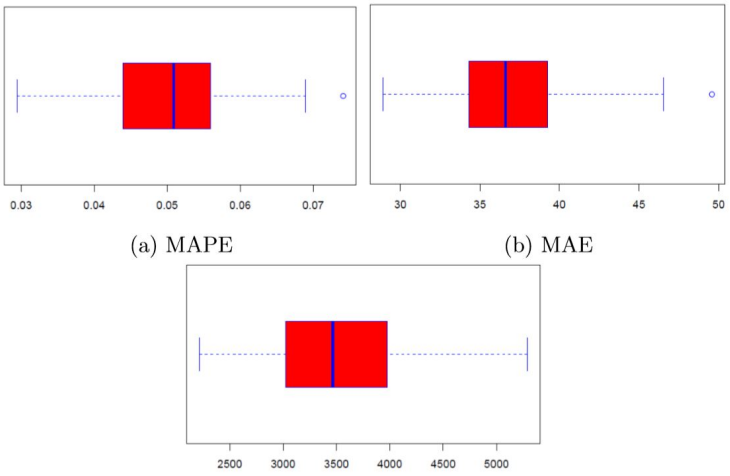

(a) MAPE (b) MAE

(c) MSE

egy, as well as this needs to be adapted to the specific case of interest. As an example, it can be argued that the neural network performances would benefit from increasing the number of observations and, specifically, by using high frequency data. In addition, as the market is highly volatile and the option market follows fast changing rules and patterns, different choices of the neural network specifications - different input layers, structure of the layers, activation functions, etc. - may result more feasible in other contexts. Nevertheless, it may be claimed that the multilayer perceptron neural network model proposed is suitable for pricing options written on Bitcoin. Moreover, it may be argued that its application can be extended to the whole cryptocurrency framework, as well as to traditional markets.

6.6 Conclusion

This chapter proposes an approach that relies on artificial neural network models for the purpose of Bitcoin option pricing. The methodology involves a first step in which options are priced according to some of the most widely employed parametric methodologies, i.e. tree models, Monte Carlo simulation and finite difference method. The option prices obtained in this way are then used as input layers in a second step by the neural network, which is capable to refine the price predictions delivered by the parametric models in the first step. We believe that the proposed model can be extended, without loss of generality, to other cryptocurrency derivatives, as well as to traditional ones.

Empirical results show that the investigated conventional pricing methodologies yield to the conclusion that Bitcoin options are extensively overpriced. In contrast, by applying the proposed neural network model one is able to better represent the real market dynamics of Bitcoin option prices. Indeed, prediction errors consistently reduce when comparing the neural network pricing model to the classical parametric ones.

Further studies may benefit and improve prediction precision by using high frequency data as well as different model specifications. As an example, improvements could be achieved by the use of different models, such as

stochastic volatility models, as input layers in the proposed neural network framework.

7 Network Models to Enhance Automated Cryptocurrency Portfolio Management

Based on the paper:
Giudici, Paolo, Pagnottoni, Paolo, & Polinesi, Gloria. 2020. Network models to enhance automated cryptocurrency portfolio management. *Frontiers in Artificial Intelligence*, **3**, 22.

7.1 Introduction

FinTech innovations are rapidly expanding nowadays, with applications including payments, lending, insurance and asset management, among others. Two technical reports from the Financial Stability Board (FSB) - FSB (2017a), FSB (2017b) - establish several key drivers for FinTech, i.e. the shift of consumer preferences on the demand side, the change of financial regulations on the supply side and the technology evolution.

In this context, services of automated financial consulting are widely spreading and, in particular robo-advisors[17]. They are supposed to match the investors' risk profile with specific class of financial assets and thereby build an efficient portfolio allocation for each specific client. However, the mechanisms underlying the portfolio construction are often obscure, as well as they arguably do not properly take into account for multivariate dependencies across securities which are key to achieve diversification and, therefore, mitigate financial risk. This is particularly true when dealing with peculiarly volatile markets such as the cryptocurrency one, which could be one of the future target market of robo-advisors, given its rapidly growing influence in the financial world.

Indeed, after its introduction by Nakamoto (2008), Bitcoin was launched

[17]An article published on "Statista" in 2019 states that assets under management in the robo-advisory segment amounts to roughly 981 billion USD, as well as that they are expected to grow at an annual growth rate (CAGR 2019-2023) of 27% (source: https://www.statista.com/outlook/337/100/robo-advisors/worldwide)

online in 2009 and paved the way for many other cryptocurrencies. As a matter of fact, as of 17 October 2019, the cryptocurrency market capitalization amounts to approximately 220 billion USD, with a daily trading volume of roughly 52 billion USD.

Along with descriptive and qualitative studies, many researches dealt with quantitative analysis applied to the cryptocurrency market. In particular, a stream of research focuses on price discovery on Bitcoin markets, aiming to determine which are the leaders and followers of the Bitcoin price formation process - see Brandvold et al. (2015), Pagnottoni and Dimpfl (2019) and Giudici and Abu-Hashish (2019). Other related researches studied the interconnectedness and spillover in the cryptocurrency market, such as Corbet et al. (2018b), Giudici and Pagnottoni (2019) and Giudici and Pagnottoni (2020). Another important area regards the study of Bitcoin derivatives - i.e. options and futures written on Bitcoin -, with studies conducted by Corbet et al. (2018a), Baur and Dimpfl (2019) and Pagnottoni (2019). Several studies are approaching the field of profitability of the Bitcoin market, such as Resta et al. (2020).

From a methodological viewpoint, we base our analysis on an important stream of literature, which focuses on stock and financial networks built on correlation matrices. The seminal paper by Mantegna (1999) uses correlation matrices to infer the hierarchical structure of stock markets, deriving a distance measure based on correlation matrices and building the so called Minimal Spanning Tree (MST), a graphical representation able to connect assets which are similar in terms of returns in a pairwise manner. After that, a research by Tola et al. (2008) uses the Random Matrix Theory (RMT) together with several clustering techniques and show that this significantly lowers portfolio risks. Subsequently, other papers about portfolio construction involving the network structure of financial assets followed - see León et al. (2017), Raffinot (2017), Ren et al. (2017) and Zhan et al. (2015).

To the best of our knowledge, there are no papers yet that exploit network topologies to build portfolios composed by cryptocurrencies. We fill this gap

proposing a model that exploits the network structure of cryptocurrencies to provide a portfolio asset allocation that well compares with traditional ones. Following Mantegna (1999) we use Markowitz' asset allocation as a benchmark, and we check whether our proposal is able to improve on it, in terms of risk/return profile.

Indeed, the originality of the current contribution is twofold. From a methodological point of view, we improve the traditional Markowitz (1952) portfolio allocation strategy by means of RMT and MST and by taking network centralities specifically into account. Moreover, throughout this technique we are able to set a parameter of systemic risk aversion that investors can tune to better match their investment strategies with their own risk profile. From an empirical viewpoint, we apply our methodology to data coming from a nascent and highly volatile market, i.e. the cryptocurrency one. This is particularly interesting, as the cryptocurrency market is rapidly expanding and its opportunities due to the high uncertainty (and volatility) around it are quite appealing, and thus a greater number of investors will likely enter it in the short run.

Our empirical findings confirm the effectiveness of our model in achieving better cumulative portfolio performances, while keeping a relatively low level of risk. In particular, we show that our proposed model which employs RMT, MST and centrality measures rapidly adapts to market conditions, and is able to yield satisfactory performances during bull market periods. During bear market periods - instead - our Network Markowitz model employing RMT and MST realizes the best performances, protecting investors from relatively high losses which are instead generated by many other asset allocation strategies tested. Furthermore, the riskiness of our strategy is still lower than most of the competing model we analyze. These outcomes suggest that a sound combination of the proposed models should be employed in order to achieve an efficient cryptocurrency allocation strategy, which could be also used as robo-advisory toolboxes to improve automated financial consultancy.

The chapter proceeds as follows. Section 2 presents our methodology

and, particularly, the Random Matrix Theory, the Minimal Spanning Tree and the portfolio construction. Section 3 illustrates our empirical results. Section 4 concludes.

7.2 Methodology

7.2.1 Random Matrix Theory

Random Matrix Theory (RMT) is widely employed in several fields such as quantum mechanics (Beenakker, 1997), condensed matter physics (Guhr et al., 1998), wireless communications (Tulino et al., 2004), as well as economics and finance (Potters et al., 2005). This technique is able to remove the noise component from the pure signal which is embedded into correlation matrices.

The algorithm tests subsequent empirical eigenvalues of the correlation matrix: $\lambda_k < \lambda_{k+1}; k = 1, \ldots, n$, against the null hypothesis that they are equal to the eigenvalues of a random Wishart matrix $\mathbf{R} = \frac{1}{T}\mathbf{A}\mathbf{A}^{\mathbf{T}}$ of the same size, being $\mathbf{A}$ a $N \times T$ matrix containing N time series of length T. The elements of $\mathbf{A}$ are *i.i.d.* random variables, with zero mean and unit variance.

Marchenko and Pastur (1967) show that as $N \to \infty$ and $T \to \infty$, and the ratio $Q = \frac{T}{N} \geq 1$ is fixed, there is convergence of the sample eigenvalues' density to:

$$f(\lambda) = \frac{T}{2\pi}\frac{\sqrt{(\lambda_+ - \lambda)(\lambda - \lambda_-)}}{\lambda}, \tag{7.1}$$

with $\lambda \in (\lambda_-, \lambda_+)$, $\lambda_\pm = 1 + \frac{1}{Q} \pm 2\sqrt{\frac{1}{Q}}$.

Provided that, if $\lambda_k > \lambda_+$ the null hypothesis is rejected from the k-th eigenvalue onwards. Hence, through a singular value decomposition the RM approach builds up a filtered correlation matrix - see Eom et al. (2009).

In our specific case, consider the continuous log return time series r_i of a generic cryptocurrency i at any time point t. i.e. :

$$r_i^t = logP_i^t - logP_i^{t-1}, \tag{7.2}$$

where P_i^t is the price of the cryptocurrency i at time t.

Considering a bunch of N cryptocurrency return time series, let $\mathbf{C}$ be the $N \times N$ correlation matrix of the cryptocurrency return time series. The random matrix approach filters the correlation matrix, thus obtaining a new matrix $\mathbf{C}^*$ as:

$$\mathbf{C}^* = \mathbf{V}\mathbf{\Lambda}\mathbf{V}^\mathbf{T}, \tag{7.3}$$

with

$$\mathbf{\Lambda} = \begin{cases} 0 & \lambda_i < \lambda_+ \\ \lambda_i & \lambda_i \geq \lambda_+ \end{cases}$$

and $\mathbf{V}$ being the matrix of the deviating eigenvectors linked to the eigenvalues which are larger than λ_+.

7.2.2 The Minimal Spanning Tree

In order to simplify the relationships given by the filtered correlation matrix $\mathbf{C}^*$ obtained from the random matrix approach, we apply the Minimal Spanning Tree representation of the cryptocurrency return time series. This is consistent with the literature on stock similarities, i.e. Mantegna and Stanley (1999), Bonanno et al. (2003) and Spelta and Araújo (2012).

Given the filtered correlation matrix obtained in the step above, we may derive an Euclidean distance for each pairwise correlation element in the matrix, i.e. :

$$d_{ij} = \sqrt{2 - 2c_{ij}^*}, \tag{7.4}$$

where c_{ij}^* is a generic element (i, j) of the matrix $\mathbf{C}^*$, with $i, j = 1, ..., N$. Each pairwise distance can be inserted in the so-called distance matrix $\mathbf{D} = \{d_{ij}\}$. The MST algorithm is able to reduce the number of links between the assets from $\frac{N(N-1)}{2}$ to $N - 1$ linking each node to its closest neighbour. In particular, we initially consider N clusters associated to the N cryptocurrencies and, at each subsequent step, we merge two generic clusters l_i and l_j if:

$$d\left(l_i, l_j\right) = \min\left\{d\left(l_i, l_j\right)\right\},$$

with the distance between clusters being defined as:

$$\hat{d}\left(l_i, l_j\right) = \min\left\{d_{pq}\right\},$$

being $p \in l_i$ and $q \in l_j$. This procedure is iteratively repeated until we remain with just one cluster at hand.

Moreover, with the aim of explaining the evolution of relationships evolve over time, Spelta and Araújo (2012) proposed the so-called residuality coefficient, which compares the relative strength of the connections above and below a threshold distance value, i.e. :

$$R = \frac{\sum\limits_{d_{i,j}>L} d_{i,j}^{-1}}{\sum\limits_{d_{i,j}\leq L} d_{i,j}^{-1}} \tag{7.5}$$

with L being the highest threshold distance value ensuring connectivity of the MST. Intuitively, the residuality coefficient R increases when the number of links increases - meaning the network becomes more sparse -, and viceversa lowers with decreasing number of links

7.2.3 Network centrality measures

In this chapter we employ of centrality measures in order to develop a portfolio allocation that takes into account the centrality of a node (cryptocurrency) in the system. Network theory includes several centrality measures such as the degree centrality, counting how many neighbours a node has, as well centrality measures based on the spectral properties of graphs - see Perra and Fortunato (2008). Among the spectral centrality measures we remark Katz's centrality - see Katz (1953) -, PageRank - Brin and Page (1998) -, hub and authority centralities - Kleinberg (1999) - and the eigenvector centrality - Bonacich (2007).

In this chapter we employ of the eigenvector centrality, as it measures the importance of a node in a network by assigning relative scores to all nodes in the network. Relative scores are based on the principle that being connected

to few high scoring nodes contributes more to the score of the node in question than equal connections to low scoring nodes. In other words, considering a generic node i, the centrality score is proportional to the sum of the scores of all nodes which are connected to it, i.e. :

$$x_i = \frac{1}{\lambda} \sum_{j=1}^{N} \hat{d_{i,j}} x_j \tag{7.6}$$

where x_j is the score of a node j, $\hat{d_{i,j}}$ is the element (i, j) of the adjacency matrix of the network, λ is a constant. The equation from above can be rewritten in a compact form as:

$$\hat{\mathbf{D}}\mathbf{x} = \lambda \mathbf{x} \tag{7.7}$$

where $\hat{\mathbf{D}}$ is the adjacency matrix, λ is the eigenvalue of the matrix $\hat{\mathbf{D}}$, with associated eigenvector $\mathbf{x}$, a vector of scores of dimension N, meaning one element for each node. Note that as our networks are based on distances between returns, the higher the centrality measure associated to a node, the more the node behaves dissimilarly with respect to the other nodes in the network.

7.2.4 Portfolio construction

Asset correlations are key items in investment theory and risk measurement, in particular for optimization problems as in the case of the widely known portfolio theory described by Markowitz (1952). As a consequence, correlation based graphs are useful tool to build optimal investment strategies. In this Subsection we show how portfolio construction can be enhanced by means of a combination of the RMT, MST and network centrality measures described above.

Several researches have investigated the relationship between the network structure of financial assets and portfolio strategies. The study Onnela et al. (2003) shows how a portfolio constructed via Markowitz theory is mainly composed by assets that lie in the periphery of the asset network structure,

i.e. outer node assets, and not in its core. Pozzi et al. (2013) find that peripheral assets in the network yield to better performances and lower portfolio risk with respect to central ones. Peralta and Zareei (2016) show that the centrality of assets within a network are negatively related with the optimal weights obtained through the Markowitz technique. Building on that, Vỳrost et al. (2018) conclude that asset allocation strategies including the network structure of financial asset are able to improve a portfolio's risk-return profile.

Another stream of literature focused on proposing alternative portfolio allocation strategies based on the network structure of financial assets. To illustrate, Plerou et al. (2002) and Conlon et al. (2007) use the random matrix theory to filter the correlation matrix to be inserted in the Markowitz minimization problem, while Tola et al. (2008) add the MST obtaining improvements with respect to the raw model.

In the present context we aim to study the differences in the risk-return profiles of our strategy, which includes topological measures in the optimization problem, with respect to the traditional Markowitz model, possibly yielding to better risk-return characteristics of the portfolios. The originality of our approach builds on the fact that we do not only use RMT and MST as alternative approaches to quantify risk diversification, but we employ an extension of the traditional Markowitz method by including these techniques in the minimization problem. Indeed, in the present case we want to solve the following problem:

$$\min_{\mathbf{w}} \mathbf{w^T \Sigma^* w} + \gamma \sum_{i=1}^{n} x_i w_i \tag{7.8}$$

subject to

$$\begin{cases} \sum_{i=1}^{n} w_i = 1 \\ \mu_P \geq \frac{\sum_{i=1}^{n} \mu_i}{n} \\ w_i \geq 0 \end{cases}$$

where $\mathbf{w}$ is the vector of portfolio weights, being w_i the weight associated to the cryptocurrency i, $\mathbf{\Sigma}^*$ is the filtered variance-covariance matrix with generic element (i, j) represented by $\sigma_i \sigma_j c^*_{i,j}$, γ is the parameter representing the risk aversion of the investor, x_i is the eigenvector centrality associated with the cryptocurrency i, μ_P indicates the return of the portfolio and μ_i the return of the generic cryptocurrency i.

Generally speaking, portfolios built upon the traditional Markowitz theory are such that the risk is minimized for a given expected return, using as input the raw variance-covariance matrix of returns. In our case, the methodological improvement is twofold. Firstly, we modify the input variance-covariance matrix, which is filtered by both RMT and MST. Secondly, we add a component derived from the MST structure which relates to an extra risk component the investor may want to control for. Indeed, by modulating γ the investor can set its own level of risk aversion towards systemic risk specifically, and not just to the portfolio risk as in the Markowitz framework. As a matter of fact, being centralities inversely related with distances, a small value of γ yields to portfolios composed by less systemically risky cryptocurrencies, which generally lie in the peripheral part of the network. Conversely, a large value of γ makes the algorithm select more systemically relevant cryptocurrencies, meaning those who are in the centre of the network structure. For the sake of completeness, we will test different values of the systemic risk aversion parameter in the course of the current application.

7.3 Empirical findings

7.3.1 Data description and network topology analysis

In our empirical application we consider 10 time series of returns referred to cryptocurrencies traded over the period 14 September 2017 - 17 October 2019 (764 daily observations). In particular, we consider the first 10 cryptocurren-

cies in terms of market capitalization as of 17 October 2019[18]. To be precise, we analyze the return time series of the following cryptocurrencies: Bitcoin (BTC), Ethereum (ETH), Ripple (XRP), Tether (USDT), Bitcoin Cash (BCH), Litecoin (LTC), Binance Coin (BNB), Eos (EOS), Stellar (XLM), Tron (TRX).

We provide some basic descriptive statistics of our data in Table 29. From Table 29 one may notice that average daily returns are all close to zero, in line with the general economic theory regarding asset returns. However, the 10 cryptocurrencies exhibit different standard deviations, meaning that the variability in returns differs quite strongly among cryptocurrencies. To illustrate, USDT is the one showing the lowest relative variability; this is in line with the fact that this cryptocurrency is classified as stable coin, therefore its price should not deviate too much on a daily basis. On the other hand, TRX is the one showing the highest standard deviation; indeed, this particular cryptocurrency witnessed a period of high fluctuations during the considered sample period. As far as kurtosis is concerned, most of the cryptocurrencies exhibit values which reflects the non-gaussian and heavy tailed behaviour of their associated distribution. This is particularly true for XLM and XRP, whose kurtosis are relatively larger than the ones of the other time series.

To better understand the dynamics of the cryptocurrency time series, we plot the normalized price series in Figure 30 and Figure 31[19]. The two figures confirm well known features of cryptocurrencies, such as their overall high volatility (with TRX being the most volatile), the stability of the stable coin (USDT) as well as the low liquidity that some of them exhibit (such as TRX).

In order to apply the filter through RMT, we divide the dataset into consecutive overlapping windows having a width $T = 120$ (4 trading months). We set the window step length to one week (7 trading days), which makes up a total of 93 weekly four-month windows.

[18] We exclude Bitcoin SV (BSV) in order to achieve a sufficiently large timespan, meaning a more than 2-year time period.

[19] We split the plot in two different figures for scale reasons.

Table 29: Summary statistics

	Mean	Std	Kurtosis	Skewness
BTC	0.0009	0.04	3.35	-0.07
ETH	-0.0007	0.05	2.90	-0.33
XRP	0.0004	0.07	15.73	1.80
USDT	0.0000	0.01	4.28	0.22
BCH	-0.0011	0.08	6.47	0.49
LTC	-0.0003	0.06	8.02	0.66
BNB	0.0033	0.07	7.74	0.78
EOS	0.0017	0.07	3.93	0.60
XLM	0.0021	0.10	26.19	2.03
TRX	0.0021	0.15	13.15	0.66

Note: The table shows relevant summary statistics for the 10 cryptocurrencies considered related to the whole sample period, i.e. 13 September 2017 - 10 October 2019.

For each time window considered, we use 15 weeks of daily observations to estimate the model, while the last week is used for validation purposes. In other words, we compute 93 correlation matrices between the 10 cryptocurrency return time series, each one based on 15 weeks of daily returns and then filter them by means of the Random Matrix approach. Applying the Random Matrix filtering, correlation matrices are rebuilt considering only the eigenvectors corresponding to the deviating eigenvalues.

In order to have a better understanding of the links existing between cryptocurrencies, the filtered correlation matrices are then used to derive the MST representation over two main periods of interest. In particular, we plot the MST structure emerging from the period of the cryptocurrency price hype (September 2017- January 2018) in Figure 32, while the MST structure related to the latest trading period analyzed (June 2019- October 2019) in Figure 33.

Figure 30: Normalized cryptocurrency price series I

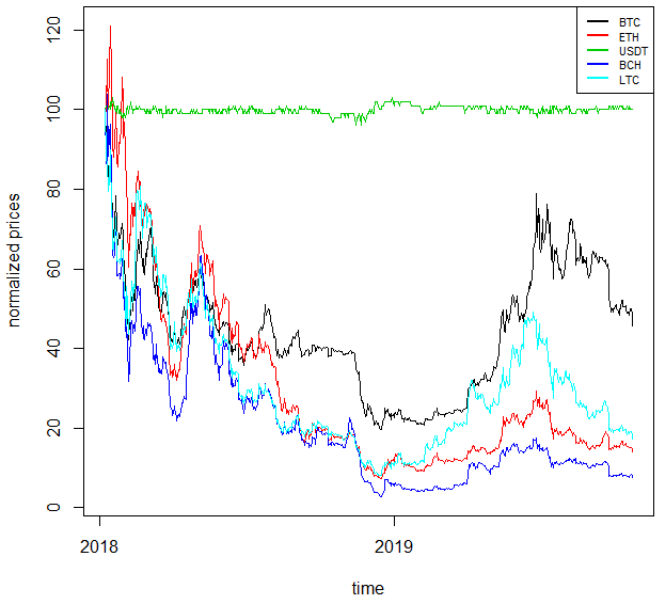

Note: The figure shows the normalized price series for 5 cryptocurrencies: BTC,ETH,USDT, BCH,LTC, relative to the period 7 January 2018 - 17 October 2019.

As it is clear from the graph, the two networks show quite similar features. Indeed, ETH is the cryptocurrency which always lies in the centre of the structure, indicating its central role in the cryptocurrency market. The only difference between the two graphical representations concerns USDT, which during the price hype is not connected directly to ETH as the other cryptocurrencies, but to LTC. This is linked to the fact that USDT is a stable coin and, therefore, behaves dissimilarly from the other cryptocurrencies considered, being it much less volatile. However, this difference in behaviour levels out during the latest period, as it emerges from Figure 33.

To better understand the dynamics of the MST among cryptocurrencies,

Figure 31: Normalized cryptocurrency price series II

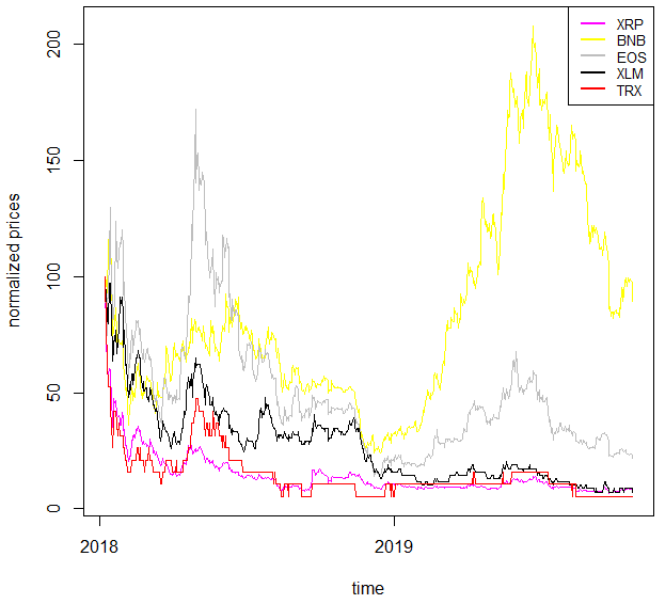

*Note:*The figure shows the normalized price series for 5 cryptocurrencies: XRP, BNB, EOS, XLM,TRX, relative to the period 7 January 2018 - 17 October 2019.

we investigate the evolution of the links over time. Indeed, we compute two different measures: the Max link, i.e. the value of the maximum distance between two pairs of nodes in the tree, and the residuality coefficient, meaning the ratio between the number of links which are dropped and the number of those who are kept by the MST algorithm. The two metrics, computed over the whole sample period, are illustrated in Figure 34.

From Figure 34 one may notice that the Max link increases during the Bitcoin price hype and fluctuates around relatively large values until roughly mid 2018, meaning that during this period correlations between cryptocurrency returns are strongly misaligned. After that, the index bounces back towards its previous values and even below, suggesting that cryptocurrency

Figure 32: MST September 2017- January 2018

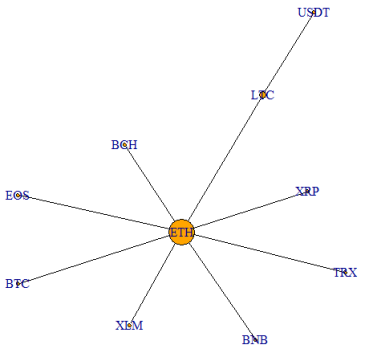

Note: The figure shows the MST representation relative to the period of the speculative bubble.

Figure 33: MST June 2019- October 2019

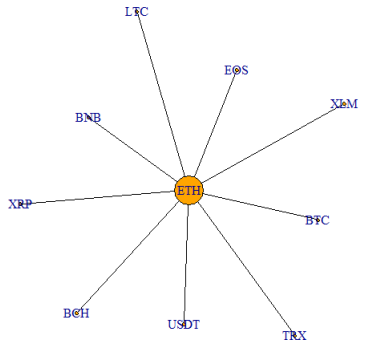

Note: The figure shows the MST relative to the period June 2019- October 2019.

returns start to behave more similarly during the latest period. Furthermore, the residuality coefficient increases during the very beginning of the sample period, while it sharply declines during the price hype phase. After the decrease, the coefficient stays quite stable and then gently increases not without fluctuations from mid 2018 to the end of the sample period. This suggests that the number of links until mid 2018 was quite limited - and, therefore, returns misaligned -, whereas the same number started to increase after that

Figure 34: MST thresholds and residuality coefficients

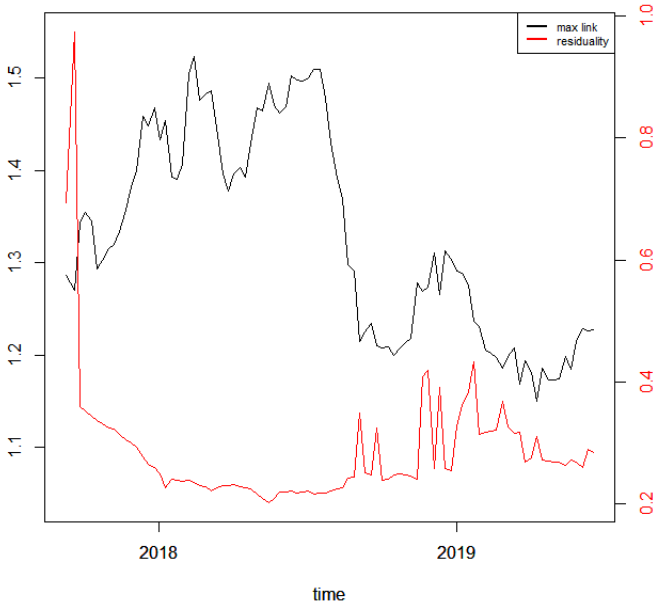

Note: The black line shows the Max link distance, while the red line shows the residuality coefficient, whose values are reported respectively on the left and right y axis.

phase, meaning there were more connections and thus more synchronicity across cryptocurrency returns.

7.3.2 Portfolio construction

In this Subsection we illustrate the results related to the proposed portfolio strategies. The optimal portfolio weights are obtained through the constrained minimization of the objective function in Equation (7.8). For the sake of completeness, we use different values of the systemic risk aversion parameter γ, meaning $\gamma = 0.005, 0.025, 0.05, 0.15, 0.7, 1$. These values have been chosen, without loss of generality, to be representative of different

aversion profiles. While $\gamma = 0$ indicates no aversion, $\gamma = 1$ indicates a high aversion, with systemic risk being given the same importance as non-systemic one.

We use fifteen weeks, i.e. to compute the optimal portfolio weights as described in Section 7.2. We then use the last week associated to each window to evaluate the out-of-sample performance of our technique, meaning to compute the portfolio returns and, therefore, the resulting Profit & Losses. We then compute portfolio returns for the period 7 January 2018 - 17 October 2019, accounting for rebalancing costs, which are supposed to amount to 10 basis points.

In Figure 35 we plot the returns of our investment strategies for the different values of γ mentioned above as well as for $\gamma = 0$ (Network Markowitz), meaning the results of the Markowitz portfolio strategy using the variance-covariance matrix filtered by RMT and MST. In doing so, we plot portfolio performances under the hypotesis of investing 100 USD at the beginning of the period, and examining how much is lost along time. The results of our strategies are compared with the performance of several strategies and indicators: the benchmark portfolio (CRIX[20]), the Markowitz portfolio with variance-covariance matrix filtered by the Glasso[21] technique (Glasso Markowitz), the naive portfolio (Equally Weighted) and the Markowitz portfolio (Classical Markowitz). To better highlight the results of our best proposed model, we plot the results only for a selection of portfolio strategies in Figure 36. To complement this information, we report the 4-month cumulative Profits & Losses of each of the considered strategy in Table 30.

Overall, we are considering a period in which the cryptocurrency market witnesses a down period - except for the first part of our analyzed timespan and several short periods consequently occurring. Therefore, as the mar-

[20]The CRIX is a cryptocurrency market index following the Laspeyres methodology for the construction of indexes. More information about CRIX can be found at https://thecrix.de/

[21]The sparsity parameter ρ has been set to 0.01, as in the reference paper by Friedman et al. (2008).

Figure 35: Performances of different portfolio strategies

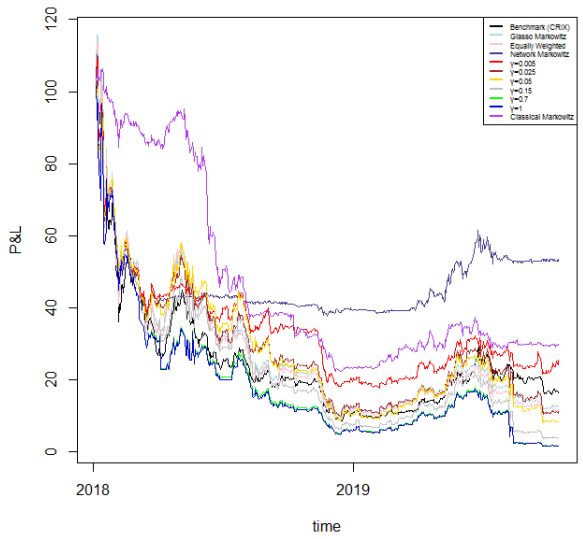

Note: The plot reports the profits and losses of a portfolio with initial value of 100 USD obtained by the CRIX benchmark index (Benchmark (CRIX)), the optimization using the Markowitz approach with the variance-covariance matrix filtered by Glasso (Glasso Markowitz), the naive portfolio (Equally Weighted), our optimization using RMT and MST applied to the variance-covariance matrix (Network Markowitz), our model based on different values of γ ($\gamma = 0.005, 0.025, 0.05, 0.15, 0.7, 1$), and the standard Markowitz portfolio (Classical Markowitz). The portfolio values are plotted for the period 7 January 2018 - 17 October 2019.

ket is not profitable during the studied period, we aim to achieve through our allocation strategies losses which are lower than those yielded by other competing methodologies.

On the one hand, during a first phase which lasts roughly until mid 2018, the traditional Markowitz porfolio seems to overperform the other portfolio allocation strategies. Indeed, the allocation by Markowitz' technique yields

Figure 36: Performances of selected portfolio strategies

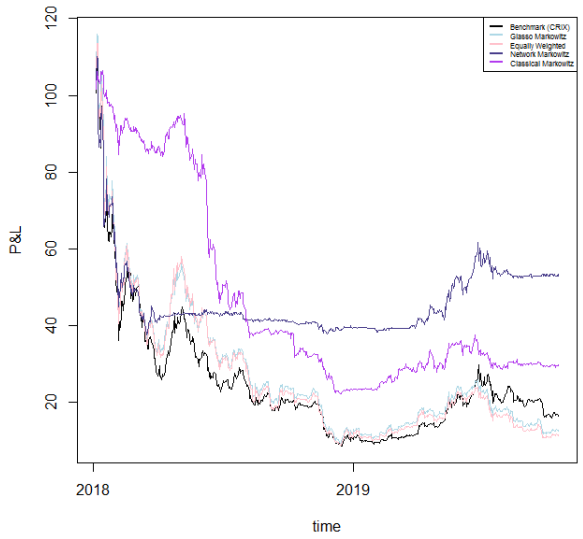

Note: The plot reports the profit and losses of a portfolio with initial value of 100 USD obtained by the CRIX benchmark index (Benchmark (CRIX)), the optimization using the Markowitz approach with the variance-covariance matrix filtered by Glasso (Glasso Markowitz), the naive portfolio (Equally Weighted), our optimization using RMT and MST applied to the variance-covariance matrix (Network Markowitz) and the standard Markowitz portfolio (Classical Markowitz). The portfolio values are plotted for the period 7 January 2018 - 17 October 2019.

to positive (cumulative) returns until January 2018 and just slightly negative ones until May 2018, however still lower than the losses provided by the other strategies in absolute terms.

On the other hand, from September 2018 onwards all portfolios start providing strong negative returns. Indeed, the returns yielded by the portfolio constructed via Markowitz start to decline dramatically, together with those of the model including the systemic risk aversion parameter. This is because the latter model takes into account the centrality of the cryptocurrencies in

Table 30: Cumulative Profits & Losses

Period	CRIX	GM	EW	CM	NW	$\gamma = 0.005$	$\gamma = 0.025$	$\gamma = 0.05$	$\gamma = 0.15$	$\gamma = 0.7$	$\gamma = 1$
Jan-2018	-0.14	-0.13	-0.16	0.04	-0.22	-0.21	-0.26	-0.27	-0.36	-0.43	-0.43
May-2018	-0.67	-0.62	-0.60	-0.12	-0.79	-0.78	-0.73	-0.66	-0.83	-1.08	-1.10
Sep-2018	-1.37	-1.37	-1.43	-0.88	-0.83	-1.02	-1.24	-1.23	-1.40	-1.60	-1.64
Jan-2019	-1.85	-1.78	-1.78	-1.32	-0.87	-1.50	-1.86	-1.98	-2.19	-2.29	-2.31
May-2019	-1.35	-1.25	-1.27	-1.01	-0.74	-1.22	-1.33	-1.29	-1.44	-1.55	-1.57
Sep-2019	-0.99	-1.45	-1.49	-1.02	-0.54	-1.19	-1.34	-1.44	-1.86	-2.13	-2.15

Note: The table shows the cumulative 4-month Profits & Losses of portfolios under different strategies. Particularly, Profits & Losses are computed for the CRIX benchmark index (CRIX), the Glasso Markowitz (GM), the naive portfolio (EW), the Network Markowitz (NW), the classical Markowitz (CM), and the proposed models with different values of γ ($\gamma = 0.005, 0.025, 0.05, 0.15, 0.7, 1$). All values are expressed in percentage terms.

the network and is therefore more adaptive to market conditions, regardless of whether they are favourable or not. Indeed it can be noticed that - overall - during bull market periods our model taking into account for risk aversion reacts very fast to upward movements and yields to good cumulative performances; conversely, during down market periods, the same model yields to worse relative performances due to declining market conditions.

However, during the second half of our sample period our proposed model with the systemic risk aversion parameter γ set to 0 (Network Markowitz) clearly overwhelms the other portfolio allocation strategies. To illustrate, if we look at the cumulative performance of the above mentioned method, we can see that it more than halves losses with respect to the equally weighted portfolio, to the Glasso Markowitz portfolio and to all portfolios including a risk aversion parameter $\gamma > 0$. Moreover, it almost halves the losses with respect to the benchmark index (CRIX) and to the traditional Markowitz methodology. This suggests that this model is capable to provide a stronger coverage for losses in case of down market periods with respect to all other considered asset allocation strategies [22].

[22] A sensitivity analysis reported in the Appendix

In Table 31 we compute the 4-month Value at Risk (VaR) with a confidence level of 0.05 % for the benchmark index (CRIX), the equally weighted portfolio, our Network Markowitz portfolio, the Glasso Markowitz and the traditional Markowitz portfolios. This is done in order to compare, together with cumulative returns, the potential riskiness of our strategy with respect to the alternative portfolio allocation methods considered.

Table 31: Value at Risk

Period	**CRIX**	**EW**	**NW**	**GM**	**CM**
Jan-2018	0.11	0.13	0.15	0.14	0.03
May-2018	0.04	0.05	0.02	0.05	0.03
Sep-2018	0.11	0.11	0.10	0.12	0.02
Jan-2019	0.07	0.10	0.05	0.07	0.01
May-2019	0.04	0.02	0.03	0.02	0.04
Sep-2019	0.05	0.05	0.02	0.05	0.01

Note: The table shows the 4-month Value at Risk of portfolios under different strategies for a confidence interval of 95 %. In particular, the VaR is computed for the CRIX benchmark index (CRIX), the naive portfolio (EW), the Network Markowitz (NW), the Glasso Markowitz (GM) and the classical Markowitz (CM). All values are expressed in absolute terms multiplied by a scale factor of 100.

Table 31 shows that, except for the price hype period, our proposed Network Markowitz approach generally yields to lower values at risk with respect to the benchmark index (CRIX), the naive portfolio and the Glasso Markowitz. The aforementioned model is instead more risky than the traditional Markowitz model, although the latter, overall, yields too far way larger negative returns. In general, the riskiness of our strategy seems to be quite satisfactory with respect to the alternative allocation strategies analyzed.

To further support our conclusions, Table 32 presents the Sharpe ratio under the different strategies.

Table 32 gives further evidence to support our conclusions: the proposed Network Markowitz approach yields better Sharpe Ratios.

Table 32: Sharpe Ratio

Period	**GM**	**EW**	**CM**	**NW**	$\gamma = 0.005$	$\gamma = 0.025$	$\gamma = 0.05$	$\gamma = 0.15$	$\gamma = 0.7$	$\gamma = 1$
Jan-2018	-0.05	-0.05	-0.03	-0.13	-0.12	-0.08	-0.06	-0.08	-0.09	-0.10
May-2018	-0.14	-0.14	-0.19	-0.03	-0.04	-0.08	-0.09	-0.08	-0.07	-0.07
Sep-2018	-0.10	-0.09	-0.17	-0.04	-0.17	-0.17	-0.20	-0.20	-0.18	-0.17
Jan-2019	0.10	0.09	0.11	0.09	0.06	0.08	0.11	0.12	0.12	0.12
May-2019	-0.02	-0.02	0.01	0.08	0.02	0.02	-0.00	-0.03	-0.04	-0.04
Sep-2019	-0.06	-0.06	-0.03	0.03	0.07	-0.11	-0.14	-0.14	-0.14	-0.14

Note: The table shows the 4-month values of Sharpe ratio of portfolios under different strategies. In particular, the SR is computed for the Glasso Markowitz (GM), the naive portfolio (EW), the classical Markowitz (CM), the Network Markowitz (NW) and for all the value of γ.

To strengthen the robustness of our conclusions, Table 33 presents the Rachev ratio, with a confidence level of 10%, under the different strategies. The Rachev ratio is a useful supplement of the Sharpe ratio, when data is non-symmetric, as in our context. It is calculated as the ratio between an extreme gain and an extreme loss.

Table 33: Rachev Ratio

Period	**GM**	**EW**	**CM**	**NW**	$\gamma = 0.005$	$\gamma = 0.025$	$\gamma = 0.05$	$\gamma = 0.15$	$\gamma = 0.7$	$\gamma = 1$
Jan-2018	0.74	0.75	0.63	0.64	0.69	0.77	0.79	0.78	0.77	0.99
May-2018	0.73	0.75	0.95	0.83	0.74	0.77	0.83	0.87	0.87	0.55
Sep-2018	0.81	0.84	0.87	0.61	0.80	0.75	0.76	0.80	0.80	0.48
Jan-2019	1.16	1.11	1.47	1.24	1.34	1.36	1.39	1.40	1.40	1.26
May-2019	0.80	0.80	1.05	0.97	0.93	0.84	0.75	0.72	0.72	0.98
Sep-2019	0.75	0.78	1	1.14	0.43	0.38	0.38	0.38	0.37	0.78

Note: The table shows the 4-month values of Rachev Ratio (RR) of portfolios under different strategies. In particular, the RR is computed for the Glasso Markowitz (GM), the naive portfolio (EW), the classical Markowitz (CM), the Network Markowitz (NW) and for all the value of γ.

Table 33 shows that the Network Markowitz approach yields the best performances in the initial and final periods, and the Classic Markowitz in

all other periods. The other strategies generally show worse performances. This is consistent with our previous findings, and with the fact that the Rachev ratio takes higher values during periods characterised by decreasing returns, such as the quarter preceding January 2019.

Overall, we cannot say that the proposed model overperforms traditional approach (such as Glasso Markowitz and Classical Markowitz). It does so in certain periods and according to certain risk aversion parameterisations.

For the sake of completeness, we plot the portfolio weights of the winning strategy over the evaluation time horizon in Figure 37. As one can clearly see, the composition of the portfolio varies quite much over time. Indeed, during the first period of the sample, approximately until February 2018, the portfolio is composed by various assets, with USDT gaining a high share over time, being it the most stable across all. After that, BTC is the cryptocurrency which is mostly selected by our algorithm, roughly until October 2018 (with some exceptions), as it is considered a proxy of the whole market. Finally, the algorithm selects different cryptocurrency compositions until the end of the sample, being the latter a highly uncertain period for the market.

Last, we present, for comparison purposes, the the portfolio weights associated with $\gamma = 1$.

While Figure 37 gives the weights relative to the situation of no systemic risk aversion, Figure 38 gives the weight corresponding to a very high systemic risk aversion, in which it has the same importance as non systemic risk.

7.4 Conclusion

In this chapter we have proposed a methodology that aims to build an allocation strategy which is suitable for highly volatile markets, such as cryptocurrency ones. In particular, we have applied our models to a set of 10 cryptocurrency return time series, selected in terms of market capitalization. We have shown that the use of network models can enhance portfolios' risk-return profiles and mitigate losses during down market periods.

We have demonstrated how the use of centrality measures, together with

Figure 37: Winning strategy portfolio weights

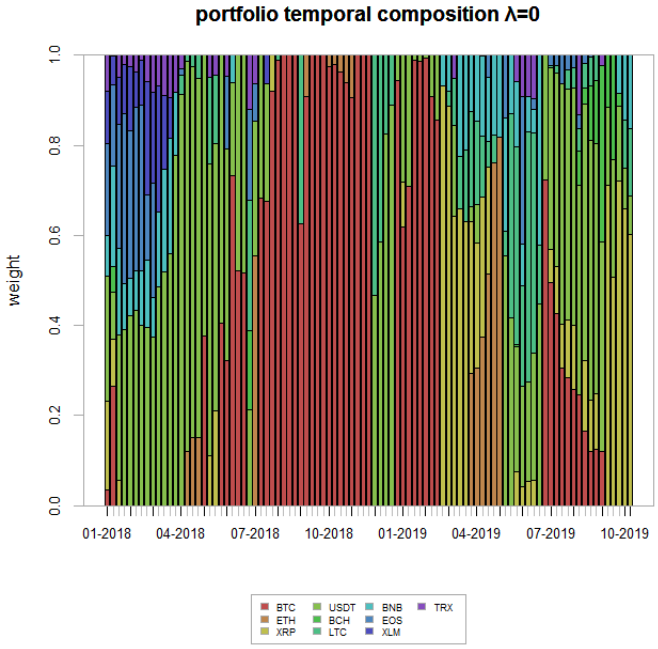

Note: The figure shows the portfolio weights associated to the winning strategy - i.e. the Network Markowitz (NW) - for the analyzed time period.

tuning an investor's systemic risk aversion, is a suitable methodology to make profits during bull market periods, as this method is rapidly adaptive to market conditions. We have also shown that, to protect investors from losses during bear market periods, the combination of Random Matrix Theory and Minimal spanning trees can yield to acceptable risk-return profiles and/or mitigate losses.

Our empirical findings show that, overall, the proposed method is acceptable, even during downturn periods. However, we cannot claim that this proposed model should always be used in automated consultancy . It should always be compared with competing alternatives, according to different market conditions and different risk aversions.

Figure 38: Highly risk adverse strategy portfolio weights

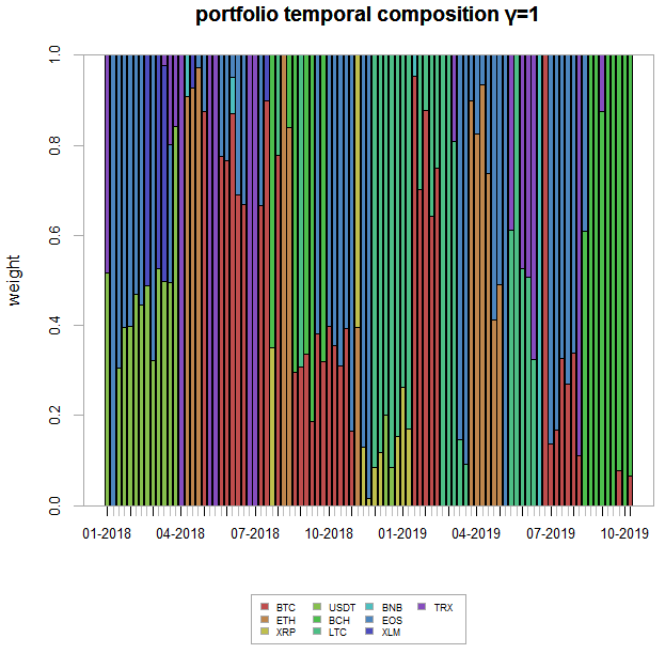

Note: The figure shows the portfolio weights associated to a highly systemic risk adverse strategy - $\gamma = 1$- for the analyzed time period.

Further research should involve, besides the application to other contexts, the consideration of different base portfolio allocation models. We have used Markowitz' as it is the most employed by robot advisory platforms.

8 Chaos Based Portfolio Selection: a Constant Chaoticity Approach

Based on the paper:
Spelta, Alessandro, Pecora, Nicoló, & Pagnottoni, Paolo. 2020. Chaos Based Portfolio Selection: a Constant Chaoticity Approach. *Working Paper*.

8.1 Introduction

The evolution of stock market data is known to be highly non-linear and to predict their future values for the formation of a profitable portfolio is undoubtedly a challenging task. The difficulties of stock returns prediction lie on the fact that data are non-stationary or non-linear in nature, and their patterns are difficult to be captured. Non-linearities are an evidence of economic life and for many financial applications the source of which is even apparent, yet empirical evidence of their existence is still weak. For instance, stock return dynamics are largely influenced by investor attitudes towards expected risk and return and by the strategic interaction between market participants, both of which are intrinsically non-linear. This translates into a plain obstacle for making effective forecasts and for selecting optimal portfolios. The foundation of portfolio theory dates back to the mean-variance model by Markowitz (1952) which constitutes the classic paradigm of the modern finance theory for asset allocation. However this approach suffers from some drawback since the estimation results that derive from this method may lead to portfolios having weights concentrated on only few stocks, thus increasing the risk of the investment. Moreover, the mean-variance model can be seen as an approach adopting a rear-view mirror for providing a portfolio selection and as a result it turns out to be inherently slower to react to changes in news and volatility.
Following Markowitz (1952), various researchers proposed enhanced models with the same goal of maximizing the expected return and to minimize risk

portfolio. These approaches include traditional linear and non-linear models as well as artificial intelligence (AI) based techniques. There exists a burgeoning literature related to traditional (linear) statistical methods such as Moving Averages, Exponential Smoothing or Auto-regressive Integrated Moving Averages (ARIMA) for financial time series prediction (see e.g. Box and Tiao 1975, Wheelwright et al. 1998). While these methods are statistically powerful, they have failed to yield accurate predictions on the test data and to capture regularities in such time series. Many non-linear time series models have been proposed in the statistical literature, such as the bilinear models of Granger and Andersen (1978), the threshold autoregressive (TAR) model of Tong and Lim (2009), the state-dependent model of Priestley (1980), and the Markov switching model of Kuan (2002). AI-based models employ artificial neural networks (ANN) which also includes multilayer perceptron (MLP) and radial basis function (RBF) as in Chen (1994), support vector machines (SVM) as or instance in Gavrishchaka and Banerjee (2006), support vector regression (SVR) as in Burges (1998); Huang et al. (2005), genetic algorithms (GA), particle swarm optimization (PSO) as in Majhi et al. (2008), artificial fish swarm (AFS) as Neshat et al. (2014) and general regression neural network (GRNN) as introduced by Specht et al. (1991). All these approaches share the aim of reducing the uncertainty of predictions by including forms of forward-looking forecasting techniques in order to take into account the continuous availability of data and news.

It is against this background that chaos theory may offer an alternative device to consider and model the underlying non-linear dynamic behaviour of financial time series. In particular, we shall show that the adoption of the tools from non-linear systems and chaos theory allows us to improve the forecasting objective through a forward-looking approach that can make long-term time series predictions.

Since several decades researchers have been looking for chaotic dynamics in economic and financial time series. The hypothesis that deterministic chaos may underlie apparently random variation in financial series has been re-

ceiving a huge interest (see LeBaron (1994), Benhabib (1996), Peters (1996), and Mandelbrot (1999) among others). Recognizing and quantifying chaos in financial time series constitutes an important step towards the understanding of the nature of such series and revealing the extent to which short and eventually long term forecasts may be improved. The possibilities of chaos in economic systems brought an enormous amount of initial interest. From forecasting movements in foreign exchange and stock markets, to understanding international business cycles, chaos in economics and finance has a broad range of potential applications. However, initial studies have been somewhat inconclusive (see Barnett and Serletis (2000)) and there have been no reports of exploitable deterministic dynamics in financial time series (see Malliaris and Stein (1999)). LeBaron (1994) argued that any chaotic dynamics that exist in financial time series are probably insignificant compared to the stochastic component and are not easy to detect. Nonetheless, in addition to the main stochastic component, we are interested in whether there is a significant non-linear determinism, and chaos, exhibited by financial series, and how such determinism may be exploited from a forecasting perspective. In an effort to quantify determinism and chaos, a variety of measures have been applied to a vast range of economic and financial time series. Examples refer to the estimation of Lyapunov exponents as in Schittenkopf et al. (2000), the correlation dimension as in Harrison et al. (1999) and Hsieh (1991), the closely related BDS statistic of Brock et al. (1991), the mutual information and other complexity measures by Darbellay and Wuertz (2000) and non-linear predictability of Agnon et al. (1999). The rationale of each of these methods was to apply a measure of non-linearity or "chaoticity" to the supposed i.i.d. returns (or log-returns). The work by Small and Chi (2003) showed that the system generating the financial time series analyzed in their paper is a non-linear dynamical system driven by noise that is either not in equilibrium or undergoing bifurcation/non-stationarity. Accordingly, despite the non-stationarity, they found a characteristic non-linear deterministic structure that persists.

Starting from these premises, we build on the literature related to the connection of chaos and dynamical systems to non-linear time series analysis. Once chaos is detected in a system, much more is known about its dynamical behavior, which is particularly useful for building investment strategies and predictions. In this chapter, we make use of non-linear measures, such as the Lyapunov exponents, which allow us to make long-term predictions that can be exploited for forecasting strategies. In particular, starting from the non-linear properties of financial time series, following an approach similar to Golestani and Gras (2014), we build a portfolio strategy that goes beyond the simple one-step ahead prediction and that features a reasonable level of accuracy and performance in terms of generated profits. Our methodology begins with the reconstruction of the attractor phase space from a single time series; once this step is accomplished, a unique characteristic that somehow represents the chaotic behaviour of the series is extracted. Then the forecasting method generates successive new values that continue the series, each value minimising the difference between the chaoticity of the new time series and the initial one. Finally, the forecasted prices are employed to build what we name the Constant Chaoticity Portfolio (CCP). We create top-bottom portfolios through stocks' single sorting, in which we generate a signal computed using price forecasts or, alternatively, past prices and which suggests the future market direction for each stock. Then, a further portfolio is generated according to a double sorting criterion, in which we simultaneously take into account signals computed using price forecasts and past prices. We test our methodology with two different datasets, namely the STOXX Europe 50 index and the Hang Seng index. The results, in terms of portfolio performances, show that our methodology is able to correctly make forecasts at a long time horizon and to generate net profits that overcome those obtained by portfolios computed by simply considering the past returns, equally weighted portfolios or ARIMA based portfolios.

The remainder of the chapter is organized as follows: Section 2 is devoted to the methodology and outlines the main steps of our forecasting procedure

which is adopted for the construction of the portfolios; Section 3 describes in detail the datasets and presents the results; Section 4 contains the sensitivity analysis which aims at checking the robustness of our method by showing how portfolio performances react to changes in the underlying model parameters and forecast horizon choice. Finally, Section 5 concludes.

8.2 The Constant Chaoticity Portfolio: methodology

This Section is devoted to shed light on the creation of the Constant Chaotic Portfolio (CCP) resulting from the stocks prices forecasts. As a reference benchmark we consider the survival components of the STOXX Europe 50 index and the Hang Seng index. These assets are those which remained within the indexes throughout the whole period under analysis.
In a nutshell, the CCP is developed by employing a dynamical system perspective. Accordingly price forecasts are obtained by choosing prediction values such that the time series is left with the same amount of chaos measured by the largest Lyapunov exponents. Top-bottom portfolios are then created by sorting stocks through a signal which exploits price forecasts and past returns.

8.2.1 Phase space Reconstruction

The modeling of a dynamical system relies on the concept of a phase space, that is the collection of the possible system states. For a system that can be mathematically modeled through differential equations, the phase space is known from these laws of motion. On the contrary, for the majority of real dynamical systems, which often exhibit chaos, the phase space and the precise mathematical description of the equations governing their dynamics are often unknown. The observation of a real process usually does not yield all possible state variables. Either not all state variables are known or not all of them can be measured. Accordingly, attractor reconstruction methods have been developed as a mean to build up the phase space and develop new

predictive models (see e.g. Rosenstein et al. 1993; Vlachos and Kugiumtzis 2008; Kliková and Raidl 2011).

The state of the system can be described by its state variables $x^{1(t)}, x^{2(t)}, ..., x^{d(t)}$. The d state variables at time t form a vector in a d-dimensional space which is called phase space. A system typically changes in time and, in turn, the vector in the phase space that describes the trajectory representing the time evolution of the system changes as well. The shape of the trajectory gives hints about the phase space portrait, whether this is periodic, quasi-periodic or even chaotic.

Due to the couplings between the system's components, it is possible to reconstruct a phase space trajectory from a single observation x_i of a time series $\mathbf{X} = \{x_1, x_2, ..., x_T\}'$ by a time delay embedding method (see Rosenstein et al. (1993)).

The reconstructed trajectory, $\mathbf{X^r}$, can be expressed as a matrix where each row is a phase space vector. That is:

$$\mathbf{X^r} = [X_1^r, X_2^r, ..., X_M^r]' \tag{8.1}$$

where $\mathbf{X_i^r}$ is the state of the system at discrete time i and M is the number of measurements. For a T-point time series, $\{x_1, x_2, ..., x_T\}$, each $\mathbf{X_i^r}$ is given by:

$$\mathbf{X_i^r} = [x_i, x_{i+\tau}, ..., x_{i+(m-1)\tau}] \tag{8.2}$$

where $i = 1, 2, ..., T - (m-1)\tau$. The parameter τ defines the reconstruction delay and m represents the embedding dimension. The delay for phase space reconstruction is estimated using Average Mutual Information (AMI). For reconstruction, the time delay is set to be the first local minimum of AMI computed as:

$$AMI = \sum_{i=1}^{T} p(x_i, x_{i+1}) \log_2 \left[\frac{p(x_i, x_{i+1})}{p(x_i)p(x_{i+1})} \right] \tag{8.3}$$

where $p(x_i, x_{i+1})$ is the joint probability density function of x_i and x_{i+1}, and where $p(x_i)$ and $p(x_{i+1})$ are the marginal density functions. The AMI, therefore, indicates how similar the joint distribution $p(x_i, x_{i+1})$ is to the products

of the factored marginal distributions. If x_i and x_{i+1} are completely unrelated (and therefore independent), then $p(x_i, x_{i+1})$ would equal $p(x_i)p(x_{i+1})$, and this measure would be zero.

The embedding dimension is the dimension of the space in which the phase portrait is reconstructed and it is specified as a scalar vector. The embedding dimension for phase space reconstruction is estimated using the False Nearest Neighbor algorithm, as in Rhodes and Morari (1997).

For a point i at dimension d, the points $\mathbf{X_i^r}$ and its nearest points $\mathbf{X_i^{r*}}$ in the reconstructed phase space $\{\mathbf{X_i^r}\}$, $i = 1, ..., T$, are false neighbors if:

$$\sqrt{\frac{R_i^2(d+1) - R_i^2(d)}{R_i^2(d)}} > thr \tag{8.4}$$

where $R_i^2(d) = ||\mathbf{X_i^r} - \mathbf{X_i^{r*}}||^2$ is the distance metric and $thr = 10$ is a tuning parameter to determine the number of points that are False Nearest Neighbors (FNN) in the reconstructed phase space. The estimated embedding dimension d is the smallest value that satisfies the condition $p_{fnn} < \omega$ where p_{fnn} is the ratio of FNN points over the total number of points in the reconstructed phase space, while $\omega = 0.1$ is a threshold such that if the percentage of false nearest neighbors (p_{fnn}) drops below the tuning parameter ω at a dimension d, then d is considered as the embedding dimension. After reconstructing the phase space, for a point i the algorithm locates the nearest neighbor i^* that satisfies $\min_{i^*} ||X_i^r - X_{i^*}^r||$ on the trajectory such that $|i - i^*| > 1$.

8.2.2 Lyapunov exponent

The subsequent step of our approach is the computation of the Lyapunov exponent (see Rosenstein et al. (1993); McCue and Troesch (2011)). The Lyapunov exponent is a useful tool to estimate the amount of chaos in a system. In particular, by considering two trajectories in the phase space with nearby initial conditions on an attracting manifold, sensitivity to initial conditions is quantified by the Lyapunov exponent. When the attractor is

chaotic, the trajectories diverge, on average, at an exponential rate characterized by the largest Lyapunov exponent. The presence of a negative Lyapunov exponent indicates convergence, while a positive Lyapunov exponent is associated with divergence and/or chaos. Mathematically, the largest Lyapunov exponent can be computed as:

$$\lambda = \frac{1}{T}\sum_{i=1}^{T}\left(\frac{1}{K}\sum_{K=K_{min}}^{K_{max}} \ln \frac{||\mathbf{X}^r_{i+K} - \mathbf{X}^r_{i^*+K}||}{||\mathbf{X}^r_i - \mathbf{X}^r_{i^*}||}\right) \tag{8.5}$$

where $K = K_{max} - K_{min}$ is the expansion range, which we select in the interval $[1, 5]$, and it is used to estimate the local expansion and to calculate the largest exponent.

8.2.3 The GenericPred Algorithm

The basic idea of GenericPred (see Golestani and Gras 2014) is to extract a unique characteristic from an existing time series that somehow represents the chaotic behaviour of the series. Subsequently the method generates successive new values that continue the series, each value minimising the difference between the chaoticity of the new time series and the initial one.
In particular, let us consider a time series $\mathbf{X} = \{x_1, x_2, ..., x_T\}$. The first step of the GenericPred method involves the reconstruction of the attractor phase space from a single time series. Then, the largest Lyapunov exponent λ is computed on $\mathbf{X}$ to have a single value which quantifies the amount of chaos in the dynamics of the time series. The value $\lambda(\mathbf{X})$ is the reference value that is used for forecasting the next k values of the time series x_{T+i}, $1 \leq i \leq k$.
The forecast of the new value x_{T+i} is chosen by randomly drawing $j = 50$ proposal x^j_{T+i} from a Normal distribution $N(x_T, \sigma^2)$ where the mean is equal to the last observed value of the series and the variance is estimated as the difference of the two last observations, i.e. $x_T - x_{T-1}$. In other words, the new value must be chosen from a set of potential values generated from the probability distribution $P(x_i|x_{i-1})$. In particular, the selected forecast $x^{j_{min}}_{T+i}$

is then computed by picking the x^j_{T+i} that minimizes the distance between the $\lambda(\mathbf{X})$ of the original time series and the one of the augmented series, where

$$j_{min} =_j (|\lambda(\mathbf{X}^j) - \lambda(\mathbf{X})|) \tag{8.6}$$

and $\mathbf{X}^j = x_1, x_2, ..., x_T, x^j_{T+1}$.
The predictions are made one step per time because the predicted value in the current step is necessary for determining the valid range of change for the next step. Therefore, after $x^{j_{min}}_{T+i}$ has been computed, the series is augmented by this new value and the method is run again in order to find the new future value.

8.2.4 The Constant Chaoticity Portfolio formation

In this Section, we describe how to employ both past and forecasted prices to build different portfolio strategies. First, we describe how we create top-bottom portfolios through stocks' single sorting. In this step we generate a signal which is computed using price forecasts or, alternatively, past prices and which suggests the future market direction for each stock. Secondly, according to a double sorting criterion, we also build portfolios using simultaneously signals computed using price forecasts and past prices.
With a rolling window of 220 days, at each step of the window, we first generate the stock price forecasts $\mathbf{X}^{j_{min}}$ for the next five days[23]. Then, we create a signal S_z associated to each stock z as the difference between the mean and the median of its five days price predictions[24]. The signal is intended for extracting a scalar measure, which is able to discriminate between bearish and bullish assets. In formula:

$$S_z = \frac{1}{Z}\sum_{z=1}^{Z} \mathbf{X}_z^{j_{min}} - \frac{\mathbf{X}_z^{j_{min}}\lceil\frac{l+1}{2}\rceil + \mathbf{X}_z^{j_{min}}\lfloor\frac{l+1}{2}\rfloor}{2} \tag{8.7}$$

[23]As a robustness exercise we also employ 10 days as an out of sample range. Results are shown in Appendix.

[24]The signal is also computed analogously using the past five days prices.

where $\mathbf{X}_z^{j_{min}}$ has been previously sorted in ascending order, l is the number of components of the vector $\mathbf{X}_z^{j_{min}}$, while $\lfloor \cdot \rfloor$ and $\lceil \cdot \rceil$ denote the floor and ceiling functions, respectively.

The signal embeds information on the shape of the price forecasts distribution of each stock. Indeed, when the mean and the median are equal, the price forecasts distribution is symmetric. On the contrary, the larger the difference between the mean and the median is, the more asymmetric the price forecasts distribution is. In particular, if the mean is lower than the median, the distribution will be skewed to the left, meaning that some predictions present low forecasted values with respect to the bulk of the distribution. We interpret this occurrence as a sell signal. On the other hand, if the mean is larger than the median, the price forecasts distribution is positively skewed: some predictions present high forecasted values with respect to the core of the distribution. This is interpreted as a buy signal.

Once the signal is generated for all the stocks, the assets associated with the lowest S_z values, i.e. stocks whose signal is below a predetermined low-percentile of the distribution, are selected as bearish assets and thus a buy position is taken over them. For those stocks returns are computed as:

$$R_t = \frac{p_{t+1} - p_t}{p_t}. \tag{8.8}$$

On the contrary, stock signals that lie above a predetermined up-percentile of the distribution are selected as bullish assets, and therefore a buy position is assumed on these instruments. For those stocks, returns are computed as:

$$R_t = \frac{p_t - p_{t+1}}{p_{t+1}}. \tag{8.9}$$

Finally, the top-bottom portfolio is computed by equally weighting the selected stocks. The top-bottom portfolio strategy foresees to take a long position on the top stocks group and a short position on the bottom stock group. The performance of the portfolio is given by the sum of profits and losses of each open position on top/bottom stock groups.

The trading strategy is back-tested using a walk forward approach. We opt

for an in-sample data time window of 220 days. Then we compute top-bottom portfolio performance in the next trading week, i.e. portfolio re-balancing is computed every working week. The in-sample time window is subsequently shifted forward by the period covered by the out of sample test, and the process is repeated. At the end, all the recorded results are used to assess the performance of the trading strategy, i.e. each top-bottom portfolio performance is connected from July 2003 to January 2018.
Moreover, we are also interested in understanding whether portfolios' profitability is influenced by both past price behavior and forecasted values. Therefore, we propose an alternative portfolio based on a double sorting procedure. This method selects the top stocks as those instruments having a signal S_z value higher than the 65th percentile of the S-distribution for both past returns and price forecasts. On the contrary, bottom stocks are identified as those assets having a signal S_z lower than the 35th percentile of the S-distribution for both past returns and price forecasts. In other words, stocks belonging to the top portfolio have both an increasing past trend as well as a predicted positive price trend, thus signaling a strong bullish market phase. On the contrary, stocks composing the bottom portfolio are characterized by both decreasing past and forecasted price trends, thus signaling a strong but negative market phase. Finally, as before, portfolio's profits and losses are computed by summing the daily returns of open long positions on top stocks and the returns of the open short positions on bottom stocks.

8.3 Data and empirical results

In this Section, we firstly describe the main qualitative and quantitative features of the datasets related to the STOXX Europe 50 and the Hang Seng indexes. Secondly, we present the results of our stock price forecasting methodology. Finally, we illustrate the portfolio performances together with those of different top-bottom strategies. In particular, the our contribution shows the empirical outcomes obtained by applying our methodology to the STOXX Europe 50 index, while results linked to the Hang Seng index are

shown in Appendix A.

8.3.1 Data

In order to test the efficacy of the CCP method, we analyze the closing price dynamics of two different indices, namely the STOXX Europe 50 and the Hang Seng indexes, and their constituents.

The STOXX Europe 50 provides a representation of supersector leaders in Europe. It is composed by the first 50 Europe's leading blue-chip stocks from 17 European countries, namely: Austria, Belgium Czech Republic, Denmark, Finland, France, Germany, Ireland, Italy, Luxembourg the Netherlands, Norway, Portugal, Spain, Sweden, Switzerland and the United Kingdom. The STOXX Europe 50 data have a daily frequency and range from 29th July 2003 to 22nd January 2018. The leader sectors presented in the index are Health and Banks accounting for the 14% and 18% of blue chips stocks belonging to these sectors respectively; Personal & Household Goods and Industrial Goods & Services, instead, impact on the index composition for almost the 12% and 10% respectively[25]. For sake of simplicity we compute portfolio selections on the 29 survival components of the STOXX Europe 50 index constituents. These assets are the ones that have remained within the index throughout the whole period under analysis.
The Hang Seng index, on the other hand, is the free-float adjusted market capitalization weighted index of the Hong Kong Stock Exchange. It is composed by 50 constituent companies, which represent about 58% of the capitalisation of the Hong Kong Stock Exchange[26]. It is used to record and monitor daily changes of the largest companies of the Hong Kong stock market and is the main indicator of the overall market performance in Hong Kong. As for the STOXX Europe 50 index, we employ the survival components of the Hang Seng index. For the Asian index we collect the daily closure price of the 47 components which have remained within the index

[25]https://www.stoxx.com/index-details?symbol=SX5P
[26]https://www.hsi.com.hk/eng

from 12th March 2014 to 11nd March 2020.

Table 34: Summary Statistics - STOXX Europe 50

Periods	**Min.**	**Max.**	**Mean**	**Std.**	**Skew.**	**Kurt.**
01-01-03 to 05-31-07	-0.0832	0.0970	0.0006	0.0126	-0.0267	5.2492
06-01-07 to 01-31-09	-0.3214	0.2565	-0.0017	0.0294	0.2418	13.7365
02-01-09 to 12-31-13	-0.2035	0.2198	0.0004	0.0211	0.0805	10.6831
01-01-14 to 01-22-18	-0.2303	0.1241	0.0002	0.0162	-0.6153	11.5442

Note: Summary statistics of the STOXX Europe 50 components divided into four sub-periods, namely from January 2003 to May 2007, from June 2007 to January 2009, from February 2009 to December 2013 and finally, from January 2014 to January 2018. For each sub-period, the table reports the minimum (Min.), the maximum (Max.), the average (Mean) values of the daily returns along with the standard deviation (Std.), the skewness (Skew.), and the kurtosis (Kurt.).

Table 34 provides some summary statistics related to the STOXX Europe 50, divided into four time-spans referring to the prior-crisis period (2003-2007), the global financial crisis (2007-2009), the European Sovereign debt crisis (2009-2013) and the post-crisis period (2014-2018). The time intervals are not equally spaced. Instead, the length of each sub-period is set according to the economic and financial events which have affected the global capital markets. The table reports the minimum, the maximum, the mean, the standard deviation, the skewness and the kurtosis of the daily return distribution of the survival components of the STOXX Europe 50 index. Summary statistics show that during both the global financial crisis and the European Debt crisis, stocks of the STOXX Europe 50 index were affected by market turmoils, which had a negative impact on the index performance. Moreover, the global financial crisis affected the markets more heavily than the European debt crisis. Indeed, the minimum return recorded in this sub-period is the highest in absolute value and the average return takes a negative value. On the contrary, despite the standard deviation of the two crisis periods are comparable, the daily average return during the European Debt crisis turns

positive and even higher than the one of the post crisis sub-interval.

Table 35: Summary Statistics - Hang Seng

Periods	**Min.**	**Max.**	**Mean**	**Std.**	**Skew.**	**Kurt.**
12-03-14 to 11-03-16	-0.2239	0.1763	0.0000	0.0196	0.1755	8.6279
12-03-16 to 11-03-18	-0.1458	0.1560	0.0010	0.0164	0.2853	8.8455
12-03-18 to 11-03-20	-0.2759	0.1207	-0.0004	0.0184	-0.1812	10.1443

Note: Summary statistics of the Hang Seng components divided into three sub-periods, namely from March 2014 to March 2016, from March 2016 to March 2018 and finally, from March 2018 to March 2020. For each sub-period, the table reports the minimum (Min.), the maximum (Max.), the average (Mean) values of the daily returns along with the standard deviation (Std.), the skewness (Skew.), and the kurtosis (Kurt.).

Table 35 shows the summary statistics related to the Hang Seng components, for three equally spaced time intervals, namely from March 2014 to March 2016, from March 2016 to March 2018 and finally, from March 2018 to March 2020. These statistics highlight that during the last considered period, the Hong Kong stock market has been affected by the turmoil due to the anti-government protests and the spread of the Covid-19 infection, which had a negative impact on the index performance. In particular, if we focus on the first three month of the year 2020, this dynamics is even more pronounced with a minimum return figure of -0.1925, a maximum of 0.0770, and an average return of -0.0026.

8.3.2 Forecasting stock prices

In this Subsection, we illustrate the outcome of the forecasting procedure obtained with a five days forecasting horizon. As an example, in Figure 39 we report the predicted and actual price patterns of a single component of the STOXX Europe 50 index. Such stock is identified with the numeric ID 405780, which refers to l'OREAL. This is the first company worldwide in

terms of turnover, operating in the beauty & cosmetics sector, specialized in cosmetics and beauty products.

Figure 39: The price pattern prediction at five days forecasting horizon for the stock component 405780 (l'OREAL) of the STOXX Europe 50

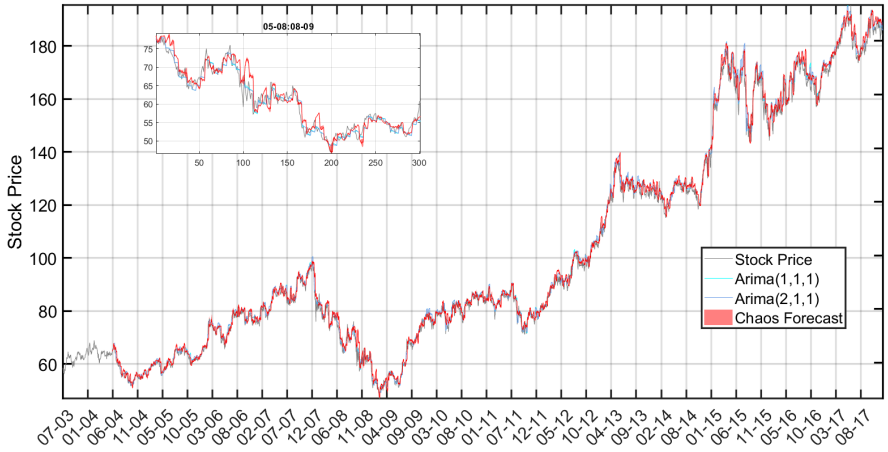

Note: The price forecast obtained by our methodology is represented by the red line; the price forecasts given by the ARIMA(1,1,1) and ARIMA(2,1,1) models are represented by the light blue and blue lines, respectively; the gray line identifies the actual stock price during the analyzed period. The y-axis refers to the stock price. The x-axis, instead, indicates the timeline. At the top left of the graph an enlargement describes the price pattern during the global financial crisis period, in particular, from May 2008 to August 2009.

Figure 39 shows the comparison between the price pattern of a representative stock composing the survival set of assets for the STOXX Europe 50 and its forecasted dynamics obtained through our proposed methodology. Additionally, we consider the predicted dynamics of several configurations

of ARIMA models as competing forecasting alternatives[27]. The in-sample period corresponds to 220 observations (one year) while the forecasting out-of-sample window is set to five days ahead. The gray line reports the stock price path, the red line refers to the price series predicted through our forecasting procedure, the light blue and blue lines are associated with the series predicted by the ARIMA(1,1,1) and ARIMA(2,1,1) models, respectively. We observe that the forecasted series, resulting from the application of our model, is able to follow quite closely the real path of the stock price. Moreover, despite being generally less accurate, ARIMA models are also able to capture the pattern of the stock price.

By analyzing the figure in detail, during the period preceding the global financial crisis, the stock features a positive performance, jumping from a 60$ price level to almost 100$, with a 67% increase in value. However, the stock price dynamics suffers from the global financial crisis: in fact, between June 2007 and January 2009, it loses about 60% of its values by dropping from a 100$ price level to almost 40$. In particular, this depreciation can be seen in the inset of Figure 39. During the post crisis period, instead, the method predicts a bullish trend of the stock dynamics. In fact, the price quadruples its value, reaching the 180$ price level at the end of the time sample. Finally, the shaded red areas represent the error bounds obtained by applying a bootstrapping procedure. In other words, for each time point forecast we have repeated the predictive methodology 10 times. The size of the bounds suggests that the methodology is robust against the re-sampling procedure, meaning that no significant improvement or reduction in forecasting accuracy can be observed by considering a larger number of random draws.

[27]In particular, throughout the analyses we illustrate configurations of ARIMA models which have been reported as good candidates for making satisfactory predictions, namely ARIMA(1,1,1) and ARIMA(2,1,1).

8.3.3 Portfolio results

This Subsection illustrates the results of the CCP method in terms of profits and losses (P&L), performances relative to the market index and risk-adjusted performances. Figure 40 represents the daily cumulative returns obtained by performing investment strategies based on different approaches. The single and the double way sorting methods employed for constructing the Constant Chaoticity Portfolios are compared against the equally weighted portfolio P&L and the ones based on ARIMA models[28], which only encompass the survival stocks of the index, and the market index performance. P&L include transaction costs of 20 basis-points per each stock composing a certain portfolio at each rebalancing. Furthermore, top-bottom portfolios are computed with the 65th and 35th percentiles as a benchmark.

From a visual inspection of Figure 40, it is possible to evaluate the horse-race of different strategies and to compare their behaviors in terms of profitability. For the sake of completeness, the performance of the top-bottom portfolio generated by past price analysis has also been inserted into the figure. Notice that, since the bootstrapping procedure creates a forecasted price distribution for each time point, we have decided to consider the median of the prediction distribution as the reference forecasted value. During the pre-crisis period, the market index associated with a buy&hold strategy (black line) is the best performing followed by the double sorting portfolio (violet line). The other approaches, instead, exhibit a lateralized trend. However, the most interesting period, seems to be the financial crisis phase: the market index (gray line) suffers from the downturn due to the banking sector turmoil, which covers a significant part of the STOXX Europe 50 dynamics. The equally weighted portfolio performance drops as expected, while the ARIMA portfolios and the single sort strategy are less responsive when the market witnesses a bearish phase. The double sorting portfolio, instead, seems to be

[28]Portfolios based on ARIMA models are constructed in the same way as CCP portfolios, with the only exception that we use ARIMA predictions rather than the forecasts given by our predictive method to derive portfolio weights.

Figure 40: Portfolio performances with five days forecasting horizon for the European case

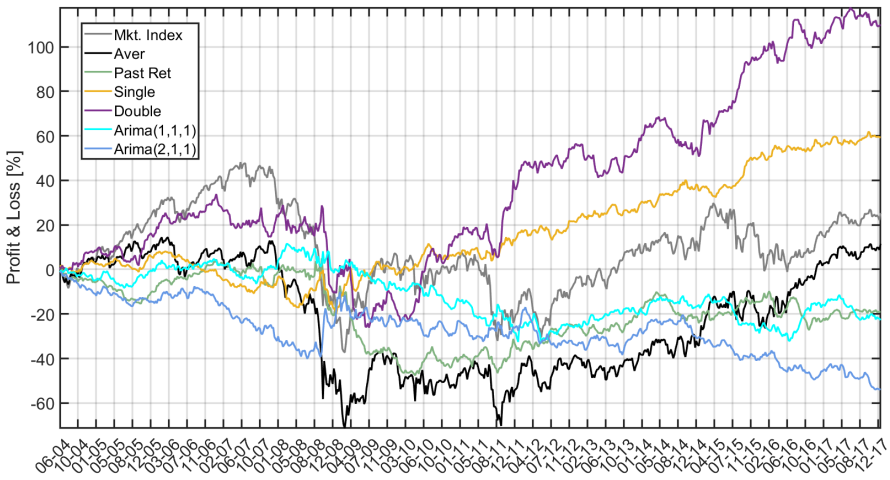

Note: The figure shows the profits and losses (P&L) of different portfolio strategies. The gray line represents the performance of the STOXX Europe 50 index, indicated as Mkt. Index. The black line represents the performance of the equally weighted portfolio obtained by selecting all the survival components of the STOXX Europe 50 (labelled as Aver). The green line shows the P&L of the past return top-bottom portfolio (Past Ret). The yellow line shows the performance of the CCP obtained with the single sort strategy computed on the forecasted prices (Single); the violet line identifies double sort strategy performance (Double); the light blue line represents the ARIMA(1,1,1) strategy performance (Arima(1,1,1)); the blue line that of ARIMA(2,1,1) (Arima(2,1,1)). The y-axis represents in percentage the P&L while the x-axis reports the timeline. Top-bottom portfolios are created by considering the 35th and 65th percentiles as reference thresholds of the signal distribution.

less affected by the financial downturn as shown by its performance during the period from June 2008 to April 2009. However, the post crisis period shows how both the single (yellow line) and the double sort strategies outperform the STOXX Europe 50 index, the equally weighted portfolio and the ARIMA-based portfolios. The single sort approach does better than all competing alternatives, but the double sort portfolio strategy, on average, turns out to be the most profitable strategy, overcoming the single sort portfolio from the second half of 2011 until the end of the sample period.

We also compute Sharpe Ratios and Jensen's Alphas for each portfolio strategy in order to support the results described through the analysis. The Sharpe Ratio is an indicator which helps investors to understand the return of an investment compared to its risk. Indeed, the ratio expresses the average return earned per unit of volatility or total risk. It is calculated by dividing the return of the portfolio by its standard deviation[29]. In formula, the Sharpe Ratio (SR) is expressed as:

$$SR = \frac{R_p}{\sigma_p} \tag{8.10}$$

where R_p is the return of portfolio and σ_p is the standard deviation of the portfolio's returns.

We also consider the Jensen's Alpha, which is a risk-adjusted performance indicator that measures the excess returns earned by the portfolio compared to the returns implied by a CAPM model (R_M). The Jensen's Alpha can be calculated using the following formula:

$$\alpha = R_p - \beta R_M. \tag{8.11}$$

This metric can assume both positive or negative (besides null) values. High positive values suggest a better portfolio performance compared to the market performance, while negative values indicate that the portfolio under

[29]Notice that the Risk-free asset of cash is absent in our computation, provided that we are interested in proposing a measure of risk adjusted returns.

Table 36: Sharpe Ratio and Jensen's Alpha of different portfolio strategies

Sharpe Ratio															
	2004	2005	2006	2007	2008	2009	2010	2011	2012	2013	2014	2015	2016	2017	TOT
Market Index	0,113	0,3	0,129	0,031	-0,243	0,09	-0,043	-0,097	0,127	0,138	0,023	-0,018	0,069	0,126	0,013
Aver. Market	0,124	0,081	-0,035	0,045	-0,237	0,038	-0,088	-0,008	0,132	-0,034	0,077	0,055	0,234	0,112	0,006
Past Returns	-0,257	-0,123	0,369	-0,179	-0,095	-0,19	0,008	0,048	0,216	0,067	-0,007	0,113	-0,121	0,132	-0,02
Single Sort	0,162	0,044	-0,169	-0,17	-0,097	0,196	0,131	0,108	0,13	0,094	0,226	0,26	0,115	0,069	0,075
Double Sort	0,227	0,1	0,267	-0,161	-0,153	-0,032	0,299	0,166	0,229	-0,044	0,011	0,395	0,075	0,089	0,074
ARIMA(1,1,1)	-0,212	0,12	0,093	-0,07	-0,026	-0,067	-0,153	-0,196	0,068	0,124	0,068	-0,24	0,212	-0,162	-0,026
ARIMA(2,1,1)	-0,508	-0,115	0,046	-0,294	0,006	0,022	-0,073	0,018	-0,131	0,075	-0,017	-0,233	-0,132	-0,129	-0,058
Jensen's Alpha															
	2004	2005	2006	2007	2008	2009	2010	2011	2012	2013	2014	2015	2016	2017	TOT
Aver. Market	0,036	-0,232	-0,283	0,035	-0,071	-0,148	-0,154	0,253	0,053	-0,267	0,125	0,213	0,452	0,003	-0,013
Past Returns	-0,228	-0,062	0,285	-0,207	-0,495	-0,329	0,018	0,076	0,198	0,079	-0,014	0,142	-0,166	0,086	-0,026
Single Sort	0,114	0,001	-0,122	-0,16	-0,342	0,373	0,131	0,157	0,151	0,098	0,238	0,25	0,127	0,058	0,088
Double Sort	0,24	0,191	0,317	-0,296	-0,906	-0,055	0,6	0,481	0,349	-0,064	0,01	0,807	0,211	0,14	0,165
ARIMA(1,1,1)	-0,168	0,058	0,063	-0,069	-0,314	-0,095	-0,153	-0,354	0,057	0,135	0,069	-0,24	0,288	-0,179	-0,032
ARIMA(2,1,1)	-0,389	-0,129	0,062	-0,284	0,037	0,119	-0,084	0,001	-0,227	0,116	-0,02	-0,192	-0,13	-0,119	-0,078

Note: The table reports the Sharpe Ratio and the Jensen's Alpha of the analyzed strategies at five days forecast horizon. The benchmark used to calculate the Jensen's Alpha is the STOXX Europe 50 index.

analysis performs worse than the market. In other words, if Alpha is positive, the portfolio outperforms the benchmark index (in this case the STOXX Europe 50 is used as the reference R_M variable), otherwise it is less profitable than the market index.

Table 36 shows the Sharpe Ratios and Jensen's Alphas computed for the different portfolio strategies considered at a five days forecasting horizon. We report both the annual measurements and the total Sharpe Ratio and Jensen's Alphas computed over the whole time period.

On the one hand, the best performing strategy in terms of risk-adjusted returns turns out to be the top-bottom portfolio generated by the single sorting method, followed by the double sorting top-bottom portfolio. Indeed, the higher the portfolio's Sharpe Ratio, the better the associated risk-adjusted-performance is. However, the magnitude of the difference between the two Sharpe Ratios is very low, meaning the two proposed strategies exhibit fairly comparable risk-return profiles.

On the other hand, Jensen's Alpha indicates that the double sorting portfolio strategy, on average, produces the best performance in terms of CAPM extra returns, while the single sorting strategy comes second. These results are also confirmed by Figure 40: indeed, even if the single sorting strategy does not differ much from the double sorting portfolio in terms of performance between 2004 and 2011, the P&L of the latter significantly exceeds that of the former from the end of 2011 onwards. Moreover, notice that the portfolio made up by sorting stocks according to their past returns shows a negative Sharpe Ratio together with a negative Jensen's Alpha, thus indicating that the index performance is larger than the P&L of this strategy.

8.4 Sensitivity analysis of the portfolio strategies

In this Section, we present the sensitivity analysis related to our portfolio strategies. We conduct three types of sensitivity analyses. Firstly, we analyse the sensitivity of portfolio performances subject to changes in the underlying model parameters. Secondly, we examine the sensitivity of our results with respect to the forecast horizon choice. Thirdly, we study the overall sensitivity of portfolio performances, that is the sensitivity to both the underlying model parameters and the forecast horizon choices. In particular, we show the sensitivity analyses related to the STOXX Europe 50 index results, whereas we illustrate those linked to the Hang Seng index in Appendix B.

8.4.1 Sensitivity to the underlying model parameters

In this Subsection, we test how a certain parametric configuration impacts the portfolios' final P&L. We let the percentiles considered for creating the top-bottom portfolio vary from $91 - 9$ to $65 - 35$. Indeed, the previous results were obtained only considering top-bottom portfolios computed with the 65th and 35th percentiles respectively, as a benchmark for the European

market.

In Figure 41 we report the sensitivity test generating different top-bottom portfolios for the past return, ARIMA(1,1,1), ARIMA(2,1,1), single and double sort cases related to the STOXX Europe 50. As a reference measure, we use the final P&L recorded at the end of the sample.

Figure 41: Sensitivity analysis with five days forecasting horizon for the European case

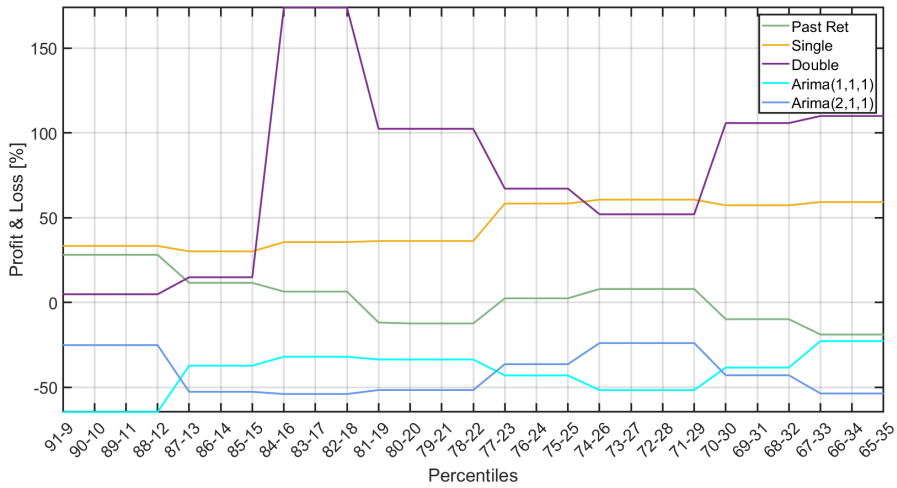

Note: The figure shows the results of the sensitivity analysis on the main portfolio strategies created with five days forecasting horizon. The figure associates the final P&L at 01-18 with various parameter configurations. Namely, the x-axis identifies the top-bottom percentiles thresholds while the y-axis reports the cumulative performance of top-bottom portfolios for the cases of single (yellow line) and double (violet) sorting along with the past returns top-bottom portfolio (green line), the ARIMA(1,1,1) portfolio (light blue line) and the ARIMA(2,1,1) portfolio (blue line).

From Figure 41 one can notice that, for a relatively wide range of percentiles, that is above $87 - 13$, the past return portfolio performs slightly better than the double sorting one. This is due to the poor number of stocks

selected with such percentile thresholds, which makes the portfolio highly sensitive to small changes in single stock prices. However, considering the same ranges, our single sorting portfolio performance dominates those of the other competing alternatives, confirming our previous findings.

When considering all parameter configurations lower than the $87 - 13$ percentiles, the performance of the double sort top-bottom portfolio and the one of the single sort turn out to be the highest, with a remarkable outperformance with respect to the backward-looking top-bottom portfolio and ARIMA portfolios. In particular, the double sorting method generates the highest P&L around the $83 - 17$ percentiles, followed by an as well outstanding performance when the range tightens to $70 - 30$ and below. Furthermore, neither the single nor the double sorting portfolio generate a negative performance, differently from the past return and ARIMA top-bottom portfolios.

8.4.2 Sensitivity to the forecast horizon choice

This Subsection analyses the sensitivity of portfolio performances with respect to changes in the forecast horizon. In particular, we perform the analyses starting from the Results Section considering a longer forecast horizon, namely 10 days.

Figure 42 shows the price predictions for l'OREAL, in the case of ten days forecasting horizon. Despite the shape of the price dynamics and the long run trend are still correctly predicted, a fair comparison with Figure 39 shows that the actual and forecasted prices diverge more consistently when considering a longer forecasting horizon, both in the case of our predictive model and ARIMA ones. Indeed, the wider predictive horizon influences the model performance, due to its updates with a delay of ten days with respect to the actual price. This fact causes a deviation between our predicted price (red line) along with ARIMA predictions (light blue and blue lines) and the actual stock price path (gray line).

Figure 42: The price pattern prediction at ten days forecasting horizon for the stock component 405780 (l'OREAL) of the STOXX Europe 50

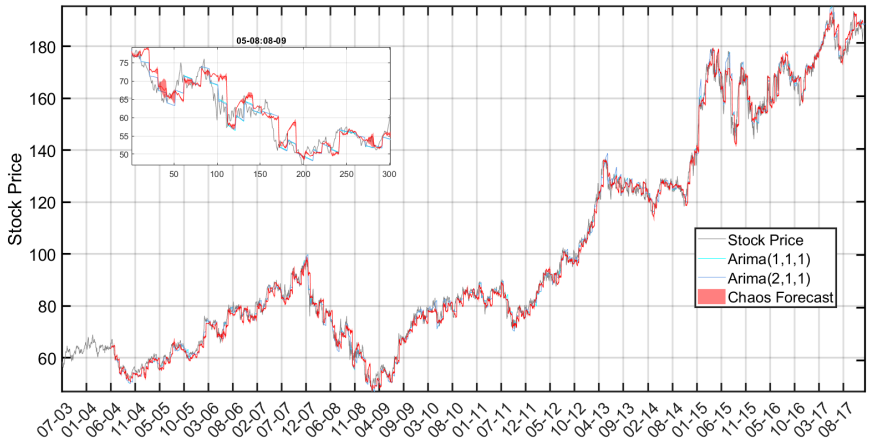

Note: The price forecast obtained by our methodology is represented by the red line; the price forecasts given by the ARIMA(1,1,1) and ARIMA(2,1,1) models are represented by the light blue and blue lines, respectively; the gray line identifies the actual stock price during the analyzed period. The y-axis refers to the stock price. The x-axis, instead, indicates the timeline. At the top left to the graph an enlargement describes the price pattern during the global financial crisis period, from May 2008 to August 2009.

Subsequently, top-bottom portfolio performances based on a forecasting horizon of ten days are derived. Between 2004 and the end of 2007, the equally weighted portfolio yields the highest P&L compared to the other strategies. However, during the global financial crisis, the double sort strategy turns out to be the most profitable choice, beating all the other alternative portfolio allocation strategies. Between 2010 and 2011, the double sorting portfolio outperforms the other strategies by lateralizing around the level of 100%. The ARIMA portfolios, instead, exhibit the lowest P&L at the end of the sample, with the single sorting method performing slightly better than them. Finally, during the global financial crisis and the post crisis, the

market index shows the worst cumulative daily returns in concurrence with the ARIMA portfolios.

Figure 43: Portfolio performance with ten days forecasting horizon

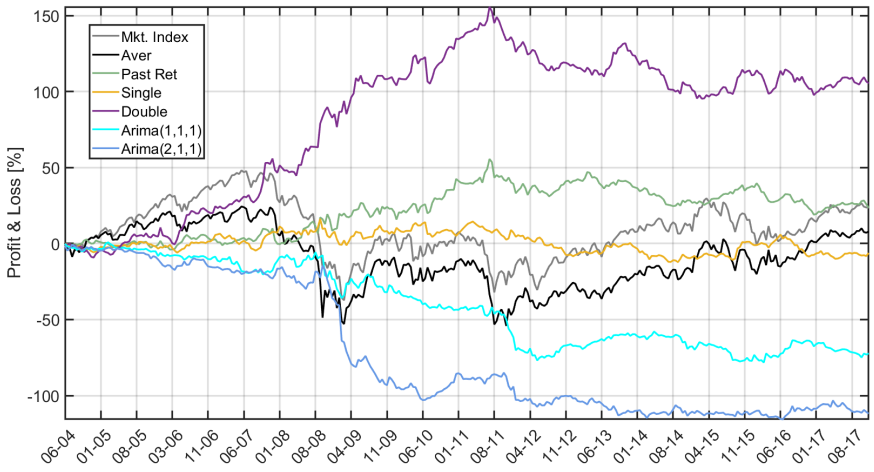

Note: The figure shows the profits and losses (P&L) of different portfolio strategies. The gray line represents the performance of the STOXX Europe 50 index, indicated as Mkt. Index. The black line represents the performance of the equally weighted portfolio obtained by selecting all the survival components of the STOXX Europe 50 (labelled as Aver). The green line shows the P&L of the past return top-bottom portfolio (Past Ret). The yellow line shows the performance of the CCP obtained with the single sort strategy computed on the forecasted prices (Single); the violet line identifies double sort strategy performance (Double); the light blue line represents the ARIMA(1,1,1) strategy performance (Arima(1,1,1)); the blue line that of ARIMA(2,1,1) (Arima(2,1,1)). The y-axis represents in percentage the P&L while the x-axis the timeline.

Overall, a comparison between Figure 42 and Figure 40 shows that the performance of the single sort top-bottom portfolio at five days horizon diverges significantly from the P&L obtained with a wider forecasting window. On the contrary, the double sort top-bottom portfolio still features the

best performance even when the forecasting window is longer. In particular, from mid 2007 onwards, the double sort portfolio outperforms all the other strategies, yielding to outstanding net profits relative to the other competing alternatives.
Results are also confirmed by the Sharpe Ratios and Jensen's alpha statistics reported in Table 37. The double sorting strategy generates the highest Sharpe Ratio, thus indicating that the portfolio creates the best risk-return performance with respect to the other strategies. This is also confirmed by the Jensen's alpha. The worst performing portfolio, instead, turns out to be the single sorting one. We believe this is mainly due to the fact that, differently from the double sorting portfolio, the single sorting one takes into account exclusively predicted values to form the top-bottom portfolio composition. Thus, being the forecast horizon longer and therefore less precise, the information coming from past returns becomes more valuable, leading to the far way better performance of the double sorting method, which is both forward and backward-looking. The latter finding deepens the conclusions drawn in Section 8.3.

8.4.3 Overall sensitivity

In this Subsection, we examine how both variations in the underlying model parameters and forecast horizon choice affect portfolio performances. In particular, we investigate how the portfolio performances react to changes in the underlying model parameters and predictive horizon by letting the percentiles considered for creating the top-bottom portfolio vary from $91 - 9$ to $65 - 35$ and - at the same time - by considering an ahead forecast period of ten days.

Figure 44 shows the sensitivity analysis on single and double sorting methods together with those based on past returns and ARIMA models. The figure displays some regularities in the parameter grid. In fact for extreme percentiles of the signal distribution the past return portfolio outperforms both the single and the double sort strategies; instead, when the top-bottom

Table 37: Sharpe Ratio and Jensen's Alphas at ten days forecasting window

Sharpe Ratio															
	2004	2005	2006	2007	2008	2009	2010	2011	2012	2013	2014	2015	2016	2017	TOT
Market Index	0,135	0,405	0,174	0,032	-0,42	0,152	-0,054	-0,156	0,18	0,19	-0,022	-0,003	0,097	0,147	0,018
Aver. Market	0,126	0,228	0,034	-0,003	-0,265	0,157	-0,068	-0,198	0,245	0,064	0,044	0,019	0,196	0,151	0,006
Past Returns	0,142	-0,161	0,129	-0,009	0,079	0,151	0,206	0,045	0,032	-0,085	-0,294	0,331	-0,385	0,061	0,031
Single Sort	-0,435	0,144	0,245	0,047	0,003	-0,021	0	0,014	-0,45	0,225	-0,213	0,206	-0,196	0,06	-0,011
Double Sort	-0,297	0,339	0,291	0,283	0,354	0,192	0,195	0,055	-0,228	0,089	-0,351	0,154	-0,119	0,084	0,098
ARIMA(1,1,1)	-0,275	-0,044	-0,125	-0,103	-0,11	-0,1	-0,392	-0,299	-0,092	0,306	-0,206	-0,26	0,248	-0,266	-0,106
ARIMA(2,1,1)	-0,175	-0,25	-0,185	-0,176	-0,18	-0,435	0,011	-0,046	-0,139	-0,241	0,006	-0,034	0,046	-0,056	-0,143
Jensen's Alpha															
	2004	2005	2006	2007	2008	2009	2010	2011	2012	2013	2014	2015	2016	2017	TOT
Aver. Market	-0,011	-0,273	-0,366	-0,084	0,861	0,07	-0,076	-0,277	0,264	-0,268	0,159	0,099	0,401	0,022	-0,044
Past Returns	0,141	-0,113	0,218	-0,025	0,196	0,517	0,568	0,213	0,197	-0,072	-0,426	0,438	-0,596	0,048	0,073
Single Sort	-0,39	0,264	0,292	0,071	0,193	-0,157	-0,052	0,023	-0,546	0,21	-0,294	0,353	-0,244	0,108	-0,019
Double Sort	-0,577	0,551	0,829	0,993	0,963	0,929	0,808	0,267	-0,49	0,188	-0,905	0,385	-0,246	0,099	0,323
ARIMA(1,1,1)	-0,313	0,035	-0,182	-0,182	-0,821	-0,499	-0,476	-0,708	-0,159	0,327	-0,326	-0,383	0,535	-0,287	-0,213
ARIMA(2,1,1)	-0,234	-0,274	-0,297	-0,194	-1,238	-2,454	0,032	-0,11	-0,291	-0,398	0,011	-0,041	0,105	-0,043	-0,331

Note: Table reports the Sharpe Ratio and the Jensen's Alpha of the analyzed strategies at ten days forecast window: the single sorting, the double sorting, the average, the past return and the reference market index which is the STOXX Europe 50. The benchmark used to calculate alphas is the STOXX Europe 50 index.

portfolios become wider, the double sort method is the best performing one. This fact confirms that by choosing stocks, which have both an increasing past trend as well as a predicted positive trend (top assets), and stocks which have both decreasing past and forecasted price trends (bottom assets), ensures to catch the most valuable market trend. Moreover, this is in line with two previous considerations: on the one hand, the low number of stocks selected with wide percentile thresholds makes the portfolio performances highly sensitive to small changes in single stock prices; on the other hand, a longer predictive horizon makes information coming from past returns become more essential to predict market directions, leading to a better performance of the double sorting method under these conditions. Overall, it is clear that by choosing the right combination of model parameters to perform top-bottom stock selection and forecast horizon, our models tend to outperform the competitive alternatives considered.

8.5 Conclusion

Stock market prediction is a task of utmost importance for investors and decision makers, in particular when dealing with portfolio allocation strategies. Nevertheless, difficulties naturally arise due to the non-stationary and non-linear behaviour of the time series under analysis, which make most of traditional allocation strategies fail in practice. Together with this, the usage of merely backward-looking techniques often yields to inefficient asset allocation, hence paving the way for the study and application of forward-looking ones.

To cope with this, we propose a forward-looking methodology built on chaos theory which is able to capture non-linearities in financial time series, thus making reliable predictions. Throughout Lyapunov exponents, we are able to make reasonably accurate forecasts in a forward-looking perspective and use such predictions to construct the Constant Chaoticity Portfolio, which is built upon signals computed by price forecasts (single sorting) and, eventually, historical prices (double sorting).

Figure 44: Sensitivity analysis with ten days forecasting horizon

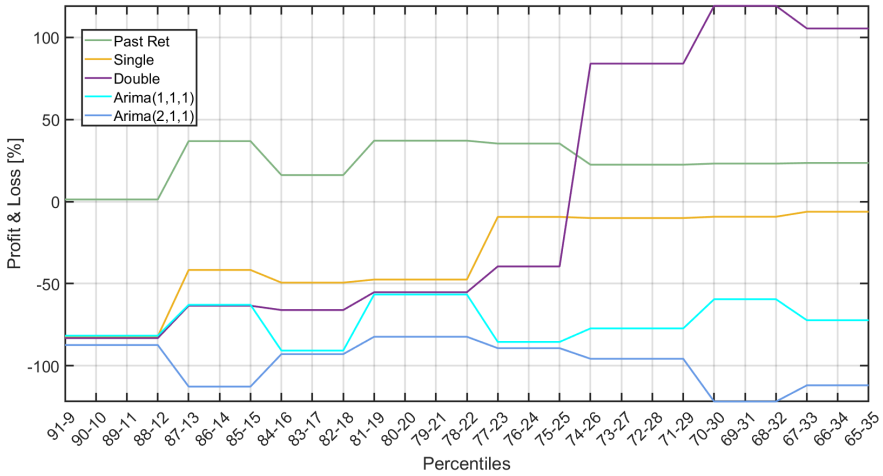

Note: The figure shows the results of the sensitivity analysis on the main portfolio strategies created with five days forecasting horizon. The figure associates the final P&L at 08-17 with various parameter configurations. Namely, the x-axis identifies the top-bottom percentiles thresholds while the y-axis reports the cumulative performance of top-bottom portfolios for the cases of single (yellow line) and double (violet) sorting along with the past returns top-bottom portfolio (green line), the ARIMA(1,1,1) portfolio (light blue line) and the ARIMA(2,1,1) portfolio (blue line).

Our methodology is tested on the survival components of the STOXX Europe 50 and the Hang Seng indexes. As far as the European case, results show that both single and double sorting CCP portfolios achieve successful performances, being their net profits at the end of the period as much as approximately 3 and 5.5 times higher than those of the corresponding market index, respectively, and overwhelming those of the considered competing alternatives. Besides net profits, Sharpe Ratios suggest that these portfolios exhibit better risk-return profiles than all competing alternatives. As far as the Asian case, the single sorting method outperforms the others in terms of portfolio returns. Also in this case, Sharpe Ratios further confirm that the CCP is able to generate a higher return on a risk-adjusted basis.

A sensitivity analysis on the underlying model parameters as well as on the forecast horizon choice confirm that results are robust with respect to different model configurations. As a matter of fact, by varying the percentile intervals for creating top-bottom portfolios in a sound way and by increasing the forecast horizon to make predictions, we show that CCP portfolios still over-perform the considered alternative allocation strategies, both in terms of net profits and risk-adjusted returns.

9 Concluding remarks

The motivation of this thesis is grounded on the growing attention of econometric methods for systemic risk analysis and investment management. The rapid development of econometric spillover and network models has paved the way to a strand of new methods to monitor the systemic risk in the financial system and enhance investment management effectiveness. The global financial system can be seen as a network of interconnected institutions, where links are of utmost importance to study the spread of contagion. The thesis contributes to the literature on econometric interconnectedness and investment management by developing new techniques capable to foster our understanding of the economic and financial systems. Financial applications are not tied exclusively to traditional financial markets, but also to the fintech sphere, particularly to the cryptocurrency market.

In chapter 2 we employed an extension of the Diebold and Yilmaz (2012) methodology with a generalized VECM to effectively monitor systemic risk and lead-lag behaviours across major cryptocurrency exchange platforms. The methodology allows to study market exchange connectedness at pairwise and system-wide levels, as well as both from a static and time-varying point of view, accounting for the common stochastic trend driving the fundamental Bitcoin price. We therefore contributed, from a methodological viewpoint, to the econometric literature - particularly for what concerns price discovery and connectedness of market exchanges - by the extension of the Diebold and Yilmaz (2012) connectedness measure, which relies on VECM rather than VAR models. The model allowed to shed further light on price discovery in Bitcoin markets, extending the conclusions in Pagnottoni and Dimpfl (2019) and Giudici and Abu-Hashish (2019) and, in particular, characterizing which are the leaders and followers in price formation among the considered exchanges, along time.

In chapter 3 we proposed an extension of the previous application to the intra-day setting. We studied directional connectedness and shed light on which are leading Bitcoin exchanges in terms of shock transmission and,

rather, which are those that follow others in the price formation process. This contributes to the stream of econometric literature studying interconnectedness and price discovery on the cryptocurrency market. Results showed that the frequency at which connectedness is measured highly influences the empirical outcomes, and that the leadership composition evolves over time, as the extant literature agrees - see Brandvold et al. (2015), Pagnottoni and Dimpfl (2019) and Giudici and Pagnottoni (2020).

In chapter 4 we proposed a methodology to construct basket based stablecoins whose value is relatively stable over time. We discussed the main policy implications of adopting a basket based stablecoin whose weights are derived by minimizing variability rather than a single digital currency, potentially more sensitive to market factors.

In chapter 5 we examined the lead-lag relationship between the sovereign CDS and bond market of a set of representative European Union countries by means of effective transfer entropy. The effective transfer entropy allowed, differently from previous studies in the literature, to examine the post sovereign crisis period, overcoming the need for the two markets to be cointegrated in order to conduct the analysis.

In chapter 6 we proposed a feasible pricing methodology to price cryptocurrency options. We have presented a two stage approach: the first stage consists of option pricing through parametric approaches such as tree models, finite difference method and Monte Carlo simulation; in the second stage, artificial neural networks are employed in order to combine the parametric option pricing approaches and capture the residual errors by learning schemes in the current status of the option market. Their performance is then compared to the conventional option pricing techniques obtained in the first stage. Results highlighted to the predominance of the neural network models with respect to the conventional methods in pricing Bitcoin options and, therefore, in capturing their real price dynamics and the non-linear dynamics typical of the option market time series.

In chapter 7 we extended the traditional Markowitz (1952) portfolio allo-

cation strategy by means of RMT and MST and by taking network centrality measures of the assets into account. By means of this technique we are able to set a parameter of systemic risk aversion that investors can tune to better match their investment strategies with their own risk profile. We have applied our methodology to the cryptocurrency domain, and our empirical findings confirm the effectiveness of our model in achieving better cumulative portfolio performances, while keeping a relatively low level of risk. In particular, we showed that our proposed model rapidly adapts to market conditions, and is able to yield satisfactory performances during bull market periods. During bear market periods - instead - our model employing RMT and MST realizes the best performances, protecting investors from relatively high losses which are instead generated by many other asset allocation strategies tested.

In chapter 8 we proposed a methodology based on chaos and dynamical systems theory for non-linear time series forecasting and investment strategy development. We constructed Constant Chaoticity Portfolios and evaluate their performances relative to several competing alternatives on the survival components of the STOXX Europe 50 index and the Hang Seng index, concluding they can enhance traditional portfolio allocation methodologies.

Overall, in this thesis we have analyzed many different data to solve cutting edge problems coming from the systemic risk and investment management spheres, both in the context of traditional financial markets and Fintech. This has been accomplished throughout the development and usage of a variety of techniques related to different mainstream domains, such as statistics, financial econometrics, financial mathematics and econophysics. The lessons learned from the current thesis are manifold. Firstly, each of the technique employed has a particular context in which it is suitable to be applied, and some may incur in pitfalls when considering specific situations (see, for instance, non-linearity). Secondly, what clearly emerges is that cryptocurrency markets widely differ from traditional financial markets - such as the stock and credit markets - from a variety of viewpoints, especially when it comes to volatility dynamics. This suggests future research to

bear in mind relevant market-specific features when dealing with quantitative analyses on interconnectedness and investment management related to traditional and nascent financial markets, also tailoring methodologies to the specific phenomenon under examination.

The methodological tools presented in this thesis have a variety of real world applications, especially in the empirical economics and finance domains. The empirical applications here developed do only partially cover the immense range of analyses which can be done and questions to be answered. Future research[30] might extend and improve the methodological frameworks presented so far, as well as provide further interesting domains of application for the methodologies proposed, given their highly interdisciplinary nature.

[30]For more detailed discussions about future research, please refer to the concluding section of each chapter.

References

[1] Acosta, P. A., Baerg, N. R., and Mandelman, F. S. (2009). Financial development, remittances, and real exchange rate appreciation. *Economic Review*, 94.

[2] Agiakloglou, C. and Deligiannakis, E. (2020). Sovereign risk evaluation for european union countries. *Journal of International Money and Finance*, 103:102117.

[3] Agnon, Y., Golan, A., and Shearer, M. (1999). Nonparametric, nonlinear, short-term forecasting: theory and evidence for nonlinearities in the commodity markets. *Economics Letters*, 65(3):293–299.

[4] Agosto, A., Giudici, P., and Raffinetti, E. (2019). A rank graduation accuracy measure. *Available at SSRN 3507530*.

[5] Agosto, A. and Raffinetti, E. (2019). Validation of parx models for default count prediction. *Frontiers in Artificial Intelligence*, 2:9.

[6] Ahelegbey, D. F., Billio, M., and Casarin, R. (2016). Bayesian graphical models for structural vector autoregressive processes. *Journal of Applied Econometrics*, 31(2):357–386.

[7] Amilon, H. (2003). A neural network versus black–scholes: a comparison of pricing and hedging performances. *Journal of Forecasting*, 22(4):317–335.

[8] Ammer, J. and Cai, F. (2011). Sovereign CDS and bond pricing dynamics in emerging markets: Does the cheapest-to-deliver option matter? *Journal of International Financial Markets, Institutions and Money*, 21(3):369–387.

[9] Antonakakis, N., Chatziantoniou, I., and Gabauer, D. (2019). Cryptocurrency market contagion: market uncertainty, market complexity, and dynamic portfolios. *Journal of International Financial Markets, Institutions and Money*, 61:37–51.

[10] Arce, O., Mayordomo, S., and Peña, J. I. (2013). Credit-risk valuation in the sovereign CDS and bonds markets: Evidence from the euro area crisis. *Journal of International Money and Finance*, 35:124–145.

[11] Augustin, P. (2014). Sovereign Credit Default Swap Premia. *Forthcoming, Journal of Investment Management*.

[12] Baba, N. and Inada, M. (2009). Price discovery of credit spreads for Japanese mega-banks: Evidence from bond and credit default swap markets. *Journal of International Financial Markets, Institutions and Money*, 19(4):616–632.

[13] Baek, S. K., Jung, W.-S., Kwon, O., and Moon, H.-T. (2005). Transfer entropy analysis of the stock market. *arXiv preprint physics/0509014*.

[14] Bank for International Settlements (1996). Implications for central banks of the development of electronic money.

[15] Barajas, A., Chami, R., Hakura, D., Montel, P., and Tressel, T. (2011). Workers' remittances and the equilibrium real exchange rate: Theory and evidence [with comment]. *Economía*, 11(2):45–99.

[16] Barnett, W. A. and Serletis, A. (2000). Martingales, nonlinearity, and chaos. *Journal of Economic Dynamics and Control*, 24(5-7):703–724.

[17] Baruník, J., Kočenda, E., and Vácha, L. (2016). Asymmetric connectedness on the us stock market: Bad and good volatility spillovers. *Journal of Financial Markets*, 27:55–78.

[18] Baruník, J. and Křehlík, T. (2018). Measuring the frequency dynamics of financial connectedness and systemic risk. *Journal of Financial Econometrics*, 16(2):271–296.

[19] Baur, D. G. and Dimpfl, T. (2019). Price discovery in bitcoin spot or futures? *Journal of Futures Markets*.

[20] Beenakker, C. W. (1997). Random-matrix theory of quantum transport. *Reviews of modern physics*, 69(3):731.

[21] Behrendt, S., Dimpfl, T., Peter, F. J., and Zimmermann, D. J. (2019). Rtransferentropy—quantifying information flow between different time series using effective transfer entropy. *SoftwareX*, 10:100265.

[22] Benhabib, J. (1996). On cycles and chaos in economics. *Studies in Nonlinear Dynamics & Econometrics*, 1(1).

[23] Billio, M., Getmansky, M., Lo, A., and Pelizzon, L. (2012). Econometric measures of connectedness and systemic risk in the finance and insurance sectors. *Journal of Financial Economics*, 104:535–559.

[24] Binner, J. M., Bissoondeeal, R. K., Elger, T., Gazely, A. M., and Mullineux, A. W. (2005). A comparison of linear forecasting models and neural networks: an application to euro inflation and euro divisia. *Applied economics*, 37(6):665–680.

[25] Black, F. and Scholes, M. (1973). The pricing of options and corporate liabilities. *Journal of Political Economy*, 81(3):637–54.

[26] Blanco, R., Brennan, S., and Marsh, I. W. (2005). An empirical analysis of the dynamic relation between investment-grade bonds and credit default swaps. *The journal of Finance*, 60(5):2255–2281.

[27] Bonacich, P. (2007). Some unique properties of eigenvector centrality. *Social networks*, 29(4):555–564.

[28] Bonanno, G., Caldarelli, G., Lillo, F., and Mantegna, R. N. (2003). Topology of correlation-based minimal spanning trees in real and model markets. *Physical Review E*, 68(4):046130.

[29] Bouri, E., Lau, C. K. M., Lucey, B., and Roubaud, D. (2019). Trading volume and the predictability of return and volatility in the cryptocurrency market. *Finance Research Letters*, 29:340–346.

[30] Box, G. E. and Tiao, G. C. (1975). Intervention analysis with applications to economic and environmental problems. *Journal of the American Statistical association*, 70(349):70–79.

[31] Boyle, P. P. (1977). Options: A monte carlo approach. *Journal of Financial Economics*, 4:323–338.

[32] Brandvold, M., Molnár, P., Vagstad, K., Valstad, A., and Ole, C. (2015). Price discovery on bitcoin exchanges. *Journal of International Financial Markets, Institutions and Money*, 36(C):18–35.

[33] Brauneis, A. and Mestel, R. (2018). Price discovery of cryptocurrencies: Bitcoin and beyond. *Economics Letters*, 165:58–61.

[34] Brennan, M. J. and Schwartz, E. S. (1977). Finite difference methods and jump processes arising in the pricing of contingent claims: A synthesis. *The Journal of Financial and Quantitative Analysis*, 12:659.

[35] Brin, S. and Page, L. (1998). The anatomy of a large-scale hypertextual web search engine. *Computer networks and ISDN systems*, 30(1-7):107–117.

[36] Brock, W. A., Hsieh, D. A., LeBaron, B. D., Brock, W. E., et al. (1991). *Nonlinear dynamics, chaos, and instability: statistical theory and economic evidence*. MIT press.

[37] Bullmann, D., Klemm, J., Pinna, A., et al. (2019). In search for stability in crypto-assets: are stablecoins the solution? Technical report, European Central Bank.

[38] Burges, C. J. (1998). A tutorial on support vector machines for pattern recognition. *Data mining and knowledge discovery*, 2(2):121–167.

[39] Calabrese, R. and Giudici, P. (2015). Estimating bank default with generalised extreme value regression models. *Journal of the Operational Research society*, 66(11):1783–1792.

[40] Carney, M. (2019). The growing challenges for monetary policy in the current international monetary and financial system. In *Remarks at the Jackson Hole Symposium*.

[41] Caserini, N. and Pagnottoni, P. (2020). Information flow in the credit risk market: Evidence from the european sovereign cds and government bonds. *Working Paper*.

[42] Chakravarty, S., Gulen, H., and Mayhew, S. (2004). Informed trading in stock and option markets. *The Journal of Finance*, 59(3):1235–1257.

[43] Chan-Lau, J. A. and Kim, Y. S. (2004). *Equity prices, credit default swaps, and bond spreads in emerging markets*. Number 4-27. International Monetary Fund.

[44] Chen, C. (1994). Neural networks for financial market prediction. In *Proceedings of 1994 IEEE International Conference on Neural Networks (ICNN'94)*, volume 2, pages 1199–1202. IEEE.

[45] Cheng, J. and Dai, Y. (2020). Is bitcoin a channel of capital inflow? evidence from carry trade activity. *International Review of Economics & Finance*, 66:261–278.

[46] Conlon, T., Ruskin, H. J., and Crane, M. (2007). Random matrix theory and fund of funds portfolio optimisation. *Physica A: Statistical Mechanics and its applications*, 382(2):565–576.

[47] Corbet, S., Lucey, B., Peat, M., and Vigne, S. (2018a). Bitcoin futures—what use are they? *Economics Letters*, 172:23–27.

[48] Corbet, S., Meegan, A., Larkin, C., Lucey, B., and Yarovaya, L. (2018b). Exploring the dynamic relationships between cryptocurrencies and other financial assets. *Economics Letters*, 165:to appear.

[49] Corbet, S., Meegan, A., Larkin, C., Lucey, B., and Yarovaya, L. (2018c). Exploring the dynamic relationships between cryptocurrencies and other financial assets. *Economics Letters*, 165:28–34.

[50] Coudert, V. and Gex, M. (2013). The interactions between the credit default swap and the bond markets in financial turmoil. *Review of International Economics*, 21(3):492–505.

[51] Cox, J. C., Ross, S., and Rubinstein, M. (1979). Option pricing: A simplified approach. *Journal of Financial Economics*, 7(3):229–263.

[52] Darbellay, G. A. and Wuertz, D. (2000). The entropy as a tool for analysing statistical dependences in financial time series. *Physica A: Statistical Mechanics and its Applications*, 287(3-4):429–439.

[53] Delatte, A.-L., Gex, M., and López-Villavicencio, A. (2012). Has the CDS market influenced the borrowing cost of european countries during the sovereign crisis? *Journal of International Money and Finance*, 31(3):481–497.

[54] Delis, M. D. and Mylonidis, N. (2011). The chicken or the egg? a note on the dynamic interrelation between government bond spreads and credit default swaps. *Finance Research Letters*, 8(3):163–170.

[55] Demirer, M., Diebold, F. X., Liu, L., and Yilmaz, K. (2018). Estimating global bank network connectedness. *Journal of Applied Econometrics*, 33(1):1–15.

[56] Dickey, D. A. and Fuller, W. A. (1979). Distribution of the estimators for autoregressive time series with a unit root. *Journal of the American statistical association*, 74(366a):427–431.

[57] Diebold, F. X. and Yilmaz, K. (2009). Measuring financial asset return and volatility spillovers, with application to global equity markets. *The Economic Journal*, 119(534):158–171.

[58] Diebold, F. X. and Yilmaz, K. (2012). Better to give than to receive: Predictive directional measurement of volatility spillovers. *International Journal of Forecasting*, 28(1):57–66.

[59] Diebold, F. X. and Yilmaz, K. (2013). Measuring the dynamics of global business cycle connectedness.

[60] Diebold, F. X. and Yılmaz, K. (2014). On the network topology of variance decompositions: Measuring the connectedness of financial firms. *Journal of Econometrics*, 182(1):119–134.

[61] Dimpfl, T. and Peter, F. J. (2013). Using transfer entropy to measure information flows between financial markets. *Studies in Nonlinear Dynamics and Econometrics*, 17(1):85–102.

[62] Duffie, D. (1999). Credit swap valuation. *Financial Analysts Journal*, 55(1):73–87.

[63] Dwyer, G. (2015a). The economics of bitcoin and similar private digital currencies. *Journal of Financial Stability*, 17:81–91.

[64] Dwyer, G. P. (2015b). The economics of bitcoin and similar private digital currencies. *Journal of Financial Stability*, 17:81–91.

[65] Engle, R. F. and Granger, C. W. (1987). Co-integration and error correction: representation, estimation, and testing. *Econometrica: journal of the Econometric Society*, pages 251–276.

[66] Eom, C., Oh, G., Jung, W.-S., Jeong, H., and Kim, S. (2009). Topological properties of stock networks based on minimal spanning tree and random matrix theory in financial time series. *Physica A: Statistical Mechanics and its Applications*, 388(6):900–906.

[67] European Central Bank (1998). Report on electronic money.

[68] Fantazzini, D., Nigmatullin, E., Sukhanovskaya, V., Ivliev, S., et al. (2017). Everything you always wanted to know about bitcoin modelling but were afraid to ask. part 2. *Applied Econometrics*, 45:5–28.

[69] Figini, S. and Giudici, P. (2011). Statistical merging of rating models. *Journal of the operational research society*, 62(6):1067–1074.

[70] Financial Stability Board (2019). Regulatory issues of stablecoins.

[71] Flore, M. (2018). How blockchain-based technology is disrupting migrants' remittances: a preliminary assessment. *Luxembourg, EUR*, 29492.

[72] Fontana, A. and Scheicher, M. (2010). An analysis of euro area sovereign CDS and their relation with government bonds. European Central Bank working paper (no. 1271).

[73] Fontana, A. and Scheicher, M. (2016). An analysis of euro area sovereign CDS and their relation with government bonds. *Journal of Banking & Finance*, 62:126–140.

[74] Friedman, J., Hastie, T., and Tibshirani, R. (2008). Sparse inverse covariance estimation with the graphical lasso. *Biostatistics*, 9(3):432–441.

[75] Fry, J. and Cheah, E.-T. (2016). Negative bubbles and shocks in cryptocurrency markets. *International Review of Financial Analysis*, 47:343–352.

[76] FSB (2017a). Financial stability implications from fintech: Supervisory and regulatory issues that merit authorities' attention. *June, Basel*.

[77] FSB (2017b). Fintech credit. *Financial Stability Board Report (27 June, 2017)*.

[78] Gavrishchaka, V. V. and Banerjee, S. (2006). Support vector machine as an efficient framework for stock market volatility forecasting. *Computational Management Science*, 3(2):147–160.

[79] Giudici, P. and Abu-Hashish, I. (2019). What determines bitcoin exchange prices? a network var approach. *Finance Research Letters*, 28:309–318.

[80] Giudici, P. and Bilotta, A. (2004). Modelling operational losses: a bayesian approach. *Quality and Reliability Engineering International*, 20(5):407–417.

[81] Giudici, P., Mezzetti, M., and Muliere, P. (2003). Mixtures of products of dirichlet processes for variable selection in survival analysis. *Journal of statistical planning and inference*, 111(1-2):101–115.

[82] Giudici, P. and Pagnottoni, P. (2019). High frequency price change spillovers in bitcoin markets. *Risks*, 7(4):111.

[83] Giudici, P. and Pagnottoni, P. (2020). Vector error correction models to measure connectedness of bitcoin exchange markets. *Applied Stochastic Models in Business and Industry*, 36(1):95–109.

[84] Giudici, P., Pagnottoni, P., and Leach, T. (2020a). Libra or librae? basket based stablecoins to mitigate foreign exchange volatility spillovers. *available at https://papers.ssrn.com/sol3/papers.cfm?abstract_id* = 3546779.

[85] Giudici, P., Pagnottoni, P., and Polinesi, G. (2020b). Network models to enhance automated cryptocurrency portfolio management. *Frontiers in Artificial Intelligence*, 3:22.

[86] Golestani, A. and Gras, R. (2014). Can we predict the unpredictable? *Scientific reports*, 4:6834.

[87] Gonzalo, J. and Granger, C. (1995a). Estimation of common long-memory components in cointegrated systems. *Journal of Business & Economic Statistics*, 13(1):27–35.

[88] Gonzalo, J. and Granger, C. (1995b). Estimation of common long-memory components in cointegrated systems. *Journal of Business & Economic Statistics*, 13(1):27–35.

[89] Gopinath, G., Boz, E., Casas, C., Díez, F. J., Gourinchas, P.-O., and Plagborg-Møller, M. (2016). Dominant currency paradigm. Working Paper 22943, National Bureau of Economic Research.

[90] Granger, C. W. and Andersen, A. (1978). On the invertibility of time series models. *Stochastic processes and their applications*, 8(1):87–92.

[91] Guhr, T., Müller-Groeling, A., and Weidenmüller, H. A. (1998). Random-matrix theories in quantum physics: common concepts. *Physics Reports*, 299(4-6):189–425.

[92] Gyntelberg, J., Hördahl, P., Ters, K., and Urban, J. (2013). Intraday dynamics of euro area sovereign CDS and bonds. BIS working paper (no.423).

[93] Gyntelberg, J., Hördahl, P., Ters, K., and Urban, J. (2017). Arbitrage costs and the persistent non-zero cds-bond basis: Evidence from intraday euro area sovereign debt markets. BIS working paper (no.631).

[94] Harrison, R. G., Yu, D., Oxley, L., Lu, W., and George, D. (1999). Nonlinear noise reduction and detecting chaos: some evidence from the s&p composite price index. *Mathematics and Computers in Simulation*, 48(4-6):497–502.

[95] Hasbrouck, J. (1995a). One security, many markets: Determining the contributions to price discovery. *The Journal of Finance*, 50(4):1175–1199.

[96] Hasbrouck, J. (1995b). One security, many markets: Determining the contributions to price discovery. *The journal of Finance*, 50(4):1175–1199.

[97] Haykin, S. S., Haykin, S. S., Haykin, S. S., Elektroingenieur, K., and Haykin, S. S. (2009). *Neural networks and learning machines*, volume 3. Pearson Upper Saddle River.

[98] Hovanov, N. V., Kolari, J. W., and Sokolov, M. V. (2004). Computing currency invariant indices with an application to minimum variance currency baskets. *Journal of Economic Dynamics and Control*, 28(8):1481–1504.

[99] Hsieh, D. A. (1991). Chaos and nonlinear dynamics: application to financial markets. *The journal of finance*, 46(5):1839–1877.

[100] Huang, W., Nakamori, Y., and Wang, S.-Y. (2005). Forecasting stock market movement direction with support vector machine. *Computers & operations research*, 32(10):2513–2522.

[101] Hull, J. and White, A. (1990a). Pricing interest-rate-derivative securities. *Review of Financial Studies*, 3(4):573–592.

[102] Hull, J. and White, A. (1990b). Valuing derivative securities using the explicit finite difference method. *The Journal of Financial and Quantitative Analysis*, 25:87.

[103] Humpage, O. (2009). Will special drawing rights supplant the dollar? `https://voxeu.org/article/sdr-vs-what-it-takes-be-international-reserve-currency`.

[104] Hutchinson, J. M., Lo, A. W., and Poggio, T. (1994). A nonparametric approach to pricing and hedging derivative securities via learning networks. *The Journal of Finance*, 49(3):851–889.

[105] Ji, Q., Bouri, E., Lau, C. K. M., and Roubaud, D. (2019). Dynamic connectedness and integration in cryptocurrency markets. *International Review of Financial Analysis*, 63:257–272.

[106] Johansen, S. (1991). Estimation and hypothesis testing of cointegration vectors in gaussian vector autoregressive models. *Econometrica: journal of the Econometric Society*, pages 1551–1580.

[107] Kaplanov, N. (2012). Nerdy money: Bitcoin, the private digital currency, and the case against its regulation. *25 Loy. Consumer L. Rev. 111.*

[108] Katsiampa, P., Corbet, S., and Lucey, B. (2019). High frequency volatility co-movements in cryptocurrency markets. *Journal of International Financial Markets, Institutions and Money*, 62:35–52.

[109] Katz, L. (1953). A new status index derived from sociometric analysis. *Psychometrika*, 18(1):39–43.

[110] Keating, J. W. (1996). Structural information in recursive var orderings. *Journal of economic dynamics and control*, 20(9-10):1557–1580.

[111] Kleinberg, J. M. (1999). Authoritative sources in a hyperlinked environment. *Journal of the ACM (JACM)*, 46(5):604–632.

[112] Kliková, B. and Raidl, A. (2011). Reconstruction of phase space of dynamical systems using method of time delay. In *Proceedings of the 20th Annual Conference WDS 2011.*

[113] Koop, G., Pesaran, M. H., and Potter, S. M. (1996). Impulse response analysis in nonlinear multivariate models. *Journal of econometrics*, 74(1):119–147.

[114] Koutmos, D. (2018). Return and volatility spillovers among cryptocurrencies. *Economics Letters*, 173:122–127.

[115] Kroll, J. A., Davey, I. C., and Felten, E. W. (2013). The economics of bitcoin mining , or bitcoin in the presence of adversaries. *Proceedings of WEIS*.

[116] Kuan, C.-M. (2002). Lecture on the markov switching model. *Institute of Economics Academia Sinica*, pages 1–30.

[117] Kullback, S. and Leibler, R. A. (1951). On information and sufficiency. *The annals of mathematical statistics*, 22(1):79–86.

[118] Kwiatkowski, D., Phillips, P. C., Schmidt, P., and Shin, Y. (1992). Testing the null hypothesis of stationarity against the alternative of a unit root: How sure are we that economic time series have a unit root? *Journal of econometrics*, 54(1-3):159–178.

[119] Kwon, O. and Yang, J.-S. (2008a). Information flow between composite stock index and individual stocks. *Physica A: Statistical Mechanics and its Applications*, 387(12):2851–2856.

[120] Kwon, O. and Yang, J.-S. (2008b). Information flow between stock indices. *EPL (Europhysics Letters)*, 82(6):68003.

[121] LeBaron, B. (1994). Chaos and nonlinear forecastability in economics and finance. *Philosophical Transactions of the Royal Society of London. Series A: Physical and Engineering Sciences*, 348(1688):397–404.

[122] León, D., Aragón, A., Sandoval, J., Hernández, G., Arévalo, A., and Nino, J. (2017). Clustering algorithms for risk-adjusted portfolio construction. *Procedia Computer Science*, 108:1334–1343.

[123] Levene, T. (2006). 'Cashless society' card that flopped. *The Guardian*.

[124] Li, N. and Huang, A. Y. (2011). Price discovery between sovereign credit default swaps and bond yield spreads of emerging markets. *Journal of Emerging Market Finance*, 10(2):197–225.

[125] Liang, X., Zhang, H., Xiao, J., and Chen, Y. (2009). Improving option price forecasts with neural networks and support vector regressions. *Neurocomputing*, 72:3055–3065.

[126] Lin, C.-T. and Yeh, H.-Y. (2005). The valuation of taiwan stock index option price-comparison of performances between black-scholes and neural network model. *Journal of Statistics and Management Systems*, 8(2):355–367.

[127] Majhi, R., Panda, G., Sahoo, G., Panda, A., and Choubey, A. (2008). Prediction of s&p 500 and djia stock indices using particle swarm optimization technique. In *2008 IEEE Congress on Evolutionary Computation (IEEE World Congress on Computational Intelligence)*, pages 1276–1282. IEEE.

[128] Malliaris, A. and Stein, J. L. (1999). Methodological issues in asset pricing: Random walk or chaotic dynamics. *Journal of Banking & Finance*, 23(11):1605–1635.

[129] Malliaris, M. and Salchenberger, L. (1996). Using neural networks to forecast the s&p 100 implied volatility. *Neurocomputing*, 10(2):183–195.

[130] Mandelbrot, B. B. (1999). A multifractal walk down wall street. *Scientific American*, 280(2):70–73.

[131] Mantegna, R. N. (1999). Hierarchical structure in financial markets. *The European Physical Journal B-Condensed Matter and Complex Systems*, 11(1):193–197.

[132] Mantegna, R. N. and Stanley, H. E. (1999). *Introduction to econophysics: correlations and complexity in finance*. Cambridge university press.

[133] Marchenko, V. A. and Pastur, L. A. (1967). Distribution of eigenvalues for some sets of random matrices. *Matematicheskii Sbornik*, 114(4):507–536.

[134] Markowitz, H. (1952). Portfolio selection. *The journal of finance*, 7(1):77–91.

[135] Marschinski, R. and Kantz, H. (2002). Analysing the information flow between financial time series. *The European Physical Journal B-Condensed Matter and Complex Systems*, 30(2):275–281.

[136] McCue, L. S. and Troesch, A. W. (2011). Use of lyapunov exponents to predict chaotic vessel motions. In *Contemporary Ideas on Ship Stability and Capsizing in Waves*, pages 415–432. Springer.

[137] Molleyres, J. (2018). Price discovery dynamics of corporate credit default swaps and bonds. *Available at SSRN 2817819*.

[138] Murphy, E., Murphy, M., and Seitzinger, M. (2015). Bitcoin: Questions, answers, and analysis of legal issues. *Congressional Research Service*.

[139] Nakamoto, S. (2008). Bitcoin: A peer-to-peer electronic cash system. *www.bitcoin.org*.

[140] Nakamoto, S. et al. (2008). Bitcoin: A peer-to-peer electronic cash system.

[141] Nelson, D. B. and Ramaswamy, K. (1990). Simple binomial processes as diffusion approximations in financial models. *Review of Financial Studies*, 3(3):393–430.

[142] Neshat, M., Sepidnam, G., Sargolzaei, M., and Toosi, A. N. (2014). Artificial fish swarm algorithm: a survey of the state-of-the-art, hybridization, combinatorial and indicative applications. *Artificial intelligence review*, 42(4):965–997.

[143] Ocampo, J. A. (2019). Is it time for a 'true global currency'? `https://www.weforum.org/agenda/2019/04/is-it-time-for-a-true-global-currency`.

[144] Onnela, J.-P., Chakraborti, A., Kaski, K., Kertesz, J., and Kanto, A. (2003). Dynamics of market correlations: Taxonomy and portfolio analysis. *Physical Review E*, 68(5):056110.

[145] Pagnottoni, P. (2019). Neural network models for bitcoin option pricing. *Frontiers in Artificial Intelligence*, 2:5.

[146] Pagnottoni, P. and Dimpfl, T. (2019). Price discovery on bitcoin markets. *Digital Finance*, 1(1-4):139–161.

[147] Palladini, G. and Portes, R. (2011). Sovereign CDS and bond pricing dynamics in the euro-area. Technical report, National Bureau of Economic Research.

[148] Patanè, M., Tedesco, M., Zedda, S., et al. (2019). Cds-bond basis dynamic and credit spread price discovery: A test for european corporate and sovereign bond markets. *Modern Economy*, 10(08):1984.

[149] Peralta, G. and Zareei, A. (2016). A network approach to portfolio selection. *Journal of Empirical Finance*, 38:157–180.

[150] Perra, N. and Fortunato, S. (2008). Spectral centrality measures in complex networks. *Physical Review E*, 78(3):036107.

[151] Pesaran, H. H. and Shin, Y. (1998a). Generalized impulse response analysis in linear multivariate models. *Economics letters*, 58(1):17–29.

[152] Pesaran, M. H. and Shin, Y. (1998b). An autoregressive distributed-lag modelling approach to cointegration analysis. *Econometric Society Monographs*, 31:371–413.

[153] Peters, E. E. (1996). *Chaos and order in the capital markets: a new view of cycles, prices, and market volatility*. John Wiley & Sons.

[154] Plerou, V., Gopikrishnan, P., Rosenow, B., Amaral, L. A. N., Guhr, T., and Stanley, H. E. (2002). Random matrix approach to cross correlations in financial data. *Physical Review E*, 65(6):066126.

[155] Potters, M., Bouchaud, J.-P., and Laloux, L. (2005). Financial applications of random matrix theory: Old laces and new pieces. *arXiv preprint physics/0507111*.

[156] Pozzi, F., Di Matteo, T., and Aste, T. (2013). Spread of risk across financial markets: better to invest in the peripheries. *Scientific reports*, 3:1665.

[157] Priestley, M. (1980). State-dependent models: A general approach to non-linear time series analysis. *Journal of Time Series Analysis*, 1(1):47–71.

[158] Raffinot, T. (2017). Hierarchical clustering-based asset allocation. *The Journal of Portfolio Management*, 44(2):89–99.

[159] Reddy, Y. and Sebastin, A. (2008). Are commodity and stock markets independent of each other? A case study in india. *The Journal of Alternative Investments*, 11(3):85–99.

[160] Ren, F., Lu, Y.-N., Li, S.-P., Jiang, X.-F., Zhong, L.-X., and Qiu, T. (2017). Dynamic portfolio strategy using clustering approach. *PloS one*, 12(1):e0169299.

[161] Rendleman, R. J. and Bartter, B. J. (1979). Two-state option pricing. *The Journal of Finance*, 34(5):1093–1110.

[162] Resta, M., Pagnottoni, P., and De Giuli, M. E. (2020). Technical analysis on the bitcoin market: Trading opportunities or investors' pitfall? *Risks*, 8(2):44.

[163] Rhodes, C. and Morari, M. (1997). False-nearest-neighbors algorithm and noise-corrupted time series. *Physical Review E*, 55(5):6162.

[164] Rosenstein, M. T., Collins, J. J., and De Luca, C. J. (1993). A practical method for calculating largest lyapunov exponents from small data sets. *Physica D: Nonlinear Phenomena*, 65(1-2):117–134.

[165] Schittenkopf, C., Dorffner, G., and Dockner, E. J. (2000). On nonlinear, stochastic dynamics in economic and financial time series. *Studies in Nonlinear Dynamics & Econometrics*, 4(3).

[166] Schreiber, T. (2000). Measuring information transfer. *Physical review letters*, 85(2):461.

[167] Segendorf, B. (2014). What is bitcoin. *Sveriges Riksbank Economic Review*, 2:71–87.

[168] Sensoy, A., Sobaci, C., Sensoy, S., and Alali, F. (2014). Effective transfer entropy approach to information flow between exchange rates and stock markets. *Chaos, solitons & fractals*, 68:180–185.

[169] Shannon, C. E. (1948). A mathematical theory of communication. *Bell system technical journal*, 27(3):379–423.

[170] Small, M. and Chi, K. T. (2003). Determinism in financial time series. *Studies in nonlinear dynamics & Econometrics*, 7(3).

[171] Specht, D. F. et al. (1991). A general regression neural network. *IEEE transactions on neural networks*, 2(6):568–576.

[172] Spelta, A. and Araújo, T. (2012). The topology of cross-border exposures: beyond the minimal spanning tree approach. *Physica A: Statistical Mechanics and its Applications*, 391(22):5572–5583.

[173] Spelta, A., Pecora, N., and Pagnottoni, P. (2020). Chaos based portfolio selection: a constant chaoticity approach. *Working Paper*.

[174] Stathakis, D. (2009). How many hidden layers and nodes? *International Journal of Remote Sensing*, 30:2133–2147.

[175] Tola, V., Lillo, F., Gallegati, M., and Mantegna, R. N. (2008). Cluster analysis for portfolio optimization. *Journal of Economic Dynamics and Control*, 32(1):235–258.

[176] Tong, H. and Lim, K. S. (2009). Threshold autoregression, limit cycles and cyclical data. In *Exploration Of A Nonlinear World: An Appreciation of Howell Tong's Contributions to Statistics*, pages 9–56. World Scientific.

[177] Tulino, A. M., Verdú, S., et al. (2004). Random matrix theory and wireless communications. *Foundations and Trends® in Communications and Information Theory*, 1(1):1–182.

[178] Vlachos, I. and Kugiumtzis, D. (2008). State space reconstruction for multivariate time series prediction. *Nonlinear Phenomena in Complex Systems*, 11(2):241–249.

[179] Vỳrost, T., Lyócsa, Š., and Baumöhl, E. (2018). Network-based asset allocation strategies. *The North American Journal of Economics and Finance*.

[180] Wheelwright, S., Makridakis, S., and Hyndman, R. J. (1998). *Forecasting: methods and applications*. John Wiley & Sons.

[181] White, L. H. (2015). The market for cryptocurrencies. *Cato Journal*, 35(2).

[182] Yao, J., Li, Y., and Tan, C. L. (2000). Option price forecasting using neural networks. *Omega*, 28:455–466.

[183] Yi, S., Xu, Z., and Wang, G.-J. (2018). Volatility connectedness in the cryptocurrency market: Is bitcoin a dominant cryptocurrency? *International Review of Financial Analysis*, 60:98–114.

[184] Zhan, H. C. J., Rea, W., and Rea, A. (2015). An application of correlation clustering to portfolio diversification. *arXiv preprint arXiv:1511.07945*.

[185] Zhu, H. (2006). An empirical comparison of credit spreads between the bond market and the credit default swap market. *Journal of Financial Services Research*, 29(3):211–235.

[186] Zięba, D., Kokoszczyński, R., and Śledziewska, K. (2019). Shock transmission in the cryptocurrency market. is bitcoin the most influential? *International Review of Financial Analysis*, 64:102–125.

A Appendix

A.1 Technical Details of Chapter 5

In this Appendix, we assess the robustness of our empirical results with respect to alternative modelling strategies.

We let the number of shuffles vary from 100 to 300. The effective transfer entropy estimates, reported in Table 38, seem just slightly influenced by the change of number of shuffles, and bi-directional information flow is still confirmed across all the sovereigns. Hence, results do not change from a qualitative viewpoint.

We then let the number of bootstrap replications vary from 300 to 600. Results are reported in Table 38. Also in this case, effective transfer entropy estimates are statistically significant for both directions, and the magnitude of information transmitted from the bond market still exceeds that of the CDS market.

We also investigate the information flow in a tighter sub-sample related to the sovereign crisis. Results for the estimated information flows from January 2010 to December 2013 are shown in Table 39. Except for Spain[31], the significance of our analysis strengthen the conclusions on the leadership of the bond market for core countries.

A.2 Technical Details of Chapter 7

To further investigate the robustness of our results, we have performed a twofold sensitivity analysis. On the one hand, we have shifted the starting point of investing 4, 8, and 12 weeks into the future and computed cumulative portfolio returns again. In this analysis we have maintained our rolling 15 weeks window for correlation estimation. Outcomes are represented in Figure 45, panels a, b and c, respectively. On the other hand, we have performed the analysis again, but using a 19-week estimation window, meaning

[31]The result is in line with the finding of Agiakloglou and Deligiannakis (2020).

Table 38: Robustness checks for the effective transfer entropy estimates significance

Country	Period	Number of shuffles = 300		Bootstrap replications = 600	
		$ETE_{CDS\to BS}$	$ETE_{BS\to CDS}$	$ETE_{CDS\to BS}$	$ETE_{BS\to CDS}$
Italy	Full sample	0.00934***	0.00981***	0.00957***	0.00964***
		(0.00139)	(0.00141)	(0.00155)	(0.00137)
Belgium	Full sample	0.02202***	0.02838***	0.02211***	0.02829***
		(0.00141)	(0.00149)	(0.00157)	(0.00136)
Austria	Full sample	0.01293***	0.02017***	0.01273***	0.02019***
		(0.00136)	(0.00142)	(0.00147)	(0.00153)
France	Full sample	0.02384***	0.03089***	0.02353***	0.03086***
		(0.00140)	(0.00146)	(0.00152)	(0.00148)
Netherlands	Full sample	0.00791***	0.00964***	0.00779***	0.00992***
		(0.00148)	(0.00151)	(0.00135)	(0.00161)
Ireland	Full sample	0.02195***	0.03364***	0.02189***	0.03368***
		(0.00153)	(0.00151)	(0.00151)	(0.00148)
Portugal	Full sample	0.02422***	0.02630***	0.02413***	0.02608***
		(0.00143)	(0.00154)	(0.00149)	(0.00152)
Spain	Full sample	0.00610***	0.00913***	0.00584***	0.00927***
		(0.00147)	(0.00140)	(0.00143)	(0.00149)

Note: The table reports the results of the effective transfer entropy estimates. The third and the fourth columns show the estimates of the effective transfer entropy from the CDS to the bond market ($ETE_{CDS\to BS}$) and from the bond to the CDS market ($ETE_{BS\to CDS}$), setting the number of shuffles equal to 300. The fifth and the sixth columns show the estimates of the effective transfer entropy from the CDS to the bond market ($ETE_{CDS\to BS}$) and from the bond to the CDS market ($ETE_{BS\to CDS}$), setting the number bootstrap replications equal to 600. Standard errors are given in parentheses. ***, **, * indicate rejection of the null hypothesis of no information flows at 1%, 5%, and 10% significance level, respectively.

Table 39: Robustness checks for the effective transfer entropy estimates during the sovereign debt crisis

Country	Period	$ETE_{CDS \to BS}$	Std. Err.	$ETE_{BS \to CDS}$	Std. Err.	NIF
Italy	2010 - 2013	0.00593**	0.00325	0.02017***	0.00327	-0.01424
Belgium	2010 - 2013	0.00083	0.00316	0.02271***	0.00304	-0.02188
Austria	2010 - 2013	0.00106	0.00272	0.00984***	0.00284	-0.00878
France	2010 - 2013	0.00584**	0.00298	0.01828***	0.00299	-0.01244
Netherlands	2010 - 2013	0.00557*	0.00319	0.00616**	0.00320	-0.00059
Ireland	2010 - 2018	0.00162	0.00334	0.01568***	0.00296	-0.01406
Portugal	2010 - 2013	0.01026***	0.00294	0.01489***	0.00319	-0.00463
Spain	2010 - 2013	0.00935**	0.00318	0.00080	0.00307	0.00856

Note: The table reports the results of the effective transfer entropy estimates. The third and the fourth columns show the estimates of the effective transfer entropy from the CDS to the bond market ($ETE_{CDS \to BS}$) and the standard error (Std. Err). The fifth and the sixth columns show the estimates of the effective transfer entropy from the bond to the CDS market ($ETE_{BS \to CDS}$) and the standard error (Std. Err.). The last column reports the net information flow (NIF), the difference between $ETE_{CDS \to BS}$ and $ETE_{BS \to CDS}$. ***, **, * indicate rejection of the null hypothesis of no information flows at 1%, 5%, and 10% significance level, respectively.

from rolling 4 months to rolling 5 months, changing both the starting point of investing and the window for correlation estimation. Results are shown in Figure 46. In both cases, outcomes suggest that our results are robust even with shifting starting points and different rolling estimation windows. Indeed, performances show that the Network Markowitz model outperforms the competitive strategies even with varying the starting point of the analysis and the estimation window choice. Moreover, the strategy results with profits rather than losses in some cases when shifting the investment starting point.

A.3 Technical Details of Chapter 8

A.3.1 Hang Seng Index Results

In this Appendix we present the results related to the Hang Seng index. We firstly introduce the stock price forecast results. After that, we examine the portfolio performances both in terms of net profits and adjusted-risk returns.

Figure 47 shows the forecasts and the price pattern of the CK Hutchison Holdings Limited (ID 0001.HK) as a reference example for the Hang Seng index. As for the STOXX Europe 50, the price forecasts are able to follow quite closely the actual path of the CK Hutchison Holdings Limited stock price. This evidence is also clearly reported in the inset of the figure where an oscillating phase is correctly recognized, in particular way by the proposed forecasting method. This is in line with what we observe for the STOXX 50 Europe stocks.

Figure 48 shows the portfolio performances related to the Asian market. As for the European case, the single and the double sorting portfolios are compared against the market index performance, the equally weighted portfolio and the ARIMA-based portfolios. Notice that, differently from the European case, P&L include transaction costs of 50 basis-points per each stock composing a certain portfolio at each rebalancing. Moreover, top-bottom portfolios are computed with the 85th and 15th percentiles as a benchmark

Table 40: Sharpe Ratio and Jensen's Alpha of different portfolio strategies

Sharpe Ratio							
	2015	2016	2017	2018	2019	2020	TOT
Market Index	-0,117	0,073	0,376	-0,129	0,077	-0,319	0,01
Aver. Market	-0,062	0,088	0,339	-0,164	0,248	-0,411	0,036
Past Returns	-0,089	-0,022	0,014	-0,249	-0,123	-0,509	-0,106
Single Sort	0,024	0,013	0,066	0,205	0,055	0,028	0,078
Double Sort	0,181	-0,139	0,189	-0,086	0,062	-0,648	0,034
ARIMA(1,1,1)	-0,004	0,051	0,247	0,05	-0,106	0,335	0,046
ARIMA(2,1,1)	-0,14	0,052	0,02	-0,07	-0,258	0,721	-0,056
Jensen's Alpha							
	2015	2016	2017	2018	2019	2020	TOT
Aver. Market	0,133	0,043	0,037	-0,129	0,355	-0,226	0,062
Past Returns	-0,172	-0,065	-0,025	-0,511	-0,162	-0,449	-0,188
Single Sort	0,049	0,031	0,013	0,442	0,048	-0,07	0,123
Double Sort	0,85	-0,416	0,389	-0,199	0,216	-2,666	0,117
ARIMA(1,1,1)	0,069	0,077	0,508	0,093	-0,148	0,456	0,085
ARIMA(2,1,1)	-0,325	0,063	0,073	-0,217	-0,369	0,986	-0,099

Table reports the Sharpe Ratio and the Jensen's Alpha of the analyzed strategies at five days forecast horizon. The benchmark used to calculate the Jensen's Alpha is the Hang Seng index.

Figure 45: Cumulative returns for selected portfolio strategies with shifting starting points.

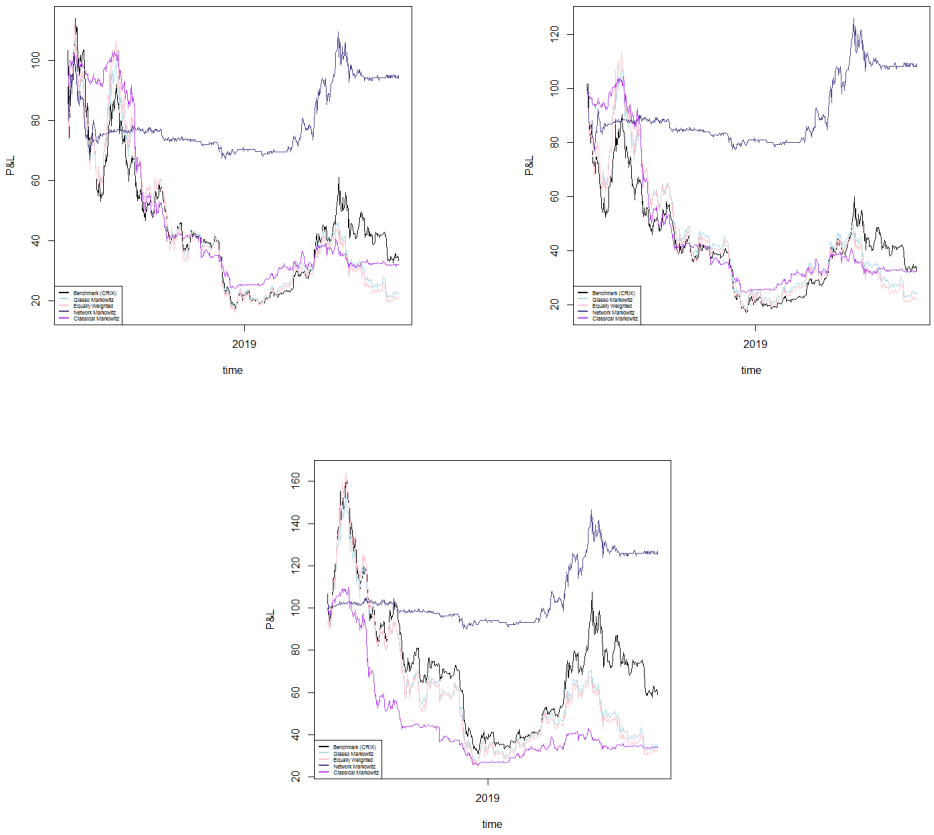

Note: The plot illustrates the profit and losses of a portfolio with initial value of 100 USD obtained by the CRIX benchmark index (Benchmark (CRIX)), the optimization using the Markowitz approach with the variance-covariance matrix filtered by Glasso (Glasso Markowitz), the naive portfolio (Equally Weighted), our optimization using RMT and MST applied to the variance-covariance matrix (Network Markowitz) and the standard Markowitz portfolio (Classical Markowitz). Starting points are shifted by 4 weeks (panel a), 8 weeks (panel b) and 12 weeks (panel c) for sensitivity purposes.

Figure 46: Cumulative returns for selected portfolio strategies with different rolling estimation windows

Note: The plot reports the profit and losses of a portfolio with initial value of 100 USD obtained by the CRIX benchmark index (Benchmark (CRIX)), the optimization using the Markowitz approach with the variance-covariance matrix filtered by Glasso (Glasso Markowitz), the naive portfolio (Equally Weighted), our optimization using RMT and MST applied to the variance-covariance matrix (Network Markowitz) and the standard Markowitz portfolio (Classical Markowitz). We use a rolling estimation window of 19 weeks for sensitivity purposes.

for the Asian case, rather than the 65th and 35th percentiles considered for the European one. This variation is due to the different number of components of each index, meaning that the Hang Seng index counts a higher

Figure 47: The price pattern prediction at five days forecasting horizon for the stock component ID 0001.HK (CK Hutchison Holdings Limited) of the Hang Seng index

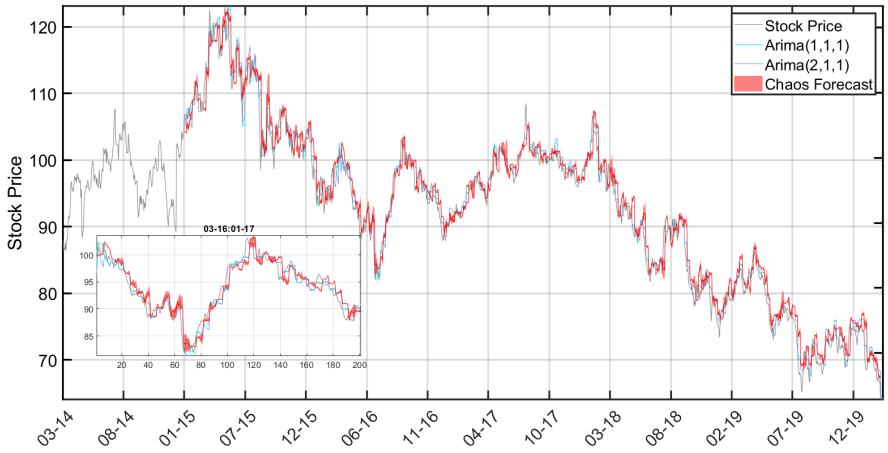

Note: The price forecast obtained by our methodology is represented by the red line; the price forecasts given by the ARIMA(1,1,1) and ARIMA(2,1,1) models are represented by the light blue and blue lines, respectively; the gray line identifies the actual stock price during the analyzed period. The y-axis refers to the stock price. The x-axis, instead, indicates the timeline. At the bottom left of the graph an enlargement describes the price pattern during the period ranging from March 2016 to January 2017.

Figure 48: Portfolio performance with five days forecasting horizon, for the Asian case

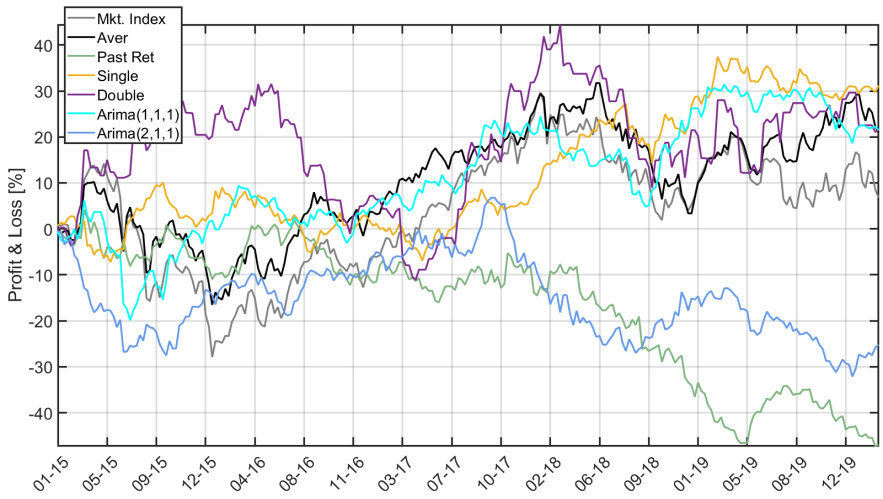

Note: The figure shows the profits and losses (P&L) of different portfolio strategies. The gray line represents the performance of the Hang Seng index, indicated as Mkt. Index. The black line represents the performance of the equally weighted portfolio obtained by selecting all the survival components of the Hang Seng (labelled as Aver). The green line shows the P&L of the past return top-bottom portfolio (Past Ret). The yellow line shows the performance of the CCP obtained with the single sort strategy computed on the forecasted prices (Single); the violet line identifies double sort strategy performance (Double); the light blue line represents the ARIMA(1,1,1) strategy performance (Arima(1,1,1)); the blue line that of ARIMA(2,1,1) (Arima(2,1,1)). The y-axis represents in percentage the P&L while the x-axis the timeline. Top-bottom portfolios are created by considering the 85th and 15th percentiles as reference thresholds of the signal distribution.

number of survival components than the STOXX Europe 50.

Results highlight that the single sort approach performs better than all the other strategies, while the double sort portfolio strategy comes second. The lower performance of the latter is mainly due to the negative P&L of its backward-looking component as also confirmed by the poorest performance of the portfolio based on past returns.

Table 40 displays the yearly Sharpe Ratios and Jensen's Alphas for the Hong-Kong stock market. As for the European case, the single sorting portfolio has the highest risk-return performance considering the whole timespan. Moreover, this portfolio strategy also features positive Sharpe Ratio values for each year and in particular it is the only strategy that does not report a negative value in 2020 since the CCP is able to capture the market downturn associated with the Covid-19 outbreak. Finally, also the Jensen's alpha confirms the previous findings being the single and the double sort portfolios the best performers.

A.3.2 Hang Seng Index Sensitivity

In this Appendix we perform a sensitivity analysis of the results concerning the Hang Seng index. We proceed as in the main text, and we firstly examine the sensitivity of our results subject to changes in the underlying model parameters. After that, we examine the sensitivity of portfolio performances to the forecast horizon choice. Finally, we analyse the sensitivity to both underlying model parameter and forecast horizon choices.

Figure 49 illustrates the sensitivity analysis with respect to the model parameters. In particular, also in this case, we let the percentiles used for creating the top-bottom portfolio vary from $91 - 9$ to $65 - 35$ and plot the corresponding portfolio net profits at the end of the period. Results are similar to the European case. Indeed, the single sorting portfolio outperforms the double sorting strategy for the highest percentiles intervals while the outcome reverts for the lowest percentiles of the grid. However, for choices of the percentile ranges of 84-16 and 71-29 the ARIMA(1,1,1) performs better

Figure 49: Sensitivity analysis with five days forecasting horizon for the Asian case

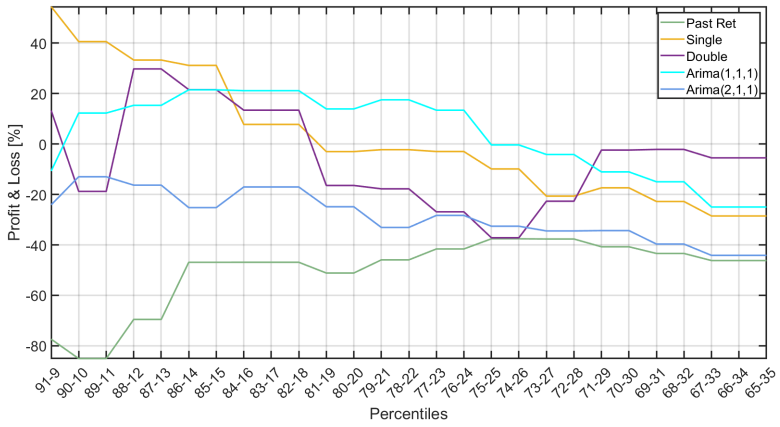

Note: The figure shows the results of the sensitivity analysis on the main portfolio strategies created with five days forecasting horizon. The figure associates the final P&L at 03-20 with various parameter configurations. Namely, the x-axis identifies the top-bottom percentiles thresholds while the y-axis reports the cumulative performance of top-bottom portfolios for the cases of single (yellow line) and double (violet) sorting along with the past returns top-bottom portfolio (green line), the ARIMA(1,1,1) portfolio (light blue line) and the ARIMA(2,1,1) portfolio (blue line).

than the single and double sorting methods. This suggests that our proposed CCPs in this case are best performing for extreme values of the percentile choices. Furthermore, we claim that a sound choice of the percentiles used to choose the top-bottom stocks to be included in the portfolio yields to CCPs able to beat the competing alternatives in terms of performances.

Figure 50 shows the price dynamics and forecasts of the CK Hutchison Holdings Limited (ID 0001.HK) as a reference example for the Hang Seng index, employing a forecast horizon of 10 days for sensitivity purposes. Results show that the predictive models are still able to capture the actual price dynamics, despite the presence of larger variations with respect to the real

Figure 50: Price pattern prediction at ten days forecasting horizon for the stock component ID 0001.HK (CK Hutchison Holdings Limited) of the Hang Seng index

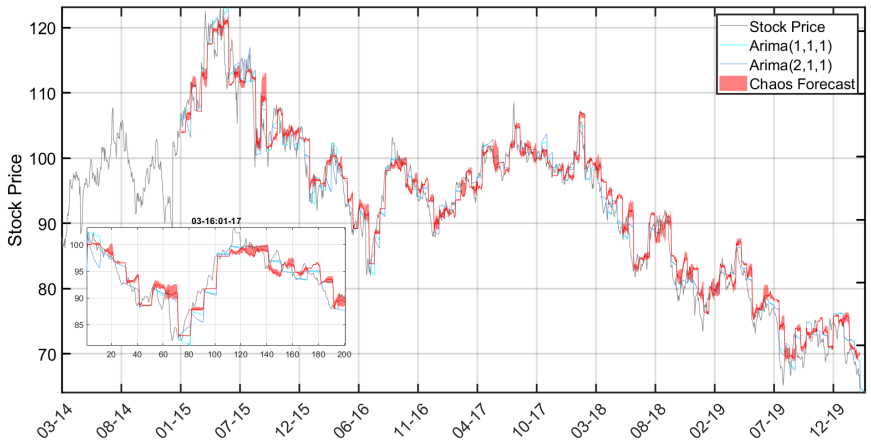

Note: The price forecast obtained by our methodology is represented by the red line; the price forecasts given by the ARIMA(1,1,1) and ARIMA(2,1,1) models are represented by the light blue and blue lines, respectively; the gray line identifies the actual stock price during the analyzed period. The y-axis refers to the stock price. The x-axis, instead, indicates the timeline.

price pattern. This is in line with what we observe for the European case, and can be imputed to the longer forecast horizon which causes a delay in the forecast updates.

Figure 51 shows the top-bottom portfolio performances based on a forecast horizon of ten days. Before 2016, there is no clear best performing portfolio, being the horse-race contested among the double sorting portfolio, the past return, the average and the ARIMA(2,1,1) one. This is in line with the considerations drawn from the European case, as the importance of past values grows together with the forecasting horizon: this is the reason why methods like the past returns, the double sorting and the ARIMA with longer memory tend to outperform the alternative allocation strategies. However,

from the beginning of 2017 onwards it is clear that the double sorting portfolio outperforms all competing alternatives, followed by the single sorting one, yielding to net profits which are as much as triple than those of the second best alternative. This is, again, in line with what we observed for the European case.

Figure 51: Portfolio performance with ten days forecasting horizon, for the Asian case

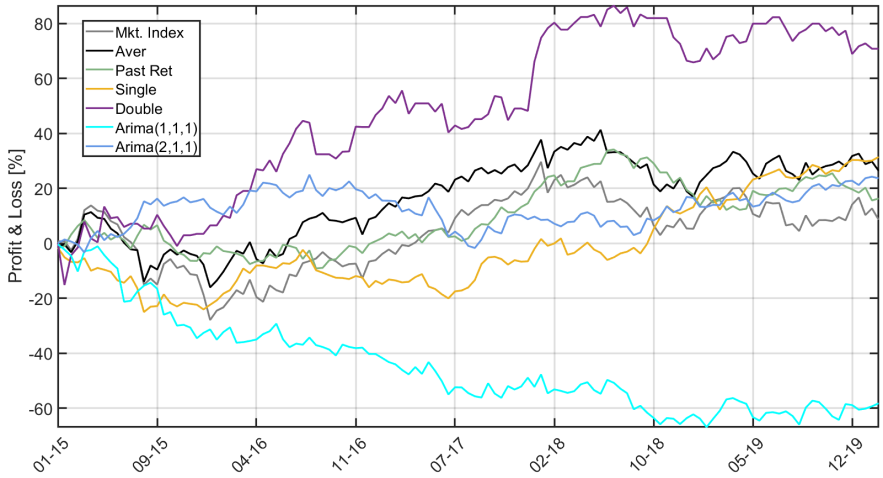

Note: The figure shows the profits and losses (P&L) of different portfolio strategies. The gray line represents the performance of the Hang Seng index, indicated as Mkt. Index. The black line represents the performance of the equally weighted portfolio obtained by selecting all the survival components of the Hang Seng (labelled as Aver). The green line shows the P&L of the past return top-bottom portfolio (Past Ret). The yellow line shows the performance of the CCP obtained with the single sort strategy computed on the forecasted prices (Single); the violet line identifies double sort strategy performance (Double); the light blue line represents the ARIMA(1,1,1) strategy performance (Arima(1,1,1)); the blue line that of ARIMA(2,1,1) (Arima(2,1,1)). The y-axis represents in percentage the P&L while the x-axis the timeline. Top-bottom portfolios are created by considering the 85th and 15th percentiles as reference thresholds of the signal distribution.

Table 41 confirms the previous findings, being the overall Sharpe Ratios and Jensen's Alphas associated to the CCPs the highest ones, with the double sorting being the best proposed method. This remarks that the two methods outperform the others also in terms of risk-adjusted returns.

Table 41: Sharpe Ratio and Jensen's Alpha of different portfolio strategies

Sharpe Ratio							
	2015	2016	2017	2018	2019	2020	TOT
Market Index	-0,179	0,125	0,684	-0,202	0,133	-0,725	0,018
Aver. Market	-0,083	0,181	0,468	-0,168	0,207	-0,971	0,061
Past Returns	-0,056	0,052	0,384	-0,018	0,013	-0,249	0,052
Single Sort	-0,388	0,149	0,259	0,242	0,305	0,52	0,103
Double Sort	0,028	0,421	0,192	-0,004	0,075	-0,305	0,137
ARIMA(1,1,1)	-0,351	-0,124	-0,177	-0,15	0,025	2,558	-0,156
ARIMA(2,1,1)	0,299	0,003	-0,087	0,127	0,102	0,639	0,076
Jensen's Alpha							
	2015	2016	2017	2018	2019	2020	TOT
Aver. Market	0,349	0,218	-0,218	0,081	0,245	-0,552	0,151
Past Returns	-0,3	0,137	0,452	-0,072	0,131	-2,749	0,136
Single Sort	-0,76	0,377	0,101	0,836	0,664	0,444	0,24
Double Sort	0,343	1,94	-1,29	-0,097	0,374	-1,524	0,687
ARIMA(1,1,1)	-1,4	-0,215	-0,676	-0,219	-0,02	0,865	-0,47
ARIMA(2,1,1)	0,46	-0,007	-0,639	0,259	0,135	0,45	0,194

Note: Table reports the Sharpe Ratio and the Jensen's Alpha of the analyzed strategies at ten days forecast horizon. The benchmark used to calculate the Jensen's Alpha is the Hang Seng index.

Figure 52 shows the sensitivity analysis with respect to variations in both model parameters and forecast horizons. In particular, we study how portfolio performances change by letting contemporaneously the percentiles for creating the top-bottom portfolio and the predictive horizon vary from $91-9$ to $65-35$ and from five to ten days, respectively. These results clearly confirm that the double sorting method for creating portfolios outperforms all the other methods and, in this case, for the whole timespan considered. The

double sorting method performances are followed by the single sorting and the ARIMA(2,1,1) portfolios and - in short stretches - by the past return portfolio. The latter outcome is in line both with the previous findings and considerations regarding the importance of the past when forecasting at a longer horizon.

Figure 52: Sensitivity analysis with ten days forecasting horizon for the Asian case

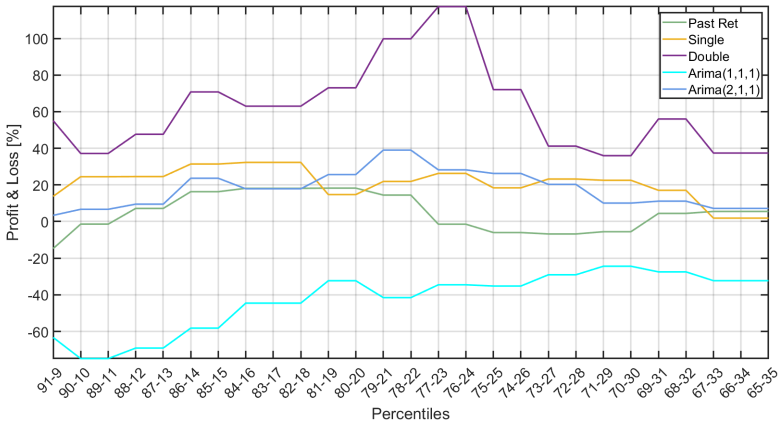

Note: The figure shows the results of the sensitivity analysis on the main portfolio strategies created with five days forecasting horizon. The figure associates the final P&L at 03-20 with various parameter configurations. Namely, the x-axis identifies the top-bottom percentiles thresholds while the y-axis reports the cumulative performance of top-bottom portfolios for the cases of single (yellow line) and double (violet) sorting along with the past returns top-bottom portfolio (green line), the ARIMA(1,1,1) portfolio (light blue line) and the ARIMA(2,1,1) portfolio (blue line).